UNIVERSIDADE DE SANTIAGO DE COMPOSTELA
FACULTAD DE FARMACIA

Departamento de Farmacia e Tecnoloxía Farmacéutica.

NANOMEDICAMENTOS PARA EL TRATAMIENTO LOCALIZADO DE PATOLOGÍAS PULMONARES

Felipe Andrés Oyarzún Ampuero
Santiago de Compostela, 2011

DOÑA DOLORES TORRES LÓPEZ Y DOÑA MARÍA JOSÉ ALONSO FERNÁNDEZ, PROFESORA TITULAR Y CATEDRÁTICA, RESPECTIVAMENTE, DEL DEPARTAMENTO DE FARMACIA Y TECNOLOGÍA FARMACÉUTICA DE LA UNIVERSIDAD DE SANTIAGO DE COMPOSTELA.

INFORMAN:

Que la presente Memoria Experimental titulada: "Nanomedicamentos para el tratamiento localizado de patologías pulmonares", elaborada por el Licenciado en Farmacia **Felipe Andrés Oyarzún Ampuero**, ha sido realizada bajo su dirección en el Departamento de Farmacia y Tecnología Farmacéutica y, hallándose concluida, autorizan su presentación a fin de que pueda ser juzgada por el tribunal correspondiente.

Y para que conste, expiden y firman el presente certificado en Santiago de Compostela, el 20 de Julio de 2011.

Fdo. Dolores Torres **Fdo. María José Alonso**

A mi familia...

"Lo escuché y lo olvidé, lo vi y lo entendí, lo hice y lo aprendí."

Confucio.

AGRADECIMENTOS

Quiero expresar mi agradecimiento a todas las personas que me han prestado su apoyo, tanto profesional como personal, durante todo el camino recorrido para finalizar esta tesis doctoral.

A mis directoras de tesis, las profesoras Dolores Torres y María José Alonso, por haberme recibido y dado la gran oportunidad de realizar este trabajo de investigación, por sus consejos, orientaciones, apoyo y gran comprensión (incluso en importantes aspectos personales) durante todo el tiempo que duró la parte práctica y escrita de esta tesis. Es importantísimo hacer notar que un trabajo de similares características habría sido muy difícil de desarrollar en mi país.

Al Ministerio de Educación de Chile y a la Xunta de Galicia, por facilitarme el apoyo económico necesario para realizar esta tesis.

A Gustavo Rivera, mi gran amigo, por su valiosísima colaboración, tanto teórica como práctica, desde su llegada al laboratorio.

A Begoña Seijo, por toda la ayuda prestada en su calidad de profesora y Coordinadora del programa de doctorado. Ésta se extiende desde antes de mi ingreso oficial al doctorado y posiblemente perdurará luego de finalizar éste.

A todos los demás profesores, investigadores y colaboraderes del grupo: Carmen Remuñán, Alejandro Sánchez, Marcos García, Noemí Csaba, Francisco Goycoolea, Purificación Domínguez, Rafael Romero, etc. Todos, absolutamente todos, tienen, además de grandes cualidades profesionales,

una inmejorable calidad humana, lo que se ha manifestado en innumerables oportunidades y con motivo de situaciones de variada índole.

A Mabel Loza, Pepo Brea, Salvador Arines y a todos los demás colaboradores del Departamento de Farmacología por su gran ayuda para el desarrollo de este trabajo.

A mis compañeros y amigos del laboratorio: Giovanni, José Vicente, Jorge, Giovanna, Patrizia, Angela, Vicky, Sonia, Celina, Pablo, Jenny, Ivana, Yolanda, Manolo, Sascha, Ester, y todos, todos, todos, (seguro, seguro, que se me olvida más de alguien) "le dan un espíritu y vida propia al laboratorio", "todos han aportado de manera tan cualitativa y cuantitativamente distinta a los metros cuadrados que compartímos, que hacen absolutamente irrepetible e intransferible esta etapa de mi vida".

A todos mis amigos chilenos y gallegos con los que compartímos tantos, tantos carretes en Santiago de Compostela (¡puchaaaaa que la pasamos bien!), todos sabemos que hemos cultivado una amistad que evidentemente perdurará en el tiempo y que recordaremos muy gustosamente cuando estemos viejitos (si llegamos…).

En este punto debo agradecer mucho a los gallegos por su gran espíritu, sencillez y capacidad para disfrutar (y los felicito por el hermoso sitio en el que tienen la posibilidad de vivir sus vidas).

Finalmente agradezco el apoyo y comprensión de toda mi familia y especialmente a aquellos que ya no están con nosotros, y que no podrán disfrutar de la culminación de esta etapa de mi vida.

Gracias, muchas, muchas, muchas, gracias “sin ustedes, no lo hubiera conseguido”.

Felipe Andrés Oyarzún Ampuero

18 de Julio, 2011.

ÍNDICE

RESUMEN, ABSTRACT

Resumen

El objetivo de la presente memoria se ha dirigido al diseño y evaluación de nanoestructuras para el tratamiento localizado de patologías pulmonares. En una primera etapa, se han desarrollado nanopartículas de quitosano, en combinación con ácido hialurónico o con carboximetil-β-ciclodextrina, conteniendo la macromolécula hidrofílica heparina. Dichos sistemas fueron evaluados en relación a su capacidad de mejora de eficacia de la heparina sobre mastocitos, en el tratamiento del asma bronquial. Se demostró por microscopía confocal de fluorescencia que los nanosistemas eran internalizados por mastocitos de rata y, en el caso de los nanosistemas con ciclodextrinas, se consiguió mejorar de manera significativa el efecto de la heparina sobre la inhibición de la liberación de histamina en mastocitos.

La segunda parte del trabajo se orientó al diseño de un nuevo nanosistema, consistente en nanocápulas de ácido hialurónico, con el fin último de dirigirlo al tratamiento del cáncer de pulmón. Los nanosistemas incrementaron significativamente el efecto citotóxico del antitumoral hidrofóbico docetaxel, sobre la línea celular de cáncer de pulmón NCI-H460, hecho que se atribuyó a la internalización de las nanocápsulas y la liberación intracelular del docetaxel. Estos resultados resaltan el enorme interés de los nanosistemas desarrollados para la liberación intracelular de fármacos en el tratamiento de enfermedades pulmonares.

Abstract

The purpose of this work has been the design and evaluation of targeted nanostructures for the treatment of lung diseases. In a first stage, we developed nanoparticles made of chitosan combined with hyaluronic acid or carboxymethyl-β-cyclodextrin, containing the hydrophilic macromolecule heparin. The final aim was to explore the potential of these nanocarriers to treat asthma. It was demonstrated that the systems were able to get inside the mast cells and, in the case of nanosystems prepared with cyclodextrins, it was obtained a significantly greater effect to prevent histamine release in mast cells compared with the heparin alone.

In a second stage, we developed a new nanocarrier, named as hyaluronic acid nanocapsules, for the intracellular delivery of hydrophobic anticancer drugs, with potential application in lung cancer. It was shown that these systems significantly improved the cytotoxic effect of docetaxel in the lung cancer cell-line NCI-H460. This result was attributed to the internalization of nanocapsules and the intracellular delivery of docetaxel. In summary, these nanostructures hold promise as intracellular drug delivery systems for the treatment of lung diseases.

LISTADO DE ABREVIATURAS

Listado de abreviaturas:

AFM: Atomic force microscopy.
ANOVA: Analysis of variance.
BKC: Benzalkonium chloride, cloruro de benzalconio.
CMβCD: Carboxymethyl-β-cyclodextrin, carboximetil-β-ciclodextrina.
CS: Chitosan, quitosano.
CTAB: Hexadeciltrymethylammonium bromide, bromuro de hexadeciltrimetilamonio.
DCX: Docetaxel
EGF: Epidermal growth factor, factor de crecimiento epidermal.
EPR: Enhanced permeability and retention effect.
HA: hyaluronic acid, ácido hialurónico.
HBSS: Hanks´ balanced salt solution.
HPLC: High performance liquid chromatography.
IP_3: Inositoltrisphosphate, trifosfato de inositol.
LMWH: Low molecular weight heparin, heparina de bajo peso molecular.
LNC: Lipid nanocapsules.
MDR: Multidrug resistance.
MTT: Tretazolium salt 3-(4,5-dimewthylthiazol-2-yl)2,5 diphenyltetrazolium bromide.
NCs: Nanocapsules.
NMR: Nuclear magnetic resonance.
ODN: Oligodeoxynucleotide.
PACA: Poly(alkylcyanoacrylate).
PBCA: Poly(isobutylcyanoacrylate).
PBS: Phosphate buffered saline.
PCL: Poly-ε-caprolactone.
PEG: Polyethyleneglycol, polietilenglicol.
PEI: Polietilenimina.
SEM: Scanning electron microscopy.
siRNA: Small interfering RNA, ARN pequeño de interferencia.
TEM: Transmission electron microscopy.
TPP: Pentasodium tripolyphosphate, tripolifosfato pentasódico.
UFH: Unfractioned heparin, heparina no fraccionada.

INTRODUCCIÓN

INTRODUCCIÓN

1. Tratamiento localizado de patologías pulmonares

La administración pulmonar de fármacos ha experimentado un notable impulso especialmente en la década pasada, como consecuencia de la creciente investigación relacionada con su uso como alternativa a la administración parenteral de macromoléculas peptídicas. Esta nueva aplicación tiene mucho que ver con las características fisiológicas especiales del tracto respiratorio, y la introducción de las partículas porosas, que permitieron maximizar el acceso del fármaco a los lugares de absorción[1;2].

El gran área superficial de la región alveolar, la delgada barrera epitelial, la gran vascularización y la relativamente baja actividad proteolítica en el espacio alveolar ofrecen grandes posibilidades a la hora de facilitar el acceso sistémico de macromoléculas problemáticas desde el punto de vista biofarmacéutico, como son las peptídicas[3;4;5]. Pero fue el descubrimiento de que extremando la porosidad de las partículas, era posible optimizar el acceso alveolar, lo que conllevó a la comercialización, aunque temporal, de la insulina pulmonar, y a los diferentes estudios clínicos en marcha hoy en día con macromoléculas inhaladas[6;7;8].

Paralelamente, y como consecuencia de la nueva experimentación en torno a la vía pulmonar, su utilización más frecuente para el tratamiento local

[1] **Edwards DA, Hanes J, Caponetti G, Hrkach J, Ben-Jebria A, Eskew ML, Mintzes J, Deaver D, Lotan N, Langer R.** (1997). Science. 276(5320):1868-71.
[2] **Garcia-Contreras L, Fiegel J, Telko MJ, Elbert K, Hawi A, Thomas M, VerBerkmoes J, Germishuizen WA, Fourie PB, Hickey AJ, Edwards D.** (2007). Antimicrob Agents Chemother. 51(8):2830-6.
[3] **Becquemin MH, Chaumuzeau JP.** (2010). Rev Mal Respir. 27(8):e54-65.
[4] **Hohenegger M.** (2010). Curr Pharm Des. 16(22):2484-92.
[5] **Andrade F, Videira M, Ferreira D, Sarmento B.** (2011). Nanomedicine (Lond). 6(1):123-41.
[6] **Heinemann L.** (2010). Int. J. Clin. Pract. Suppl. 166:29-40.
[7] **Neumiller JJ, Campbell RK.** (2010). BioDrugs. 24(3):165-72.
[8] **Hohenegger M. (2010).** Curr. Pharm. Des. 16(22):2484-92.

de patologías de las vías aéreas, experimentó un considerable repunte, abriéndose nuevas posibilidades en el tratamiento de patologías como el asma[9;10], tuberculosis[11;12] o cáncer de pulmón[3;13;14]. A ello contribuye la incorporación del nuevo conocimiento disponible acerca de los distintos factores implicados, como por ejemplo, el mecanismo de acción de los fármacos utilizados en terapias localizadas, las moléculas capaces de unirse específicamente a receptores presentes en las células diana, o bien los nuevos vehículos transportadores de fármacos, entre los que destacan las nanoestructuras poliméricas, objeto de la presente Memoria.

2. Nanosistemas orientados al *targeting* pulmonar

El pulmón es una diana muy atractiva para la liberación de fármacos que buscan un efecto localizado. Así, a través de una vía no invasiva, se puede lograr una elevada concentración del principio activo, evitando el efecto de primer paso y teniendo la posibilidad de desencadenar un rápido inicio de acción. Este hecho, junto con el reciente desarrollo de los nanotransportadores terapéuticos, ha generado nuevas expectativas en las terapias localizadas (Figura 1).

[9] **Niven AS, Argyros G.** (2003) Chest. 123(4):1254-65.
[10] **Barnes PJ.** (2010). Trends Pharmacol. Sci. 31(7):335-43.
[11] **Mitchison DA, Fourie PB**. (2010). Tuberculosis (Edinb). 90(3):177-81.
[12] **Ohashi K, Kabasawa T, Ozeki T, Okada H.** (2009). J. Control Release. 135(1):19-24..
[13] **Kurmi BD, Kayat J, Gajbhiye V, Tekade RK, Jain NK.** (2010).Expert Opin. Drug Deliv. 7:781-794.
[14] **Yi D, Wiedmann T.S.** (2010). J. Aerosol Med. Pulm. Drug Deliv. 23(4):181-7.

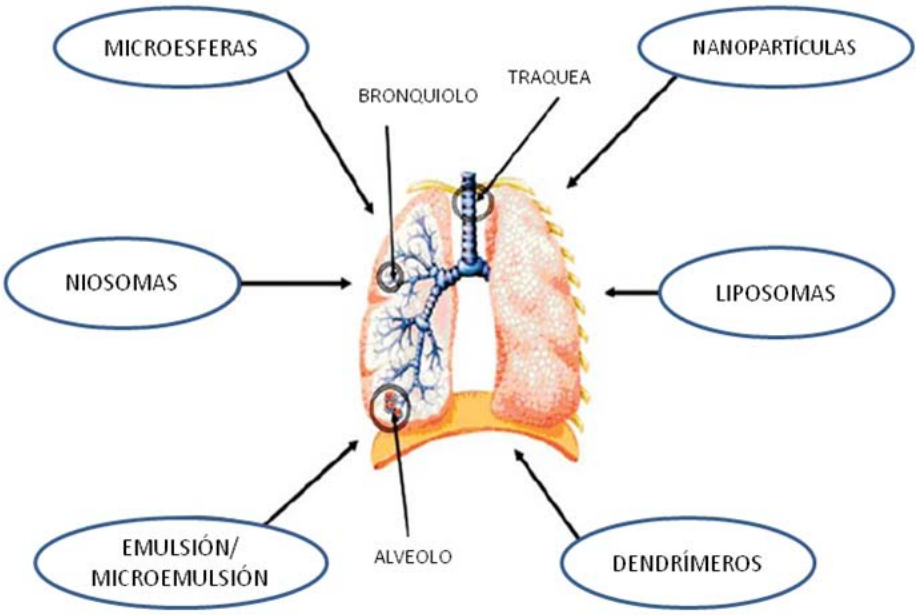

Figura 1. Algunos de los sistemas nanopartículares propuestos para el *targeting* pulmonar (tomado de ref 13).

Los sistemas nanoparticulares ofrecen distintas ventajas potenciales en cuanto a la optimización de:

1) adhesión a la mucosa pulmonar y modulación de la liberación del fármaco, lo que permitiría reducir la frecuencia de dosificación, disminuir los efectos adversos y mejorar el cumplimiento del paciente.

2) protección de fármacos macromoleculares, asegurando su liberación en forma activa.

3) mejora de la interacción del fármaco con las células diana, favoreciendo el acceso intracelular cuando fuese necesario, y maximizando así su eficacia[15].

En la Tabla 1 se recogen distintos ejemplos de sistemas nanoparticulares administrados por vía pulmonar para tratar diferentes

[15] **Manzour HM, Rhee YS, Wu X.** (2009). Int. J. Nanomed. 4:299-319.

afecciones localizadas en dicho órgano. Destacan en este sentido los relacionados con el tratamiento de tuberculosis y cáncer.

En el caso de la tuberculosis, las nanoestructuras resultan especialmente adecuadas, ya que se busca el *targeting* en las células diana que son los macrófagos alveolares; por lo tanto, la captura de las nanoestructuras por estas células, favorecería de manera rotunda el éxito del tratamiento. Existen una serie de estudios en los que se evalúa la administración de nanopartículas poliméricas de diversa composición, conteniendo antibioticos (rifampicina, isoniazida y pirazinamida) a cobayas infectadas con *micobacterium tuberculosis*. Dichas nanopartículas se administraron mediante nebulización cada 10-15 días hasta un total de 3-5 dosis o bien, como control, se administraron diariamente por vía oral. En el caso de los sistemas nanoparticulares constituídos por poli(ácido láctico-ácido glicólico) (PLGA), se mantuvieron niveles terapéuticos plasmáticos de los fármacos durante los 8 días postadministración, y en el pulmón estos niveles se mantuvieron durante 11 días[16]. Otra interesante alternativa consistió en modificar superficialmente las nanopartículas de PLGA con la lectina aglutinina de germen de trigo. Dicha lectina, además de ser mucoadhesiva, ofrece la posibilidad de que las nanopartículas interaccionen con los receptores de esta molécula ubicados en el epitelio alveolar, lo que permitiría prolongar aún más el control en la liberación del fármaco en el pulmón. Los citados sistemas fueron capaces de mantener niveles terapéuticos de los fármacos durante 14 días en el plasma y 15 días en el pulmón[17]. Otra apuesta resaltable para el tratamiento de la tuberculosis consistió en la utilización de nanopartículas de quitosano-alginato. En este caso, se pudo apreciar igualmente que los niveles plasmáticos de los fármacos se mantuvieron en plasma durante 14 días y en el pulmón hasta 15

[16] **Pandey R, Sharma A, Zahoor A, Sharma S, Khuller GK, Prasad B. (2003)** J. Antimicrob. Chemother. 52(6): 981-6.
[17] **Sharma A, Sharma S, Khuller GK.** (2004). J. Antimicrob. Chemother. 54(4): 761-6.

días[18]. La liberación sostenida de los fármacos en el pulmón, apreciada en todos los nanosistemas comentados, redujo significativamente la dosis total de fármaco requerida para el tratamiento. De hecho, al final del tratamiento, ninguno de los animales infectados presentó la enfermedad, lo que fue comparable con lo obtenido con la dosis oral diaria.

En el caso de la administración pulmonar de nanosistemas para el tratamiento de cáncer de pulmón, el cisplatino y sus derivados han sido utilizados como fármacos modelo en distintas ocasiones. Estos sistemas han sido evaluados en cuanto a sus parámetros de formulación y a su eficacia *in vitro* e *in vivo* en diversos modelos celulares de cáncer[19;20;21]. Destacamos los resultados obtenidos con nanopartículas de gelatina cargadas con cisplatino y funcionalizadas con el factor de crecimiento epidermal (EGF). El receptor para el EGF se sobreexpresa en distintos tipos de cáncer, especialmente en el de células no pequeñas de pulmón[22]. Los autores demostraron *in vitro* que los nanosistemas tenían más afinidad por células que sobrexpresan el receptor para el EGF, y que su eficacia era mayor que la del fármaco solo o la de las nanopartículas con cisplatino, pero sin funcionalizar. También demostraron que la potencia de las nanopartículas funcionalizadas era superior cuando se administraban intratumoralmente en un modelo animal de cáncer. Finalmente, los autores administraron mediante nebulización los nanosistemas funcionalizados y demostraron que éstos podían localizarse en células tumorales que sobreexpresan el receptor para el EGF y alcanzar allí altas concentraciones de fármaco[23].

[18] **Ahmad Z, Sharma S, Khuller GK.** (2005). Int .J. Antimicrob. Agents. 26(4): 298:303.
[19] **Cafaggi S, Russo E, Stefani R, Leardi R, Caviglioli G, Parodi B, Bignardi G, De Totero D, Aiello C, Viale M.** (2007). J. Control Rel. 121(1-2):110-23.
[20] **Brown SD, Nativo P, Smith JA, Stirling D, Edwards PR, Venugopal B, Flint DJ, Plumb JA, Graham D, Wheate NJ.** (2010). J. Am. Chem. Soc. 132(13):4678-84.
[21] **Paraskar AS, Soni S, Chin KT, Chaudhuri P, Muto KW, Berkowitz J, Handlogten MW, Alves NJ, Bilgicer B, Dinulescu DM, Mashelkar RA, Sengupta S.** (2010). Proc. Natl. Acad. Sci. U S A. 13;107(28):12435-40.
[22] **Rusch V, Klimstra D, Venkatraman E, Pisters PW, Langenfeld J, Dmitrovsky E.** (1997). Clin. Cancer Res. 3(4):515-22.
[23] **Tseng CL, Su WY, Yen KC, Yang KC, Lin FH.** (2009). Biomaterials. 30(20):3476-85.

Otro sistema que podemos destacar es el constituído por nanopartículas poliméricas de poli (ácido glutámico)-dextrano recubiertas por alcohol cetílico-tripalmitina, cargadas con 5-fluorouracilo. Dichos sistemas se atomizaron y administraron a hámsters para evaluar su eficacia sobre tumores de células escamosas, obteniéndose niveles efectivos de fármaco de un modo prolongado[24].

En el caso de la administración de material genético para el tratamiento del cáncer, un trabajo interesante se refiere al tratamiento de un modelo de metástasis pulmonar con nanosistemas constituídos por polietilenimina y el plásmido del gen *p*53. Se ha encontrado que la mutación/deleción de dicho gen está presente en la mayoría de los cánceres de pulmón de células pequeñas y no pequeñas, por lo que transfectar dichas células con el plásmido en cuestión resultaría favorable. Dichos sistemas fueron nebulizados y administrados a ratas, obteniéndose reducciones muy significativas en el tamaño y número de tumores[25]. También destaca el trabajo realizado Xu y col. (2008), que diseñaron nanosistemas constituídos por policaprolactona y polietilenimina conteniendo el RNA de interferencia akt1 (siRNA). La proteína Akt (proteína kinasa B) es un importante regulador de la supervivencia y proliferación celular y la amplificación de los genes que la codifican ha sido evidenciada en varios tumores. La nebulización de estos sistemas en ratas demostró una significativa disminución de la progresión del tumor de pulmón, a través de la inhibición de las señales celulares dependientes del gen Akt[26].

[24] **Hitzman CJ, Wattenberg LW, Wiedmann TS.** (2006). J. Pharm. Sci. 95(6):1196-211.
[25] **Densmore CL, Kleinerman ES, Gautam A, Jia SF, Xu B, Worth LL, Waldrep JC, Fung YK, T'Ang A.** (2001). Cancer Gene Ther. 8(9):619-27.
[26] **Xu CX, Jere D, Jin H, Chang SH, Chung YS, Shin JY, Kim JE, Park SJ, Lee YH, Chae CH, Lee KH, Beck GR Jr, Cho CS, Cho MH.** (2008). Am. J. Respir. Crit. Care Med. 178(1):60-73.

Tabla 1: Ejemplos de sistemas nanoparticulares administrados por vía pulmonar para el tratamiento de patologías pulmonares.

Composición nanosistema	Tamaño (nm)	Fármaco(s)	Especie animal	Forma de administración	Respuesta biológica y referencia
PLGA, PLGA modificado con aglutinina de germen de trigo	186-400	Rifampicina, isoniazida, pirazinamida	Cobayas	Nebulización	Mejora la biodisponiblidad y permite reducir la frecuencia de dosis en tuberculosis[16;17].
Quitosano-Alginato	235	Rifampicina, isoniazida, pirazinamida	Cobayas	Nebulización	Mejora la biodisponiblidad y permite reducir la frecuencia de dosis en tuberculosis[18].
PLGA	213	Rifampicina	Rata	Nanopartículas incluidas en microesferas de manitol administradas en inhalador de polvo seco	Retención pulmonar prolongada del nanosistema y localización en macrófagos alveolares[27].
Quitosano	376	pDNA	Ratón	Instilación intratraqueal	Eficacia inmunogénica contra tuberculosis[28].
Gelatina modicada con EGF	230	Cisplatino	Ratón	Nebulización	Alta concentración del fármaco en tumores localizados en pulmón[23].
Poli(ácido glutámico)-dextrano; recubrimiento con alcohol cetílicotripalmitina	800	5-fluorouracilo	Hámsters	Nebulización	Se demuestra retención pulmonar y efecto prolongado del fármaco[24].
PEI	No disponible	pDNA	Ratón	Nebulización	Reducción significativa en número y tamaño de tumores[23].

[27] **Ohashi K, Kabasawa T, Ozeki T, Okada H.** (2009). J. Control Release. 135(1):19-24.
[28] **Bivas-Benita M, van Meijgaarden KE, Franken KL, Junginger HE, Borchard G, Ottenhoff TH, Geluk A.** (2004). Vaccine. 22(13-14):1609-15.

Policaprolactona y PEI	150	siRNA	Ratón	Nebulización	Mayor eficacia en la supresión tumoral[23].
Quitosano modificado con ácido urocánico	No disponible	Proteína de programación de muerte celular 4 (PPMC4)	Ratón	Nebulización	Facilita la apoptosis, inhibe importantes vías de proliferación celular y suprime eficientemente las vías de angiogénesis tumoral[29].
PLGA	201-240	TAS-103 (fármaco antineoplásico)	Rata	Nanopartículas incluidas en microesferas de trealosa administradas en inhalador de polvo seco	Concentración del fármaco en pulmón superior a la detectada en plasma y superior que tras administración IV[30].
PLGA-PEG	44	Oligonucleótido secuestrador del factor nuclear κB (regula la expresión de importantes citoquinas inflamatorias)	Rata	Instilación intratraqueal	Atenúa el desarrollo de hipertensión pulmonar arterial y de la remodelación arterial[31].

PLGA: poli(ácido láctico-ácido glicólico); PEI:polietilenimina; PEG:polietilenglicol; EGF: factor de crecimiento epidermal; pDNA:ADN plasmídico; siRNA:ARN pequeño de interferencia.

[29] **Jin H, Kim TH, Hwang SK, Chang SH, Kim HW, Anderson HK, Lee HW, Lee KH, Colburn NH, Yang HS, Cho MH, Cho CS.** (2006). Mol. Cancer Ther. 5(4):1041-9.

[30] **Tomoda K, Ohkoshi T, Hirota K, Sonavane GS, Nakajima T, Terada H, Komuro M, Kitazato K, Makino K.** (2009). Colloids Surf. B Biointerfaces. 71(2):177-82.

[31] **Kimura S.; Egashira K.; Chen L.; Nakano K.; Iwata E.; Miyagawa.; Tsujimoto H.; Hara K.; Morishita R.; Sueishi K.; Tominaga R.; Sunagawa K.** (2009).Hypertension. 53(5):877-83.

2.1. Asma bronquial y heparina

La heparina es una macromolécula que pertenece a la compleja familia de los glucosaminoglucanos. Está compuesta por unidades disacarídicas altamente sulfatadas (Figura 2), de tal manera que su naturaleza polianiónica favorece la interacción con una gran variedad de proteínas que poseen aminoácidos cargados positivamente[32].

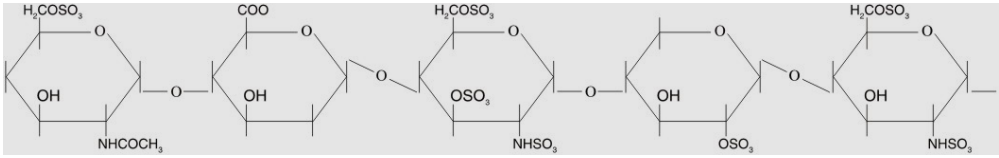

Figura 2: Estructura molecular de heparina.

De estas interacciones, la mejor caracterizada es la que lleva a la formación del complejo heparina-antitrombina III, que posee importantes repercusiones en el proceso de coagulación sanguínea[33;34]. Adicionalmente a su actividad antiacoagulante, la heparina ha demostrado poseer interesantes propiedades antiinflamatorias en enfermedades alérgicas. Ejemplo de ello, es la demostrada interacción entre la heparina y el receptor intracelular de trifosfato de inositol (IP_3) en mastocitos[35;36]. El resultado de dicha interacción es la inhibición de la movilización intracelular de calcio, lo que impide la activación de mediadores intracelulares y la contracción del citoesqueleto, previniéndose finalmente la liberación de histamina (Figura 3). Este efecto

[32] **Wong WS, Koh DS.** (2000). Biochem. Pharmacol. 59(11):1323-35.
[33] **Jaques LB.** (1980). Pharmacol. Rev. 31: 99-166.
[34] **Lindhal U, Backstrom G, Thundberg L.** (1983). J. Biol. Chem. 258: 9826-9830.
[35] **Lucio J, D'Brot J, Guo CB, Abraham WM, Lichtenstein LM, Kagey-Sobotka A, Ahmed T.** (1992). Appl. Physiol. 73(3):1093-101.
[36] **Ahmed T, Syriste T, Mendelssohn R, Sorace D, Mansour E, Lansing M, Abraham WM, Robinson M.J.** (1994). J. Appl. Physiol. 76(2):893-901.

induce a pensar el interesante rol que puede tener esta molécula en el tratamiento del asma alérgico[37;38].

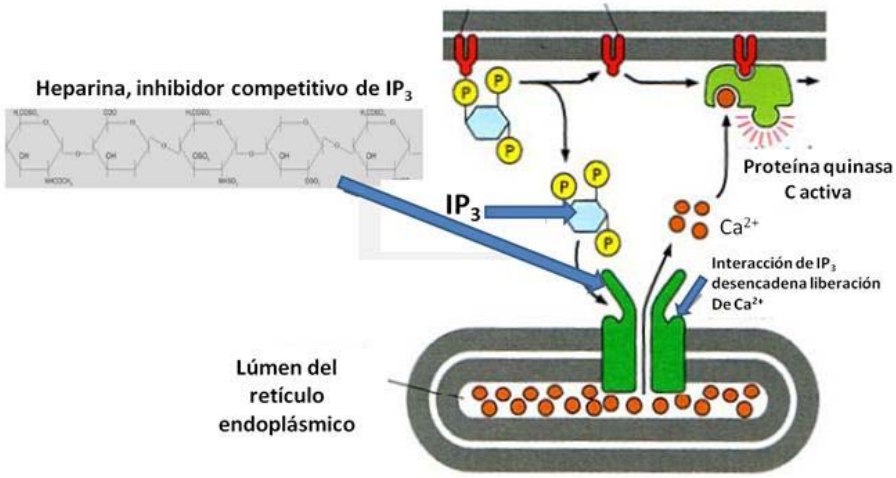

Figura 3: Mecanismo de acción de heparina para prevenir la degranulación de los mastocitos.

Confirmando la información anterior, se ha demostrado en distintos estudios que la inhalación de heparina de pesos moleculares diferentes (con y sin actividad antiacoagulante) es efectiva para prevenir las respuestas de broncoconstricción aguda y de hipersensibilidad bronquial, típicas de la enfermedad asmática[39;40;41;42]. De hecho, se llegó a demostrar que la potencia de las heparinas para prevenir dichas respuestas es inversamente proporcional a su peso molecular.

Otro hallazgo interesante de la heparina, y que complementa su utilidad para el tratamiento del asma, es su potencial para prevenir la remodelación de las vías aéreas. Esta remodelación, mediada principalmente

[37] **Tyrrel DJ, Kilfeather S, Page CP.** (1995). TiPS. 16:198-204.
[38] **Diamant Z, Page CP.** (2000). Pulm. Pharmacol. Ther. 13(1):1-4.
[39] **Martinez-Salas J, Mendelssohn R, Abraham WM, Hsiao B, Ahmed T**. (1998). J. Appl. Physiol. 84:222–228.
[40] **Molinari JF, Campo C, Shahida S, Ahmed T.** (1998). Am. J. Respir. Crit. Care Med. 157: 887–893.
[41] **Campo C, Molinari JF, Ungo J, Ahmed T.** (1999). J. Appl. Physiol. 86: 549–557.
[42] **Ahmed T, Ungo J, Zhou M, Campo C**. (2000). J. Appl. Physiol. 88, 1721–1729.

por la acumulación de células musculares lisas, induce un estrechamiento excesivo de las vía aéreas y conduce a hipersensibilidad y dificultad para respirar[43]. La heparina ha demostrado una alta eficacia al inhibir la proliferación de células musculares lisas extraídas de las vías aéreas de humanos[44], bovinos[45] y perros[46].

2.2. Docetaxel y su vehiculización tumoral

Los taxanos (paclitaxel y docetaxel; Figura 4) son potentes agentes quimioterápicos cuyo núcleo químico fundamental es de origen natural y se extrae a partir de árboles del género "*Taxus"*. Su mecanismo de acción consiste en promover el ensamblaje intracelular de tubulina y en inhibir la despolimerización de los microtúbulos, impidiendo el crecimiento celular[47]. Estas moléculas han contribuido de manera trascendental a la supervivencia de pacientes con cáncer, siendo eficaces frente a un amplio rango de tumores sólidos como el cáncer avanzado de mama, de ovarios y de células no pequeñas de pulmón[48;49;50], entre otros. Algunos estudios, como el publicado por Jones y col. (2005), indican que el docetaxel resulta más eficaz que el paclitaxel cuando se evalúa la sobrevida en pacientes con cáncer metastásico de mama[51].

[43] **Kanabar V, Hirst SJ, O'Connor BJ, Page CP.** (2005). Br. J. Pharmacol. 146, 370–377.
[44] **Johnson PR, Armour CL, Carey D, Black JL.** (1995). Am. J. Physiol. 269, L514–L519.
[45] **Kilfeather SA, Tagoe S, Perez AC, Okona-Mensa K, Matin R, Page C.P.** (1995). Br. J. Pharmacol. 114, 1442–1446.
[46] **Halayko AJ, Recto E, Sthepens NL.** (1997). Can. J. Physiol. Pharmacol. 75, 917–919.
[47] **Abal M.; Andreu J.M.; Barasoain I.** (2003). Curr Cancer Drug Targets. 3(3):193-203.
[48] **Rowinsky RK, Donehower RCN.** (1995). Engl. J. Med. 332: 1004-1014.
[49] **Trudeau ME, Eisenhauer EA, Higgins BP, Letendre F, Lofters WS, Norris BD, Vandenberg TA, Delorme F, Muldal AM.** (1996). J. Clin. Oncol. 14: 422-428.
[50] **Piccart MJ, Gore M, Huinink WTB, Vanoosterom A, Verweij J, Wanders J, Franklin H, Bayssas M, Kaye S.** (1995). J. Natl. Cancer Inst. 87: 676-681.
[51] **Jones SE, Erban J, Overmoyer B, Budd GT, Hutchins L, Lower E, Laufman L, Sundaram S, Urba W J, Pritchard KI, Mennel R, Richards D, Olsen S, Meyers ML, Ravdin PM.** (2005). J. Clin. Oncol. 2005, 23, 5542–5551.

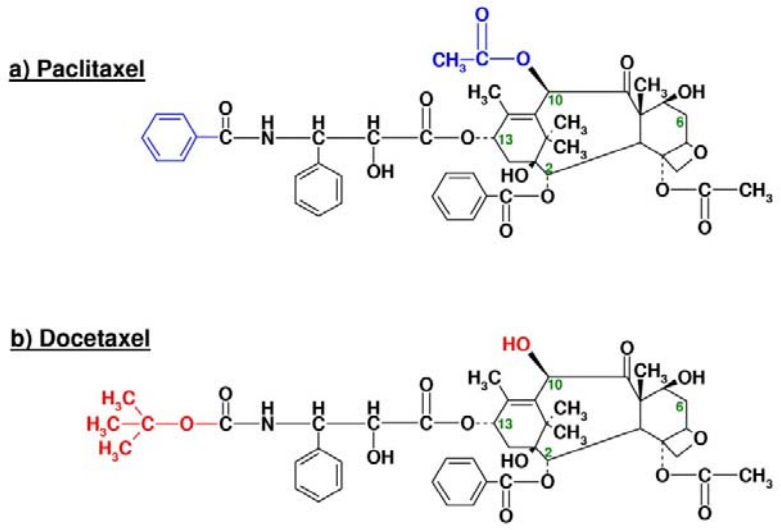

Figura 4: Estructura molecular de los taxanos (en azul y rojo se destaca la diferencia estructural entre las moléculas).

Independientemente de su potencia, ambas moléculas se caracterizan por su elevado carácter hidrofóbico, lo que obliga a incluir agentes solubilizantes como el Cremophor EL y Tween 80, ambos en combinación con etanol, en las formulaciones endovenosas de paclitaxel y docetaxel, respectivamente. Desgraciadamente, estos vehículos son responsables de efectos secundarios severos, lo que limita la cantidad de fármaco que puede ser administrada al paciente de modo seguro. Entre estos efectos podemos mencionar: hipersensibilidad anafilactoide severa, neuropatía periférica, agregación de eritrocitos y patrones anormales de lipoproteínas[52;53;54].

Además de este problema de toxicidad, los taxanos son fármacos que comparten los problemas asociados a los antitumorales, es decir, su baja permanencia plasmática, y su biodistribución indiscriminada. Para superar estas limitaciones, se han propuesto nuevas formulaciones que no requieren

[52] **Gelderblom H, Verweij J, Nooter K, Sparreboom A.** (2001). Eur J Cancer. 37(13):1590-8.
[53] **Van Zuylen L, Verweij J, Sparreboom A.** (2001).Invest. New Drugs. 19(2):125-41.
[54] **Engels FK, Mathot RA, Verweij J.** (2007). Anticancer Drugs. 18(2):95-103.

la hidrosolubilización de los fármacos, y modifican su perfil farmacocinético. Entre ellas, destacan las basadas en nanoestructuras poliméricas, como por ejemplo, el sistema denominado Abraxane®, constituído por nanopartículas de albúmina conteniendo paclitaxel, la primera formulación de nanopartículas en clínica, introducida en el año 2005[55]. Es importante recalcar que este hito impulsó de manera importante el desarrollo de nuevas formulaciones que contienen taxanos, entre ellas podemos destacar: liposomas[56], lipoplejos[57], nanopartículas[58;59;60;61], nanocápsulas[62;63] y conjugados[64;65;66]. En general, todos estos nanosistemas proveen al fármaco de una mayor citoespecificidad lo que puede verse traducido en menos efectos no deseados y una mayor eficacia en el tratamiento.

Los sistemas nanocapsulares basados en estructuras de tipo reservorio (núcleo de aceite recubierto por una capa polimérica), son vehículos muy adecuados para el transporte de fármacos hidrofóbicos como el docetaxel pues, además de obviar la necesidad de utilizar solubilizantes en la formulación, permiten obtener una elevada eficacia de encapsulación y

[55] **Sparreboom A, Scripture CD, Trieu V, Williams PJ, De T, Yang A, Beals B, Figg WD, Hawkins M, Desai N.** (2005). Clin. Cancer Res. 11, 4136-43.
[56] **Eliaz RE, Szoka FCJr.** (2001). Cancer Res. 61(6):2592-601.
[57] **Surace C, Arpicco S, Dufaÿ-Wojcicki A, Marsaud V, Bouclier C, Clay D, Cattel L, Renoir JM, Fattal E.** (2009). Mol. Pharm. 6(4):1062-73.
[58] **Hyung W**, **Ko H**, **Park J**, **Lim E**, **Park SB**, **Park YJ**, **Yoon HG**, **Suh JS**, **Haam S**, **Huh Y.M**. (2008). Biotechnol. Bioeng. 99(2):442-54.
[59] **Pandita D, Ahuja A, Lather V, Dutta T, Velpandian T, Khar RK.** (2011). Pharmazie. 66(3):171-7.
[60] **Hong GY, Jeong YI, Lee SJ, Lee E, Oh JS, Lee HC.** (2011). Arch Pharm Res. 34(3):407-17.
[61] **Liu D, Wang L, Liu Z, Zhang C, Zhang N.** (2010). J Biomed Nanotechnol. 6(6):675-82.
[62] **Lozano MV, Torrecilla D, Torres D, Vidal A, Domínguez F, Alonso MJ.** (2008) Biomacromol. 9(8):2186-93.
[63] **Hureaux J, Lagarce F, Gagnadoux F, Rousselet MC, Moal V, Urban T, Benoit J.** (2010). Pharm Res. 27(3):421-30.
[64] **Luo Y, Bernshaw NJ, Lu ZR, Kopecek J, Prestwich GD.** (2002). Pharm Res. 19(4):396-402.
[65] **Rosato A, Banzato A, De Luca G, Renier D, Bettella F, Pagano C, Esposito G, Zanovello P, Bassi P.** (2006). Urol. Oncol. 24(3):207-15.
[66] **Xin D, Wang Y, Xiang J.** (2010). Pharm. Res. 27(2):380-9.

modificar su perfil de distribución[67;68]. El Capítulo 1 de la presente tesis doctoral es una revisión acerca de los citados sistemas, en la que se puede obtener una visión más general y detallada de las nanocápsulas en aspectos relacionados con su elaboración, caracterización y evaluación *in vitro/in vivo*.

En distintas investigaciones, se ha propuesto la utilización de nanocápsulas para la vehiculización tumoral de docetaxel. Un ejemplo, es el sistema propuesto por Khalid y col. (2006)[69], quienes desarrollaron nanocápsulas lipídicas recubiertas de polietilenglicol para obtener tiempos prolongados de circulación en sangre. Este trabajo fue el primero que demostró que la encapsulación de docetaxel en sistemas coloidales podía ser utilizada para dirigir pasivamente el fármaco a los tejidos neoplásicos. De hecho, las nanocápsulas demostraron una mejora en la acumulación del fármaco en el tumor cuando se comparaban con la formulación convencional (Taxotere®). Lozano y col. (2010)[62] demostraron que la inclusión de docetaxel en nanocápsulas recubiertas con quitosano da lugar a una rápida captura de los sistemas en líneas celulares de cáncer de mama (MCF-7) y pulmón (A-549) y que, tras 24 horas, el efecto sobre la viabilidad celular obtenido con las nanocápsulas cargadas con docetaxel fue significativamente mejor que el obtenido con el fármaco solo. Se demostró igualmente que las nanocápsulas de quitosano mostraban, tras inyección intratumoral, un efecto similar en la reducción del volumen tumoral al de la formulación comercial de docetaxel, siendo un efecto más lento, pero más duradero en el período de seguimiento del proceso[70].

[67] **Mora-Huertas CE, Fessi H, Elaissari A.** (2010). Int. J. Pharm. 385(1-2):113-42.
[68] **Huynh NT, Passirani C, Saulnier P, Benoit JP. (2009)** Int. J. Pharm. 379(2):201-9.
[69] **Khalid M N, Simard P, Hoarau D, Dragomir A, Leroux J C.** (2006). Pharm. Res. 23, 752–758.
[70] **Lozano M.V.; Torrecilla D.; Lallana E.; Vidal A.; Fernández-Megía R.; Riguera R.; Dominguez F.; Alonso M. J. and Torres D.** Chitosan nanocapsules for active tumor targeting, 7th World Meeting on Pharmaceutics, Biopharmaceutics and Pharmaceutical Technology, Malta, 2010.

Capitulo 1

Nanocapsules as carries for the transport and targeted delicery os bioactive molecules

Introduction

Nanocapsules, first developed by Couvreur *et al.* [1], offer unique opportunities with the poupose of improving the biological profile of drugs in terms of transport across biological barriers, biodistribution and cellular uptake. They have a vesicular organization whose internal reservoir can be composed of aqueous or oily components, and they are surrounded by a polymeric coating [2, 3]. This reservoir system offers the possibility of great loadings of either lipophilic or hydrophilic drugs, depending on the nature of the liquid core (Figure). Additionally, the core has the role of protecting the drug from the physiological environment. Finally, the liquid nature of nanocapsules and, thus, their elasticity, may facilitate the contact of the nanostructures with the ephithelia and further internalization.

Polymeric Nanocapsules: Production and Characterization

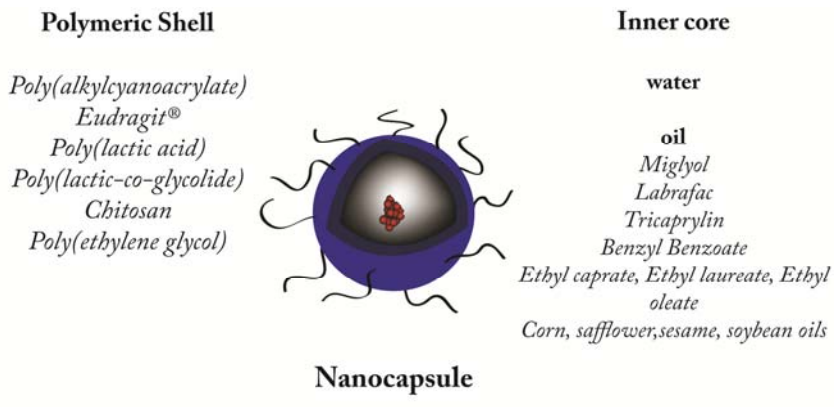

Figure 1: Schematic diagram of nanocapsules containing an aqueous or oily core.

Several methods have been developed to date for the production of nanocapsules and the encapsulation of drugs. These methods are based on different physicochemical principles including (i) interfacial polymerization[1, 4], (ii) interfacial deposition or solvent displacement [5], (iii) phase inversion temperature[6] and (iv) polymer adsorption onto a preformed emulsion [7-9]The choice of the most appropriate materials and methods for the preparation of the nanocapsules is critical. The specific details of the different approaches and formulations will be described in detail in the next section.

A deep characterization of the nanocapsules is essential as there are specific parameters, such as size, morphology and stability, which can significantly affect their biopharmaceutical behavior [10-12].

Most of the techniques employed to characterize the morphology of nanocapsules are based on microscopy, such as scanning electron microscopy (SEM), atomic force microscopy (AFM) or transmission electron microscopy (TEM). These techniques have been widely used to elucidate not only the shape but also the size and wall thickness of nanocapsules structure. These techniques can also be combined with other methods like freeze-fracture, cryogenic techniques or negatively stained preparations in order to obtain deep information on the structural organization of the different components of the nanocapsules [3, 6, 13].

Regarding the size of the nanocapsules, several techniques can give accurate values of diameter and wall thickness. Scattering methods are the most recommended for obtaining accurate values of particle size distributions. The dynamic light scattering technique, also named as photon correlation spectroscopy, is a measurement of the dynamics of the Brownian motion of particles, this being related to their hydrodynamic diameter. This is a suitable method for particles with diameters between a few nanometers and a few microns[14]. Recently, small angle neutron scattering has proved to be a very powerful tool for calculating the size and the wall thickness of the nanocapsules.[15].

The characterization of the surface properties of the nanocapsules can be made through the measurement of zeta potential by laser doppler anemometry[16]. Nuclear Magnetic Resonance (NMR) can also be employed for a deeper characterization of the nanocapsule surface: the hydratation and the physical state of the shell forming polymer can be determined by cross polarization NMR [17], while Pulsed Field Gradient NMR can be used to study the permeability, hydratation and the mobility of the nanocapsule shell[18].
A brief description of nanocapsule drug delivery systems developed to date is presented in Table 1.

Table1: Polymers used as wall materials in nanocapsules for the delivery of different therapeutics, using varied administration routes.

Polymer	***Drug***	***Drug effect***	***Route***	***ref***
PACA NC	Nucleic Acids	Antitumor		19,28,90
(water core)	Salmon calcitonin	Hypocalcemic	Oral	29
PACA NC	Insulin	Hypoglucemic	Oral	52-55
	Phtalocyanines	Imaging	i.t.	80
	siRNA, ODNs	Antitumor	i.t.	90, 19
	Cyclosporin	Immunosuppresor	Ocular	68,66
	Pilocarpine	Antiglaucomatous		
Eudragit	Tacrolimus	Immunosuppresor	Oral	31,56,59
	Cyclosporine	Immunosuppresor		
PLA	Indometacin,	Antiinflamatory	Oral	57
	Diclofenac			
PCL	Spironolactone	Diuretic	Oral	58
	Betaxolol, Carteolol,	Antiglaucomatous	Ocular	63-65
	Metipranolol			
	Indomethacin	Antiinflamatory	Ocular	70,71
	Cyclosporine	Immunosuppresor	Ocular	67,70
Chitosan	Calcitonin	Hypocalcemic	Oral	38
	Calcitonin	Hypocalcemic	Nasal	7
	Docetaxel	Antitumor		9
LNC	Paclitaxel	Antitumor	Oral	60
	Paclitaxel	Antitumor	i.v.	79

Docetaxel	Antitumor	i.v.	[45]

i.t.= intratumoral; i.v.= intravenous

Nanocapsules made of synthetic polymers

Polyacrylate nanocapsules

The first generation of nanocapsules was developed by the group of Couvreur in the late 1970s employing poly(alkylcyanoacrylates) (PACA) as wall material[1, 4]. Since then, PACA nanocapsules have been widely used in drug delivery.

PACA nanocapsules can be prepared following two main methods: interfacial polymerization or interfacial deposition [19, 20] (Figure 2 and 3). In the first case, nanocapsules are formed due to the fast polymerization of the alkylcyanoacrylate monomers at the interface of o/w or w/o emulsions leading to the production of oil or water containing nanocapsules, respectively. Aprotic solvents and a suitable oil/solvent ratio are necessary to achieve an adequate yield of nanocapsules [21, 22]. Oil-containing nanocapsules prepared by this method allow the efficient encapsulation of lipophilic drugs because of their solubility in the oily phase [23]. Water soluble molecules, i.e. insulin or calcitonin, can also be entrapped in the form of a suspension in the oily phase [24, 25] due to the instantaneous formation of the shell around the oily droplets. The mean diameter of the nanocapsules formed by interfacial polymerization is normally in the range 200-350 nm. However, recently, the possibility of reducing the size of the nanocapsules down to 100 nm was reported, thanks to the use of the appropriate combination of surfactants [26].

Nanocapsules consisting of an aqueous core are of special interest for the encapsulation of water-soluble molecules such as peptides [27] and nucleic acids, including antisense oligonucleotides [28]. In these cases, the nanocapsules are formed in an external oily phase and need to be isolated and

resuspended in water prior to their use. Nanocapsules with aqueous core have mean diameters ranging from 50 to 350 nm depending on the type of surfactants used for their preparation[19, 29].

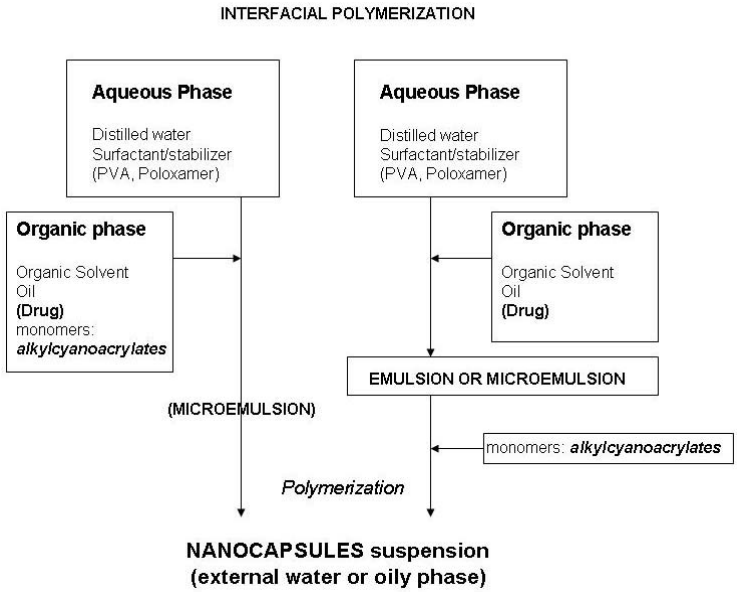

Figure 2: Preparation of nanocapsules by interfacial polymerization

PACA nanocapsules can also be obtained by interfacial deposition of a preformed polymer (Figure .3). This technique was first described by Fessi et al.[5] and is based on the spontaneous emulsification of the oil due to the diffusion of a organic solvent, where the polymer and oil are dissolved, into water. The nanocapsules are formed due to the precipitation of the preformed polymer at the interface of the emulsion[5, 30].The size of the nanocapsules prepared by this method usually ranges from 150 to 300 nm.

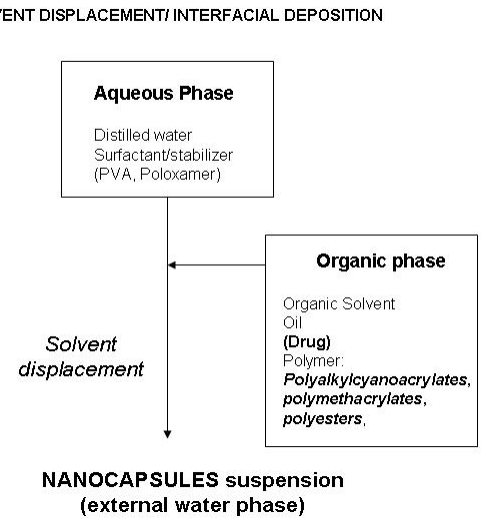

Figure 3: Preparation of nanocapsules by interfacial polymer deposition following solvent displacement

Other interesting polyacrylates, also used to prepare nanocapsules, are polymethacrylates (Eudragit®). These nanocapsules have been obtained by interfacial deposition of the preformed Eudragit®. The interest of these systems relies in their pH sensitive character that can be employed to improve the stability and bioavailability of therapeutic drugs after oral administration [31].

Polyester nanocapsules

Polyesters such as poly-ε-caprolactone (PCL), poly lactic acid (PLA) and its copolymer poly(lactic-co-glycolic) acid (PLGA) have also been used for the preparation of nanocapsules. To date, all polyester nanocapsules have been prepared by the interfacial deposition of a preformed polymer following solvent displacement [5, 13, 14]. This effective and reproducible method allows the production of polyester nanocapsules with size ranges between 100-350 nm and wall thickness of 1 to 20 nm[15, 32, 33].

The surface properties of polyester nanocapsules can be modified in order to reach the therapeutical purpose. For example, chitosan, a bioadhesive polymer, can be attached to the surface of polyester nanocapsules by incubation [16]. In addition, it is possible to obtain PEG-coated polyester nanocapsules by using the amphiphilic PEGylated copolymer, i.e. PEG-PCL, PEG-PLA or PEG-PLGA[34-37]. The polymer deposition technique leads to the orientation of the hydrophobic segment towards the oily phase whereas the PEG portion protrudes towards the external aqueous medium.

Nanocapsules made of natural polymers

Naturally occurring polymers such as polysaccharides have also been used for the formation of nanocapsules. Among these, chitosan has received increasing attention for a number of years as a biomaterial for transmucosal drug delivery. Our group described for the first time the preparation of chitosan nanocapsules according to an interfacial deposition method slightly modified when compared to that used for PACA or polyester nanocapsules described above (Figure). In this case, chitosan is incorporated into the external aqueous phase and its deposition at the oil/water interphase occurs because of its electrostatic interaction with the negatively charged phosphatidylcholine, which is used as a stabilizer of the nanodroplets. [7, 8, 34] We have also proposed an alternative method which involves first, the formation of a nanoemulsion and, the incubation of the nanoemulsion in an aqueous solution of chitosan [7-9]. This method has also been employed for the formation of PEG-chitosan nanocapsules[38]. In this case, the PEG molecule gets oriented towards the external phase due to the cationic nature of chitosan and its natural tendency to associate to the negatively charged nanodroplets.

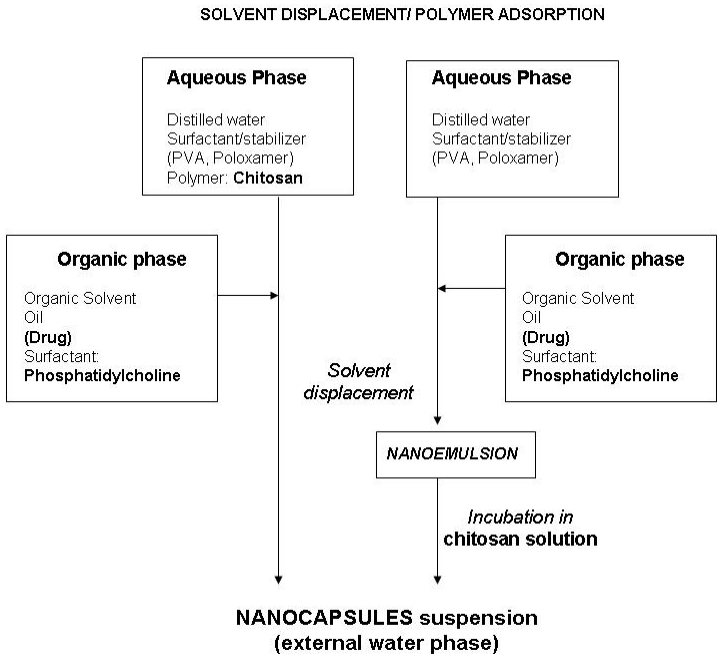

Figure 4: Preparation of nanocapsules by polymer adsorption following solvent displacement

The incubation approach has been recently proposed for the formation of nanocapsules with a double polysaccharic wall consisting of chitosan and lambda-carrageenan [39]. In this case, the nanoemulsion was formed by high pressure homogenization using a modified starch as negatively charged stabilizer; then, it was incubated first in a chitosan solution and afterwards in a lambda-carrageenan solution.

Lipid nanocapsules

A new generation of nanocapsules, named lipid nanocapsules, were first prepared by the group of Benoit[6, 40-42]. These systems consists of an oil core surrounded by a thick polymeric shell, made of PEG-hydroxystearate and phosphatidylcholine. These nanocapsules can be prepared via a novedous, solvent-free, phase inversion process (Figure). In this process, all the components of the system are mixed together with the aqueous phase and, then, exposed to several cycles of heating and cooling (usually between temperatures around 65 and 85ºC). The size and polydispersity of the nanocapsules decrease as a function of the number and temperature cycles and a thick interfacial layer is created with this cycling process, since the surfactant is forced to overconcentrate at the interface of the oily droplets.[43] Finally, the process is quenched at a temperature below the phase inversion temperature (o/w emulsion), followed by addition of cold water. This fast cooling-dilution process led to the formation of lipid nanocapsules with particle sizes between 20 and 100 nm[42]. These nanocapsules showed a rigid shell surrounding the oily core and were physically stable for at least 18 months without fusion of the dispersed oily phase[41]. These nanocapsules are very versatile as they can be produced using different types of oils and lipids, thus exhibiting high drug encapsulation efficiency values [44, 45].

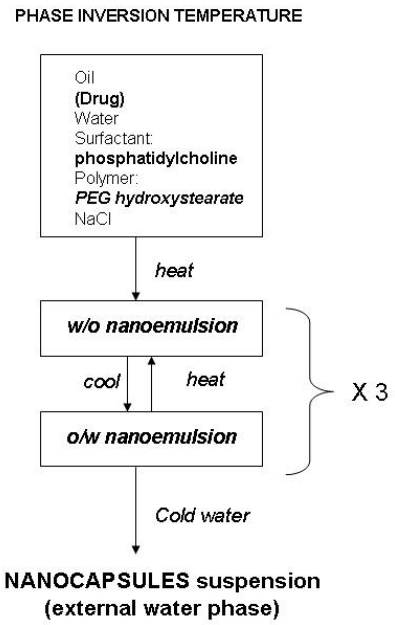

Figure 5: Preparation of nanocapsules by phase inversion temperature.

Therapeutical applications of nanocapsules

The use of nanocapsules has been reported as a promising strategy for improving the oral bioavailability of therapeutic molecules [46]. It has been shown that due to their colloidal size, nanocapsules are able to interact favorably with the mucosal barrier and, simultaneously, protect the encapsulated drug from the harsh environment of the gastrointestinal tract [46, 47]. For these reasons, nanocapsules have been extensively studied as vehicles for improving the oral bioavailability of poorly absorbed drugs such as peptides or some lipophilic compounds, as well as for obtaining drug controlled release[48].

Nanocapsules for oral peptide delivery

The oral administration of peptides and proteins continue to be a challenge because of their susceptibility to the enzymatic degradation and their low permeability across the intestinal ephitelium. The encapsulation of these macromolecules into polymeric nanocapsules is nowadays considered a promising approach towards this ambitious goal[49,50]. An example is represented by the nanocapsules made of mucoadhesive polymers, such as chitosan, as described for transmucosal absorption of calcitonin [51]. Chitosan nanocapsules loaded with calcitonin were able to enhance and prolong the systemic absorption of the drug, thus leading to an improvement of the hypocalcemic effect (Figure). The *in vitro* studies performed in the Caco-2 cells cocultured with the a model of mucus-secreting cells (HT29-M6) suggested that chitosan nanocapsules do not cross the monolayer, but rather they remain at the apical side of the cells [51].

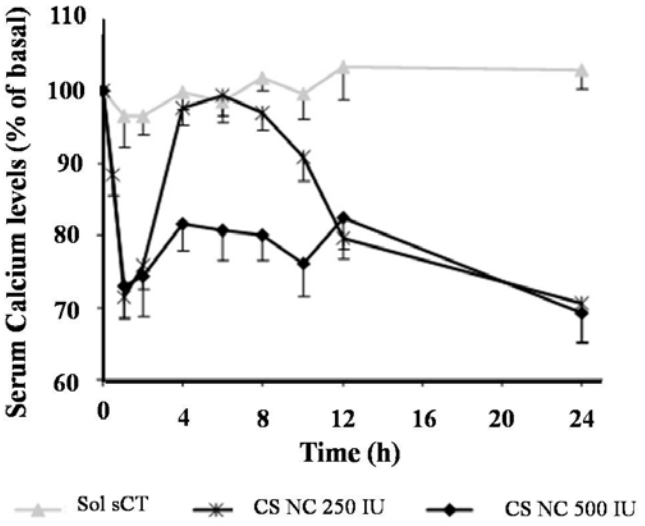

Figure 6: Serum calcium levels in rats after oral administration of salmon calcitonin in an aqueous solution (sCT Sol) or encapsulated in chitosan nanocapsules (CS NC) at two different doses (250 and 500 IU/Kg), (mean ± SE; n = 6).[51] Reproduced by permission of Springer.

Promising results have also been obtained with poly (isobutylcyanoacrylate) (PBCA) nanocapsules containing calcitonin. The

results of the *in vivo* studies performed on rats indicated that these nanocapsules allowed a great decrease of calcium levels to occur[29].

On the other hand, Damgé et al. investigated the potential of PACA nanocapsules for the oral administration of insulin[52,53]. Following intragastric administration of insulin loaded nanocapsules (12.5, 25 and 50 IU of insulin per kg) to diabetic rats (diabetes induced by the administration of 65 mg/kg of spreptozocin), the authors observed that the nanocapsules remained intact in simulated gastric fluid, thus ensuring a good protection of the peptide. Moreover, the new formulation produced a significant reduction of the glycemia (50-60%), a response that was maintained for up to 20 days. The authors attributed this long-term effect to the adsorption of the nanocapsules across the intestinal epithelium and the subsequent release of the encapsulated peptide[54].

More recently, other authors studied the bioavailability of orally administered insulin loaded PBCA nanocapsules (50 IU of insulin per kg) in diabetic rats (diabetes induced by the administration of 65 mg/kg of spreptozocin [55]. These results showed that the oral administration of nanocapsules allows the delivery of noticeable levels of insulin into the bloodstream in diabetic rats, however decrease in glycemia could not be observed. The low reproducibility of the results in animal models hampered the comprehensive analysis of the results from the different studies.

Nanocapsules were also investigated for the delivery of hydrophobic peptides such as cyclosporine. The oral absorption of this peptide was tested using nanocapsules made of an oily core consisting of Cremophor® or Maisine® and surrounded by Eudragit RL® or RS®. Unfortunately, the absolute bioavailability achieved with the nanocapsules ranged from 4 to 7.5 %, a result that is far below that observed with the marketed Neoral® premicroemulsion (about 22%) [56]. The authors related the lower cyclosporine bioavailability to the size of the nanocapsules, more than to the constituents of the systems, however, the low bioadhesion of the polymers used to the

intestinal epithelium could also play an important role in the absorption of the drug.

Nanocapsules for oral delivery of lipophilic low molecular weight drugs

Nanocapsules have also been used for oral delivery of low molecular weight compounds. Anti-inflammatory agents are known to exhibit important gastrointestinal side effects such as irritation and mucosal damage. Moreover, they are characterized by very low water solubility, a property which makes these good candidates for the encapsulation within oily core nanocapsules [57]. Nanocapsules made of PLA were investigated for their potential of improving the gastrointestinal tolerance to indometacin and diclofenac[57]. The encapsulation of these drugs into PLA nanocapsules led to a great reduction of the irritation of the gastrointestinal mucosa.

The diuretic drug, spironolactone, used in premature infants to reduce lung congestion, has also been efficiently encapsulated in PCL nanocapsules[58]. Nowadays there is no commercially available oral liquid preparation of spironolactone due to its poor water solubility and its dissolution rate. Its incorporation into nanocapsules solved these problems, although further pharmacokinetics studies are needed in order to fully demonstrate their *in vivo* effectiveness.

The use of nanocapsules has also been proposed for the oral administration of drugs which suffer the efflux transport, mediated by P-glycoprotein (P-gp), across the apical membrane of the intestinal ephitelium. This transport is known to drastically reduce the absorption of antibiotics, antivirals, antitumorals and other drugs. Recently, it was shown that the encapsulation of tacrolimus, an immunosuppresor agent substrate of P-gp, into Eudragit® nanocapsules, protect the drug from the efflux transports and increase the concentration of the drug within the cell and therefore its bioavailability[59]. This evidence was observed in two animal models, rats and

minipigs. In addition, in these studies it was also observed that the small lipophilic oil cores were able to enter the enterocytes and reach the lamina propria behind the P-gp. Similar results were obtained with the encapsulation of the antitumor drug, paclitaxel, into lipid nanocapsules. Due to the effect of P-gp and its low water solubility, paclitaxel is currently admistered intravenously. Following *in vivo* administration of lipidic nanocapsules containing placlitaxel to rats, an increase in its absorption when compared to that of the control was observed (Taxol®, paclitaxel dissolved in Cremophor® and ethanol). The positive role of the nanocapsules was attributed to two mechanisms: first, as could be expected, the presence of lipids in the formulation increased the intestinal lymphatic transport and, second, the entrapment of the molecule in the nanocapsules could reduce the P-gp-mediated transport of the drug. Nevertheless, these promising results should be taken into account cautiously due to the high interindividual variability and need to be confirmed by further experimentation[60].

Overall, nanocapsules can be considered as potential vehicles for promoting the oral absorption of peptides and lipophilic low molecular weight drugs. Particularly noticeable is their capacity to overcome multidrug resistance (MDR) mechanisms, such as the P-gp efflux transport. Despite this evidence, the validation of the efficacy of these nanosystems in large-scale animals, in fed and fasted conditions will have to be proved in order to make sure of their potential for clinical use.

Nanocapsules as nasal drug carriers

The intranasal delivery is an attractive non-invasive route which offers several unique advantages for peptide drugs, such as the ease of administration, the looseness of the epithelium and the avoidance of the hepatic first-pass metabolism. Our group has explored the potential of chitosan nanocapsules for increasing the nasal absorption of the peptide salmon calcitonin[7]. The results observed in the rat model indicated that, as expected, the response of this peptide could be significantly enhanced and prolonged following its association to the nanocapsules (Figure). These results highlight the critical role of the polymer in enhancing the transport of the associated peptide and consequently the potential of chitosan nanocapsules for nasal peptide delivery.

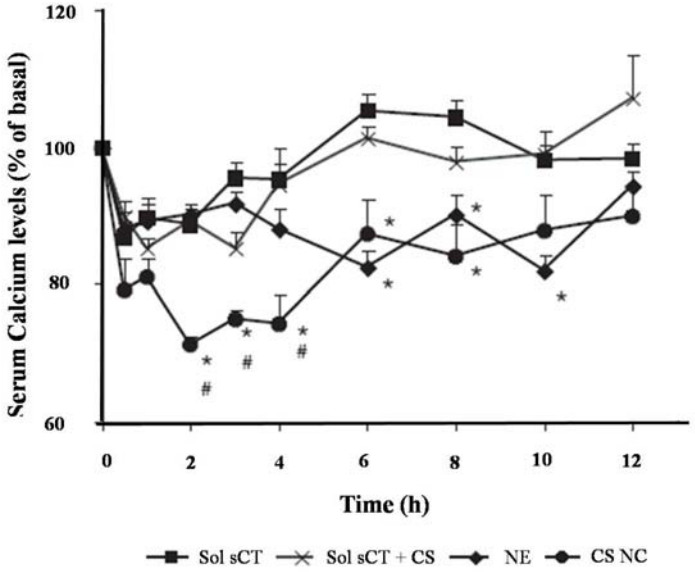

Figure 7: Serum calcium levels in rats after nasal administration of salmon calcitonin (sCT, dose: 15 IU/kg) in aqueous solution (with or without CS) or encapsulated in the control nanoemulsion (NE) or in chitosan nanocapsules (CS NC); (mean ± SE; n = 6). *Significantly different from salmon calcitonin solutions ($p < 0.05$). #Significantly different from nanoemulsion ($p < 0.05$).[7] Reproduced by permission of Ed. Sante.

Nanocapsules as ocular drug carriers

The vast majority of intraocular diseases are treated by the instillation of aqueous solution eye-drops in the *cul-de-sac*. In order to penetrate into the eye, drugs must diffuse through different hurdles, such as the cornea, that acts as a barrier for hydrophilic and lipophilic drugs, limiting dramatically the intra-ocular penetration[61]. Another impediment is represented by the lachrymal fluid which is continuously spread over the surface of the cornea and is quickly drained, together with the instilled drug, into the nasolachrymal ducts [61]. In conclusion, less than 5% of the instilled drug is able to enter into the eye [62], therefore several instillations of the drug solution are required to obtain a sustained therapeutic effect. Importantly, drugs which are drained into the nasolachrymal ducts can be absorbed directly into the systemic circulation, thereby it could be possible to observe secondary effects [63-65].

The use of nanocapsules has been proposed as a strategy to increase the penetration of lipophilic drugs into the eye by prolonging their precorneal residence time. The strategy has been explored for a number of β-blocking antiglaucomatous agents such as betaxolol, carteolol and metipranolol. In the case of betaxolol and carteolol it was found that their association to PCL nanocapsules led to a significant improvement of their pharmacological effect (intraocular pressure) [64, 65]. Additionally, in all cases, the association of the drug to the nanocapsules resulted in a significant reduction of their side effects [63-65]. As an approach to further improving the efficacy of the nanocapsules, Desai *et al.* [66] associated the antiglaucomatous drug pilocarpine to PCL nanocapsules that were dispersed in a Pluronic® F127 gel. This formulation was more effective than the nanocapsules without the gel or than the pilocarpine incorporated into the gel. The authors explained the positive effect of Pluronic® F127 in terms of the ability of the gel to increase the contact time of the nanocapsules within the ocular mucosa.

Another interesting study was conducted by Calvo *et al.* [67] who demonstrated an improvement in ocular absorption of cyclosporine A by encapsulation into PCL nanocapsules. The corneal levels of this drug were 5-fold higher than the drug formulated in oily solution, and significant differences in the concentration of cyclosporine A were even found for up three days. Le Bourlais *et al*. also studied formulations with cyclosporine A showing that the absorption of this drug was higher when the drug was included in PACA nanocapsules, poly(acrylic) gels, or a combination of both compared with the drug being dispersed in oil [68]. Importantly, nanocapsules dispersed in gel did not show any toxic effect differing from the other carriers.

In an attempt to understand the mechanism of action of nanocapsules following topical ocular administration, our research group has conducted several studies. In an initial study we could demonstrate by confocal microscopy that PCL nanocapsules penetrate selectively into the corneal epithelium by endocityc process, without cause a disruption in the cells membrane [69]. In addition, we identified that the size of the particles, but not the inner structure or the composition, was a critical factor for their effectiveness as drug carriers across the epithelial barrier. More specifically, following topical instillation of different carriers containing indomethacin: PCL nanoparticles, PCL nanocapsules, and a submicron emulsion (Figure). We found that all nanostructured formulations behaved significantly better than the commercial eye drops (Indocollyre®)[70] in terms of increasing the corneal permeation of the associated drug, while PCL microparticles failed to produce this benefit in a different study[71].

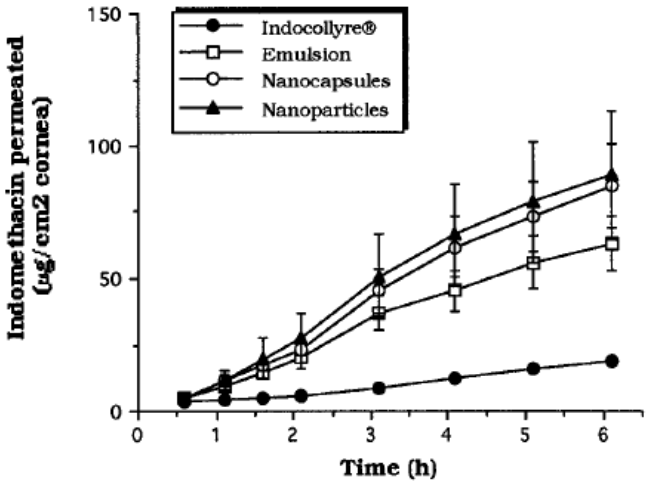

Figure 8: Permeation of indomethacin through isolated rabbit cornea: (▲) PCL nanoparticles, (❍) PCL nanocapsules, (□) submicron emulsion, and (●) commercial eye drops (Indocollyre®).[70] Reproduced by permission of Wiley InterScience.

In addition to the influence of the particle size, we also studied the importance of the surface charge and composition of the nanocapsules in their ability to work as drug carriers. More specifically, we compared the behavior of indomethacin-loaded PCL nanocapsules with that of chitosan-coated and poly-L-lysine-coated PCL nanocapsules following topical instillation to rabbits. The results indicated that the chitosan-coated nanocapsules provide better corneal drug penetration than poly-L-lysine or uncoated nanocapsules[16]. Given the fact that chitosan and poly-L-lysine are both polycationic polymer, the positive behavior of the chitosan-coated nanocapsules could not be simply attributed to the positive surface charge but to the specific properties of chitosan, i.e. mucoadhesive and permeability-enhancing properties of this polymer [72].

In an attempt to explore further the effect of the surface polymer composition in the interaction of the nanostructures with the ocular barriers, we comparatively investigated chitosan- and PEG-coated PCL nanocapsules[34]. These studies were conducted using nanocapsules loaded with a fluorescent dye and their ocular distribution was observed by confocal

microscopy. Two main conclusions were extracted from this study: (i) both formulations were internalized by the corneal epithelium; (ii) the chitosan formulations were favourably retained in the superficial layers while the PEG formulations were able to reach deep layers of the corneal epithelium.

All the above information indicates that nanocapsules are interesting tools for improving the drug ocular bioavailability and reducing the systemic side effects of drugs administered topically onto the eye. Additionally, these results underline the importance of the particle size and surface composition on the therapeutic efficacy of the nanocapsules.

Nanocapsules in cancer therapy

The main limitations in cancer therapies are related to their lack of specificity and subsequent toxicity. Moreover, in many cancers, there are specific biological barriers, such as the MDR mechanisms, which limit the efficacy of the treatments [73, 74]. Finally, from the formulation point of view, most of the anticancer drugs suffer from poor water solubility and instability. In this context, nanocapsule technology emerges as an important approach for the formulation of anticancer drugs, as it offers the possibility of incorporating hydrophobic drugs and protecting them in the biological fluids[3]. The size and large surface-to-volume ratios [75] of the nanocapsules facilitate their accumulation in the tumor by the well-known enhanced permeability and retention effect (EPR) [76, 77] and their capacity to be internalized by the tumor cells. Moreover, it has been shown that lipid nanocapsules behave as a MDR-inhibiting system.[78, 79].

There are a number of reports showing the advantages of nanocapsules for specific anticancer drugs. For example, Lenaerts *et al.* [80] encapsulated phtalocyanines, important agents in photodynamic tumor therapy, in poloxamer surface modified-PACA nanocapsules. They found that the presence of some types of poloxamer significantly decreased the

uptake of nanocapsules by organs rich in phagocytic cells and increased the accumulation of phtalocyanines in primary tumors. The concentration of photosensitizers in the tumor was maximal 12 h post-administration, these carriers allowing a 200-fold higher accumulation in the tumor.

In different reports it has been shown that lipid nanocapsules are adequate vehicles for the delivery of taxanes. More specifically, the encapsulation of paclitaxel into lipid nanocapsules led to a significant concentration increase in the tumoral tissue, and significantly reduced the tumor mass compared to the commercial product (Taxol ®) as we can see in Figure [79]. Additionally, *in vivo* studies in rats have shown that lipid nanocapsules enhanced around 3-fold the oral bioavailability of the anticancer drug, in comparison with the commercial product [60, 81]. Docetaxel is another taxane that has been encapsulated into lipid nanocapsules; these nanocapsules showed an enhanced drug deposition in mice tumors which was characterized by a 5-fold increase in the area under the curve of the tumor (AUC_{tumor}) when compared to the control formulation (Taxotere®)[45].

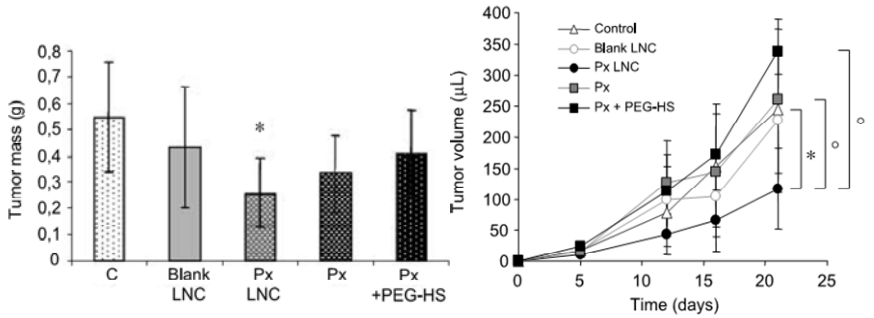

Figure 9: *In vivo* effects of paclitaxel-loaded lipid nanocapsules (LNC) treatment on the growth of F98 glioma cells implanted. (C, control; Px-LNC, paclitaxel-loaded LNC; Px, Taxol only; Px + PEG-HS, Taxol with Solutol HS15 solution) *, $P<0.05$ (Dunnett´s test). º, $P<0.05$ (Fisher´s test). Statistical analysis by pairs show significant diferences on day 21 between formulations.[79] Reproduced by permission of American Association for Cancer Research, Inc.

Our group has also proposed an alternative carrier for the intracellular delivery of docetaxel consisting of oligomer chitosan

nanocapsules [9]. The results have shown that chitosan nanocapsules are able to facilitate the rapid internalization of the drug into the cancer cells, leading to a significant increase of the antiproliferative effect of the drug.

Overall, the results presented here indicate that nanocapsules represent an alternative for the intracellular delivery of hydrophobic anticancer drugs. This potential is related to their capacity to be internalized by the cells and inhibit the MDR mechanisms, thus maximizing the antitumoral drug effects.

Nanocapsules as carriers for gene therapy

The discovery of antisense oligodeoxynucleotides (ODNs) and more recently siRNA, has opened wide perspectives in therapeutics for the treatment of cancer, infectious and inflammatory diseases, or to block cell proliferation and diseases caused thereby. However, the clinical use of these molecules is limited by their poor stability in biological media and their important hydrophilic character, which strongly limit tissular, cellular and subcellular internalization[82, 83]. Besides, another disadvantage of the ODNs and siRNA is the toxicity related with the cationic charge, and the poor activity of these naked molecules.

A few research groups have explored the potential of nanotechnology for the development of suitable carriers for gene delivery. Among the different options, nanocapsule technology has been shown to offer some specific advantages. Due to its hydrophilic character, siRNA and ODNs molecules are usually adsorbed onto the polymeric surface of nanoparticles or polymeric micelles[84, 85], however, water containing nanocapsules can eficiently encapsulate these molecules within its aqueous core. An interesting method for the encapsulation of ODNs into PACA nanocapsules was that described by Lambert *et al.* [28]. These aqueous core-containing nanocapsules improved the ODNs stability against enzymatic degradation and considerably

increased their half-life in serum in comparison with the naked molecules or those adsorbed onto nanospheres[86]. Moreover, the ODNs cell uptake was significantly improved when the molecule was included in the nanocapsules[87].

The encapsulation into the aqueous core of PBCA nanocapsules of an antisense-siRNA (siRNA-AS) against a fusion oncogen (*Fli1*) overexpressed in Ewing sarcoma, resulted in an important inhibition of tumor growth tested in a murine model of Ewing sarcoma-related tumor (Figure)[88, 89].

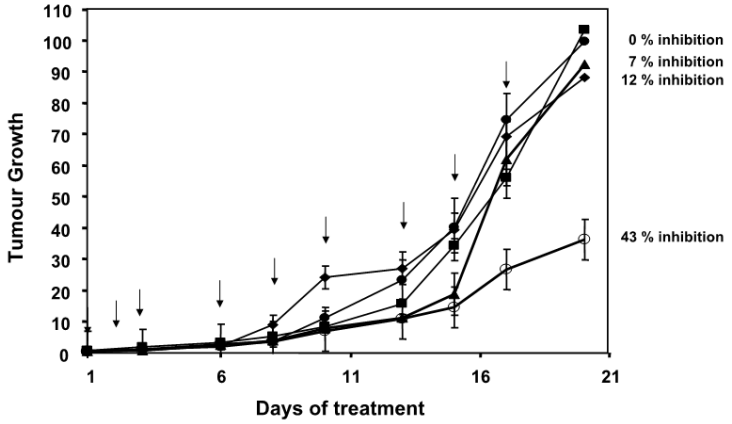

Figure 10: Inhibition of Erwing sarcoma fusion oncogen (EWSFli1)-expressing tumor growth in nude mice by: ○ siRNA-antisense (siRNA-AS) loaded NCs; ▲siRNA-control loaded NCs; ■, siRNA-AS naked; ♦, siRNA-control naked; ●, saline.[89] Reproduced by permission of Springer.

Hillaireau *et al.*[19] described the incorporation of ODNs to PBCA nanocapsules. They observed that the association could be significantly improved when ODN is associated first to a cationic polymer, such as chitosan or poly(ethylenimine), and afterwards this complex being encapsulated into a water containing nanocapsule. In a different work, Bouclier *et al.*[90] reported the encapsulation of a specific siRNA (target to estrogen receptor alfa [ERα-siRNA]) in three different systems: PBCA nanocapsules, PEG-PLGA nanoparticles and PEG-PCL-malic acid nanoparticles. The *in vitro* studies indicated that PBCA nanocapsules showed

a high efficiency in MCF-7 cancer cells, whereas the other systems showed no antiproliferative effect in the same cancer cell lines. In a preliminary *in vivo* study, these nanocapsules showed a slight decrease in tumor growth in comparison to scramble-siRNA loaded nanocapsules or the siRNA naked[90], showing the benefits of the nanocapsules over other nanosystems for the encapsulation of siRNA.

Conclusions

The liquid nature of nanocapsules and, thus, their fluidity and elasticity make them ideal nanovehicles able to facilitate the contact with the epithelia and target cells, as well as to enter intracellularly. They have unique properties as their simplicity and their capacity of obtaining great loadings of either lipophilic or hydrophilic drugs. Moreover, nanocapsules have shown to be capable of inhibiting multidrug resistance cellular mechanisms, specially important in cancer therapy. In conclusion, polymeric or lipid nanocapsules are a promising tool for transmucosal drug delivery as well as for cancer therapeutics, particularly for drugs which are water-insoluble and that, until recently, have required solvents to be formulated. Concerning gene therapy, nanocapsules emerge as an interesting approach, due to the high affinity of nucleic acids for their water core and to the possibility of adapting these systems to the requirements of this novel therapy.

In addition, the use of reservoir structures composed by inorganic nanoparticles (iron, silica or gold nanoparticles, quantum dots, carbon nanotubes, etc.) surronded by a polymer and, optionally, a targeting ligand, represents a promising and powerful tool to enhance the biocompatibility and the biodistribution of these nanostructures widely used in the diagnostics and threatment of several diseases. This composite nanocapsules will be discussed widely in following chapters.

Abbreviations

AFM – Atomic force microscopy

EPR – Enhanced permeability and retention effect

LNC – Lipid nanocapsules

MDR – Multidrug resistance

NCs – Nanocapsules

NMR – Nuclear magnetic resonance

ODN – Oligodeoxynucleotide

PACA – Poly(alkylcyanoacrylate)

PBCA – Poly(isobutylcyanoacrylate)

PCL – Poly-ε-caprolactone

PEG – Polyethylene glycol

PLA – Poly lactic acid

PLGA – Poly(lactic-co-glycolic) acid

SEM – Scanning electron microscopy

TEM – Transmission electron microscopy

siRNA – Small interfering RNA

siRNA – AS – siRNA antisense.

Bibliography

1. Couvreur, P., Tulkens, P., and Roland, M. (1977).Nanocapsules: a new type of lysosomotropic carrier. *FEBS Lett.*84.pp 323-326.
2. Legrand, P., Barratt, G., Mosqueira, V., Fessi, H., and Devissaguet, J.P. (1999).Polymeric nanocapsules as drug delivery systems: A review. *STP Pharm. Sci.*9.pp 411-418.
3. Couvreur, P., Barratt, G., Fattal, E., Legrand, P., and Vauthier, C. (2002).Nanocapsule technology: A review. *Crit Rev Ther Drug Carrier Syst.*19.pp 99-134.

4. Couvreur, P., Kante, B., and Roland, M. (1979).Polycyanoacrylate nanocapsules as potential lysosomotropic carriers: Preparation, morphological and sorptive properties. *J Pharm Pharmacol.*31.pp 331-332.
5. Fessi, H., Puisieux, F., Devissaguet, J.P., Ammoury, N., and Benita, S. (1989).Nanocapsule formation by interfacial polymer deposition following solvent deplacement. *Int J Pharm.*55.pp 25-28.
6. Heurtault, B., Saulnier, P., Pech, B., Proust, J.E., and Benoit, J.P. (2002).A novel phase inversion-based process for the preparation of lipid nanocarriers. *Pharm Res.*19.pp 875-880.
7. Prego, C., Torres, D., and Alonso, M.J. (2006).Chitosan nanocapsules: A new carrier for nasal peptide delivery. *JDDST.*16.pp 331-337.
8. Prego, C., Torres, D., and Alonso, M.J. (2006).Chitosan nanocapsules as carriers for oral peptide delivery: Effect of chitosan molecular weight and type of salt on the in vitro behaviour and in vivo effectiveness. *J Nanosci Nanotechnol.*6.pp 2921-2928.
9. Lozano, M.V., Torrecilla, D., Torres, D., Vidal, A., Dominguez, F., and Alonso, M.J. (2008).Highly efficient system to deliver taxanes into tumor cells: Docetaxel-loaded chitosan oligomer colloidal carriers. *Biomacromolecules.*9.pp 2186-2193.
10. Desai, M.P., Labhasetwar, V., Amidon, G.L., and Levy, R.J. (1996).Gastrointestinal Uptake of Biodegradable Microparticles: Effect of Particle Size. *Pharm Res.*13.pp 1838-1845.
11. Vila, A., Gill, H., McCallion, O., and Alonso, M.J. (2004).Transport of PLA-PEG particles across the nasal mucosa: effect of particle size and PEG coating density. *J Control Release.*98.pp 231-244.
12. Yin Win, K. and Feng, S. (2005).Effects of particle size and surface coating on cellular uptake of polymeric nanoparticles for oral delivery of anticancer drugs. *Biomaterials.*26.pp 2713-2722.

13. Quintanar-Guerrero, D., Allemann, E., Doelker, E., and Fessi, H. (1998).Preparation and characterization of nanocapsnles from preformed polymers by a new process based on emulsification-diffusion technique. *Pharm Res.*15.pp 1056-1062.
14. Moinard-Checot, D., Chevalier, Y., Briancon, S., Beney, L., and Fessi, H. (2008).Mechanism of nanocapsules formation by the emulsion-diffusion process. *J Colloid Interface Sci.*317.pp 458-468.
15. Rube, A., Hause, G., Mader, K., and Kohlbrecher, J. (2005).Core-shell structure of Miglyol/poly(D,L-lactide)/Poloxamer nanocapsules studied by small-angle neutron scattering. *J Control Release.*107.pp 244-252.
16. Calvo, P., Vila-Jato, J.L., and Alonso, M.J. (1997).Evaluation of cationic polymer-coated nanocapsules as ocular drug carriers. *Int J Pharm.*153.pp 41-50.
17. Guinebretiere, S., Briancon, S., Lieto, J., Mayer, C., and Fessi, H. (2002).Study of the emulsion-diffusion of solvent: Preparation and characterization of nanocapsules. *Drug Dev Res.*57.pp 18-33.
18. Wohlgemuth, M. and Mayer, C. (2003).Pulsed field gradient NMR on polybutylcyanoacrylate nanocapsules. *J Colloid Interface Sci.*260.pp 324-331.
19. Hillaireau, H., Le Doan, T., Chacun, H., Janin, J., and Couvreur, P. (2007).Encapsulation of mono- and oligo-nucleotides into aqueous-core nanocapsules in presence of various water-soluble polymers. *Int J Pharm.*331.pp 148-152.
20. Vauthier, C. and Bouchemal, K. (2008).Methods for the Preparation and Manufacture of Polymeric Nanoparticles. *Pharm Res.*1-34.
21. Gallardo, M., Couarraze, G., Denizot, B., Treupel, L., Couvreur, P., and Puisieux, F. (1993).Study of the mechanisms of formation of nanoparticles and nanocapsules of polyisobutyl-2-cyanoacrylate. *Int J Pharm.*100.pp 55-64.

22. Puglisi, G., Fresta, H.T.M., Giammona, G., and Ventura, C.A. (1995).Influence of the preparation conditions on poly(ethylcyanoacrylate) nanocapsule formation. *Int J Pharm.*125.pp 283-287.
23. Fresta, M., Cavallaro, G., Giammona, G., Wehrli, E., and Puglisi, G. (1996).Preparation and characterization of polyethyl-2-cyanoacrylate nanocapsules containing antiepileptic drugs. *Biomaterials.*17.pp 751-758.
24. Aboubakar, M., Puisieux, F., Couvreur, P., Deyme, M., and Vauthier, C. (1999).Study of the mechanism of insulin encapsulation in poly(isobutylcyanoacrylate) nanocapsules obtained by interfacial polymerization. *J Biomed Mater Res.*47.pp 568-576.
25. Lowe, P.J. and Temple, C.S. (1994).Calcitonin and insulin in isobutylcyanoacrylate nanocapsules: Protection against proteases and effect on intestinal absorption in rats. *J Pharm Pharmacol.*46.pp 547-552.
26. Vauthier, C., Labarre, D., and Ponchel, G. (2007).Design aspects of poly(alkylcyanoacrylate) nanoparticles for drug delivery. *J Drug Target.*15.pp 641-663.
27. Watnasirichaikul, S., Davies, N.M., Rades, T., and Tucker, I.G. (2000).Preparation of biodegradable insulin nanocapsules from biocompatible microemulsions. *Pharm Res.*17.pp 684-689.
28. Lambert, G., Fattal, E., Pinto-Alphandary, H., Gulik, A., and Couvreur, P. (2000).Polyisobutylcyanoacrylate nanocapsules containing an aqueous core as a novel colloidal carrier for the delivery of oligonucleotides. *Pharm Res.*17.pp 707-714.
29. Vranckx, H., Demoustier, M., and Deleers, M. (1996).A new nanocapsule formulation with hydrophilic core: Application to the oral administration of salmon calcitonin in rats. *Eur J Pharm Biopharm.*42.pp 345-347.

30. Al Khouri Fallouh, N., Roblot-Treupel, L., and Fessi, H. (1986).Development of a new process for the manufacture of polyisobutylcyanoacrylate nanocapsules. *Int J Pharm.*28.pp 125-132.
31. Nassar, T., Rom, A., Nyska, A., and Benita, S. (2008).A novel nanocapsule delivery system to overcome intestinal degradation and drug transport limited absorption of P-glycoprotein substrate drugs. *Pharm Res.*25.pp 2019-2029.
32. Guinebretiere, S., Briançon, S., Fessi, H., Teodorescu, V.S., and Blanchin, M.G. (2002).Nanocapsules of biodegradable polymers: Preparation and characterization by direct high resolution electron microscopy. *Mater Sci Eng C.*21.pp 137-142.
33. Cauchetier, E., Deniau, M., Fessi, H., Astier, A., and Paul, M. (2003).Atovaquone-loaded nanocapsules: Influence of the nature of the polymer on their in vitro characteristics. *Int J Pharm.*250.pp 273-281.
34. De Campos, A.M., Sanchez, A., Gref, R., Calvo, P., and Alonso, M.J. (2003).The effect of a PEG versus a chitosan coating on the interaction of drug colloidal carriers with the ocular mucosa. *Eur J Pharm Sci.*20.pp 73-81.
35. Mosqueira, V.C.F., Legrand, P., Gulik, A., Bourdon, O., Gref, R., Labarre, D., and Barratt, G. (2001).Relationship between complement activation, cellular uptake and surface physicochemical aspects of novel PEG-modified nanocapsules. *Biomaterials.*22.pp 2967-2979.
36. Mosqueira, V.C.F., Legrand, P., Morgat, J.L., Vert, M., Mysiakine, E., Gref, R., Devissaguet, J.P., and Barratt, G. (2001).Biodistribution of long-circulating PEG-grafted nanocapsules in mice: Effects of PEG chain length and density. *Pharm Res.*18.pp 1411-1419.
37. Bouclier, C.l., Moine, L., Hillaireau, H., Marsaud, V.r., Connault, E., Opolon, P., Couvreur, P., Fattal, E., and Renoir, J.-M. (2008).Physicochemical Characteristics and Preliminary in Vivo

Biological Evaluation of Nanocapsules Loaded with siRNA Targeting Estrogen Receptor Alpha. *Biomacromolecules.*9.pp 2881-2890.

38. Prego, C., Torres, D., Fernandez-Megia, E., Novoa-Carballal, R., Quinoa, E., and Alonso, M.J. (2006).Chitosan-PEG nanocapsules as new carriers for oral peptide delivery: Effect of chitosan pegylation degree. *J Control Release.*111.pp 299-308.
39. Preetz, C., Rube, A., Reiche, I., Hause, G., and Mader, K. (2008).Preparation and characterization of biocompatible oil-loaded polyelectrolyte nanocapsules. *Nanomedicine.*4.pp 106-114.
40. Heurtault, B., Saulnier, P., Pech, B., Benoit,t, J.P., and Proust, J.E. (2003).Interfacial stability of lipid nanocapsules. *Colloids Surf B Biointerfaces.*30.pp 225-235.
41. Heurtault, B., Saulnier, P., Pech, B., Proust, J.E., and Benoit, J.P. (2003).Physico-chemical stability of colloidal lipid particles. *Biomaterials.*24.pp 4283-4300.
42. Heurtault, B., Saulnier, P., Pech, B., Venier-Julienne, M.C., Proust, J.E., Phan-Tan-Luu, R., and Benoit, J.P. (2003).The influence of lipid nanocapsule composition on their size distribution. *Eur J Pharm Sci.*18.pp 55-61.
43. Anton, N., Gayet, P., Benoit, J.P., and Saulnier, P. (2007).Nano-emulsions and nanocapsules by the PIT method: An investigation on the role of the temperature cycling on the emulsion phase inversion. *Int J Pharm.*344.pp 44-52.
44. Babu Dhanikula, A., Mohamed Khalid, N., Lee, S.D., Yeung, R., Risovic, V., Wasan, K.M., and Leroux, J.C. (2007).Long circulating lipid nanocapsules for drug detoxification. *Biomaterials.*28.pp 1248-1257.
45. Khalid, M.N., Simard, P., Hoarau, D., Dragomir, A., and Leroux, J.C. (2006).Long circulating poly(ethylene glycol)-decorated lipid

nanocapsules deliver docetaxel to solid tumors. *Pharm Res.*23.pp 752-758.

46. Prego, C., Garcia, M., Torres, D., and Alonso, M.J. (2005).Transmucosal macromolecular drug delivery. *J Control Release.*101.pp 151-162.
47. Csaba, N., Garcia-Fuentes, M., and Alonso, M.J. (2006).The performance of nanocarriers for transmucosal drug delivery. *Expert Opin Drug Deliv.*3.pp 463-478.
48. Pinto Reis, C., Neufeld, R.J., Ribeiro, A.J., and Veiga, F. (2006).Nanoencapsulation II. Biomedical applications and current status of peptide and protein nanoparticulate delivery systems. *Nanomedicine.*2.pp 53-65.
49. Alonso, M.J. (2004).Nanomedicines for overcoming biological barriers. *Biomed Pharmacother.*58.pp 168-172.
50. des Rieux, A., Fievez, V., Garinot, M., Schneider, Y.J., and Preat, V. (2006).Nanoparticles as potential oral delivery systems of proteins and vaccines: A mechanistic approach. *J Control Release.*116.pp 1-27.
51. Prego, C., Fabre, M., Torres, D., and Alonso, M.J. (2006).Efficacy and mechanism of action of chitosan nanocapsules for oral peptide delivery. *Pharm Res.*23.pp 549-556.
52. Damge, C., Michel, C., Aprahamian, M., and Couvreur, P. (1988).New approach for oral administration of insulin with polyalkylcyanoacrylate nanocapsules as drug carrier. *Diabetes.*37.pp 246-251.
53. Damge, C., Vranckx, H., Balschmidt, P., and Couvreur, P. (1997).Poly(alkyl cyanoacrylate) nanospheres for oral administration of insulin. *J Pharm Sci.*86.pp 1403-1409.
54. Pinto-Alphandary, H., Aboubakar, M., Jaillard, D., Couvreur, P., and Vauthier, C. (2003).Visualization of insulin-loaded nanocapsules: In vitro and in vivo studies after oral administration to rats. *Pharm Res.*20.pp 1071-1084.

55. Cournarie, F., Auchere, D., Chevenne, D., Lacour, B., Seiller, M., and Vauthier, C. (2002).Absorption and efficiency of insulin after oral administration of insulin-loaded nanocapsules in diabetic rats. *Int J Pharm.*242.pp 325-328.

56. Ubrich, N., Schmidt, C., Bodmeier, R., Hoffman, M., and Maincent, P. (2005).Oral evaluation in rabbits of cyclosporin-loaded Eudragit RS or RL nanoparticles. *Int J Pharm.*288.pp 169-175.

57. Staniscuaski Guterres, S., Fessi, H., Barratt, G., Puisieux, F., and Devissaguet, J.P. (1995).Poly(D,L-Lactide) nanocapsules containing non-steroidal anti-inflammatory drugs: Gastrointestinal tolerance following intravenous and oral administration. *Pharm Res.*12.pp 1545-1547.

58. Limayem Blouza, I., Charcosset, C., Sfar, S., and Fessi, H. (2006).Preparation and characterization of spironolactone-loaded nanocapsules for paediatric use. *Int J Pharm.*325.pp 124-131.

59. Nassar, T., Rom, A., Nyska, A., and Benita, S. (2009).Novel double coated nanocapsules for intestinal delivery and enhanced oral bioavailability of tacrolimus, a P-gp substrate drug. *J Control Release.*133.pp 77-84.

60. Peltier, S., Oger, J.M., Lagarce, F., Couet, W., and Benoit, J.P. (2006).Enhanced oral paclitaxel bioavailability after administration of paclitaxel-loaded lipid nanocapsules. *Pharm Res.*23.pp 1243-1250.

61. Barar, J., Javadzadeh, A.R., and Omidi, Y. (2008).Ocular novel drug delivery: Impacts of membranes and barriers. *Expert Opin Drug Deliv.*5.pp 567-581.

62. Lang, J.C. (1995).Ocular drug delivery conventional ocular formulations. *Adv Drug Deliv Rev.*16.pp 39-43.

63. Losa, C., Marchal-Heussler, L., Orallo, F., Vila-Jato, J.L., and Alonso, M.J. (1993).Design of new formulations for topical ocular

administration: Polymeric nanocapsules containing metipranolol. *Pharm Res.*10.pp 80-87.

64. Marchal-Heussler, L., Fessi, H., Devissaguet, J.P., Hoffman, M., and Maincent, P. (1992).Colloidal drug delivery systems for the eye. A comparison of the efficacy of three different polymers: Polyisobutylcyanoacrylate, polylactic-co-glycolic acid, poly-epsilon-caprolactone. *STP Pharma Sciences.*2.pp 98-104.
65. Marchal-Heussler, L., Sirbat, D., Hoffman, M., and Maincent, P. (1993).Poly(ε-caprolactone) nanocapsules in carteolol ophthalmic delivery. *Pharm Res.*10.pp 386-390.
66. Desai, S.D. and Blanchard, J. (2000).Pluronic® F127-based ocular delivery system containing biodegradable polyisobutylcyanoacrylate nanocapsules of pilocarpine. *Drug Delivery: J Delivery and Targeting Therapeutic Agents.*7.pp 201-207.
67. Calvo, P., Sanchez, A., Martinez, J., Lopez, M.I., Calonge, M., Pastor, J.C., and Alonso, M.J. (1996).Polyester nanocapsules as new topical ocular delivery systems for cyclosporin A. *Pharm Res.*13.pp 311-315.
68. Le Bourlais, C.A., Chevanne, F., Turlin, B., Acar, L., Zia, H., Sado, P.A., Needham, T.E., and Leverge, R. (1997).Effect of cyclosporine A formulations on bovine corneal absorption: Ex-vivo study. *J Microencapsulation.*14.pp 457-467.
69. Calvo, P., Thomas, C., Alonso, M.J., Vila-Jato, J.L., and Robinson, J.R. (1994).Study of the mechanism of interaction of poly(E-caprolactone) nanocapsules with the cornea by confocal laser scanning microscopy. *Int J Pharm.*103.pp 283-291.
70. Calvo, P., Vila-Jato, J.L., and Alonso, M.J. (1996).Comparative in vitro evaluation of several colloidal systems, nanoparticles, nanocapsules, and nanoemulsions, as ocular drug carriers. *J Pharm Sci.*85.pp 530-536.

71. Calvo, P., Alonso, M.J., Vila-Jato, J.L., and Robinson, J.R. (1996).Improved Ocular Bioavailability of Indomethacin by Novel Ocular Drug Carriers. *J Pharm Pharmacol.*48.pp 1147-1152.

72. Alonso, M.J. and Sanchez, A. (2003).The potential of chitosan in ocular drug delivery. *J Pharm Pharmacol.*55.pp 1451-1463.

73. Gottesman, M.M., Fojo, T., and Bates, S.E. (2002).Multidrug resistance in cancer: Role of ATP-dependent transporters. *Nat Rev Cancer.*2.pp 48-58.

74. Ehdaie, B. (2008).Application of Nanotechnology in Cancer Research: Review of Progress in the National Cancer Institute's Alliance for nanotechnology.

75. McNeil, S.E. (2005).Nanotechnology for the biologist. *J Leukoc Biol.*78.pp 585-594.

76. Iyer, A.K., Khaled, G., Fang, J., and Maeda, H. (2006).Exploiting the enhanced permeability and retention effect for tumor targeting. *Drug Discov Today.*11.pp 812-818.

77. Greish, K. (2007).Enhanced permeability and retention of macromolecular drugs in solid tumors: A royal gate for targeted anticancer nanomedicines. *J Drug Target.*15.pp 457-464.

78. Brigger, I., Dubernet, C., and Couvreur, P. (2002).Nanoparticles in cancer therapy and diagnosis. *Adv Drug Deliv Rev.*54.pp 631-651.

79. Garcion, E., Lamprecht, A., Heurtault, B., Paillard, A., Aubert-Pouessel, A., Denizot, B., Menei, P., and Benoit, J.P. (2006).A new generation of anticancer, drug-loaded, colloidal vectors reverses multidrug resistance in glioma and reduces tumor progression in rats. *Mol Cancer Ther.*5.pp 1710-1722.

80. Lenaerts, V., Labib, A., Chouinard, F., Rousseau, J., Ali, H., and Van Lier, J. (1995).Nanocapsules with a reduced liver uptake: Targeting of phthalocyanines to EMT-6 mouse mammary tumor in vivo. *Eur J Pharm Biopharm.*41.pp 38-43.

81. Lacoeuille, F., Hindre, F., Moal, F., Roux, J., Passirani, C., Couturier, O., Cales, P., Le Jeune, J.J., Lamprecht, A., and Benoit, J.P. (2007).In vivo evaluation of lipid nanocapsules as a promising colloidal carrier for paclitaxel. *Int J Pharm.*344.pp 143-149.

82. Fattal, E. and Bochot, A. (2008).State of the art and perspectives for the delivery of antisense oligonucleotides and siRNA by polymeric nanocarriers. *Int J Pharm.*364.pp 237-248.

83. Li, X. and Chan, W.K. (1999).Transport, metabolism and elimination mechanisms of anti-HIV agents. *Adv Drug Deliv Rev.*39.pp 81-103.

84. Nakada, Y., Fattal, E., Foulquier, M., and Couvreur, P. (1996).Pharmacokinetics and biodistribution of oligonucleotide adsorbed onto poly(isobutylcyanoacrylate) nanoparticles after intravenous administration in mice. *Pharm Res.*13.pp 38-43.

85. Schwab, G., Chavany, C., Duroux, I., Goubin, G., Lebeau, J., Helene, C., and Saison-Behmoaras, T. (1994).Antisense oligonucleotides adsorbed to polyalkylcyanoacrylate nanoparticles specifically inhibit mutated Ha-ras-mediated cell proliferation and tumorigenicity in nude mice. *Proc Natl Acad Sci U S A.*91.pp 10460-10464.

86. Lambert, G., Fattal, E., Pinto-Alphandary, H., Gulik, A., and Couvreur, P. (2001).Polyisobutylcyanoacrylate nanocapsules containing an aqueous core for the delivery of oligonucleotides. *Int J Pharm.*214.pp 13-16.

87. Lambert, G., Bertrand, J.R., Fattal, E., Subra, F., Pinto-Alphandary, H., Malvy, C., Auclair, C., and Couvreur, P. (2000).EWS Fli-1 antisense nanocapsules inhibits Ewing sarcoma-related tumor in mice. *Biochem Biophys Res Commun.*279.pp 401-406.

88. Toub, N., Bertrand, J.R., Malvy, C., Fattal, E., and Couvreur, P. (2006).Antisense oligonucleotide nanocapsules efficiently inhibit EWS-Fli1 expression in a Ewing's sarcoma model. *Oligonucleotides.*16.pp 158-168.

89. Toub, N., Bertrand, J.R., Tamaddon, A., Elhamess, H., Hillaireau, H., Maksimenko, A., Maccario, J., Malvy, C., Fattal, E., and Couvreur, P. (2006).Efficacy of siRNA nanocapsules targeted against the EWS-Fli1 oncogene in Ewing sarcoma. *Pharm Res.*23.pp 892-900.

90. Bouclier, C., Moine, L., Hillaireau, H., Marsaud, V., Connault, E., Opolon, P., Couvreur, P., Fattal, E., and Renoir, J.M. (2008).Physicochemical characteristics and preliminary in vivo biological evaluation of nanocapsules loaded with siRNA targeting estrogen receptor alpha. *Biomacromolecules.*9.pp 2881-2890.

ANTECEDENTES, HIPÓTESIS Y OBJETIVOS

ANTECEDENTES

1. Las nanoestructuras poliméricas administradas por inhalación, han demostrado ser capaces de proporcionar niveles terapéuticos de fármacos durante períodos prolongados, al potenciar el acceso de éstos hacia las dianas localizadas a nivel pulmonar[71;72;73;74;75].

2. Algunos polisacáridos mucoadhesivos, como el quitosano y el ácido hialurónico, ofrecen interesantes posibilidades como constituyentes de nanoestructuras capaces de interaccionar con el epitelio pulmonar y maximizar su período de contacto[76;77]. Ambos polímeros pueden, además, formar nanoestructuras híbridas gracias a la interación iónica de sus cargas opuestas[78;79], lo que aporta ventajas en cuanto al perfil de seguridad ofrecido por el quitosano[79].

3. La combinación del quitosano con ciclodextrinas en nanopartículas, aporta mejoras a las propiedades de los nanosistemas constituídos únicamente por el polisacárido, al disminuir posibles alteraciones de la función barrera del epitelio y ofrecer mayor protección a las macromoléculas encapsuladas[80;81].

71 **Pandey R, Sharma A, Zahoor A, Sharma S, Khuller GK, Prasad B.** (2003). J. Antimicrob. Chemother. 52(6): 981-6.
72 **Sharma A, Sharma S, Khuller GK.** (2004). J. Antimicrob. Chemother. 54(4): 761-6.
73 **Ahmad Z, Sharma S, Khuller GK.** (2005). Int .J. Antimicrob. Agents. 26(4): 298:303.
74 **Hitzman CJ, Wattenberg LW, Wiedmann TS.** (2006). J Pharm Sci. 95(6):1196-211.
75 **Ohashi K, Kabasawa T, Ozeki T, Okada H.** (2009). J. Control Release. 135(1):19-24.
76 **Yamamoto H, Kuno Y, Sugimoto S, Takeuchi H, Kawashima Y.** (2005). J Control Release. 102(2):373-81.
77 **Liu XB, Ye JX, Quan LH, Liu CY, Deng XL, Yang M, Liao YH.** (2008). Eur J Pharm Biopharm.
78 **de la Fuente M, Seijo B, Alonso MJ.** (2008). Macromol Biosci. 8(5):441-50.
79 **de la Fuente M, Seijo B, Alonso MJ.** (2008). Invest. Ophthalmol. Vis. Sci. 49(5):2016-24.
80 **Teijeiro-Osorio D, Remuñán-López C, Alonso MJ.** (2009). Biomacromol. 10(2):243-9.
81 **Chen Y, Siddalingappa B, Chan PH, Benson HA.** (2008). Biopolymers. 90(5):663-70.

4. La heparina es una macromolécula que ofrece un potencial terapéutico para el tratamiento del asma bronquial, al prevenir la desgranulación de los mastocitos[82;83]. Este potencial se ve limitado por su acceso restringido al interior celular[84], donde se encuentran localizados los receptores.

5. El docetaxel constituye un tratamiento antitumoral de elección, sin embargo su extremada hidrofobicidad obliga a la inclusión de disolventes en su formulación endovenosa, que dan lugar a importantes reacciones de sensibilización que se suman a los efectos secundarios provocados por el propio citostático[85;86].

6. Nuestro grupo de investigación ha demostrado el potencial de nanocápsulas de polisacáridos y poliaminoácidos catiónicos como transportadores intracelulares de antitumorales hidrofóbicos, como el docetaxel, consiguiendo vehículos eficaces sin necesidad de la inclusión de solventes tóxicos[87;88].

7. Se ha demostrado que en distintos tumores sólidos, entre ellos varios de pulmón, hay sobreexpresión del receptor CD-44, que es la diana endógena del ácido hialurónico[89;90]. La incorporación de ácido hialurónico en diferentes

[82] **Tyrrel DJ, Kilfeather S, Page CP.** (1995). TiPS. 16:198-204.
[83] **Diamant Z, Page CP.** (2000). Pulm. Pharmacol. Ther. 13(1):1-4.
[84] **Motlekar NA, Youan BB.** (2006). J. Control Release. 113(2):91-101.
[85] **Engels FK, Mathot RA, Verweij J.** (2007). Anticancer Drugs. 18(2):95-103.
[86] **Ten Tije AJ, Verweij J, Loos WJ, Sparreboom A.** (2003). Clin. Pharmacokinet. 42(7), 665-85.
[87] **Lozano MV, Torecilla D, Torres D, Vidal A, Dominguez F, Alonso MJ.** (2008). Biomacromol. 9, 2186-2193.
[88] **Lozano MV, Lollo G, Brea J, Torres D, Loza MI, Alonso MJ.** Polyarginine nanocapsules: a new platform for intracellular drug delivery (submitted).
[89] **Penno MB, August JT, Baylin SB, Mabry M, Linnoila RI, Lee VS, Croteau D, Yang XL, Rosada C.** (1994). Cancer Res. 54(5):1381-7.
[90] **Tran TA, Kallakury BV, Sheehan CE, Ross JS.** (1997). Hum Pathol. 28(7):809-14.

tipos de transportadores ha confirmado la especificidad del *targeting* hacia el receptor CD-44[91;92;93;94].

HIPÓTESIS

1.- El desarrollo de nanoestructuras constituídas por polisacáridos mucoadhesivos como el quitosano y/o el ácido hialurónico, puede constituir una estrategia adecuada para tratar localmente patologías que cursan a nivel pulmonar, como el asma bronquial o el cáncer de pulmón. El éxito de esta estrategia residirá fundamentalmente en favorecer la accesibilidad de los fármacos a las células diana, a la vez que prolongar su contacto con las mismas y potenciar su captura intracelular.

2.- La combinación del quitosano con ciclodextrinas en sistemas nanoparticulares es una alternativa que puede aportar ventajas al sistema puro en su administración pulmonar, en lo que se refiere a mejora de su perfil de seguridad, promoción de su captura intracelular, y protección de la macromolécula encapsulada.

3.- El diseño de un nuevo sistema constituído por nanocápsulas de ácido hialurónico puede resultar de interés para la vehiculización pulmonar del antitumorales hidrofóbicos. El nuevo nanosistema contendrá en su núcleo oleoso la molécula activa, mientras que el ácido hialurónico potenciará la interacción con células tumorales que sobreexpresan receptores CD-44 en su superficie.

---

[91] **Akima K, Ito H, Iwata Y, Matsuo K, Watari N, Yanagi M, Hagi H, Oshima K, Yagita A, Atomi Y, Tatekawa I.** (1996). J Drug Target. 1996;4(1):1-8.
[92] **Auzenne E, Ghosh SC, Khodadadian M, Rivera B, Farquhar D, Price RE, Ravoori M, Kundra V, Freedman RS, Klostergaard J.** (2007). Neoplasia. 9(6):479-86.
[93] **Eliaz RE, Szoka FCJr.** (2001). 61(6), 2592-601.
[94] **Peer D, Margalit R.** (2004). Neoplasia 6, 343-353.

OBJETIVOS

El objetivo de esta Tesis se ha dirigido a evaluar el potencial que presentan distintos nanotransportadores para vehiculizar y promover el efecto intracelular de fármacos tan distintos, como la macromolécula hidrofílica heparina o el antitumoral hidrofóbico docetaxel, en células diana pulmonares.

Este objetivo se cubrirá a través de las siguientes etapas:

1.- Desarrollo de nanosistemas híbridos de quitosano conteniendo heparina y evaluación *ex vivo* de su interacción y de su actividad antiinflamatoria sobre mastocitos.

Esta parte de la memoria se ha dirigido en primer lugar a optimizar los nanosistemas de quitosano-ácido hialurónico y quitosano-ciclodextrinas en cuanto a su contenido en heparina, para asegurar la producción del efecto antiasmático. En segundo lugar, se estudió la capacidad de los nanosistemas para interaccionar y ser internalizados en mastocitos extraídos de rata. Finalmente, se ha evaluado el potencial de estos vehículos para inhibir la liberación de histamina por parte de los mastocitos.
Los resultados de este apartado se recogen en los capítulos experimentales 2 y 3.

2.- Desarrollo de un nuevo sistema constituído por nanocápsulas de ácido hialurónico conteniendo docetaxel y evaluación de su eficacia antitumoral sobre cultivos celulares de cáncer de pulmón.

Para poner a punto el nuevo nanosistema, se llevó a cabo la optimización del proceso de recubrimiento con el polímero aniónico, evaluando sus características tras la incorporación de distintos tensoactivos catiónicos en el núcleo oleoso. Se determinó finalmente la eficacia antitumoral de las nanocápsulas conteniendo docetaxel sobre el modelo celular de cáncer de pulmón NCI-H460.

Los resultados de este apartado se recogen en el capítulo experimental 4.

PARTE I: DESARROLLO DE NANOSISTEMAS HÍBRIDOS DE QUITOSANO CONTENIENDO HEPARINA Y EVALUACIÓN *EX VIVO* DE SU INTERACCIÓN Y DE SU ACTIVIDAD ANTIINFLAMATORIA SOBRE MASTOCITOS.

Capitulo 2

Chitosan-hyaluronic acid nanoparticles loaded with heparin for the treatment of asthma

Abstract

The purpose of this study was to produce mucoadhesive nanocarriers made from chitosan (CS) and hyaluronic acid (HA), and containing the macromolecular drug heparin, suitable for pulmonary delivery. For the first time, this drug was tested in *ex-vivo* experiments performed in mast cells, in order to investigate the potential of the heparin-loaded nanocarriers in antiasthmatic therapy. CS and mixtures of HA with unfractionated or low-molecular-weight heparin (UFH and LMWH, respectively) were combined to form nanoparticles by the ionotropic gelation technique. The resulting nanoparticles loaded with UFH were between 162 and 217 nm in size, and those prepared with LMWH were 152 nm. The zeta potential of the nanoparticle formulations ranged from +28.1 to +34.6 mV, and in selected nanosystems both types of heparin were associated with a high degree of efficiency, which was approximately 70%. The nanosystems were stable in phosphate buffered saline (PBS), pH 7.4, for at least 24 h, and released 10.8% of UFH and 79.7% of LMWH within 12 h of incubation. Confocal microscopy experiments showed that fluorescent heparin-loaded CS-HA nanoparticles were effectively internalized by rat mast cells. *Ex-vivo* experiments aimed at evaluating the capacity of heparin to prevent histamine release in rat mast cells indicated that the free or encapsulated drug exhibited the same dose-response behaviour.

Keywords: Nanoparticles; Chitosan; Hyaluronic Acid; Heparin; Asthma; Mast Cells; Histamine.

Introduction

Although mast cells produce a variety of lipid mediators, chemokines, cytokines and enzymes that can interact with airway smooth muscle cells to cause hyperresponsiveness (Page et al., 2001; Robinson, 2004), they are the only endogenous source of heparin in mammals, which plays a protective role by limiting inflammation and airway remodelling (Page, 1991). Heparin is released on degranulation of mast cells (Green et al., 1993) and inhibits the proliferation of smooth muscle cells isolated from the airways of several species including humans (Johnson et al., 1995), bovines (Kilfeather et al., 1995) and dogs (Halayko et al., 1997).

Furthermore, several studies have demonstrated that the inhalation of high, medium and low-molecular-weight heparin (with or without anticoagulant activity) is effective in preventing acute bronchoconstrictor responses and airway hyperresponsiveness, with the potency of these types of heparin being inversely proportional to their molecular weight (Martinez-Salas et al., 1998; Molinari et al., 1998; Campo et al., 1999; Ahmed et al., 2000). This effect was attributed to the capacity of heparin to prevent mast cell degranulation. Interestingly, ultra-low-molecular-weight heparin was also effective in the treatment of late airway responses (pre or post antigen challenge); the effect was independent of the anticoagulant activity of the heparin and was mediated by an unknown biological action (Molinari et al., 1998; Ahmed et al., 2000). This is convincing evidence of the potential role of heparin in asthma therapy.

With the aim of enhancing the potential role of heparin in the treatment of asthma, we propose encapsulating this macromolecule in selected nanocarriers capable of positively interacting with mast cells, be internalized by these cells and released the encapsulated heparin in a controlled manner, thereby also preventing the possible degradation of the drug by enzymatic attack in the airways.

CS is a natural, non-toxic, biodegradable polycationic polysaccharide. We, and other groups, have previously used the polymer to elaborate different nanocarriers (Garcia-Fuentes et al., 2005; Köping-Höggård et al., 2005; Prego et al., 2005; De la Fuente et al; 2008a); these nanosystems have been shown, among other advantages, to prolong its residence time at the target site of absorption. These results were mainly attributed to the capacity of the polymer to interact with the negatively charged cell surfaces.

HA is a natural, non-toxic, biodegradable polysaccharide that is distributed widely throughout the human body, mainly in the connective tissue, eyes, intestine and lungs. Several *ex-vivo* studies have demonstrated that particulate HA systems have beneficial effects on the mucociliary transport rate in airways, due to the mucoadhesivity of the polymer (Prichtard et al., 1996; Lim et al., 2000). It has also been found that HA has a discreet hypoproliferative effect on proliferating airway smooth muscle cells (Kanabar et al., 2005). This may also indicate that HA alone, or in synergy with heparin (Johnson et al., 1995), may be useful in preventing narrowing of the airway in asthmatic patients.

Taking into account this information and the previous experience of our group on the development of CS-HA nanoparticles loaded with hydrophilic and hydrophobic macromolecules (De la Fuente et al., 2008b), the present study aimed to combine the virtues of CS and HA in the development of heparin-loaded nanoparticles, intended for pulmonary administration. Finally, the interaction between these nanosystems and mast cells will be investigated, and their potential for preventing rat mast cell degranulation evaluated, to our knowledge, for the first time.

Materials and methods

Materials

Ultrapure chitosan hydrochloride salt (CS; UP CL 113, molecular weight ~125 KDa and degree of acetylation 14%) was purchased from Pronova Biopolymer AS (Oslo, Norway). Sodium hyaluronate ophthalmic grade (HA, molecular weight ~165 KDa) was a gift from Bioiberica (Barcelona, Spain). Unfractionated heparin sodium salt (UFH, molecular weight ~18 KDa, 202 USP units/mg), low-molecular-weight heparin sodium salt (LMWH, molecular weight ~4 KDa, 53 USP units/mg) and pentasodium tripolyphosphate (TPP) were purchased from Sigma Aldrich (Madrid, Spain). All other solvents and chemicals were of the highest commercially available grade.

Preparation of heparin-loaded CS-HA nanoparticles

CS-HA nanoparticles loaded with heparin were prepared according to the procedure previously developed by our group (De la Fuente et al., 2008a). Nanoparticles were spontaneously obtained by ionotropic gelation between the positively charged amino groups of CS and the negatively charged HA, TPP and heparin. Briefly, 3.5 mL of a mixture of an aqueous solution of HA (0.17-0.34 mg/mL), TPP (0.06 mg/mL) and UFH (0.29-0.46 mg/mL) or LMWH (0.4 mg/mL) were added to 3.5 mL of a solution of CS (0.11% w/v, pH 4.9) under magnetic stirring at room temperature. Magnetic stirring was maintained for 10 min to enable complete stabilization of the system. The nanoparticles were transferred to Eppendorf tubes and isolated by centrifugation in 20 μL of a glycerol bed (16000×*g*, 30 min, 25º C). Supernatants were collected and the nanoparticles were then resuspended in ultrapure water by shaking on a vortex mixer.

The production yield of the systems was obtained by centrifugation of fixed volumes of the nanoparticle suspensions (16000×*g*, 30 min, 25° C), without a glycerol bed. The supernatants were discarded and the sediments were freeze-dried. The yield was calculated as follows:

$$\text{Yield} = \frac{\text{Weight of nanoparticles}}{\text{Total amount of the components}} \times 100$$

Physicochemical characterization of heparin-loaded CS-HA nanoparticles

The size and zeta potential of the colloidal systems were determined by photon correlation spectroscopy and laser Doppler anemometry, with a Zetasizer Nano-ZS (Malvern Instruments, United Kingdom). Each batch was analyzed in triplicate.

Morphological examination of the nanoparticles was performed by transmission electron microscopy (TEM) (CM12 Philips, Netherlands). The samples were stained with 1% w/v phosphotungstic acid for 10 sec., immobilized on copper grids with Formvar® and dried overnight for viewing by TEM.

Association efficiency and drug loading of heparin-loaded CS-HA nanoparticles

The association efficiencies of the selected formulations were determined after isolation of nanoparticles by centrifugation, as described in Section 2.2. The amount of unbound heparin in the supernatant was determined by a colorimetric method (Stachrom® Heparin, Diagnostica Stago, France).

The association efficiency of heparin and the drug loading were calculated as follows:

$$\text{Association efficiency} = \frac{\text{Total amount of drug - Amount of unbound drug}}{\text{Total amount of drug}} \times 100$$

$$\text{Drug Loading} = \frac{\text{Total amount of drug - Amount of unbound drug}}{\text{Weight of nanoparticles}} \times 100$$

Stability study of heparin-loaded CS-HA nanoparticles in different media

Selected nanoparticle formulations were prepared and centrifuged in the presence of glycerol. Nanoparticles were tested for their stability taking into account the change in size of nanoparticles and possible precipitations in different media at 37º C, including: Hanks´ balanced salt solution (HBSS) at pH 6.4 and 7.4, and phosphate buffered saline (PBS), at pH 7.4 (for composition of these solutions, see below). Nanoparticles were incubated in these media and samples were collected at several time intervals (0, 1, 3, 5, 10 and 24 h), and the size distribution of the nanoparticles was measured by photon correlation spectroscopy.

The composition of HBSS was: 137 mM NaCl, 5.4 mM KCl, 0.25 mM Na_2HPO_4, 0.44 mM KH_2PO_4 and 4.2 mM $NaHCO_3$.

The composition of PBS was: 137 mM NaCl, 2.7 mM KCl, 1.4 mM NaH_2PO_4 and 1.3 mM Na_2HPO_4.

***In vitro* heparin release studies from CS-HA nanoparticles**

Heparin release studies were performed by incubating 0.1 mg of the selected nanoparticles in 1 mL of PBS (pH 7.4) at 37º C. The samples were

centrifuged at appropriate time intervals (1, 5 and 12 h), and the amount of heparin released was evaluated with the heparin kit described above. The concentration of heparin was quantified and calculated by interpolation from the corresponding standard curve.

Study of interaction of fluorescent heparin-loaded CS-HA nanoparticles with rat mast cells by confocal microscopy

Fluorescein labelling of CS

Chitosan was labelled with fluorescein following a slight modification of the method described by De Campos et al. (2004). The covalent attachment of fluorescein to CS was by the formation of amide bonds between primary amino groups of the polymer and the carboxylic acid groups of fluorescein. Briefly, 250 mg of CS was dissolved in 25 mL of water, and 10 mg of fluorescein (Sigma Aldrich, Spain) was dissolved in 1 mL of ethanol. These solutions were then mixed, and EDAC (1-ethyl-3-(dimethylaminopropyl) carbodiimide hydrochloride) (Sigma Aldrich, Spain) was added to a final concentration of 0.05 M, to catalyze the formation of amide bonds. The reactive mixture was incubated under permanent magnetic stirring for 12 h in the dark, at room temperature. The resulting conjugate was finally isolated by dialysis for 72 h (cellulose dialysis tubing, pore size 12400 Da; Sigma Aldrich, Spain) against demineralised water, and freeze-dried. The pH of fluorescent CS was adjusted to the same value as the raw CS solution (pH 4.9) with HCl, for the preparation of fluorescent nanoparticles.

Preparation of fluorescent heparin-loaded CS-HA nanoparticles

Fluorescent nanoparticles were prepared according to the same procedure described in 2.2. The selected mass distribution for the preparation of fluorescent nanoparticles was: 4 mg of fluorescent CS, 0.6 mg of HA, 0.21 mg of TPP and 1.4 mg of UFH.

Confocal laser scanning microscopy study

An aqueous solution (50 μL) containing 0.3 mg of isolated fluorescent UFH-loaded CS-HA nanoparticles was incubated with 450 μL of a suspension of mast cells ($10x10^3$ cells/100 μL) in Umbreit (for composition, see below) containing 0.05% w/v of BSA. The mixture was incubated for 2 h at 37 °C, and the cells were then separated by centrifugation (10 min, 200x*g*) and discarding the supernatants. Two hundred μL of Umbreit+BSA solution (at 4 °C) were then added to the cell pellet. The pellet was resuspended and centrifuged again to extract the non-internalized nanoparticles. This procedure was repeated once more. Mast cells were fixed for 5 minutes in paraformaldehyde (2% w/v, 100 μL) and washed 3 times with the Umbreit+BSA solution, by centrifugation. Two hundred μL of a Bodipi® phalloidin solution (Invitrogen, USA) were added to the cell pellet and the cells were incubated for 30 min at room temperature. The cells were washed 3 times (Umbreit+BSA) by centrifugation, the supernatant was discarded, and the pellet was resuspended in 20 μL of the Umbreit+BSA solution. The resuspended sample was placed on the surface of a positively charged microscope slide (Superfrost Ultra Plus, Menzel-Glaser, Irland) and dried at room temperature overnight. The sample was prepared in Vectashield medium (Vector, USA) for visualization by confocal microscopy (CLSM, Zeiss 501, Germany) (all of the described procedures were carried

out in darkness to prevent the loss of the fluorescent signal from the nanoparticles and mast cells).

The composition of Umbreit saline solution was: 1.2 mM $MgSO_4$, 1.2 mM $NaPO_4H_2$, 22.85 mM $NaHCO_3$, 5.94 mM KCl, 1 mM $CaCl_2$, 119 mM NaCl and 0.1% glucose.

***Ex vivo* studies with rat mast cells: Inhibition of histamine release by heparin-loaded CS-HA nanoparticles**

Rat mast cell purification and viability

Mast cells were obtained by lavage of pleural and peritoneal cavities of female Sprague–Dawley rats (400–800 g) with Umbreit saline solution, following procedures similar to those described in other studies (Lago et al., 2001; Buceta et al., 2008). The suspension obtained from each rat was centrifuged at 100x*g* for 5 min (4 ºC) and suspended in a final volume of 1 mL of Umbreit containing 0.05% w/v of BSA. Purification was carried by centrifugation on 4 mL of an isotonic Percoll gradient at 600 *g* for 10 min (4 ºC). The mast cells were washed twice with the Umbreit+BSA solution and maintained at 4 °C in this solution until use. Mast cells were quantified by toluidin blue staining (95% purity) and the viability assessed by trypan blue staining (the procedure is described below).

Trypan blue staining procedure: Mast cell viability studies were carried out by trypan blue staining in an inverted microscope, as described by Lago et al. (2001). This involved visual counting of the stained cells in the five fields of a counting chamber. The percentage of viability was calculated with the following formula:

$$\text{Trypan blue stained cells} = \frac{\text{Arithmetic mean from the five fields}}{\text{Total number of mast cells}} \times 100$$

In order to test the mast cell viability after contact with heparin-loaded nanoparticles, the same procedure was used, and the UFH or LMWH-loaded CS-HA nanoparticles added to the rat mast cell suspension ($1x10^5$ cells per test tube). The tested dose of nanoparticles was equivalent to 200 μg/mL of UFH or LMWH.

Measurement of histamine release in rat mast cells

Rat mast cells ($1x10^5$ cells per test tube) were pre-warmed at 37 ºC (10 min) in BSA-free Umbreit saline solution containing the UFH or LMWH solutions or the nanoparticles loaded with UFH or LMWH. Histamine release from mast cells was then initiated by incubating the cells with 100 μM of compound 48/80 (Sigma Aldrich, Spain) for 20 min at 37 ºC. The cells were then centrifuged at 1100x*g* for 3 min at 4 ºC, and two aliquots (100 μl) of the supernatants were collected in a 96-well microplate. The rest of the supernatants were discarded and the pellets were resuspended in 500 μl of 0.1 mM HCl, sonicated for 1 min and centrifuged at 1100 x *g* for 6 min. Two aliquots of 100 μL of the supernatants were collected for residual histamine determination. Histamine was assayed fluorometrically, as described by Lago et al. (2001); briefly, 80 μL NaOH 1 M were added to 100 μL of the sample, then 50 μl phthaldialdehyde 0.04% w/v were added to each well and plate was incubated for 4 min at 25° C. After this time, 50 μl of 3 M HCl were added and fluorescence was measured within 20 min, at excitation and emission wavelengths of 360 nm and 465 nm respectively, in a Tecan Ultra Evolution reader (Tecan, Switzerland).

Data analysis for measurement of histamine release in rat mast cells

Results were expressed as percentage of the total histamine released after stimulation with compound 48/80. The results were corrected for spontaneous histamine release in the absence of any chemical and under the same conditions. The equation used for the calculation was HR=[(S−ER)/(S+P−ER)]×100, where HR is the percentage histamine release; S, supernatant fluorescence; ER, fluorescence of spontaneous release supernatants and P, pellet fluorescence.

IC_{50} values were obtained by fitting the data with non-linear regression, with Prism 2.1 software (GraphPad, San Diego, CA).

Statistical analysis

The statistical significance of the differences between formulations was determined by application of two-way analysis of variance (ANOVA) followed by a two-tailed paired Student's test. Differences were considered significant at $p<0.05$.

Results and discussion

Preparation and characterization of heparin-loaded CS-HA nanoparticles

Nanoparticles loaded with heparin were prepared by the ionotropic gelation technique. The ability of CS to form a gel after contact with polyanions by promoting inter and intramolecular linkages (Calvo et al., 1997) enables the formation of the nanoparticles. In this case, an ionic interaction occurs between the positively charged CS and the negatively charged HA, heparin and the polyanion TPP. The ionic gelation process is extremely simple and involves mixing two aqueous phases at room temperature.

When the nanoparticles loaded with UFH were prepared, it was necessary to establish the best ratio between components that enabled formation and also adequate isolation of the nanosystems. The size, polydispersity index, zeta potential and appearance of the tested formulations are shown in Table 1. In general, it is possible to argue that when the amount of polyanions was too low (relative to CS), nanoparticles could not be formed, or that the quantity of the formed nanoparticles was too low. Nanoparticles with different characteristics were obtained when greater amounts of polyanions were used. However, if the amount of polyanions was too high, it was impossible to isolate the particles, because the nanosystems were not resuspendable or, in extreme cases, precipitation occurred. In addition, when the amount of polyanions was higher, slight decreases in the positive zeta potential values were observed. This may be caused by increased shielding of free positively charged groups of CS.

All the resulting nanosystems ranged in size from 162 to 217 nm; polydispersity values were between 0.11-0.45 and the positive zeta potential ranged from +28.1 to +34.6 (Table 1). This positive zeta potential indicates that the surface of the nanosystems is preferably composed by CS. Among the tested formulations, we selected those formed by the following mass distribution for subsequent studies: 4 mg of CS, 0.6 mg of HA, 0.21 mg of TPP and 1.4 mg of UFH. This formulation was able to encapsulate the highest amount of UFH tested, showed reasonable polydispersity, and high turbidity (related to a higher production yield).

Table 1: Physicochemical properties of the nanoparticles prepared with different ratios of CS-HA-TPP-heparin (mean ± S.D., n=3).

Amount (mg) CS-HA-TPP-heparin	Size (nm)	Polydispersity Index	Zeta potential (mV)	Appearance
4-1.2-0.21-1.0[a]	201 ± 24	0.22 – 0.36	+32.1 ± 1.6	Medium turbidity
4-1.2-0.21-1.2[a]	217 ± 30	0.23 – 0.35	+28.1 ± 0.9	High turbidity
4-1.2-0.21-1.4[a]	Not resuspendable	---	---	---
4-1.2-0.21-1.6[a]	Precipitation	---	---	---
4-0.6-0.21-1.2[a]	162 ± 17	0.11 – 0.30	+34.6 ± 0.6	Medium turbidity
4-0.6-0.21-1.4[a]	193 ± 32	0.24 – 0.45	+32.5 ± 1.7	High turbidity
4-0.6-0.21-1.5[a]	Not resuspendable	---	---	---
4-0.6-0.21-1.4[b]	152 ± 10	0.17 – 0.27	+33.0 ±1.3	Low turbidity

[a]= UFH; [b]= LMWH

The loading capacity, association efficiency and yield of the selected formulation are shown in Table 2. The association efficiency was 72.3% and therefore 1.01 mg of UFH (of the initial 1.4 mg) formed nanoparticles. The drug loading was about 34%, with the remaining mass corresponding to CS, HA and TPP.

The same formulation prepared with LMWH was similar in size, zeta potential and association efficiency, but showed lower values of polydispersity and yield and higher drug loading (see Tables 1 and 2).
Interestingly, the drug loading of the formulation with LMWH is approximately twice that of the formulation with UFH, and it is possible that LMWH may induce greater displacement of the anionic molecules (HA and TPP) from the nanoparticles and, consequently, lead to a lower yield.

Table 2: Loading characteristics and yield of selected CS-HA nanoparticles containing UFH or LMWH (mean ± S.D., n=3).

Amount (mg) CS-HA-TPP-heparin	Loading capacity (%)	Association Efficiency (%)	Yield (%)
4-0.6-0.21-1.4[a]	33.6 ±1.2	72.3 ± 2.7	49.0 ± 1.2
4-0.6-0.21-1.4[b]	60.6 ± 0.3	69.7 ± 7.6	24.9 ± 4.3

[a] = UFH; [b] = LMWH

Considering that the only difference between the prepared formulations was the type of heparin, these changes should be attributed, on one hand, to the different molecular weight (~18 KDa for UFH and ~4 KDa for LMWH) and, on the other hand, to possible chemical differences between UFH and LMWH, associated with very different values of anticoagulant activities (202 and 53 USP units/mg, respectively).

The TEM micrographs shown in Figures 1a and 1b indicate that the selected nanosystems loaded with UFH or LMWH were spherical. Interestingly, the systems with UFH appeared denser in the center than at the surface, and differed from those containing LMWH, which appeared more homogeneous.

Figure 1: Electron transmission micrographs of selected CS-HA nanoparticles containing UFH (a) or LMWH (b).

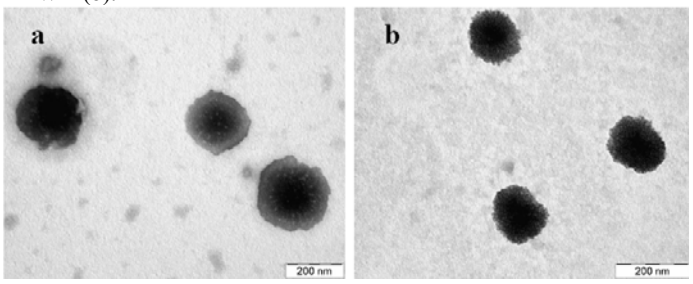

Stability studies of heparin-loaded CS-HA nanoparticles

Determination of nanoparticle colloidal stability under conditions similar to those used for cell culture is crucial for future studies. Therefore, the stability of the selected systems was investigated in media usually used for cell culture studies. These media included: HBSS (pH 7.4), HBSS (pH 6.4) and PBS (pH 7.4). The stability of the selected nanoparticles was better in media of pH 7.4, and was maximal for PBS, where the size was maintained for up to 24 h (Fig. 2) (the stability in HBSS (pH 6.4), is not shown because the nanosystems aggregated immediately). The explanation

for this difference between PBS (pH 7.4) and HBSS (pH 7.4), may be related to the different composition of these media (HBSS contains CO_3^{-2} ions and a concentration of PO_4^{-2} ions eight times lower than in PBS). This may directly affect the hydration shell of the counterions located at the surface of the nanoparticles, as well as the structure of water surrounding the systems. In PBS these effects appeared to result in an increase in repulsive hydration forces, and hence, greater stability. Interestingly, the zeta values of UFH and LMWH-loaded nanoparticles was slightly negative (-10.5±2 mV) throughout all the stability studies in which HBSS (pH 7.4) and PBS (7.4) were used.

Figure 2: Stability of heparin-loaded CS-HA nanosystems in different media: UFH-loaded nanoparticles (▲) and LMWH-loaded nanoparticles (×) in PBS (pH 7.4); UFH-loaded nanoparticles (■) and LMWH-loaded nanoparticles (□) in HBSS (pH.7.4) (mean ± S.D., n=3).

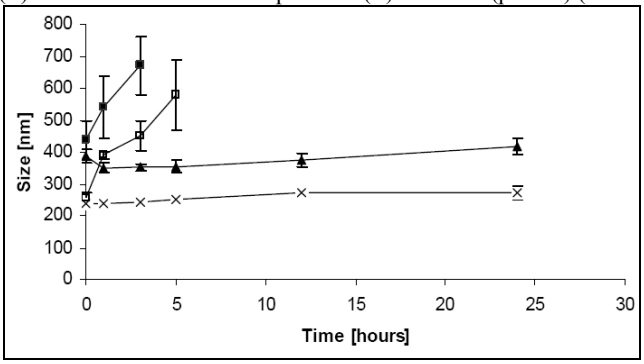

The contact between the nanoparticle formulations with both media produced an increase in size (relative to the corresponding sizes in water, see Table 1). This increase may be related to swelling, attributed to the combination of electrostatic intermolecular repulsion of TPP, HA and heparin (CS chains are partially uncharged at pH 7.4 and the interactions with polyanions become weaker) and the ionic strength of these media, as demonstrated by Lopez-Leon et al. (2005).

The stability of the nanoparticles was also assayed in water at 4°C, and the nanosystems were stable for up to three months (data not shown).

Heparin release studies from CS-HA nanoparticles

Taking into account the stability profiles of the selected systems, the release studies were performed in PBS (pH 7.4). The release kinetics of the different heparins was quite different (Fig. 3). In the case of the systems loaded with UFH, the drug was released very slowly, with final release of approximately 10% of the drug within 12 hours of incubation. Otherwise, the LMWH was released in a faster, continuous manner, with a final release of approximately 80% in the same period. Considering the high net negative charge of heparin and the positive charge of CS, a strong electrostatic interaction between these oppositely charged macromolecules is expected, resulting in slow drug release. The faster release rate observed for LMWH may be attributed to its smaller molecular weight, which allows better diffusion of the drug from the nanoparticles. There was also an appreciable difference between the drug loading values of the selected systems containing UFH and LMWH (33.6 and 60.6%, respectively). These different values may also affect the release profiles obtained for the two systems.

Figure 3: Heparin release from UFH-loaded CS-HA nanoparticles (□) and LMWH-loaded CS-HA nanoparticles (■) in PBS (pH 7.4) (means ± S.D., n=3).

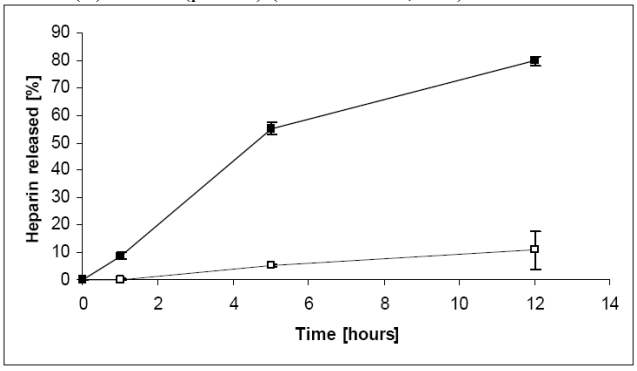

Confocal microscopy study of interaction between heparin-loaded CS-HA nanoparticles and rat mast cells

Taking into account that heparin prevents mast cell degranulation via an intracellular receptor (Ahmed et al., 2000; Wong and Koh, 2000; Niven and Argyros, 2003), we aimed to establish whether inclusion of the drug in CS-HA nanoparticles provides intracellular access to the mast cells. Thus, the interaction of fluorescent UFH-loaded CS-HA nanoparticles was observed by confocal microscopy. The overlapping of the fluorescent signal from the incubated nanoparticles (green) with that corresponding to the mast cells (red), resulted in an orange colour (Fig. 4.2). This means that the fluorescent nanoparticles effectively interacted with the mast cells after a period of contact of two hours. We confirmed that this interaction enables the nanoparticles to be internalized in mast cells by observing the fluorescent nanoparticles in sequential slides from the "z" axis of mast cells (Fig. 4.3). The positive control (Fig. 4.1) indicates that fluorescent mastocytes did not emit the signal of fluorescent nanoparticles, thus validating the results obtained.

Figure 4: Confocal laser scanning microscopy images of fluorescent mastocytes and fluorescent UFH-loaded CS-HA nanoparticles. (1) Mastocytes not incubated with nanoparticles (positive control): (a) excitation signal for mastocytes (red); (b) excitation signal for nanoparticles (no signal); (c) overlapping of both signals (red), and (d) optical signal. (2) Mastocytes after incubation with nanoparticles: (a) excitation signal for mastocytes (red); (b) excitation signal for nanoparticles (green); (c) overlapping of both signals (orange), and (d) optical signal. (3) Slides of mastocytes taken every 1.5 microns in the "z" axis, after incubation with nanoparticles. First line: excitation signal for mastocytes (red); second line: excitation signal for nanoparticles (green).

Figure 4.1

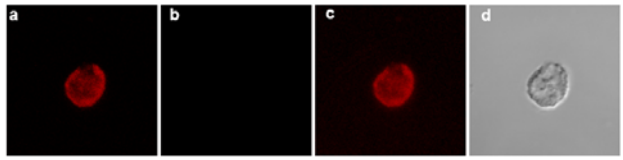

Figure 4.2

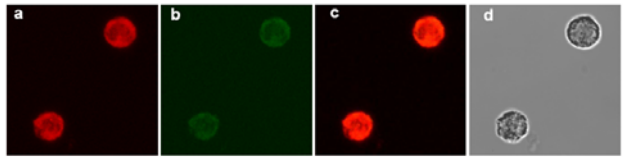

Figure 4.3

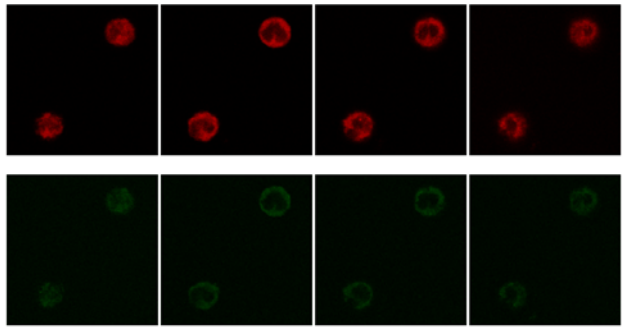

We also tested LMWH-loaded CS-HA nanoparticles, with similar results, but finally selected the systems containing UFH as that they are larger than the former and therefore may be less well internalized by rat mast cells.

Viability test of mast cells after extraction from rats and contact with UFH or LMWH-loaded nanoparticles.

The viability of rat mast cells was higher than 90% in both cases, as assessed by trypan blue staining (see Materials and Methods). The selected dose of UFH or LMWH-loaded nanoparticles to be tested in mast cells corresponded to the highest dose to be administered in the subsequent histamine release studies (equivalent to 200 μg/mL of heparin).

***Ex vivo* studies with rat mast cells: Inhibition of histamine release by heparin-loaded CS-HA nanoparticles**

Considering that heparin-loaded CS-HA nanoparticles were effectively internalized by the mast cells, we decide to evaluate and compare the capacity of heparin -administered in the form of solution or loaded in the selected nanoparticles- to prevent histamine release in rat mast cells. To our knowledge, this is the first time that such experiments have been carried out and reported.

Firstly, we tested the effect of different doses of UFH or LMWH in solution on histamine release by rat mast cells; the cells were previously stimulated with a standard substance that elicits degranulation by binding to mast cell granules (compound 48/80) (Ortner and Chignell, 1981). A dose-dependent effect was found, with no significant differences between the different types of heparin (Figure 5). This confirmed that, under these conditions, heparin was effective at preventing histamine release (IC_{50} (μg/mL) = 6.8±1.2 for UFH and 12.3±3.1 for LMWH), and demonstrated the effective range of concentrations required for this effect.

Figure 5: Effect of UFH and LMWH solutions on histamine-release from rat mast cells. Histamine release was initiated by incubating the cells with a 100 μM solution of compound 48/80 (black bar), and preincubating different concentrations of UFH (vertical-line bars) or LMWH (horizontal-line bars) before the addition of compound 48/80 (n=3, $p<0.05$).

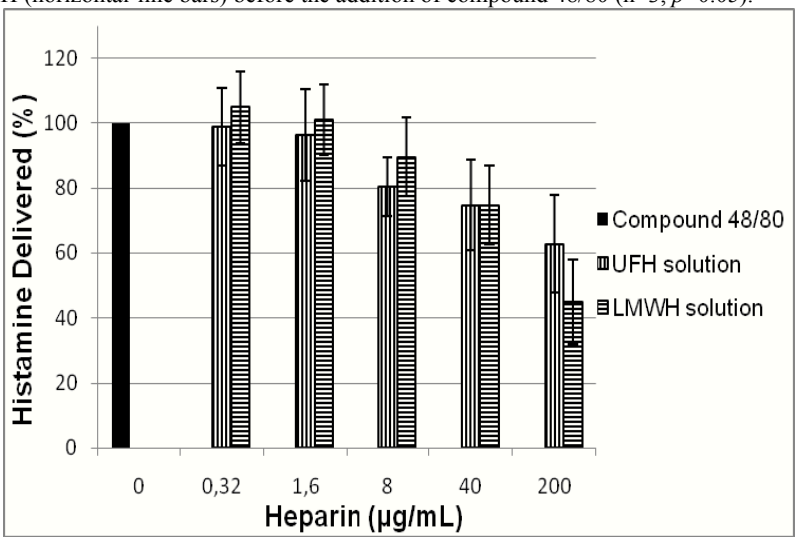

The effect of the UFH-loaded CS-HA nanoparticles in preventing histamine release, compared with that obtained with UFH solution is shown in Fig. 6a. The dose-dependent effect was maintained, with no significant differences between the UFH solution and the UFH-loaded CS-HA nanoparticles (IC_{50} (μg/mL) = 6.9±1.4 and 3.6±1.8, respectively). Blank nanoparticles did not have any effect on the release of histamine from mastocytes (the concentration of the tested blank nanoparticles was chosen according to the highest dose of heparin-loaded nanoparticles tested, thus equivalent to 200 μg/mL of heparin). A similar finding was observed on comparison of the results obtained with the LMWH in solution and LMWH encapsulated in the nanoparticles (IC_{50} (μg/mL) = 5.5±2.1 and 9.6±2.3, respectively) (Figure 6b).

Figure 6: Effect of heparin solutions and heparin-loaded CS-HA nanoparticles on histamine release from rat mast cells. Histamine release was initiated by incubating the cells with a 100 μM solution of compound 48/80 (black bar) and preincubating different concentrations of (a) UFH solution (vertical-line bars), UFH-loaded CS-HA nanoparticles (horizontal-line bars) or (b) LMWH solution (vertical-line bars), LMWH-loaded CS-HA nanoparticles (horizontal-line bars), before the addition of compound 48/80. As a control, the cells were preincubated with a fixed concentration of blank CS-HA nanoparticles (squared bars) before the addition of compound 48/80 (n=3, p<0.05).

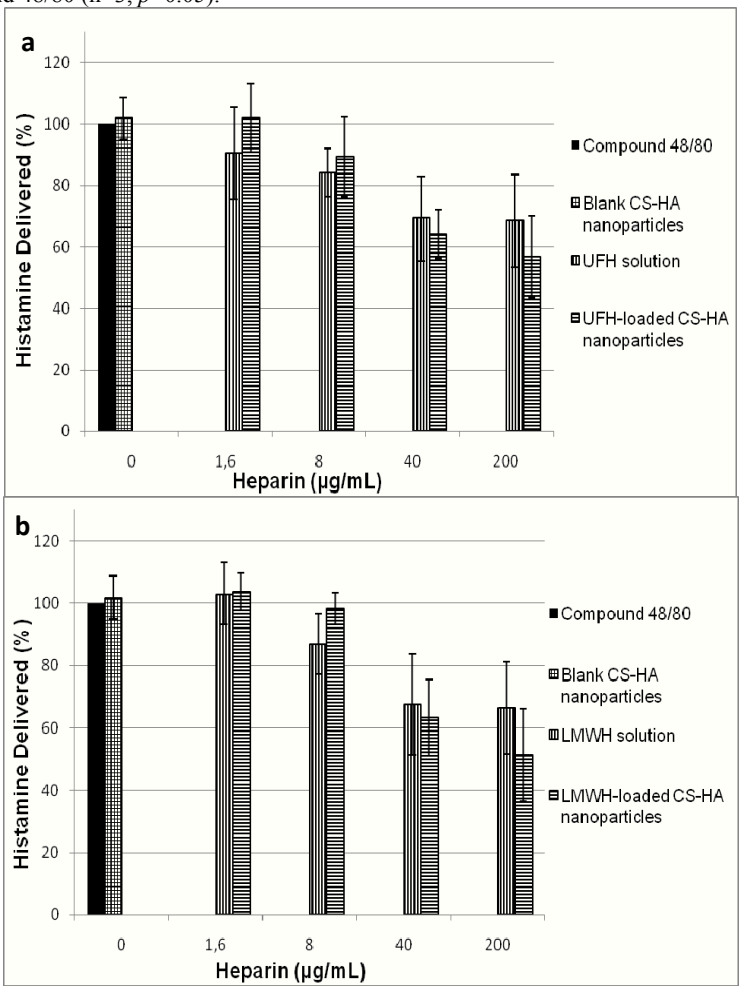

The results obtained with heparin-loaded nanoparticles are not so promising if they are compared with those obtained with heparin solutions. However, the experimental conditions do not reflect physiological barriers in airways such as mucociliary clearance (via the mucociliary escalator) and enzymatic activity. These barriers may be better overcome by the described

polysaccharide nanosystems because of the mucoadhesive-properties of CS (Aspden et al., 1997; Lim et al., 2000) and HA (Prichtard et al., 1996; Lim et al., 2000) and because of the intrinsic capacity of nanoparticles to protect the loaded drug from the enzymatic attack. Additionally, the nanoparticulate formulations may improve the effect of a conventional heparin formulation because of slow drug release, thus prolonging the antiasthmatic effect. Unfortunately, the experimental *ex-vivo* conditions do not allow long-term experiments to be carried out.

Whether CS-HA nanoparticles loaded with heparin can really improve the effect of heparin in preventing mast cell degranulation can only be answered by conducting *in-vivo* experiments. This is the next challenge in validating our hypothesis.

Conclusions

Nanosystems were produced from CS and HA and their suitability as heparin carriers for the treatment of asthma was investigated. Confocal microscopy revealed that heparin-loaded CS-HA nanoparticles were internalized by rat mast cells. However, the capacity of free heparin and of heparin encapsulated in the nanosystems to prevent histamine release was very similar, and showed the same dose-response dependence.

Acknowledgements

The authors acknowledge financial support from the Spanish Government (SAF 2004-08319-C02-01 and Consolider-Ingenio CSD 2006-00012); Felipe Oyarzun-Ampuero was in receipt of a CONICYT scholarship. J.B. received financial support from the Programa Isabel Barreto (Xunta de Galicia). We also thank Mr. Salvador Arines for technical assistance with the mast cells assays.

References

1. Ahmed, T., Ungo, J., Zhou, M., Campo, C., 2000. Inhibition of allergic late airway responses by inhaled heparin-derived oligosaccharides. J. Appl. Physiol., 88, 1721-1729.
2. Aspden, T.J., Mason, J.D., Jones, N.S., Lowe, J., Skaugrud, O., Illum, L., 1997. Chitosan as a nasal delivery system: the effect of chitosan solutions on in vitro and in vivo mucociliary transport rates in human turbinates and volunteers. J. Pharm. Sci. 86(4), 509-13.
3. Buceta, M., Dominguez, E., Castro, M., Brea, J., Alvarez, D., Barcala, J., Valdes, L., Alvarez-Calderon, P., Dominguez, F., Vidal, B., Diaz, J.L., Miralpeix, M., Beleta, J., Cadavid, M.I., Loza, M.I., 2008. A new chemical tool (C0036E08) supports the role of adenosine A(2B) receptors in mediating human mast cell activation. Biochem. Pharmacol., 76(7), 912-21.
4. Calvo, P., Remuñan-Lopez, C., Vila-Jato, J.L., Alonso, M.J., 1997. Novel hydrophilic chitosan-polyethylene oxide nanoparticles as protein carriers. J. Appl. Pol. Sci., 63, 125-132.
5. Campo, C., Molinari, J.F., Ungo, J., Ahmed, T., 1999. Molecular-weight-dependent effects of nonanticoagulant heparins on allergic airway responses. J. Appl. Physiol., 86(2), 549-557.
6. De Campos, A.M., Diebold, Y., Carvalho, E.L., Sanchez, A., Alonso, M.J., 2004. Chitosan nanoparticles as new ocular drug delivery systems: in vitro stability, in vivo fate, and cellular toxicity. Pharm. Res., 21(5), 803-10.
7. De la Fuente, M., Seijo, B., Alonso, M.J., 2008a. Bioadhesive hyaluronan-chitosan nanoparticles can transport genes across the ocular mucosa and transfect ocular tissue. Gene Ther., 15(9), 668-76.

8. De la Fuente, M., Seijo, B., Alonso, M.J., 2008b. Novel hyaluronan-based nanocarriers for transmucosal delivery of macromolecules. Macromol. Biosci., 8(5), 441-50.
9. Garcia-Fuentes, M., Prego, C., Torres, D., Alonso, M.J., 2005. A comparative study of the potential of solid triglyceride nanostructures coated with chitosan or poly(ethylene glycol) as carriers for oral calcitonin delivery. Eur. J. Pharm. Sci., 25(1), 133-43.
10. Green, W.F., Konnaris, K., Woolcock, A.J., 1993. Effect of salbutamol, fenoterol, and sodium cromoglicate on the release of heparin from sensitized human lung fragments challenged with *Dermatophagoides pteronyssinus* allergen. Am. J. Respir. Cell Mol. Biol., 8, 518-521.
11. Halayko, A.J., Recto, E., Sthepens, N.L., 1997. Characterization of molecular determinants of smooth muscle cells heterogeneity. Can. J. Physiol. Pharmacol., 75, 917-919.
12. Johnson, P.R., Armour, C.L., Carey, D., Black, J.L., 1995. Heparin and PGE2 inhibit DNA synthesis in human airway smooth muscle cells in culture. Am. J. Physiol., 269, L514-L519.
13. Kanabar, V., Hirst, S.J., O´Connor, B.J., Page, C.P., 2005. Some structural determinants of the antiproproliferative effect of heparin-like molecules on human airway smooth muscle. Br. J. Pharmacol., 146, 370-377.
14. Kilfeather, S.A., Tagoe, S., Perez, A.C., Okona-Mensa, K., Matin, R., Page, C.P., 1995. Inhibition of serum-induced proliferation of bovine tracheal smooth muscle cells in culture by heparin and related glycosaminoglycans. Br. J. Pharmacol., 114, 1442-1446.
15. Köping-Höggård, M., Sanchez, A., Alonso, M.J., 2005. Nanoparticles as carriers for nasal vaccine delivery. Expert Rev. Vaccines., 4(2),185-96.
16. Lago, J., Alfonso, A., Vieytes, M.R., Botana, L.M., 201. Ouabain-induced enhancement of rat mast cells response. Modulation by protein phosphorylation and intracellular pH. Cell Signal., 13(7), 515-24.

18. Lim, S.T., Martin, G.P., Berry, D.J., Brown, M.B., 2000. Preparation and evaluation of the in vitro drug release properties and mucoadhesion of novel microspheres of hyaluronic acid and chitosan. J. Control. Rel., 66, 281-292.
18. Lopez-Leon, T., Carvalho, E.L., Seijo, B., Ortega-Vinuesa, J.L., Bastos-Gonzalez, D., 2005. Physicochemical characterization of chitosan nanoparticles: electrokinetic and stability behavior. J. Colloid Interface Sci., 283(2), 344-51.
19. Martinez-Salas, J., Mendelssohn, R., Abraham, W.M., Hsiao, B., Ahmed, T., 1998. Inhibition of allergic airway responses by inhaled low-molecular-weight heparins: molecular-weight dependence. J. Appl. Physiol., 84(1), 222-228.
20. Molinari, J.F., Campo, C., Shahida, S., Ahmed, T., 1998. Inhibition of antigen-induced airway hyperresponsiveness by ultralow molecular-weight heparin. Am. J. Respir. Crit. Care Med., 157, 887-893.
21. Niven, A.S., Argyros, G., 2003. Alternate treatments in asthma. Chest., 123(4), 1254-65.
22. Ortner, M.J., Chignell, C.F., 1981. The effect of concentration on the binding of compound 48/80 to rat mast cells: a fluorescence microscopy study. Immunopharmacology, 3(3), 187-91.
23. Page, C.P., 1991. One explanation of the asthma paradox: inhibition of natural anti-inflammatory mechanism by beta 2-agonist. Lancet, 337, 717-720.
24. Page, S., Ammit, A.J., Black, J.L., Armour, C.L., 2001. Human mast cell and airway smooth muscle cell interactions: implications for asthma. Am. J. Physiol. Lung Cell. Mol. Physiol., 281, L1313-L1323.
25. Prego, C., García, M., Torres, D., Alonso, M.J., 2005. Transmucosal macromolecular drug delivery. J. Control Release., 101(1-3), 151-62.
26. Prichtard, K., Lansley, A.B., Martin, G.P., Helliwell, M., Marriot, C., Benedetti, L.M., 1996. Evaluation of the bioadhesive properties of

hyaluronan derivates: detachment weight and mucocilliary transport studies. Int. J. Pharm., 129, 137-145.

27. Robinson, D.S., 2004. The role of the mast cell in asthma: induction of airway hyperresponsiveness by interaction with smooth muscle? J. Allergy Clin. Immunol., 114, 58-65.
28. Wong, W.S., Koh, D.S., 2000. Advances in immunopharmacology of asthma. Biochem Pharmacol., 59(11), 1323-35.

Capitulo 3

A potential nanomedicine consisting in heparin-loaded polysaccharide nanocarriers for the treatment of asthma

Abstract

The aim of this study is to produce and characterize a new nanomedicine consisting of chitosan (CS)/carboxymethyl-β-cyclodextrin (CMβCD) loaded with unfractioned or low-molecular-weight heparin (UFH or LMWH, respectively), and evaluate its potential in asthma treatment. The nanoparticles are prepared by ionotropic gelation showing a size ranged between 221 and 729 nm with a positive zeta potential. The drug association efficiency is higher than 70%. Developed nanosystems are stable in Hank's balanced salt solution pH 6.4, releasing slowly the drug. Ex vivo assays, show that nanocarriers led to an improvement of heparin at preventing mast cell degranulation. These results agree with the effective cellular internalization of the fluorescently-labelled nanocarriers, and postulate these nanomedicines as promising formulations for asthma treatment.

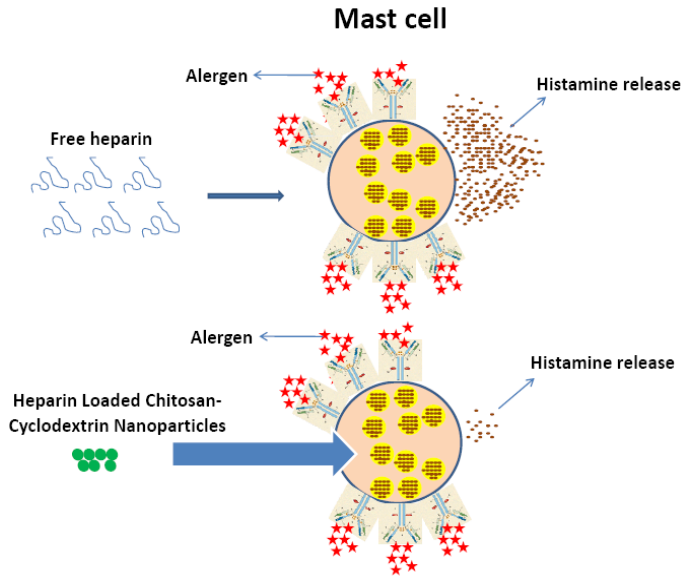

Keywords: chitosan; cyclodextrins; heparin delivery; mast cells; nanoparticles.

Introduction

Over the last few decades, the design of new delivery approaches for the administration of drugs by the pulmonary route has received increasing attention. These delivery efforts have taken advantage of the physiological characteristics of this organ (i.e. large superficial area, thin epithelial barrier, great vascularization, and low proteolitic activity) which offer possibilities for systemic and local treatments.[1] Within this context, the use of polymeric carriers represents an attractive strategy for the pulmonary delivery of macromolecular compounds.[1-3]

A variety of nanocarriers have been investigated for the delivery of macromolecules to the respiratory tract.[4-10] Among these, chitosan (CS)-based nanocarriers have shown a degree of success for the delivery of macromolecules across the nasal and pulmonary mucosae.[11-18] Overall, these reports have shown that CS-based nanocarriers have an important capacity for the association of macromolecular drugs and are able to facilitate their intracellular access, thus leading to a significant enhancement of their in vivo efficacy.

In our view, a particularly promising CS-based nanocarrier for pulmonary drug delivery is the one composed of CS and cyclodextrins. Indeed, using the CALU-3 model epithelial cell line, we have shown that these hybrid nanoparticles are able to enter in the intracellular space. Moreover, we could confirm this ability to overcome the epithelial barrier in vivo following nasal administration.[19-20] These facts together with the reduction of the cellular toxicity of the nanostructures due to the presence of cyclodextrins suggest the potential of this nanocarrier for nasal and pulmonary drug delivery.

Taking into account the favorable characteristics of CS-cyclodextrins nanoparticles for pulmonary drug delivery, we selected heparin as a drug which could potentially benefit from this delivery approach. Heparin is a

macromolecular drug that has been classically used as an anti-coagulant, however, recently, there has been an accumulated evidence of the antiasthmatic activity of this molecule. In particular, the activity of inhaled heparin has been systematically studied by Ahmed and co-workers in a sheep model,[21-23] and also in humans.[24-26] This previous work has led to a number of conclusions such as i) the antiashmatic activity of heparin is related to its capacity for inhibiting the degranulation of mast cells by interacting with the intracellular receptor of inositoltrisphosphate (IP_3); (ii) the potency of heparin is inversely proportional to its molecular weight; iii) the antiasthmatic effect of heparin is independent to its antiacoagulant activity.

Therefore, our aim in this work was to explore the potential of CS-cyclodextrin nanoparticles for the targeted intracellular delivery of heparin into mast cells. Therefore, we associated heparin to the nanoparticles and evaluated their capacity to enter mast cells and preventing histamine release.

Experimental Section

Materials

Ultrapure CS hydrochloride salt (CS; UP CL 113, molecular weight ~125 kDa and degree of acetylation 14%) was purchased from Pronova Biopolymer AS (Oslo, Norway). Na-carboxymethyl-β-cyclodextrin (CMβCD, molecular weight 1375 Da) having a substitution degree of 3.0-3.5 was purchased from Fluka GmbH (Buchs, Switzerland). Unfractionated heparin sodium salt (UFH, molecular weight ~18 kDa, 202 USP units/mg), low-molecular-weight heparin sodium salt (LMWH, molecular weight ~4 kDa, 53 USP units/mg) and pentasodiumtripolyphosphate (TPP) were purchased from Sigma Aldrich (Madrid, Spain). All other solvents and chemicals were of the highest commercially available grade.

Preparation of Nanoparticles

CS-CMβCD nanoparticles loaded with heparin were prepared according to the procedure previously developed by our group.[27] Nanoparticles were spontaneously obtained by ionotropic gelation between the positively charged amino groups of CS and the negatively charged CMβCD, TPP and heparin. Briefly, 1.5 mL of a mixture of an aqueous solutions of CMβCD (0-1.33 mg/mL), TPP (0-0.23 mg/mL) and UFH (0.67-1.4 mg/mL) or LMWH (1.07 mg/mL) were added to 3 mL of a CS solution (0.2% w/v, pH 4.9) under magnetic stirring at room temperature. Magnetic stirring was maintained for 10 min to enable complete stabilization of the system. The nanoparticles were transferred to Eppendorf tubes and isolated by centrifugation in 20 μL of a glycerol bed (16000 × *g*, 30 min, 25º C). Supernatants were collected and the nanoparticles were then suspended in ultrapure water by shaking on a vortex mixer.

The production yield of the systems was obtained by centrifugation of fixed volumes of the nanoparticle suspension (16000 × *g*, 30 min, 25º C), without the glycerol bed. The supernatants were discarded and the systems were freeze-dried. The yield was calculated as follows:

$$\text{Yield} = \frac{\text{Nanoparticles Weight}}{\text{Total Amount of the Components}} \times 100 \quad (1)$$

Physicochemical Characterization of Heparin-Loaded CS-CMβCD Nanoparticles

The size and zeta potential of the colloidal systems were determined by photon correlation spectroscopy and laser Doppler anemometry, with a Zetasizer Nano-ZS (Malvern Instruments, United Kingdom). Each batch was analyzed in triplicate.

Morphological examination of the nanoparticles was performed by transmission electron microscopy (TEM) (CM12 Phillips, Netherlands). The samples were stained with 1% (w/v) phosphotungstic acid for 10 s, immobilized on copper grids with Formvar® and dried overnight for viewing by TEM.

Association Efficiency and Drug Loading of Heparin-Loaded CS-CMβCD Nanoparticles

The association efficiencies of the selected formulations were determined after isolation of nanoparticles by centrifugation as described in Section 2.2. The amount of unbound heparin in the supernatant was determined by a colorimetric method (Stachrom® Heparin, DiagnosticaStago, France).

The association efficiency of heparin and the drug loading were calculated as follows:

$$\text{Association efficiency} = \frac{\text{Total amount of drug} - \text{Amount of unbound drug}}{\text{Total amount of drug}} \times 100 \quad (2)$$

$$\text{Drug Loading} = \frac{\text{Total amount of drug} - \text{Amount of unbound drug}}{\text{Nanoparticles weight}} \times 100 \quad (3)$$

Stability Study

Selected nanoparticles formulations were prepared and centrifuged in the presence of glycerol. Nanoparticles were tested for their stability taking into account the change in size of nanoparticles and possible precipitations in different media at 37º C, including: Hank's balanced salt solution (HBSS) at pH 6.4 and 7.4, and phosphate buffered saline (PBS), at pH 7.4 (for

composition of these solutions, see below). Nanoparticles were incubated in these media and samples were collected at several time intervals (0, 1, 3, 5, 10 and 24 h), and the size distribution of the nanoparticles was measured by photon correlation spectroscopy.

The composition of HBSS was: 137 mMNaCl, 5.4 mMKCl, 0.25 mM Na_2HPO_4, 0.44 mM KH_2PO_4 and 4.2 mM $NaHCO_3$.

The composition of PBS was: 137 mMNaCl, 2.7 mMKCl, 1.4 mM NaH_2PO_4 and 1.3 mM Na_2HPO_4.

In Vitro Heparin Release Studies from CS-CMβCD Nanoparticles

Heparin release studies were performed by incubating 0.1 mg of the selected nanoparticles in 1 mL of HBSS (pH 6.4) at 37º C. The sample were centrifuged at appropriate time intervals (1, 5 and 12 h), and the amount of heparin released was evaluated with the heparin kit described above.

Study of Interaction of Fluorescent Heparin-Loaded CS-CMβCD Nanoparticles with Rat Mast Cells by Confocal Microscopy

Fluorescein Labelling to CS: CS was labelled with fluorescein following a slight modification of the method described by De Campos et al.[28] The covalent attachment of fluorescein to CS was by the formation of amide bonds between primary amino groups of the polymer and the carboxylic acid groups of fluorescein. Briefly, 250 mg of CS was dissolved in 25 mL of water, and 10 mg of fluorescein (Sigma Aldrich, Spain) was dissolved in 1 mL of ethanol. These solutions were then mixed, and EDAC (1-ethyl-3-(dimethylaminopropyl) carbodiimide hydrochloride) (Sigma Aldrich, Spain) was added to a final concentration of 0.05 M, to catalyze the formation of amide bonds. The reactive mixture was incubated under permanent magnetic stirring for 12 h in the dark, at room temperature. The resulting conjugate

was finally isolated by dialysis for 72 h (cellulose dialysis tubing, pore size 12400 Da; Sigma Aldrich, Spain) against demineralised water, and freeze-dried. The pH of fluorescent CS was adjusted to the same value as the raw CS solution (pH 4.9) with HCl, for the preparation of fluorescent nanoparticles.

Preparation of Fluorescent Heparin-Loaded CS-CMβCD Nanoparticles: Fluorescent nanoparticles were prepared according to the same procedure explained in 2.2. The selected mass distribution for the preparation of fluorescent nanoparticles was: 6 mg of fluorescent CS, 0.85 mg of CMβCD, 0.34 mg of TPP and 1.6 mg of UFH.

Confocal Laser Scanning Microscopy Study: An aqueous solution (50 μL) containing 0.3 mg of isolated fluorescent UFH-loaded CS-CMβCD nanoparticles was incubated with 450 μL of a suspension of mast cells ($10x10^3$ cells/100 μL) in Umbreit (for composition, see below) containing 0.05% w/v of BSA. The mixture was incubated for 2 h at 37 °C, and the cells were then separated by centrifugation (10 min, 200x*g*) and discarding the supernatants. Two hundred μL of Umbreit+BSA solution (at 4 °C) were then added to the cell pellet. The pellet was resuspended and centrifuged again to extract the non-internalized nanoparticles. This procedure was repeated once more. Mast cells were fixed for 5 minutes in paraformaldehyde (2% w/v, 100 μL) and washed 3 times with the Umbreit+BSA solution, by centrifugation. Two hundred μL of a Bodipi® phalloidin solution (Invitrogen, USA) were added to the cell pellet and the cells were incubated for 30 min at room temperature. The cells were washed 3 times (Umbreit+BSA) by centrifugation, the supernatant was discarded, and the pellet was resuspended in 20 μL of the Umbreit+BSA solution. The resuspended sample was placed on the surface of a positively charged microscope slide (Superfrost Ultra Plus, Menzel-Glaser, Irland) and dried at room temperature overnight. The

sample was prepared in Vectashield medium (Vector, USA) for visualization by confocal microscopy (CLSM, Zeiss 501, Germany) (all of the described procedures were carried out in darkness to prevent the loss of the fluorescent signal from the nanoparticles and mast cells).

The composition of Umbreit saline solution was: 1.2 mM $MgSO_4$, 1.2 mM $NaPO_4H_2$, 22.85 mM $NaHCO_3$, 5.94 mMKCl, 1 mM $CaCl_2$, 119 mMNaCl and 0.1% glucose.

Ex Vivo Studies With Rat Mast Cells: Inhibition of Histamine Release by Heparin-Loaded CS-CMβCD Nanoparticles

Animal procedures were conducted in accordance with the standard ethical guidelines (National Institutes of Health, 1995; Council of Europe, 1996) and approved by the local ethical committees.

Rat Mast Cell Purification and Viability: Mast cells were obtained by lavage of pleural and peritoneal cavities of female Sprague - Dawley rats (400–800 g) with Umbreit saline solution, following procedures similar to those described in other studies.[29-30] The suspension obtained from each rat was centrifuged at 100x*g* for 5 min (4 ºC) and suspended in a final volume of 1 mL of Umbreit containing 0.05% w/v of BSA. Purification was carried by centrifugation on 4 mL of an isotonic Percoll gradient at 600 *g* for 10 min (4 ºC). The mast cells were washed twice with the Umbreit+BSA solution and maintained at 4 °C in this solution until use. Mast cells were quantified by toluidin blue staining (95% purity) and the viability (90%) assessed by trypan blue staining (the procedure is described below).

Trypan blue staining procedure: Mast cell viability studies were carried out by trypan blue staining in an inverted microscope, as described by Lago et al.[29] This involved visual counting of the stained cells in the five fields of a counting chamber. The percentage of viability was calculated with the following formula:

$$\text{Trypan Blue Stained Cells} = \frac{\text{Aritmetic Mean From the Five Fields}}{\text{Total Number of Mast Cells}} \times 100 \quad (4)$$

In order to test the mast cell viability after contact with heparin-loaded nanoparticles, the same procedure was used, and the UFH or LMWH-loaded CS-CMβCD nanoparticles added to the rat mast cell suspension ($1x10^5$ cells per test tube). The tested dose of nanoparticles was equivalent to 200 μg/mL of UFH or LMWH.

Measurement of Histamine Release in Rat Mast Cells: Rat mast cells ($1x10^5$ cells per test tube) were pre-warmed at 37 ºC (10 min) in BSA-free Umbreit saline solution containing the UFH or LMWH solutions or the nanoparticles loaded with UFH or LMWH. Histamine release from mast cells was then initiated by incubating the cells with 100 μM of compound 48/80 (Sigma Aldrich, Spain) for 20 min at 37 ºC. The cells were then centrifuged at 1100x*g* for 3 min at 4 ºC, and two aliquots (100 μl) of the supernatants were collected in a 96-well microplate. The rest of the supernatants were discarded and the pellets were resuspended in 500 μL of HCl 0.1 M, sonicated for 1 min and centrifuged at 1100 x*g* for 6 min. Two aliquots of 100 μL of the supernatants were collected for residual histamine determination. Histamine was assayed fluorometrically, as described by Lago et al.[29]; briefly, 80 μL NaOH 1 M were added to 100 μL of the sample, then 50 μl phthaldialdehyde 0.04% w/v were added to each well and plate was incubated for 4 min at 25° C. After this time, 50 μl of 3 M HCl were added and fluorescence was measured within 20 min, at excitation and emission wavelengths of 360 nm

and 465 nm respectively, in a Tecan Ultra Evolution reader (Tecan, Switzerland).

Data Analysis for Measurement of Histamine Release in Rat Mast Cells: Results were expressed as percentage of the total histamine released after stimulation with compound 48/80. The results were corrected for spontaneous histamine release in the absence of any chemical and under the same conditions. The equation used for the calculation was HR=[(S−ER)/(S+P−ER)]×100, where HR is the percentage histamine release; S, supernatant fluorescence; ER, fluorescence of spontaneous release supernatants and P, pellet fluorescence.

IC_{50} values were obtained by fitting the data with non-linear regression, with Prism 2.1 software (GraphPad, San Diego, CA).

Statistical Analysis

The statistical significance of the differences between formulations was determined by application of two-way analysis of variance (ANOVA) followed by a two-tailed paired Student's test. Differences were considered significant at $p<0.05$.

Results and Discussion

It has been reported that heparin could potentially be used for the treatment of asthma. However, this potential use is constrained by its limited access into the mast cells where target receptors for preventing degranulation are located.[31-32] This limited access could be related to the electrostatic repulsion between this highly negative macromolecule and the mastocyte membranes. Therefore, the hypothesis of this work was that the incorporation

of heparin into nanocarriers could neutralize its charge and facilitate the internalization and controlled release of the drug into the mast cells.

Preparation and Characterization of Heparin-Loaded CS-CMβCD Nanoparticles

Nanoparticles loaded with heparin were prepared by the ionotropic gelation technique. The ability of CS to form a gel after contact with polyanions by promoting inter and intramolecular linkages enables the formation of the nanoparticles.[33] In this case, an ionic interaction occurs between the positively charged CS and the negatively charged CMβCD, heparin and the polyanion TPP. The ionic gelation process is extremely simple and involves mixing two aqueous phases at room temperature.

As a first approximation for the formation of adequate nanoparticle formulations, we assayed different ratios of the three anionic components of the nanomedicines. Then, we identified the ratio between components that enabled the formation and also the adequate isolation of nanosystems. Table 1 shows size, polydispersity index, and zeta potential of a variety of formulations tested with UFH. Valuable information extracted from these experiments is that when the amount of polyanions was too low (relative to CS), nanoparticles could not be formed. However, if the amount of polyanions was too high, the particles precipitated or aggregated during the isolation process. This behavior could be attributed to the gradual counterionization of the positively charged CS, as noted by the reduction in the positive zeta potential values of the nanosystems.

All the resulting nanosystems loaded with UFH exhibited a size in the range of 350-730 nm; polydispersity values were between 0.2-1 and the positive zeta potential ranged from +33.2 to +40.7 (Table 1). These ranges of values are similar to those previously presented by Krauland et. al.[27] who developed different formulations of UFH loaded in CS-CMβCD or CS-TPP

nanoparticles. Among the formulation developed in this study, the one comprising 6 mg of CS, 0.85 mg of CMβCD, 0.34 mg of TPP and 1.6 mg of UFH was selected for further studies including in vitro characterization and ex vivo efficacy.

Table 1: Physicochemical properties of the nanoparticles prepared with different ratios of CS-CMβCD-TPP-heparin (mean ± S.D., n=3).

Amount [mg] CS-CMβCD-TPP-heparin	Size [nm]	Polydispersity Index	Zeta potential [mV]
6-1-0-1[a]	359 ± 21	0.3 – 0.4	+40.7 ± 1.0
6-2-0-2[a]	729 ± 54	0.8 – 1	+33.2 ± 0.8
6-2-0-2.1[a]	Non resuspendable	---	---
6-0.85-0.34-1.6[a]	375±69	0.3 – 0.5	+37.0 ± 1.6
6-1-0.34-1.6[a]	473 ± 24	0.6 – 0.9	+34.7 ± 1.2
6-1.15-0.34-1.6[a]	Non resuspendable	---	---
6-1.3-0.34-1.6[a]	Precipitation	---	---
6-0.85-0.34-1.6[b]	221± 26	0.2 – 0.3	+36.8 ± 0.7

[a]= UFH; [b] = LMWH

Importantly, the association efficiency of UFH in the selected formulation was 77.0%. This high association value is related to the capacity of the polyanion to interact avidly with the polycationic CS as previously shown for other CS-based nanosystems.[27,30]

With the aim of elucidating the influence of the heparin Mw in the in vitro and ex vivo behavior of the heparin-loaded nanoparticles, we also used a low-molecular-weight-heparin (LMWH). This new formulation exhibited similar values of zeta potential and association efficiency, however the size and polydispersity values were smaller when compared to those of high Mw heparin-loaded nanoparticles (Table 1). This could be attributed to a tighter assembling of the components forming the nanoparticles. The differences between the two formulations are also illustrated in the TEM micrographs presented in Figure 1a and b. It should be noted that the nanosystems containing LMWH form a smaller and denser structure than those containing

UFH. The photographs also show the spherical shape of nanosystems, this is in agreement with previous works describing nanoparticles prepared following the same method.[27,30]

Figure 1: Electron transmission micrographs of CS-CMβCD nanoparticles containing UFH (a) or LMWH (b).

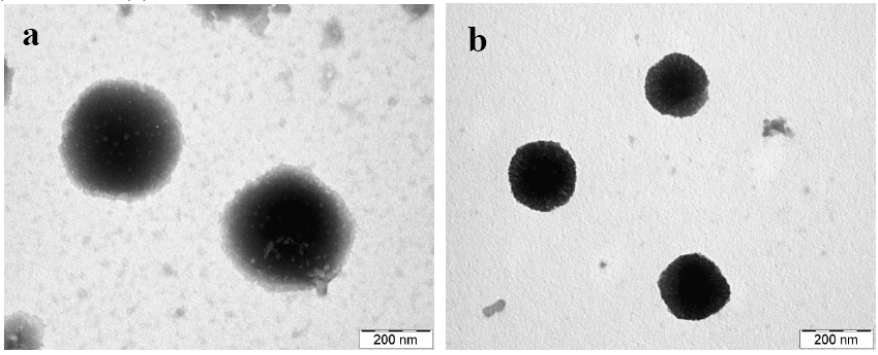

Stability Studies

The stability of the selected systems was investigated in media that mimics biological conditions and that are usually used in cell culture studies. These media included: HBSS (pH 6.4 and 7.4) and PBS (pH 7.4). The stability of the selected nanoparticles loaded with UFH and LMWH was maintained for up to 24 h in HBSS pH 6.4 (Figure 2) while in the other media the nanoparticles aggregated immediately (data not shown). The zeta values of the selected UFH/LMWH-loaded nanoparticles in HBSS pH 6.4 were approximately +14 mV, due to the presence of ionizable groups of CS in this medium. In contrast, the zeta values of the systems in HBSS pH 7.4 and PBS 7.4 were neutral (≈0 mV), thus, making the systems vulnerable to aggregation. The stability of the nanoparticles was also assayed in water at 4° C, where formulations maintained stable for up three months (data not shown).

Figure 2: Stability of heparin-loaded CS-CMβCD nanosystems in HBSS pH 6.4: UFH-loaded nanoparticles (■) and LMWH-loaded nanoparticles (×) (mean ± S.D., n=3).

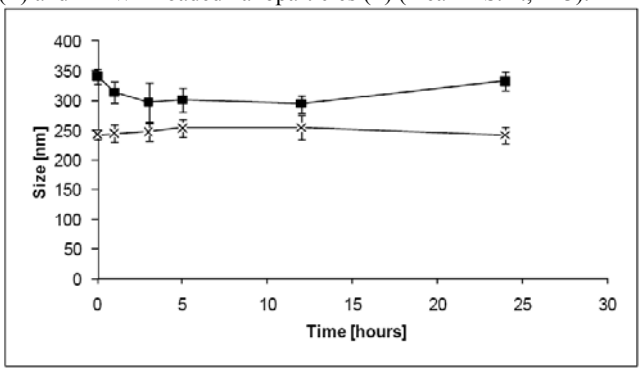

Release Studies From Selected Nanosystems

As shown in Figure 3, the release kinetics of heparins in HBSS pH 6.4 was slow and clearly dependent on their molecular weight. In the case of the systems comprising LMWH, the drug was released very slowly during the first hour (approximately 10% of the encapsulated drug) followed by a plateau phase with little further change up to 12 h of incubation. Otherwise, the UFH was released in a faster, continuous manner, with a final release of approximately 50% in the same period of incubation. The slower release rate observed for LMWH could be attributed to the more packed structure of these nanosystems as we previously argument. The slow release rate observed for nanosystems loaded with UFH or LMWH agrees with the results obtained for other formulations comprising CS and heparin and is attributed to the strong ionic interaction among the anionic drug and the cationic polymer.[30]

Figure 3: Heparin release from UFH-loaded CS-CMβCD nanoparticles (□) and LMWH-loaded CS-CMβCD nanoparticles (■) in HBSS pH 6.4 (means ± S.D., n=3).

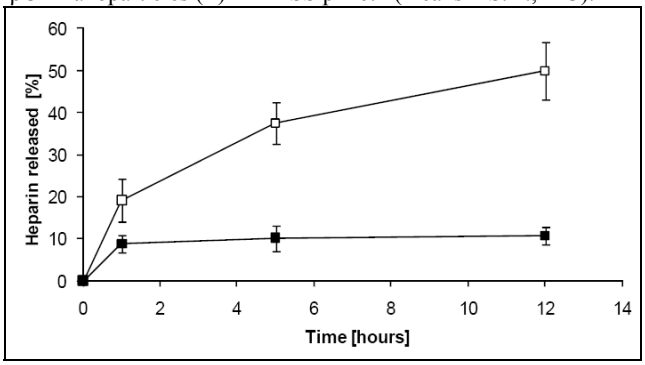

Study of Interaction of Heparin-Loaded CS-CMβCD Nanoparticles with Rat Mast Cells by Confocal Microscopy

Taking into account that the antiasthmatic effect of heparin is attributed to its capacity of preventing the mast cell degranulation via the intracellular receptor of IP_3,[34-35] the capacity of the selected nanosystems to gain intracellular access is a fundamental requisite. Thus, we performed confocal microscopy experiments for visualizing the interaction-transport of fluorescent heparin-loaded CS-CMβCD nanoparticles in rat-mast cells. In Figure 4.2, it can be seen that the overlapping of the fluorescent signal from the incubated UFH-loaded CS-CMβCD nanoparticles (green) with that corresponding to the mast cells (red), resulted in an orange color. This means that the fluorescent nanoparticles effectively interacted with the mast cells after a period of contact of two hours. We confirmed that this interaction enables the nanoparticles to be internalized in mast cells by observing the fluorescent nanoparticles in sequential slides from the "z" axis of mast cells (Fig. 4.3). The positive control (Fig. 4.1) indicates that fluorescent mastocytes did not emit the signal of fluorescent nanoparticles. The confocal images obtained upon treatment of cells with fluorescent LMWH-loaded CS-CMβCD nanoparticles, were similar to those reported in Figure 4.3. Overall,

this capacity of heparin-loaded CS-CMβCD nanoparticles for entering in the rat mast cells is similar to that previously observed for heparin-loaded CS-hyaluronic acid nanoparticles.[30] This capacity could be attributed to the nanometric characteristic of the systems and also to the capacity CS for interacting with cellular membranes and promoting the intracellular access of the nanosystems.[20, 36]

Figure 4: Confocal laser scanning microscopy images of fluorescent mastocytes and fluorescent UFH-loaded CS-CMβCD nanoparticles. (1) Mastocytes not incubated with nanoparticles (positive control): (a) excitation signal for mastocytes (red); (b) excitation signal for nanoparticles (no signal); (c) overlapping of both signals (red), and (d) optical signal. (2) Mastocytes after incubation with nanoparticles: (a) excitation signal for mastocytes (red); (b) excitation signal for nanoparticles (green); (c) overlapping of both signals (orange), and (d) optical signal. (3) Slides of mastocytes taken every 1.5 microns in the "z" axis, after incubation with nanoparticles. First line: excitation signal for mastocytes (red); second line: excitation signal for nanoparticles (green).

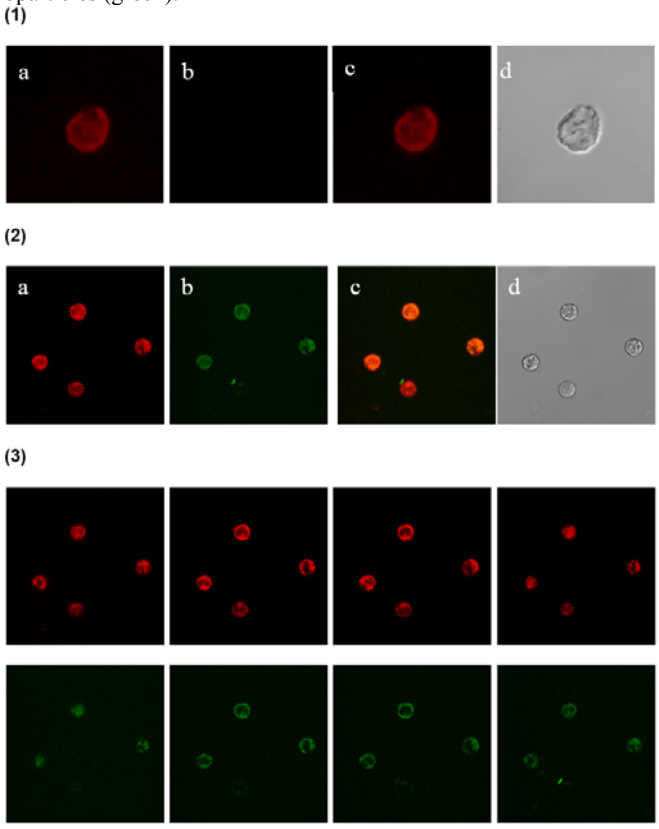

Ex Vivo Studies with Mast Cells for Preventing the Histamine Release

With the aim of evaluating the potential of these new prototypes as nanomedicines for treating asthma, we tested and compared the capacity of heparin solutions and heparin-loaded CS-CMβCD nanoparticles to prevent histamine release in rat mast cells. The histamine release was initiated by stimulating the cells with a standard substance that elicits degranulation by binding to mast cell granules (compound 48/80).[37] Figure 5a shows the effect of the formulation containing UFH on histamine release. The results show a dose-dependent effect for both UFH solution and UFH-loaded nanoparticles. This behavior is similar to the one previously reported for UFH-loaded CS-hyaluronic acid nanoparticles.[30] Importantly, a dramatic effect in terms of preventing histamine release was achieved for the highest dose of UFH-loaded CS-CMβCD nanoparticles (≈90% of inhibit inhibition); an effect that was much less important for UFH in solution (≈55% of inhibition). This positive behavior contrasts with the one reported for CS-AH nanoparticles, which effect at preventing histamine release was similar than that obtained with heparin administered in solution.[30] Consequently, we attributed such positive effect to the presence of CMβCD in the formulation and its recognized role in improving the permeability of drugs through cellular membranes. Moreover, the dose-dependent positive effect of nanoparticles could be related to the dose-dependent permeabilizing effect of ciclodextrins. Blank nanoparticles did not have any significant effect on the release of histamine from mastocytes (the concentration of the tested blank nanoparticles was equivalent to those administered when 200 μg/mL of heparin was administered in the nanoparticles).

On the other hand, as shown in Figure 5b, the systems containing LMWH, produce an effect that is similar to those observed for the UFH-loaded nanosystems. Again, the effect obtained with the highest tested dose

of heparin-loaded nanoparticles significantly improved those obtained upon treatment with LMWH in the solution.

Figure 5: Effect of heparin solutions and heparin-loaded CS-CMβCD nanoparticles on histamine release from rat mast cells. Histamine release was initiated by incubating the cells with a 100 μM solution of compound 48/80 and preincubating different concentrations of (a) UFH solution and UFH-loaded CS-CMβCD nanoparticles or (b) LMWH solution and LMWH-loaded CS-CMβCD nanoparticles, before the addition of compound 48/80. As a control, the cells were preincubated with a fixed concentration of blank CS-CMβCD nanoparticles before the addition of compound 48/80 (n=3, p<0.05).

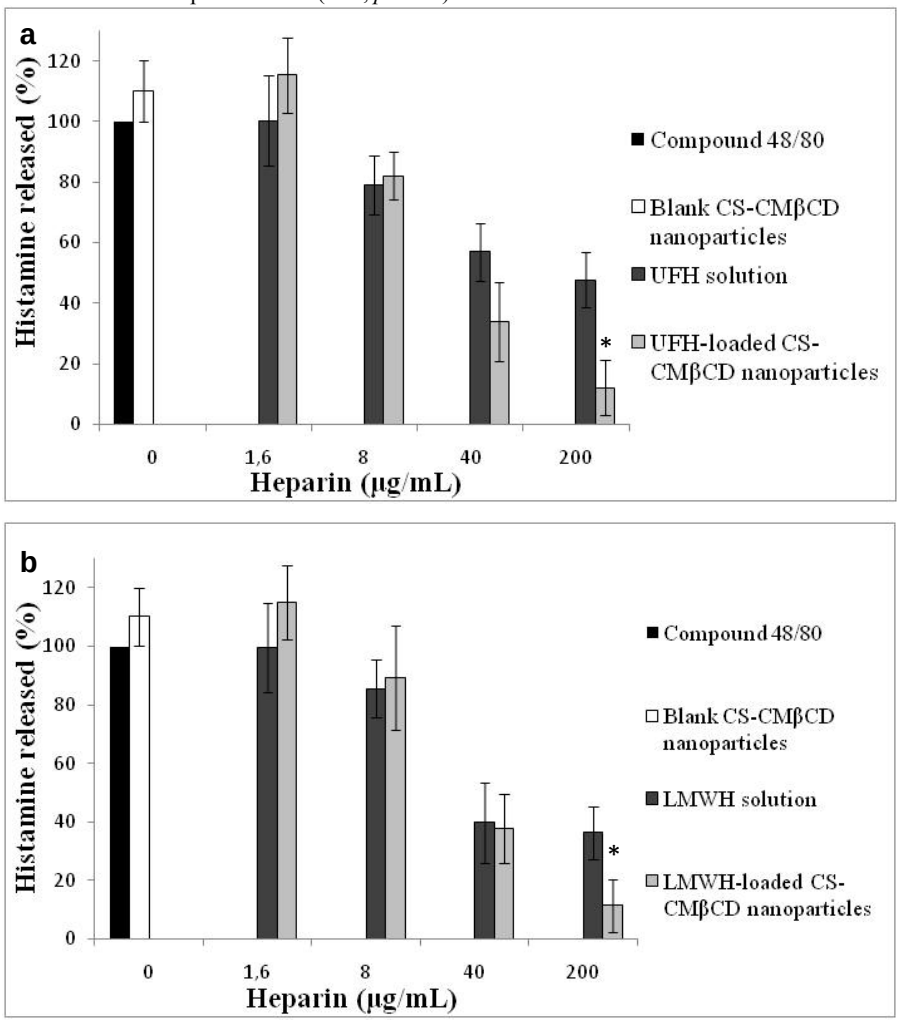

Importantly, the viability of the mast cells after the addition of the UFH/LMWH-loaded nanoparticles was, in all cases, similar to that presented

by mastocytes after the extraction from rats (90%), thus discarding any toxic effect of the tested nanoparticles-doses.

The results obtained with heparin-loaded CS-CMβCD nanoparticles in terms of preventing histamine release are promising and indicate that nanoparticle-composition is crucial in order to achieve the desired effect.[30] These results together with those previously reported on the low toxicity of CS-CMβCD nanoparticles in CALU-3 cells,[20] support the potential use of these nanoparticles for the treatment of asthma.

Finally, it is important to note that the ex vivo conditions carried out in these works do not reflect the physiological barriers in the airways such as mucociliary clearance (via the mucociliary escalator) and enzymatic activity. These barriers should be overcome by the described polysaccharide nanosystems because of the mucoadhesive-properties of CS,[38-39] and the intrinsic capacity of nanoparticles to protect the loaded drug from enzymatic attack. In fact, there are some examples in the literature showing the topical efficacy of CS nanoparticles for the pulmonary delivery of active molecules for treating tuberculosis[40-41] and cancer[42].

In addition, it could be expected that the nanoparticle-formulations presented here would improve the effect of a conventional heparin formulation because of the slow drug release. Unfortunately, the experimental conditions do not allow long-term experiments to be carried out for validating the above hypothesis. Ultimately, in vivo experiments would be necessary in order to validate the potential of these new nanomedicines for the treatment of asthma.

Conclusion

Nanosystems were produced from CS and CMβCD and their suitability as heparin carriers for the treatment of asthma was investigated. Confocal microscopy revealed that heparin-loaded CS-CMβCD nanoparticles were internalized by rat mast cells. Experiments in mast cells indicated that the association of heparin to the nanocarriers led to a significant improvement of the efficacy of this drug measured in terms of preventing mast cell degranulation. To the best of our knowledge, this is the first evidence of the enhanced efficacy of heparin presented in the form of a nanomedicine for the treatment of asthma.

Acknowledgements: The authors acknowledge financial support from the Spanish Government (SAF 2004-08319-C02-01 and Consolider-Ingenio CSD 2006-00012); Felipe Oyarzun-Ampuero was in receipt of a CONICYT scholarship. J.B. received financial support from the Programa Isabel Barreto (Xunta de Galicia). We also thank Mr. Salvador Arines for technical assistance with the mast cells assays.

References

1. M. Bur, A. Henning, S. Hein, M. Schneider, C.M. Lehr, *Inhalation Toxicology* 2009, *21(S1)*, 137.
2. B.D. Curmi, J. Kayat, V. Gajbhiye, R.K. Tekade, N.K. Jain, *Expert Opin. Drug Deliv.* 2010, *7(7)*, 781.
3. H.H. Mansour, Y.S. Rhee, X. Wu, *Int. J. Nanomed.* 2009, *4*, 299.
4. M.N.V.R. Kumar, S.S. Mohapatra, X. Kong, P.K. Jena, U. Bakowsky, C.M. Lehr, *J. Nanosci. Nanotech.* 2004, *48*, 990.

5. N. Nafee, S. Taetz, M. Schneider, U.F. Schaefer, C.M. Lehr, *Nanomedicine* 2007, *3(3)*, 173.
6. M. Bivas-Benita, S. Romeijn, H.E. Junginger, G. Borchard, *Eur. J. Pharm. Biopharm.* 2004a, *58(1)*, 1.
7. M. Bivas-Benita, R. Zwier, H.E. Junginger, G. Borchard, *Eur. J. Pharm. Biopharm.* 2005, *61*, 214.
8. M. Bivas-Benita, T.H.M. Ottenhoff, H.E. Junginger, G. Borchard, *J. Control. Rel.* 2005*, 107*, 1.
9. A. Misra, A.J. Hickey, C. Rossi, G. Borchard, H. Terada, K. Makino, P.B. Fourie, Colombo, P. *Tuberculosis*, 2011, *91(1)*, 71.
10. S. Taetz, N. Nafee, J. Beisner, K. Piotrowska, C. Baldes, T.E. Muedter, H. Huwer, M. Schneider, U.F. Schaefer, U. Klotz, C.M. Lehr, C.M, *Eur. J. Pharm. Biopharm.* 2008, *722*, 358.
11. M. Köping-Höggård, A. Sanchez, M.J. Alonso, *Expert Rev. Vaccines* 2005, *4(2)*, 185.
12. M. Köping-Höggård, M.M. Issa, T. Köhler, A. Tronde, K.M. Vårum, P. Artursson, *J. Gene Med.* 2005, *7(9)*, 1215.
13. M.M. Issa, M. Köping-Höggård, K. Tømmeraas, K.M. Vårum, B.E. Christensen, B.E, S.P. Strand, P. Artursson, *J Control Rel.* 2006, *115(1)*, 103.
14. N. Csaba, M. Köping-Höggård, M.J. Alonso, *Int. J. Pharm.* 2009, *382(1-2)*, 205.
15. N. Csaba, M. Garcia-Fuentes, M.J. Alonso, *Adv. Drug Deliv. Rev.* 2009, *61(2)*, 140.
16. N. Csaba, M. Köping-Höggård, E. Fernandez-Megia, R. Novoa-Carballal, R. Riguera, M.J. Alonso, *J. Biomed. Nanotechnol.* 2009, *5(2)*, 162.
17. C. Prego, M. García, D. Torres, M.J. Alonso, *J. Control Rel.* 2005 *101(1-3)*, 151.

18. A. Vila, A. Sánchez, K. Janes, I. Behrens, T. Kissel, J.L. Vila-Jato, M.J. Alonso, *Eur. J. Pharm. Biopharm.* 2004, *57(1)*, 123.
19. D. Teijeiro-Osorio, C. Remuñan-Lopez, M.J. Alonso, *Biomacromol.* 2009, *10(2)*, 243.
20. D. Teijeiro-Osorio, C. Remuñan-Lopez, M.J. Alonso, *Eur. J. Pharm. Biopharm.* 2009, *71(2)*, 257.
21. T. Ahmed, C. Campo, M.K. Abraham, J.F. Molinari, W.M. Abraham, D. Ashkin, T. Syriste, L.O. Andersson, C.M. Svahn, *Am. J. Respir. Crit. Care. Med.* 1997, *155(6)*, 1848.
22. J. Martinez-Salas, R. Mendelssohn, W.M. Abraham, B. Hsiao, T. Ahmed, *J. Appl. Physiol.* 1998, *84(1)*, 222.
23. C. Campo, J.F. Molinari, J. Ungo, T. Ahmed, *J. Appl. Physiol.* 1999, *86(2)*, 549.
24. T. Ahmed, J. Garrigo, I. Danta, *N. Engl. J. Med*. 1993, *329(2)*, 90.
25. T. Ahmed, B.J. Gonzalez, I. Danta, *Am. J. Respir. Crit. Care. Med.* 1999, *160(2)*, 576.
26. J. Garrigo, I. Danta, T. Ahmed, *Am. J. Respir. Crit. Care. Med.* 1996, *153(5)*, 1702.
27. A.H. Krauland, M.J. Alonso, *Int. J. Pharm*. 2007, *340*, 134.
28. A.M. De Campos, Y. Diebold, E.L. Carvalho, A. Sanchez, M.J. Alonso, *Pharm. Res.* 2004, *21(5)*, 803.
29. J. Lago, A. Alfonso, M.R. Vieytes, L.M. Botana, *Cell Signal* 2001, *13(7)*, 515.
30. F.A. Oyarzun-Ampuero, J. Brea, M.I. Loza, D. Torres, M.J. Alonso. Int. J. Pharm. 2009, *381(2)*, 122.
31. J. Lucio, J. D'Brot, C.B. Guo, W.M. Abraham, L.M. Lichtenstein, A. Kagey-Sobotka, T. Ahmed, *Appl. Physiol.* 1992, *73(3)*, 1093.

32. T. Ahmed, T Syriste, R. Mendelssohn, D. Sorace, E. Mansour, M. Lansing, W.M. Abraham, M.J. Robinson, *J. Appl. Physiol.* 1994, *76(2)*, 893.

33. P. Calvo, C. Remuñan-Lopez, J.L. Vila-Jato, M.J. Alonso, *J. Appl. Pol. Sci.* 1997, *63*, 125.

34. W.S. Wong, D.S. Koh, *Biochem. Pharmacol.* 2000, *59(11)*, 1323.

35. A.S. Niven, G. Argyros, *Chest* 2003, *123(4)*, 1254.

36. M. de la Fuente, N. Csaba, M. Garcia-Fuentes, M.J. Alonso, *Nanomedicine* (Lond.). 2008, *3(6)*, 845.

37. M.J. Ortner, C.F. Chignell, *Immunopharmacology* 1981, *3(3)*, 187.

38. T.J. Aspden, J.D. Mason, N.S. Jones, J. Lowe, O. Skaugrud, L. Illum, *J. Pharm. Sci.* 1997, *86(4)*, 509.

39. S.T. Lim, G.P. Martin, D.J. Berry, M.B. Brown, *J. Control. Rel.* 2000, *66*, 281.

40. M. Bivas-Benita, K.E. van Meijgaarden, K.L. Franken, H.E. Junginger, G. Borchard, T.H. Ottenhoff, A. Geluk, *Vaccine* 2004b, *22(13-14)*, 1609.

41. Z. Ahmad, S. Sharma, G.K. Khuller, *Int. J. Antimicrob. Agents* 2005, *26(4)*, 298.

42. H. Jin, T.H. Kim, S.K. Hwang, S.H. Chang, H.W. Kim, H.K. Anderson, H.W. Lee, K.H. Lee, N.H. Colburn, H.S. Yang, M.H. Cho, C.S. Cho, *Mol. Cancer Ther.* 2006, *5(4)*, 1041.

DISCUSIÓN

Como se ha mencionado en la sección de Introducción, la heparina posee un interesante potencial como tratamiento del asma bronquial. Sin embargo, este potencial se ve notablemente limitado por su acceso restringido al interior de los mastocitos, donde se encuentran localizados los receptores que pueden prevenir la desgranulación de estas células[95;96]. La dificultad en el acceso intracelular de la macromolécula se relaciona con la repulsión electrostática entre la heparina, que posee una gran densidad de carga negativa, y las membranas celulares de los mastocitos. Por lo tanto, la incorporación de la heparina en sistemas nanoparticulares se abre como una posibilidad de ocultar su carga y, con ello, facilitar su internalización, además de ofrecer la posibilidad de modular su liberación en el interior de los mastocitos.

Para la elaboración de los nanosistemas, se seleccionó el polisacárido quitosano, en combinación con el ácido hialurónico (HA), o con el oligosacárido carboximetil-β-ciclodextrina (CMβCD). La técnica elegida para la elaboración de los nanosistemas fue la gelificación ionotrópica y las principales variables de formulación investigadas en la formación de las nanopartículas, fueron la proporción de los componentes en cada tipo de sistema y el peso molecular de la heparina.

[95] **Lucio J, D'Brot J, Guo CB, Abraham WM, Lichtenstein LM, Kagey-Sobotka A, Ahmed T.** (1992). **Appl. Physiol.** 73(3):1093-101.

[96] **Ahmed T, Syriste T, Mendelssohn R, Sorace D, Mansour E, Lansing M, Abraham WM, Robinson MJ.** (1994). J. Appl. Physiol. 76(2):893-901.

Preparación de las nanopartículas

Las nanopartículas se prepararon de acuerdo con el procedimiento de gelificación iónica, previamente desarrollado en nuestro grupo de investigación[97]. Esta técnica consiste en mezclar dos fases que contienen disoluciones acuosas con moléculas de carga positiva y negativa (Fig. 1). Las nanopartículas se obtienen espontáneamente tras la nanogelificación que se produce por la interacción entre los grupos amino cargados positivamente del quitosano y las cargas negativas de los polímeros u oligómeros, en presencia del agente reticulante (tripolifosfato; TPP). Es un procedimiento extremadamente simple y suave que se realiza a temperatura ambiente.

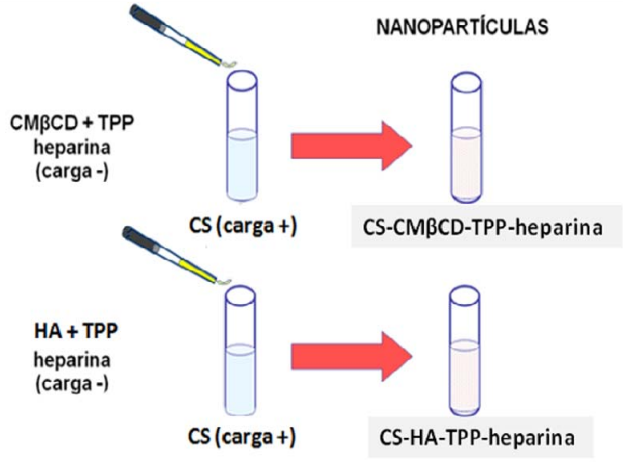

Figura 1. Esquema de preparación de los nanosistemas mediante el procedimiento de gelificación iónica (CS:quitosano).

[97] **Calvo P, Remuñan-Lopez C, Vila-Jato JL, Alonso MJ.** (1997) J. Appl. Polymer Sci. 63, 125-132.

Para la preparación de los nanosistemas de quitosano-CMβCD y quitosano-HA, conteniendo heparina, fue necesario establecer las proporciones más adecuadas de los componentes que permitían su apropiada formación y aislamiento. En general, independientemente de la composición específica de cada sistema, las condiciones de formación se ajustaron a una pauta similar.

En las Tablas 1a y 1b se puede apreciar que, en la medida en que se añadieron cantidades crecientes de los polianiones, se observó un aumento de tamaño en los sistemas junto con una disminución en el valor absoluto del potencial zeta. Esto es explicable en términos de la contraionización que el policatión (quitosano) va sufriendo producto de la adición de cantidades crecientes de polianiones. Cuando los sistemas se vuelven irresuspendibles, o precipitan, se supone una la completa contraionización del policatión, que impide a los sistemas tener una carga eléctrica superficial suficientemente alta que les permita repelerse electrostáticamente y mantener su estabilidad coloidal[98].

Tabla 1. Características físico-químicas de las nanopartículas preparadas usando diferentes proporciones de (1) CS-HA-TPP-heparina y (2) CS-CMβCD-TPP-heparina (media ± d.e.; n=3).

1)

Cantidad (mg) CS-HA-TPP-heparina	**Tamaño (nm)**	**Índice de polidispersión**	**Potential Z (mV)**
4-1.2-0.21-1.0 [a]	201 ± 24	0.2 – 0.4	+32.1 ± 1.6
4-1.2-0.21-1.2 [a]	217 ± 30	0.2 – 0.4	+28.1 ± 0.9
4-1.2-0.21-1.4 [a]	No resuspendible	---	---
4-1.2-0.21-1.6 [a]	Precipitación	---	---
4-0.6-0.21-1.2 [a]	162 ± 17	0.1 – 0.3	+34.6 ± 0.6
4-0.6-0.21-1.4 [a]	**193 ± 32**	**0.2 – 0.5**	**+32.5 ± 1.7**
4-0.6-0.21-1.5 [a]	No resuspendible	---	---
4-0.6-0.21-1.4 [b]	**152 ± 10**	**0.2 – 0.3**	**+33.0 ±1.3**

CS= quitosano; [a]= UFH; [b]= LMWH.

[98] **Krauland AH, Alonso MJ.** (2007). Int. J. Pharm. 340:134-42.

2)

Cantidad (mg) CS-CMβCD-TPP-heparina	Tamaño (nm)	Índice de polidispersión	Potencial Z (mV)
6-1-0-1[a]	359 ± 21	0.3 – 0.4	+40.7 ± 1.0
6-2-0-2[a]	729 ± 54	0.8 – 1	+33.2 ± 0.8
6-2-0-2.1[a]	No resuspendible	---	---
6-0.85-0.34-1.6[a]	**375±69**	**0.3 – 0.5**	**+37.0 ± 1.6**
6-1-0.34-1.6[a]	473 ± 24	0.6 – 0.9	+34.7 ± 1.2
6-1.15-0.34-1.6[a]	No resuspendible	---	---
6-1.3-0.34-1.6[a]	Precipitación	---	---
6-0.85-0.34-1.6[b]	**221± 26**	**0.2 – 0.3**	**+36.8 ± 0.7**

Caracterización de las nanopartículas

Como se puede apreciar en la Tabla 1.1, todos los sistemas de quitosano-HA presentaron un rango de valores de tamaño, polidispersión y potencial zeta relativamente estrecho (152-217 nm, 0.1-0.5, y 33.2-40.7 mV, respectivamente). Por otro lado, los sistemas de quitosano-CMβCD (Tabla 1.2) presentaron una mayor dispersión en los citados parámetros (221-729 nm, 0.2-1, y +33-+41 mV), siendo estos valores similares a los presentados por Krauland y col. (2007) para diferentes formulaciones nanopartículas de quitosano-TPP y quitosano-CMβCD conteniendo heparina no fraccionada (UFH)[98]. En las formulaciones en las que sustituyó la UFH por heparina de bajo peso molecular (LMWH), los parámetros de tamaño y polidispersión fueron los más bajos de todos los sistemas ensayados, lo que, evidentemente, se relaciona con el menor peso molecular del fármaco. En el caso del potencial zeta, se puede apreciar que, en todas las formulaciones, se obtienen valores altamente positivos, lo cual es indicativo de que la superficie de los nanosistemas está compuesta principalmente por quitosano.

Para las siguientes etapas de caracterización y evaluación, se seleccionaron las formulaciones destacadas en negrita en las Tablas 1.1 y 1.2. El criterio utilizado para dicha selección se basó principalmente en la menor

polidispersión de estas formulaciones y en el hecho de que éstas están elaboradas con una adecuada cantidad de heparina.

En las Tablas 2.1 y 2.2 se presentan los valores de contenido en heparina, eficacia de asociación y rendimiento de las formulaciones de quitosano-HA y quitosano-CMβCD. La eficacia de asociación fue, en todos los casos, similar (~70%), lo que coincide con otros trabajos en los que se describen nanosistemas de quitosano y heparina [4;99]. Esta elevada asociación se atribuye al alto potencial para interaccionar iónicamente que presentan dos macromoléculas con carga complementaria, como quitosano y heparina. En cuanto al contenido de heparina encapsulada, se puede apreciar que este valor fue siempre mayor para los sistemas que contienen LMWH y, especialmente alto para las nanopartículas de quitosano-HA (~61%). Ello se puede atribuir a un mejor ensamblaje de la LMWH en la matriz nanopartícular, lo que puede inducir un mayor desplazamiento de los demás polianiones (HA, CMβCD, TPP) que interaccionan con el quitosano y que explicaría también el menor rendimiento obtenido para los sistemas con LMWH.

Tabla 2. Contenido en heparina, eficacia de encapsulación y de las nanopartículas de a) CS-HA y b) CS-CMβCD (media ± d.e.; n=3).

1)

Cantidad CS-HA-TPP-heparina (mg)	Contenido en heparina (%)	Eficacia de encapsulación (%)	Rendimiento (%)
4-0.6-0.21-1.4[a]	33.6 ±1.2	72.3 ± 2.7	49.0 ± 1.2
4-0.6-0.21-1.4[b]	60.6 ± 0.3	69.7 ± 7.6	24.9 ± 4.3

CS= quitosano; [a]= UFH; [b]= LMWH.

2)

Cantidad CS-CMβCD-TPP-heparina (mg)	Contenido en heparina (%)	Eficacia de encapsulación (%)	Rendimiento (%)
6-0.85-0.34-1.6[a]	38.7 ± 2.5	77.0 ± 2.1	39.4 ± 2.5
6-0.85-0.34-1.6[b]	44.0 ± 1.1	70.6 ± 2.5	29.3 ± 0.6

[99] **Chen MC, Wong HS, Lin KJ, Chen HL, Wey SP, Sonaje K, Lin YH, Chu CY, Sung HW. (**2009). Biomaterials. 30(34):6629-37.

Las imágenes de microscopía electrónica (Figura 2) indican que las formulaciones son esféricas, independientemente del tipo de contraión (HA o CMβCD) o de heparina utilizados. Es interesante hacer notar que los sistemas desarrollados con LMWH se ven aparentemente mejor ensamblados que los que contienen UFH, lo que concuerda con el argumento que acabamos de exponer.

(1)

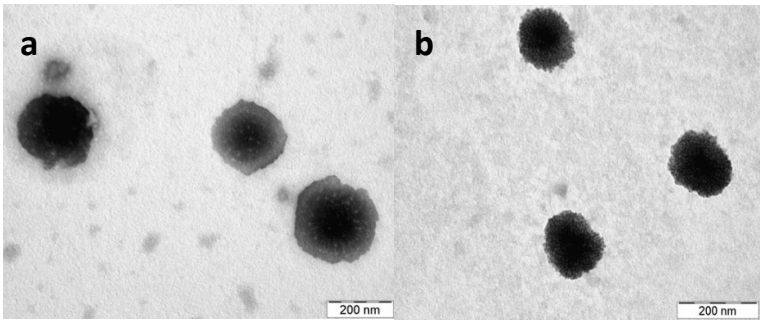

(2)

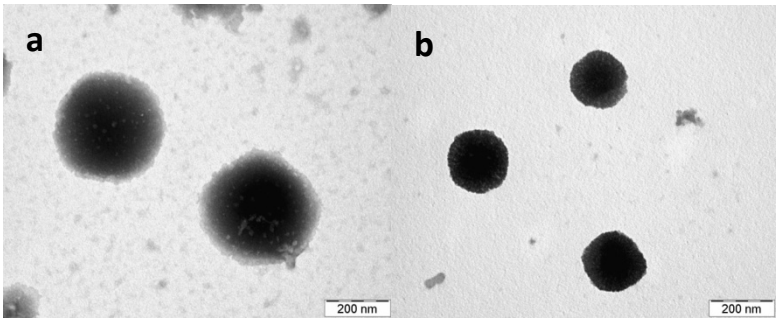

Figura 2. Imágenes de microscopía electrónica de transmisión de las nanopartículas de (1) CS(quitosano)-HA y (2) CS-CMβCD conteniendo a) UFH y b) LMWH.

Estudios de estabilidad de las nanopartículas

Evaluar la estabilidad coloidal de los nanosistemas es un punto clave para la planificación de estudios posteriores. Para ello se realizaron estudios de estabilidad con las formulaciones seleccionadas en condiciones similares a

las utilizadas en cultivos celulares, esto es, a 37°C y utilizando como medios HBSS a pH 6.4 y 7.4 y PBS a pH 7.4.

La estabilidad de los nanosistemas se valoró a través del seguimiento de su tamaño en las diferentes condiciones. La composición de los nanosistemas y de los medios utilizados fueron factores determinantes en su estabilidad. En el caso de las nanopartículas de quitosano-HA, su tamaño no experimentó cambios significativos en 24 horas cuando se incubó en PBS a pH 7.4 (Figura 3), mientras que en HBSS a pH 7.4 sí experimentó un incremento significativo. A pH 6.4, se agregaron de inmediato, hecho que se relaciona con el cambio en el potencial zeta de las formulaciones, que presentó valores cercanos a la neutralidad. A pH 7.4, el potencial zeta de los sistemas se mantuvo en torno a -10 mV. Esta inversión en la carga superficial es consecuencia del bajo grado de ionización del quitosano (pKa ~ 6.2) en medios a pH 7.4. La diferencia entre los perfiles de estabilidad para HBSS pH 7.4 y PBS pH 7.4 tiene que ver con la distinta composición de estos tampones (HBSS posee iones CO_3^{2-} y una concentración de iones PO_4^{2-} 8 veces superior).

En el caso de los sistemas de quitosano-CMβCD, la estabilidad se mantuvo hasta 24 h en HBSS pH 6.4 (Figura 4), mientras que en los otros medios las nanopartículas se agregaron inmediatamente. En HBSS pH 6.4 el potencial zeta de las formulaciones era cercano a +14 mV, mientras que a pH 7.4, los valores fueron neutros (~0 mV), lo que confirma la desestabilización.

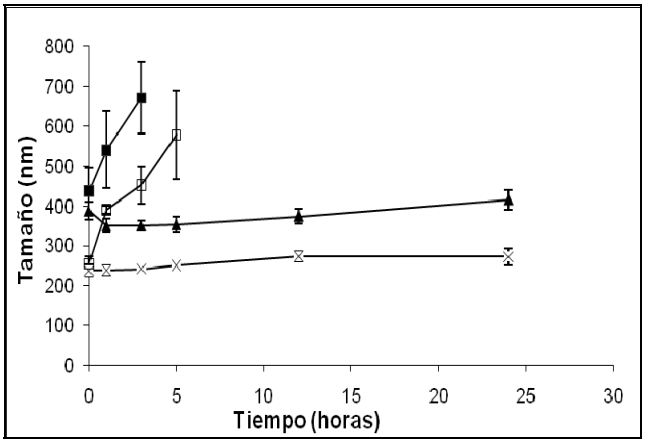

Figura 3: Evolución del tamaño de las nanopartículas de quitosano-HA conteniendo heparina, en medios a pH 7.4: UFH (▲) y LMWH (×) en PBS; UFH (■) y LMWH (□) en HBSS (media ± d.e., n=3).

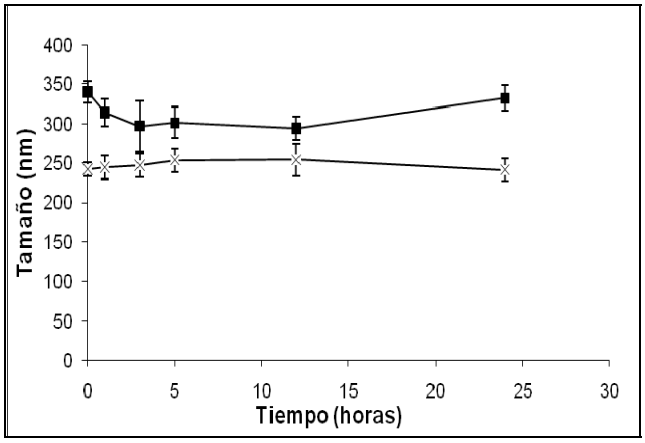

Figura 4: Evolución del tamaño de las nanopartículas de quitosano-CMβCD conteniendo UFH (■) y LMWH (×) en medio HBSS pH 6.4 (media ± d.e., n=3).

Finalmente, todas las formulaciones seleccionadas mantuvieron su tamaño sin alteraciones apreciables durante 3 meses en suspensión acuosa a 4 °C (resultados no mostrados).

Estudios de liberación de heparina a partir de las nanopartículas

Se evaluó la liberación de UFH y LMWH a partir de las formulaciones seleccionadas, en los medios en que éstas alcanzaron la

máxima estabilidad, esto es, en PBS pH 7.4 para los sistemas de quitosano-HA y en HBSS pH 6.4 para los sistemas de quitosano-CMβCD. Considerando la alta densidad de carga negativa que posee la heparina y la carga positiva del quitosano, se espera que la liberación del fármaco a partir de la matriz de los nanosistemas sea lenta, como consecuencia de una fuerte interacción electrostática entre las macromoléculas con carga opuesta[98].

Como se puede apreciar en las Figuras 6a y 6b, si bien la liberación de las heparinas fue lenta en todos los casos, su perfil varió significativamente dependiendo de su peso molecular y de la composición de cada nanosistema. En el caso de los sistemas de quitosano-HA, la UFH se liberó muy lentamente alcanzándose una liberación final de un 10% tras 12 h de incubación. La LMWH se liberó de una manera más rápida y continua alcanzándose una liberación final de aproximadamente un 80% (Figura 6a).

a)

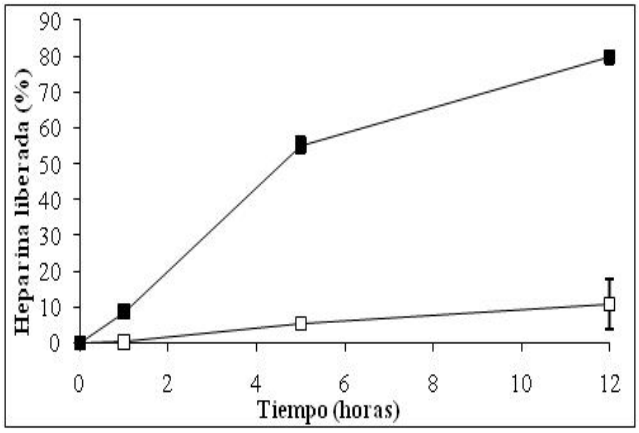

b)

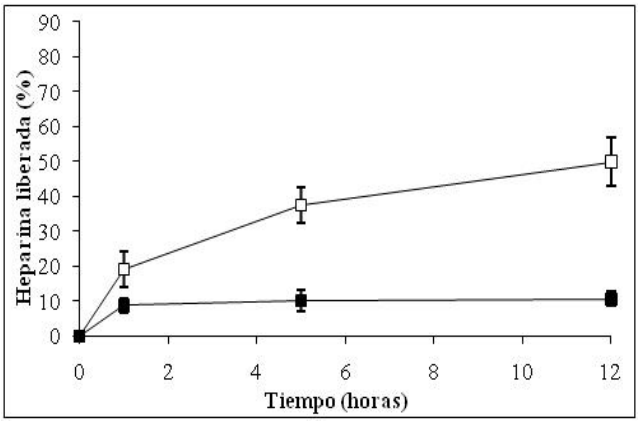

Figura 6: Perfiles de liberación de UFH (□) y LMWH (■) a partir de las nanopartículas de a) CS(quitosano)-HA en PBS pH 7.4; y b) CS-CMβCD en HBSS pH 6.4 (media ± d.e., n=3).

La liberación más rápida de la LMWH se atribuye a su menor peso molecular, que facilitaría la mejor difusión de la heparina. También debe tomarse en consideración la gran diferencia en los valores de contenido en heparina de los sistemas desarrollados con UFH y LMWH (~34% y ~61%, respectivamente), que apoyaría los resultados expuestos.

Por otro lado, como se puede apreciar en la Figura 6b, la cinética de liberación de las heparinas a partir de las nanopartículas de quitosano-CMβCD se ajustó a una pauta diferente. Los nanosistemas conteniendo LMWH, liberaron el fármaco de manera muy lenta durante la primera hora (~ 10%), tras lo cual apenas hay cambios hasta las 12 h de duración del estudio. La UFH se liberó de una manera más rápida y continua, con una liberación final de aproximadamente un 50%. La menor liberación observada para la LMWH puede relacionarse con un mejor ensamblamiento de ésta molécula en la matriz de los sistemas, como ya se sugirió previamente en relación al tamaño de los nanosistemas (221 vs 375 nm).

Estudio de la interacción entre las nanopartículas conteniendo heparina y los mastocitos

Considerando que la heparina previene la desgranulación de los mastocitos debido a la interacción que establece con el receptor intracelular de trifosfato de inositol (IP_3)[100;101;102], es importante elucidar si su inclusión en los nanosistemas de quitosano-HA y quitosano-CMβCD facilitará el acceso de este fármaco al interior de los mastocitos. Para hacer un seguimiento de las nanopartículas fluorescentes en contacto con mastocitos de rata, se utilizó la microscopía confocal.

El solapamiento de la señal verde transmitida por las nanopartículas conteniendo UFH, con la señal roja transmitida por los mastocitos, resultó en un color naranja (Figura 7). Esto nos confirma que las nanopartículas, independientemente de su composición, son capaces de interaccionar con los mastocitos tras un periodo de incubación de 2 h.

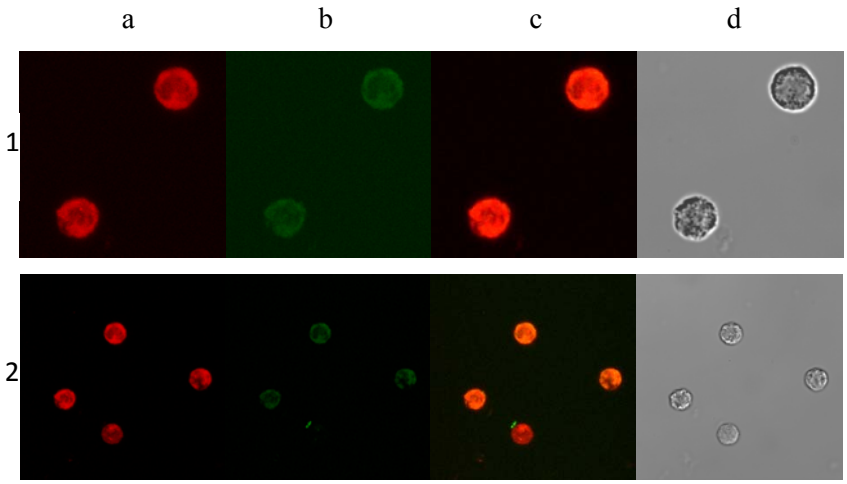

Figura 7. Imágenes de microscopía confocal de mastocitos fluorescentes tras un contacto de 2 horas con nanopartículas fluorescentes de (1) CS-HA y (2) CS-CMβCD conteniendo UFH: (a)

[100] **Ahmed T, Ungo J, Zhou M, Campo C.** (2000). J. Appl. Physiol. 88:1721–1729.
[101] **Wong WS, Koh DS.** (2000). Biochem. Pharmacol. 59:1323–1335.
[102] **Niven AS, Argyros G.** (2003). Chest 123:1254–1265.

señal transmitida por los mastocitos (rojo); (b) señal transmitida por las nanopartículas (verde); (c) solapamiento de ambas señales (naranja) y (d) señal óptica.

Para confirmar que esta interacción transcurre a nivel intracelular, y no sólo a nivel superficial, se obtuvieron secuencialmente planos del eje "z" de los mastocitos tras su incubación con las nanoparticulas (Figura 8). En estas imágenes se puede apreciar que, efectivamente, las nanopartículas son capaces de acceder al interior de los mastocitos distribuyéndose aquí de una manera relativamente homogénea. Esta información coincide con lo observado en otros trabajos en los que se ha demostrado, por esta y otras técnicas, que las nanopartículas que poseen una cubierta de quitosano son capaces de acceder al interior del espacio celular[103;104;105;106], en diferentes cultivos celulares. Sin embargo, ésta es la primera vez que, utilizando microscopia confocal, se evalúa y demuestra que las nanopartículas son internalizadas en mastocitos. Finalmente, los nanosistemas conteniendo LMWH demostraron un comportamiento similar a los sistemas cargados con UFH (imágenes no mostradas).

[103] **Ma Z, Lim LY.** (2003). Pharm. Res. 20(11):1812-9.
[104] **Csaba N, Köping-Höggård M, Fernandez-Megia E, Novoa-Carballal R, Riguera R, Alonso MJ.** (2009). J. Biomed. Nanotechnol. 5(2):162-71.
[105] **Lee DW, Yun KS, Ban HS, Choe W, Lee SK, Lee KY.** (2009). J. Control Rel.139(2):146-52.
[106] **Raviña M, Cubillo E, Olmeda D, Novoa-Carballal R, Fernandez-Megia E, Riguera R, Sánchez A, Cano A, Alonso MJ.** (2010). Pharm. Res. 27(12):2544-2555.

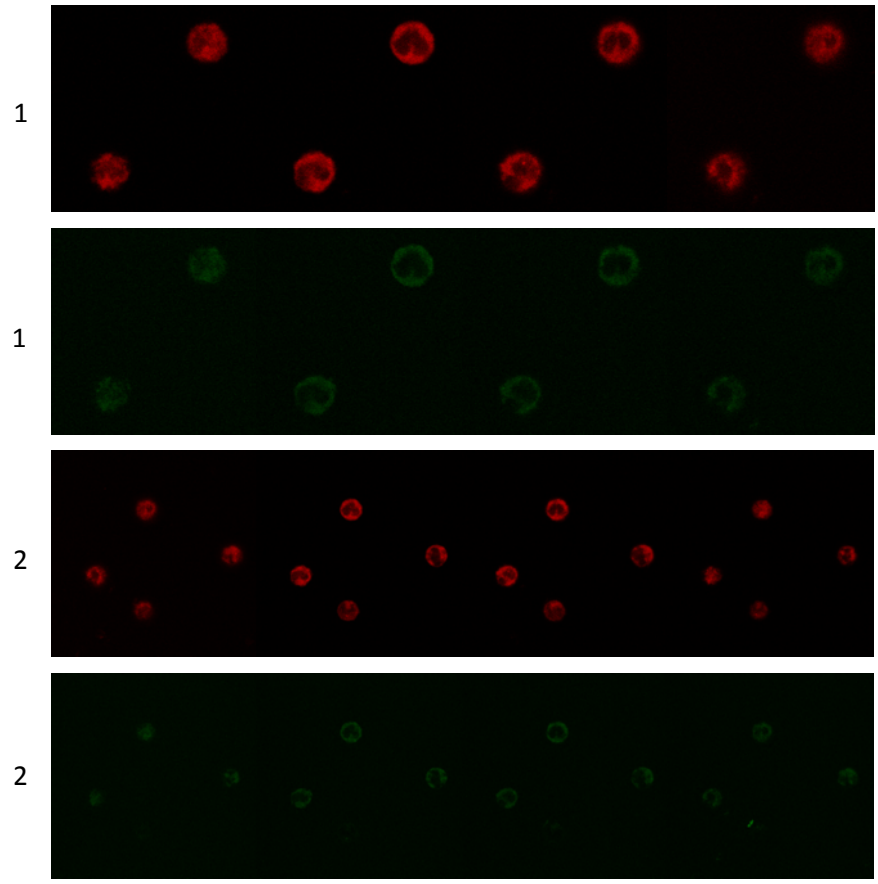

Figura 8. Imágenes de microscopía confocal de mastocitos de rata fluorescentes tras 2 horas de incubación con nanopartículas fluorescentes de (1) CS-HA y (2) CS-CMβCD conteniendo UFH. Planos de los mastocitos tomados cada 1.5 μm del eje "z".. Señal de exitación para mastocitos (rojo); señal de exitación para nanopartículas (verde).

Estudio de viabilidad celular

La viabilidad de los mastocitos tras su extracción a partir de las cavidades peritoneales y pleurales de rata fue, en todos los casos, superior a un 90%. Ésto se comprobó mediante microscopia óptica empleando el método del azul tripano[107]. El método utilizado para la extracción de los

[107] **Oyarzun-Ampuero FA, Brea J, Loza MI, Torres D, Alonso MJ.** (2009). Int. J. Pharm. 381:122–129.

mastocitos fue el descrito por Lago y col.[108], y los valores de viabilidad obtenidos fueron similares a los obtenidos previamente[109]. Tras un tiempo de 2 horas de contacto con los nanosistemas, la viabilidad fue siempre superior al 90%, lo que indica la inocuidad de los nanosistemas en el modelo celular ensayado. La cantidad de nanopartículas utilizada en estos estudios, correspondió a la más alta que sería administrada a los mastocitos en los estudios de liberación de histamina que se presentan a continuación.

Estudio de inhibición de la liberación de histamina en mastocitos

Como método de evaluación de la eficacia antiasmática de la heparina encapsulada, se estudió su capacidad para prevenir la liberación de histamina por parte de los mastocitos. De acuerdo con la información que disponemos, ésta es la primera vez que este tipo de experimentos se lleva a cabo con nanosistemas.

Estudio preliminar: En primer lugar, se evaluó el efecto de diferentes dosis de UFH y LMWH en solución para prevenir la liberación de histamina inducida por el compuesto estándar de origen sintético 48/80. El compuesto 48/80 es conocido por su capacidad de desgranulación de los mastocitos, promoviendo así la liberación al medio extracelular de la histamina localizada en el interior de dichos gránulos[110]. En la Figura 9 se puede apreciar que tanto la UFH como la LMWH poseen, en el rango de concentración ensayado, un efecto dosis dependiente similar, para prevenir la liberación de histamina (IC50 μg/mL = 6.8±1.2 para UFH y 12.3±3.1 para LMWH).

[108] **Lago J, Alfonso A, Vieytes MR, Botana LM. (**2001). Cell Signal. 13:515–524.
[109] **Buceta M, Dominguez E, Castro M, Brea J, Alvarez D, Barcala J, Valdes L, Alvarez-Calderon P, Dominguez F, Vidal B, Diaz JL, Miralpeix M, Beleta J, Cadavid MI, Loza MI.** (2008). Biochem. Pharmacol. 76, 912–921.
[110] **Ortner MJ, Chignell CF.** (1981). Immunopharmacology 3:187–191.

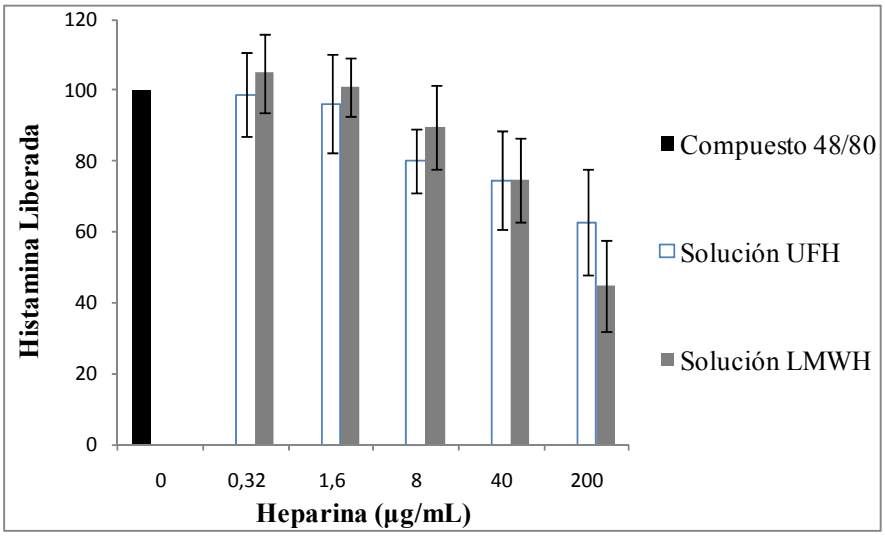

Figura 9. Efecto de la concentración de UFH y LMWH en solución sobre la liberación de histamina en mastocitos. La liberación de histamina se inició tras la incubación de las células con una solución 100 µM del compuesto 48/80. Las células se preincubaron con diferentes concentraciones de UFH y LMWH antes de la adición del compuesto (n=3, $p< 0.05$).

Se confirmó que en las condiciones del ensayo, la heparina es capaz de prevenir la liberación de histamina y, por otro lado, evidencia el rango efectivo de concentraciones de UFH y LMWH. Ambos tipos de heparina inhibieron la liberación de histamina en una magnitud similar, sin apreciarse diferencias significativas entre ellas. Ésto contrasta con la información presentada en diferentes publicaciones en las que se evidencian diferencias significativas entre los efectos de las heparinas inhaladas de alto y bajo peso molecular para prevenir la liberación de la histamina[111;112;113]. De hecho, se indica que la potencia de las distintas heparinas ensayadas es inversamente proporcional a su tamaño molecular. La diferencia entre estos resultados puede deberse a la comparación del contacto directo de las heparinas con los

[111] **Ahmed T, Campo C, Abraham MK, Molinari JF, Abraham WM, Ashkin D, Syriste T, Andersson LO, Svahn CM.** (1997). Am. J. Respir. Crit. Care Med. 155(6):1848-55.
[112] **Martinez-Salas J, Mendelssohn R, Abraham WM, Hsiao B, Ahmed T.** (1998). J. Appl. Physiol. 84(1):222-8.
[113] **Campo C, Molinari JF, Ungo J, Ahmed T.** (1999). J. Appl. Physiol. 86(2):549-57.

mastocitos *ex vivo*, con la administración *in vivo* de las heparinas por nebulización. En el último caso, las características propias de la fisiología pulmonar (aclaramiento mucociliar, actividad enzimática, etc.) pueden influenciar de manera significativa el efecto de una u otra heparina.

Efecto de las nanopartículas conteniendo heparina sobre la liberación de histamina en mastocitos: En el caso de los sistemas de quitosano-HA conteniendo UFH (Figura 10a), se evidencia un efecto dosis-dependiente sobre la inhibición de la liberación de histamina, sin apreciarse diferencias significativas entre la formulación nanoparticular y el control de heparina en solución.

En el caso de los sistemas de quitosano-CMβCD conteniendo UFH (Figura 10b), también se observa un efecto dosis-dependiente para prevenir la liberación de histamina. Sin embargo, se evidencia una mejora significativa en este parámetro cuando se ensaya la dosis más alta de UFH (200 μg/mL), que es capaz de inhibir casi completamente el efecto estimulante de degranulación del compuesto 48/80 (~90% de inhibición), mientras que la misma dosis de UFH en solución inhibe sólo un 55%.

Resultados muy similares a los presentados en el presente apartado se obtuvieron cuando la LMWH estaba contenida en sistemas de quitosano-HA y quitosano-CMβCD (**Capitulo 2, Figura 6b y Capitulo 3, Figura 5b**).

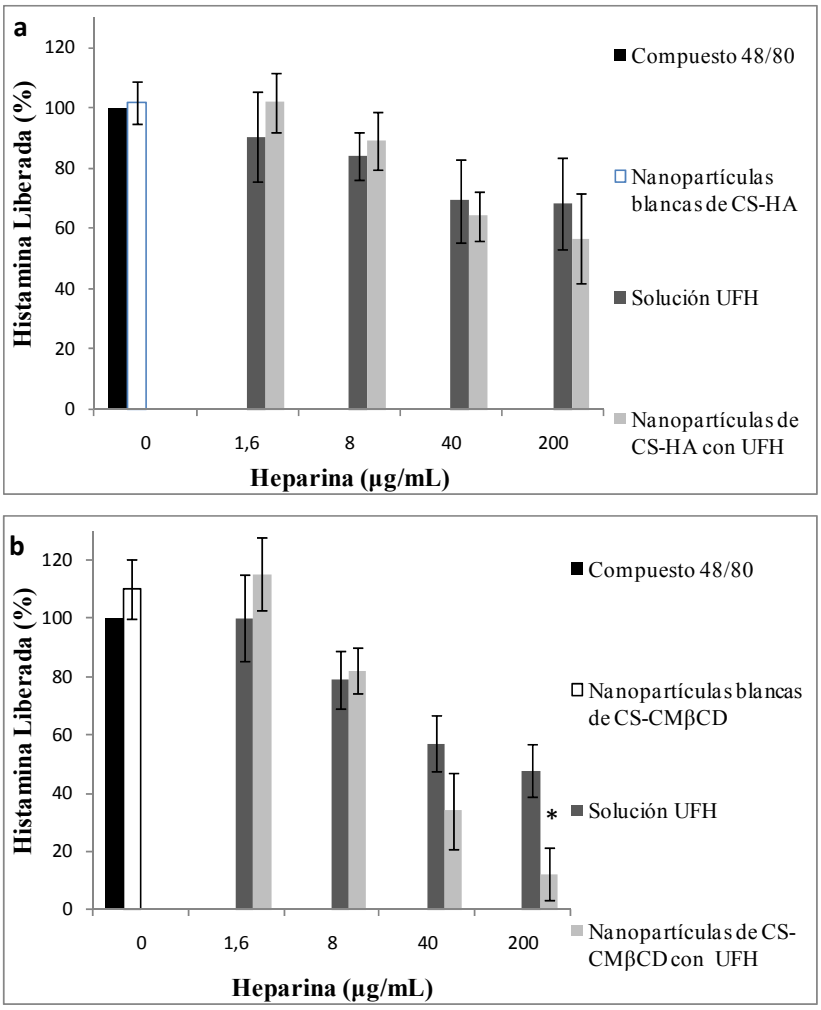

Figura 10. Efecto de la heparina encapsulada en las nanopartículas de (a) CS(quitosano)-HA y (b) CS-CMβCD sobre la liberación de histamina en mastocitos. La liberación de histamina se inició tras la incubación de las células con una solución 100 µM del compuesto 48/80. Las células se preincubaron con diferentes concentraciones de UFH en solución (barras grises) y UFH encapsulada en las nanopartículas (barras crema). Como control, se incubaron también las nanopartículas blancas (n=3, $p< 0.05$).

Como control negativo de los experimentos, y en todos los casos, se evaluó el efecto las formulaciones nanoparticulares blancas, sobre la liberación de histamina, apreciándose que ningún sistema *per se* tiene un efecto significativo sobre este parámetro.

Los resultados presentados evidencian la importancia que tiene la composición de las nanopartículas sobre el efecto de la heparina sobre mastocitos. En el caso de las nanopartículas de quitosano-CMβCD, independientemente del peso molecular de la heparina, se observó siempre una mejora significativa sobre el efecto obtenido con la heparina en solución. Nuestra hipótesis es que dicha mejora se relaciona con un efecto promotor de la CMβCD en el acceso intracelular de la heparina en mastocitos, que se hace notar a la concentración más alta de heparina, con la que hay también una mayor concentración de ciclodextrinas. Una situación diferente se presenta con los nanosistemas de quitosano-HA, que no llegaron a demostrar, al menos a las dosis ensayadas, un efecto superior al de la heparina en solución, lo que indica una menor capacidad internalizante. De cualquier modo, resulta complicado comparar las dos formulaciones de nanopartículas, ya que además de las diferencias atribuidas a las propiedades de los contraiones, HA y CMβCD, existen otras diferencias que pueden tener un efecto significativo sobre la eficacia de la heparina, como por ejemplo la relación final entre polímeros y heparina, valor difícil de estimar, al ser diferentes los rendimientos obtenidos para cada formulación.

Otras diferencias significativas entre las formulaciones en parámetros como el tamaño, los perfiles de estabilidad y liberación de la heparina, pueden también condicionar el efecto biológico de la heparina.

Finalmente, es importante considerar que las condiciones *ex vivo* utilizadas en los experimentos no reflejan las barreras fisiológicas de las vías aéreas como son el aclaramiento mucociliar y la actividad enzimática. Dichas barreras pueden ser superadas eficazmente por los nanosistemas propuestos, debido a la demostrada propiedad mucoadhesiva del quitosano[114;115] y del

[114] **Aspden TJ, Mason JD, Jones NS, Lowe J, Skaugrud O, Illum L.** (1997). J. Pharm. Sci. 86: 509–513.
[115] **Lim ST, Martin GP, Berry DJ, Brown MB.** (2000). J. Control. Rel. 66, 281–292.

HA[9;116] y a la capacidad de las nanopartículas para proteger el fármaco encapsulado de la actividad enzimática. Un buen ejemplo en el que se demuestra la eficacia de las nanopartículas recubiertas con quitosano para promover el efecto localizado de un fármaco macromolecular administrado por vía pulmonar, ha sido previamente publicado por Bivas-Benita y col. (2004)[117]. El enfoque del citado trabajo fue el desarrollo una vacuna conteniendo un plásmido de DNA para prevenir la tuberculosis.

De manera adicional, las formulaciones nanoparticulares propuestas pueden mejorar el efecto de una formulación convencional de heparina debido a su potencial para liberar lentamente el fármaco, lo que prolongaría su efecto antiasmático. Desafortunadamente, las condiciones experimentales *ex vivo* utilizadas en el presente trabajo no permiten realizar experimentos de mayor duración, lo que no permite verificar esta teoría.

[116] **Pritchard K, Lansley AB, Martin GP, Helliwell M, Marriot C, Benedetti LM.** (1996). Int. J. Pharm. 129:137–145.
[117] **Bivas-Benita M, van Meijgaarden KE, Franken KL, Junginger HE, Borchard G, Ottenhoff TH, Geluk A.** (2004). Vaccine 22(13-14), 1609-15.

PARTE II: DESARROLLO DE UN NUEVO SISTEMA CONSTITUÍDO POR NANOCÁPSULAS DE ÁCIDO HIALURÓNICO CONTENIENDO DOCETAXEL Y EVALUACIÓN DE EFICACIA ANTITUMORAL SOBRE CULTIVOS CELULARES DE CÁNCER DE PULMÓN.

Capitulo 4

Hyaluronan nanocapsules: a new safe and effective nanocarrier for the intracellular delivery of anticancer drugs

Abstract

Here we report a new drug nanocarrier for the intracellular delivery of hydrophobic anticancer drugs. The nanocarrier -named as nanocapsules- is composed of a lipid core surrounded by a shell made of hyaluronic acid (HA). This polymer was chosen because of its ability to prolong the circulation time and the interaction with certain cancer tumors. HA nanocapsules were produced by a modified solvent displacement technique, which allows the formation of the polymer shell around the oily core, as a consequence of the interaction between a cationic surfactant and the anionic polysaccharide. The resulting HA nanocapsules have average sizes from 170 to 250 nm and a zeta potential values ranging from -30 and -60 mV. They showed a capacity to efficiently encapsulate the hydrophobic drug docetaxel (DCX) and retain it in the oily core upon dilution in a simulated biological fluid. As expected, the nanoencapsulated DCX exhibited an enhanced cytotoxicity (3-fold increase as compared to a control solution) upon *in vitro* incubation with the cancer cell line NCI-H460. This result was attributed to the internalization of the nanocapsules and the intracellular delivery of DCX. Moreover, the nanocapsules suspension could be freeze-dried and remained stable during storage. In summary, these novel nanostructures hold promise as intracellular drug delivery systems.

Keywords: Nanocapsules, hyaluronic acid, cancer, hydrophobic drugs, intracellular delivery.

Introduction

Currently, it is known that the use of nanoscale drug delivery vehicles represents a very promising strategy for improving the biodistribution and intracellular delivery of anticancer drugs. Taxanes (paclitaxel, docetaxel) are good examples of potent chemotherapeutic agents, which could greatly benefit from these delivery carriers. Indeed, despite their efficacy, these drugs display significant draw-backs related to their indiscriminate biodistribution and the necessity to use toxic solubilizers for their intravenous administration (Ten Tije et al., 2003). Besides the marketed formulation of albumin nanoparticles (Abraxane), a number of nanocarriers have been disclosed in the literature for the delivery of these specific compounds. Particularly attractive for this purpose are the nanocapsules, which can easily accommodate hydrophobic (Heurtault et al., 2002a, b; Bae et al., 2007; Lozano et al., 2008; 2011b). For example, the group of Benoit and co-workers has reported the potential of PEG-coated lipid nanocapsules loaded with paclitaxel in different cancer animal models. Overall, the authors observed that PEGylated nanocapsules have long circulating properties as well as the ability to improve the intracellular accumulation of drugs in the tumor cells (Garcion et al., 2006; Lacoeuille et al., 2007). An alternative nanocapsule-type carrier was recently reported by our group for the delivery of docetaxel (DCX) (Lozano et al., 2008; 2011b). These nanocapsules are made of chitosan and polyarginine and display a number of properties, among which it is important to highlight: I) their capacity to be internalized by different cell lines, such as the breast cancer (MCF-7) and lung cancer (A-549) cell lines, II) the improved efficacy of DCX-loaded nanocapsules in MCF-7, A-549 and NCI-H460 (non small cell lung cancer) cell lines compared with DCX alone; and III) the possibility to functionalize them with ligands such as anti-TMEFF-2 in order to target them to TMEFF-2, a

transmembrane protein, that is overexpressed in non microcytic tumors (Torrecilla et al., 2011).

Following this experience, we found it important to modify the polymer corona of the nanocapsules by using hydrophilic negatively charged polymers such as hyaluronic acid (HA). This polysaccharide attracted our attention because of its reported ability to prolong the plasma circulation time of liposomes and nanoparticles (Peer and Margalit, 2004a, b; Peer et al., 2007; Choi et al., 2009; Ossipov, 2010). Additionally, HA offers the possibility of targeting the drug-loaded nanocarrier to the cancer cells that overexpress the endogenous receptor for this polymer (called CD-44 receptors). As a consequence of these properties, HA-based nanocarriers have resulted in an improved tumor growth inhibition and a decreased systemic toxicity, when compared to the free drug (Akima et al., 1996; Luo and Prestwich., 1999; Elias and Szocka., 2001; Eliaz et al., 2004; Peer and Margalit., 2004 a, b; Rosato et al., 2006; Auzenne et al. 2007; Hyung et al., 2008).

Taking this background information into account our aim in this work has been to develop a new and alternative HA-based anticancer drug delivery nanocarrier exhibiting unique pharmaceutical properties such as: I) acceptable from the safety point of view, II) able to load important amounts of lipophilic anticancer drugs, III) ability to target and enter cancer cells providing intracellular drug delivery and, finally, IV) easy to produce and scale-up and stable under storage. The results presented in this report clearly show that HA nanocapsules fulfill such interesting profile.

Materials and methods

Chemicals: Docetaxel (DCX, from Fluka), poloxamer (Pluronic F-68®), benzalkonium chloride (BKC) and hexadeciltrymethylammonium bromide (CTAB) were purchased from Sigma-Aldrich (Spain). Miglyol 812®, which is neutral oil formed by esters of caprylic and capryc fatty acids and glycerol, was donated by Sasol Germany GmbH (Germany). The surfactant Epikuron 145V, which is a phosphatidylcholine-enriched fraction of soybean Lecithin, was donated by Cargill (Spain). Hyaluronic acid of 29 kDa was purchased from Imquiaroma (Barcelona, Spain) and that of 160 kDa was kindly donated by Bioiberica (Barcelona, Spain).

Preparation of HA nanocapsules:

HA nanocapsules were prepared following two different procedures that have been previously described by our group (Prego et al., 2005; Lozano et al., 2008). The first one, called "two-stage procedure" consist in adding 125 μL of Miglyol 812 to an organic phase comprising 30 mg of lecithin, and 4 mg of BKC or 1.8 mg of CTAB, dissolved in 0.5 ml of ethanol and 9.5 ml of acetone. This organic phase was added to an aqueous phase (20 mL). The formation of the cationic nanoemulsions was instantaneous, which was evident due to the milky appearance of the mixture (interestingly, the cationic nanoemulsion was also obtained after the addition of the organic phase to a homogenizer/sonicator, data not shown). The above solution was rotaevaporated until a volume of 10 mL, and then incubated with an aqueous solution of HA (0.1-50 mg) in a volume ratio 4:1.5 (cationic nanoemulsion:HA solution); when the anionic HA interacts with the cationic nanoemulsion, it forms a polymer corona at the oil/aqueous interface thus originating HA nanocapsules. The second one, called "one-stage procedure" involves adding 125 μL of Miglyol 812 to an organic phase comprising 30

mg of lecithin, and 4 mg of BKC or 1.8 mg of CTAB, dissolved in 0.5 ml of ethanol and 9.5 ml of acetone. This organic phase was added to an aqueous phase (20 mL) that contains the polymer HA (0.1-50 mg). The above solution was rotaevaporated until a volume of 10 mL, here the formation of HA nanocapsules occurs concomitantly to the evaporation of the solvent due to adsorption of the polymer onto the nanocarrier-surface. In both cases, the incorporation of DCX, required the previous dissolution of this molecule in ethanol to obtain a final concentration of 1 mg/mL. Next, an aliquot of the stock solution was added to the organic phase and the same procedure was followed. The final DCX concentration obtained in HA nanocapsules carriers was 7.27 μM.

Physicochemical Characterization of HA nanocapsules

The size and zeta potential of the colloidal systems were determined by photon correlation spectroscopy and laser Doppler anemometry, with a Zetasizer Nano-ZS (Malvern Instruments, United Kingdom). Each batch was analyzed in triplicate.

The morphological examination of the systems was performed by transmission electron microscopy (TEM) (CM12 Phillips, Netherlands). The samples were stained with 2% (w/v) phosphotungstic acid and immobilized on copper grids with Formvar® for viewing by TEM.

Encapsulation Efficiency of DCX-Loaded HA nanocapsules

The encapsulation efficiency of DCX in the nanocarriers was determined indirectly by the difference between the total amount of DCX and the free drug recovered in the continuous phase. The total amount of drug was estimated by dissolving an aliquot of non isolated DCX-loaded HA nanocapsules with acetonitrile. This sample was centrifuged during 20 min at

4000 × *g* and the supernatant was measured with a high performance liquid chromatography (HPLC) system. The non encapsulated drug was determined by the same method following separation of the nanocapsules from the aqueous medium by ultracentrifugation (27500 *g*, 60 min). DCX was assayed by a slightly modified version of the method proposed by Lee et al (1999). The HPLC system consisted of an Agilent 1100 series instrument equipped with a UV detector set at 227 nm and a reverse phase Zorbax Eclipse XDB-C8 column (4.6 × 150 mm i.d., pore size 5 μm Agilent, U.S.A.). The mobile phase consisted of a mixture of acetonitrile and 0.1% v/v orthophosphoric acid (55:45, v/v) and the flow rate was 1 mL/min. The standard calibration curves of DCX were linear ($r2 > 0.999$) in the range of concentrations between 0.3-2 μg/mL.

In vitro Release Studies

The release studies of DCX from HA carriers were performed by incubating a sample of the formulation with milli-Q water at an appropriate concentration to ensure sink conditions. The vials were placed in an incubator at 37 °C with horizontal shaking. A total of 3 mL of the suspension were collected and ultracentrifuged (27500 *g*, 60 min) by using Herolab high speed centrifuge labware tubes (Herolab GmbH, Germany) at different time intervals. The DCX released was calculated indirectly by determining how much of it was left in the system by processing the isolated HA nanocapsules with acetonitrile before HPLC analysis.

Cellular assays

Cell viability assay and IC_{50} estimation: Human non-small cell lung cancer cell line NCI-H460 was cultured in RPMI 1640 medium (ATCC), supplemented with 10% (v/v) fetal bovine serum (FBS) at 37° C in a humidified atmosphere containing 5% carbon dioxide. Tretazolium salt 3-(4,5-dimewthylthiazol-2-yl)2,5 diphenyltetrazolium bromide (MTT, Acros Organics) was used for mytocondrial activity evaluation. Briefly, cells were plated onto 96-well plates, with a seeding density of $15x10^3$ cells/well in 100 µL culture medium. After 24 h, the medium was renewed but containing the following three treatments: DCX, DCX- loaded HA nanocapsules and blank HA nanocapsules. Finally, after 48 h cell survival was measured by the MTT assay (Mossmann., 1983). In brief, medium was removed and the cells were washed twice with 100 µL Hank`s Balanced Salt Serum (HBSS). Then 20 µL of a MTT solution (5 mg/mL in PBS) and 100 µL HBSS were added to the wells and maintained at 37°C in an atmosphere with 5% CO_2 for 4h. Afterwards, buffers were replaced by 100 µL DMSO per well and maintained at 37° C in an atmosphere with 5% CO_2 overnight. Absorbance (λ= 515 nm) was measured in a spectrophotometer (Tecan, Ultra evolution) removing background absorbance (λ= 630 nm). Moreover, short incubation times of 2 h were assayed in order to determine the efficacy of HA nanocapsules to quickly interact with the cells and deliver the drug intracellularly. Thus, after 2 h of incubation with the three treatments, medium was replaced by fresh one and cells were grown for 48 h. Finally, cell viability was measured as described.

The percentage of cell viability was calculated by the absorbance measurements of control growth in the presence of the formulations at various concentration levels. IC_{50} values were obtained by fitting the data with non linear regression, with Prism 2.1 software (GraphPad, San Diego, CA).

Stability study at storage conditions

The suspension stability of HA nanocapsules prepared with the surfactants BKC and CTAB were evaluated according to terms of time and temperature of storage. Therefore, aliquots of the nanocapsules suspension without dilution were placed in sealed tubes at 4 and 37°C for storage. Size and polydispersity index of the nanocarriers were measured for a period of three months, meanwhile zeta potential values were controlled at the end of the study. Each sample corresponds to a different HA nanocapsules batch.

Freeze-dried studies of HA nanocapsules

Concentrations of HA nanocapsules (0.25, 0.5 and 1% w/v) and of the cryoprotectant trealose (5 and 10%) were considered the variables for the lyophilization study. Therefore, 2 mL dilutions of HA NCs were transferred in 5 mL volume glass vials and were frozen at -20°C. The lyophilization procedure consisted in an initial drying step for 60 h at -35°C, followed by a secondary drying for 24 h in a high vacuum atmosphere. Finally, temperature was slowly increased up to 20°C until the end of the process (Labconco Corp., USA). HA nanocapsules were recovered by adding 2 mL of ultrapure water ot the freeze-dried powders followed by manual resuspension and were characterized as explained above.

Statistical analysis

Cell culture results were evaluated in order to determine the statistical significance between the different formulations studied. The statistical evaluation of the cell viability results was performed by an ANOVA test followed by the post hoc Tukey test comparison analysis (SigmaStat Program, Jandel Scientific, version 3.5).

Results and discussion

The main aim of this work was the development of a new anticancer drug nanocarrier consisting of a lipid core surrounded by a shell made of HA. The conceptual bases of the system were: simplicity (minimum amount of components and easy to produce), acceptability (from the regulatory stand point) and efficacy (improvement of citoxicity in cancer cells). For this, DCX was chosen as a model compound and its efficacy was evaluated in lung cancer cell line NCI-H460. As indicated in the introduction, the biopolymer HA was chosen because of its interesting biopharmaceutical properties (Eliaz and Szoka, 2001; Surace et al., 2009; Ossipov et al., 2010).

Development and characterization of HA nanocapsules

HA nanocapsules were prepared by a number of simple techniques, which involved the formation of a cationic nanoemulsion and the attachment of the outer HA corona. One of the techniques was the solvent displacement technique, which allowed the emulsification process to occur simultaneously to the attachment of the polymer corona. Other techniques involved two steps, i.e. an emulsification process either by the solvent displacement technique, homogenization or sonication, followed by the coating with the polymer. In all cases, the formation of the polymer capsule is driven by the

ionic interaction of the positively charged surfactant with the negatively charged HA. Following an initial screening of different experimental approaches, we chose the two-step solvent diffusion technique previously used for the formation of chitosan (Lozano et al., 2008) and polyarginine nanocapsules (Lozano et al., 2011b), and investigated the influence of different formulation parameters on the physicochemical properties of the resulting systems. The formulation parameters were the type and concentration of cationic surfactant, and the concentration of HA. The cationic surfactants selected on the basis of their acceptable toxicological profile (Rowe et al., 2009) were BKC and hexadecyltrimethylammonium bromide (CTAB). On the other hand, the quantity of the surfactants used was the minimum that allowed us the formation of stable systems. In the case of CTAB this amount was 1.8 mg, and in the case of BKC 4.0 mg.

Table 1a and b show the characteristics of nanocapsules prepared by the two-stage procedure using the surfactants BKC or CTAB, respectively. As can been noted, the use of adequate concentrations of HA with the cationic nanoemulsions results in the formation of homogenous populations of nanocapsules of around 250 nm. The results also show a shielding of the original positive zeta potential of the nanoemulsion, which leads to an inversion to negative values, as the concentration of HA increases. This dependency of the zeta potential with the amount of HA evidences the surface localization of HA molecules and indicates the necessity to use a minimum amount of HA in order to obtain a stable nanocapsules. The formation of the HA corona results in a minor increase in the size of the nanocapsules with respect to the nanoemulsions, a result that supports the idea that HA is tightly attached to the oily droplets.

Tables 1a and b also indicate that the viability of the system is compromised under certain conditions. More specifically, we observed a precipitation of the system due to the neutralization of the positive surface charge caused by the addition of increasing amounts of HA. After the inflection point, the addition of subsequent amounts of HA leads to the inversion of the zeta potential and the subsequent stabilization of the system. Finally, there is another precipitation point that is related to the excess of the HA in the formulation. Here, the precipitation phenomenon could be attributed to a combination of factors such as the high ionic strength in the medium (Hiemenz and Rajagopalan, 1997) (due to the high concentration of sodium ions added together with the hyaluronate), combined with the increase in the viscosity, which might modify the kinetic of adsorption of the polymer onto the cationic nanoemulsion (Cowman and Matsuoka, 2005).

Table 1. Physicochemical properties of the nanocapsules prepared following a two-stage procedure, with different quantities of HA (29 kDa) and a fixed amount of the surfactants (a) BKC (4.0 mg) or (b) CTAB (1.8 mg) (mean± S.D., n≥3).

(a)

HA 29 kDa (mg)	Size (nm)	Polydispersity Index	Zeta potential (mV)
0.0	223.3 ± 10.3	0.1	+27.1 ± 3.5
0.5	249.8 ± 10.2	0.2	+9.6 ± 2.5
1.0	pp.	---	---
3.1	pp.	---	---
6.2	248.7 ± 10.0	0.2	-42.3 ± 2.1
12.5	235.3 ± 13.3	0.1	-45.6 ± 4.7
25.0	252.2 ± 19.1	0.1	-46.7 ± 2.9
50.0	pp.	---	---

(b)

HA 29 kDa (mg)	Size (nm)	Polydispersity Index	Zeta potential (mV)
0.0	215.2 ± 7.3	0.1	+35.3 ± 2.1
0.1	231.7 ± 8.3	0.1	+18.3 ± 2.2
0.5	pp.	---	---
1	pp.	---	---
3.1	238.2 ± 2.4	0.1	-35.3 ± 2.4
6.2	238.4 ± 3.3	0.1	-37.6 ± 2.2
12.5	260.3 ± 20.0	0.2	-31.3 ± 3.2
25.0	pp.	---	---
50.0	pp.	---	---

pp.: Precipitation.

Tables 2a and 2b display the results of size and zeta potential of the HA nanocapsules prepared according to a single stage procedure. Overall, the conclusion is that the incorporation of HA either during or after the emulsification process does not affect the formation of the HA corona (similar zeta potential values and precipitation conditions). However, the size of the nanocapsules elaborated by a single stage procedure was smaller than that of nanocapsules obtained by a two-stage procedure (~170nm and ~250nm, respectively). This difference in size has also been observed for chitosan nanocapsules prepared following a single or two-stage procedure (Prego et al., 2005; Lozano et al., 2008) and could be attributed to the stabilizing role of the polymer during the emulsification process.

Table 2. Physicochemical properties of the nanocapsules prepared following a single stage procedure with different quantities of HA (29 kDa) and a fixed amount of the surfactants (a) BKC (4.0 mg) or (b) CTAB (1.8 mg) (mean± S.D., n≥3).

(a)

HA 29 kDa (mg)	Size (nm)	Polydispersity Index	Zeta potential (mV)
0.0	223.3 ± 10.3	0.1	+27.1 ± 3.5
0.5	251.2 ± 5.2	0.1	+27.2 ± 1.4
1.0	pp.	pp.	pp.
3.1	pp.	pp.	pp.
6.2	pp.	pp.	pp.
12.5	185.2 ± 4.6	0.1	-44.2 ± 2.3
25.0	186.4 ± 6.6	0.1	-47.4 ± 2.3
50.0	pp.	pp.	pp.

(b)

HA 29 kDa (mg)	Size (nm)	Polydispersity Index	Zeta potential (mV)
0.0	215.7 ± 7.2	0,1	+35 ± 2.5
0.1	228.6 ± 17.3	0.1	+33.7 ± 3.0
0.5	pp.	pp.	pp.
1.0	pp.	pp.	pp.
3.1	168.4 ± 3.4	0.1	-35.9 ± 2.7
6.2	170.3 ± 6	0.1	-35.6 ± 1.0
12.5	273.4 ± 12.7	0.2	-35.7 ± 2.8
25.0	pp.	pp.	pp.
50.0	pp.	pp.	pp.

pp.: Precipitation.

The size and appearance of the nanocapsules has also been observed by transmission electron microscopy (TEM). As an example, figure 1 illustrates the size and structure of those prepared with the BKC surfactant (figure 1). Overall, the nanocapsules exhibited a round shape and the core-corona structure typically observed for polymeric nanocapsules (Prego et al., 2005; Lozano et al., 2008).

Figure 1: Transmission electron microscopy images of HA nanocapsules obtained with 12.5 mg of HA (29 kDa) and containing BKC (4 mg).

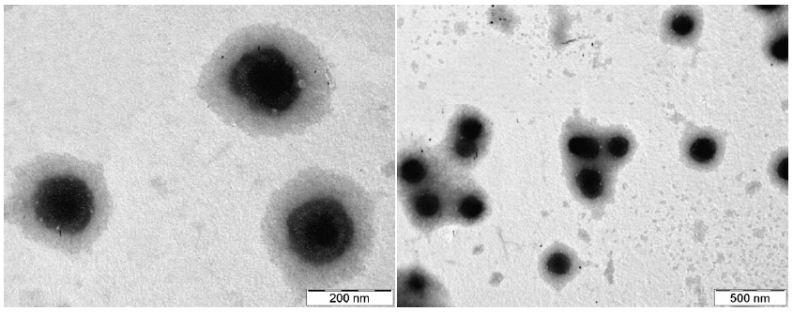

In a second part of the development process, we evaluated the influence of the HA MW (160 kDa vs. 29 kDa used in the original study) in the characteristics of the nanocapsules prepared by the two-step solvent diffusion technique. Table 3 shows the characteristics of the formulations prepared by incubation of the preformed emulsion containing BKC with high MW HA. Overall, the values corresponding to size, polidispersity, and zeta potential are larger than those obtained with HA of 29 kDa (table 1a and b). Similar results were obtained when the surfactant used was CTAB (data not shown). This behavior correlates very well with the previously observed for chitosan nanocapsules (Santander-Ortega et al. 2011) and was attributed to the different thickness of the HA coating around the oily nanodroplets. Namely, the use of high MW led to an increase in the thickness of the coating and, thus, to an increase of the size of the nanocapsules. In addition, an increase of the zeta potential values was also observed as compared to the low MW HA nanocapsules, a result that could be a consequence of the greater number of carboxylic groups of AH at the shell surface.

Table 3. Physicochemical properties of the nanocapsules prepared following a two-stage procedure with different quantities of HA (160 kDa), with the surfactant BKC (4 mg) (mean± S.D., n≥3).

HA 160 kDa (mg)	Size (nm)	Polydispersity Index	Zeta potential (mV)
0.0	207.6 ± 5.5	0.1	+27.3 ± 3.1
0.5	235.2 ± 10.3	0.2	+27.3 ± 3.6
1.0	271.4 ± 53.8	0.5	+3.9 ± 1.8
3.1	pp.	---	---
6.2	256.6 ± 11.4	0.5	-52.4 ± 8.8
12.5	294.5 ± 40.6	0.4	-62.3 ± 8.1
25.0	410.7 ± 70.0	0.5	-59.9 ± 6.1
50.0	pp.	pp.	pp.

pp.:Precipitation.

Encapsulation and release of docetaxel (DCX) from HA nanocapsules

The high efficacy of DCX in the treatment of a wide range of solid tumors (Crown and O'Leary., 2000), together with its hydrophobic character makes this molecule an attractive candidate for inclusion in the developed nanocapsules. Among the tested blank nanocapsules formulations, we selected the one containing 12.5 mg of 29 KDa HA (see tables 1a and 1b) for the further studies as it contained the greatest amount of HA without causing precipitation. As shown in table 3, DCX could be efficiently encapsulated in the HA nanocapsules prepared with the surfactants BKC or CTAB hardly affecting the characteristics of the original blank formulations. These data of encapsulation correlates very well with previously published works where DCX was also encapsulated in lipid nanocapsules, and is attributed to the affinity of the drug for the core components (Khalid et al., 2006, Lozano et al., 2008).

Table 3. Characteristics of the selected blank and DCX-loaded HA nanocapsules prepared with the surfactants BKC or CTAB. (mean ± S.D., n≥3).

Formulation	Size (nm)	Polydispersity Index	Zeta potential (mV)	Association efficiency (%)
HA NCs (BKC)	235.5 ± 13.2	0.1	-45.0 ± 4.3	---
DCX- loaded HA NCs (BKC)	250.3 ± 20.5	0.1	-52.3 ± 11.3	65.5 ± 3.1
HA NCs (CTAB)	267.2 ± 23.4	0.1	-31.1 ± 3.4	---
DCX- loaded HA NCs (CTAB)	276.2 ± 10.3	0.1	-36.7 ± 1.4	65.1 ± 3.8

In an additional experiment, we evaluated the release pattern of the encapsulated DCX upon incubation of highly diluted nanocapsules prepared with the surfactants BKC or CTAB in aqueous medium. The results showed similar drug release profiles for nanocapsules containing BKC or CTAB with only critical differences in the initial time-release point (figure 2). The release follows a biphasic profile, characterized by a rapid initial release, followed by a second stage in which no further changes were observed. The initial release stage, which is typically observed in oily systems (Prego et al., 2006; Lozano et al., 2008; 2011b), has been attributed to the dilution of the nanocapsules in the incubation medium and the subsequent partition of the drug between the oily core and the external aqueous phase. The absence of release in the second stage confirms the high affinity of the DCX by the oil core. While these data provide us with information about mechanistic details, in their interpretation it is important to point out that the release behavior observed *in vitro* is not expected to correlate with the *in vivo* behavior. In the *in vivo* situation, the presence of physiological occurring macromolecules and ions could significantly influence the release profile as reported Ahmed et al (2011).

Figure 2: *In vitro* DCX release from DCX- loaded HA nanocapsules using BKC (X) or CTAB (■) as surfactants (mean± S.D., n=3).

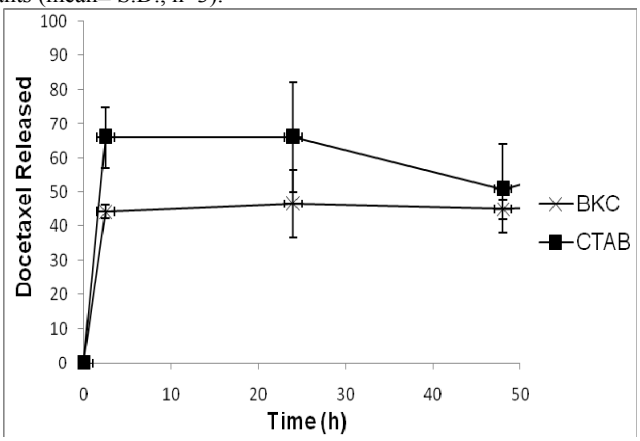

In vitro efficacy of the DCX- loaded HA nanocapsules in human lung cancer cell line

Cell viability studies were performed in order to assess the efficacy of the HA nanocapsules in the non-small cell lung cancer NCI-H460 cell line. Figures 3a and b show the cellular viability profiles of DCX-loaded HA nanocapsules (formulation containing 1.8 mg of CTAB and 12.5 mg of HA 29 KDa) upon cell exposure for up to 2 and 48 h respectively. The results indicate that the encapsulation of DCX in HA nanocapsules leads to a significant increase of its citotoxicity. The toxicity values were multiplied by a factor of 2 or 3 depending upon the incubation time. The results also show that blank nanocapsules do not cause any noticeable damage to the cells. These results are summarized in table 4, which illustrates the citotoxicity values of DCX-loaded nanocapsules measured by their IC_{50}. Overall, the potency of DCX was increased up to more than 3 times upon its encapsulation into HA nanocapsules.

Figure 3: Effect of DCX encapsulation into HA nanocapsules (HA= 29 KDa, 12.5 mg) containing CTAB (1.8 mg) on NCI-H460 cell viability after (a) 2 or (b) 48 h incubation. Blank HA NCs (white bars), free DCX (grey bars) and DCX- loaded HA NCs (black bars) (n=4). # p<0.005: DCX- loaded HA NCs vs. free DCX.

(a)

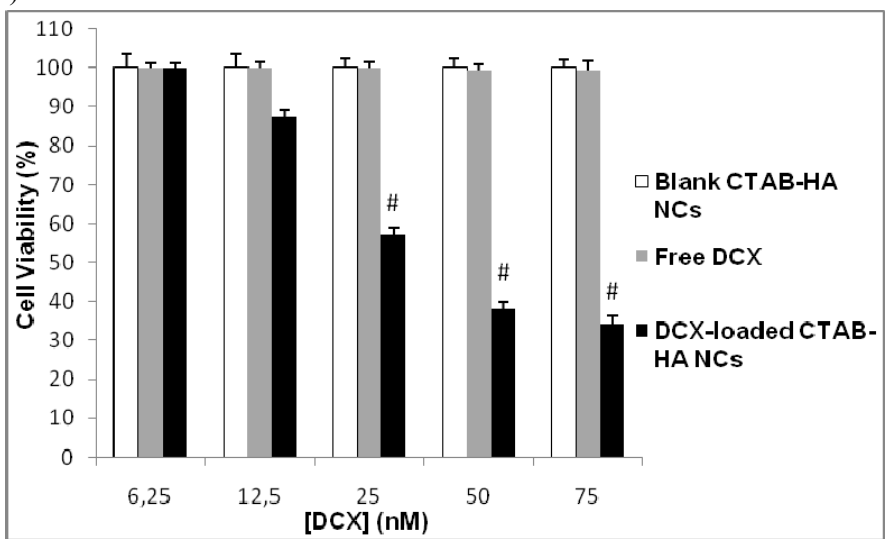

(b)

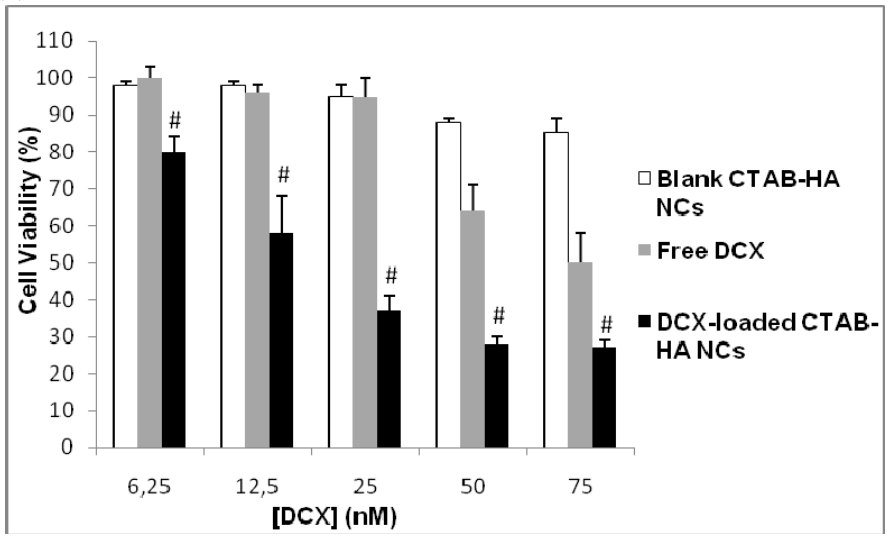

Table 4: IC_{50} values (drug concentration resulting in a 50% of cell viability) expressed in nM. Mean values of 4 independent experiments; n.d.: none of the concentrations tested resulted in a significant reduction in the viability.

Formulation	2 h exposure	48 h exposure
Blank HA CTAB NCs	n.d.	n.d.
Blank HA BKC NCs	n.d.	*
DCX	105.0 ± 9.0	36.4 ± 4.0
DCX- loaded HA CTAB NCs	31.5 ± 2.1[#]	10.8 ± 1.1[#]
DCX- loaded HA BKC NCs	29.1 ± 1.8[#]	15.3 ± 2.0[#]

[*] The maximum reduction in cell viability was 39.0 ± 8.0%. [#] $P<0.01$ with respect to IC_{50} of DCX (One-way ANOVA test, post-hoc Tukey test).

Figures 4a and b show the cytotoxicity profiles of cell exposed to HA nanocapsules prepared with the surfactant BKC for up to 2 and 48 h, respectively. The cellular behavior displayed in figure 4a is similar to that observed for nanocapsules prepared with the surfactant CTAB. Accordingly, the results in table 4 show that DCX-loaded nanocapsules are 3.6 times more efficient than the free drug in terms of the IC_{50} values. This improved efficacy was also observed after 48 h incubation (figure 4b), leading to a 3-fold reduced IC_{50} value (table 4). In this case, a certain reduction of cell viability was also observed at high concentrations of blank nanocapsules (figure 4b), a result that was attributed to the higher toxicity of BKC over CTAB (Rowe, 2009) and the necessity of using a greater amount of BKC *vs*. CTAB for the formation of stable nanocapsules.

Figure 4: Effect on NCI-H460 cell viability of HA nanocapsules (AH= 29 KDa, 12.5 mg) prepared with the surfactant BKC (4 mg) after (a) 2 or (b) 48 h of contact with the cells. Blank HA NCs (white bars), free DCX (grey bars) and DCX- loaded HA NCs (black bars) (n=4). # p<0.005: DCX- loaded HA NCs vs. free DCX.

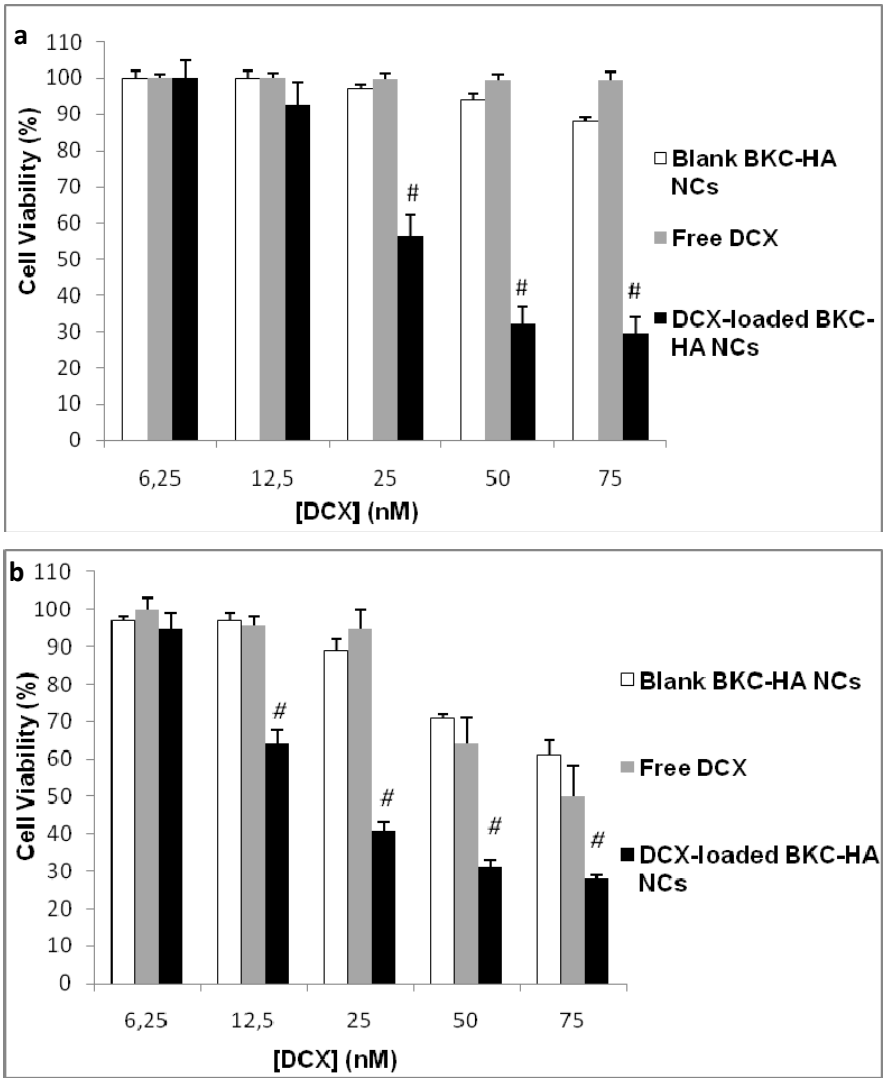

The significant improvement in cytotoxicity observed for HA nanocapsules loaded with DCX is in agreement with the results observed for other nanocapsules coated with polyethyleneglycol (Garcion et al., 2006), chitosan (Lozano et al., 2008) or polyarginine (Lozano et al., 2011b) tested in a variety of cell lines, including: glyoma cells (9L and F98 cell lines), human

breast carcinoma (MCF-7), and human lung cancer (A-549, and NCI-H460). The improvement in cytotoxicity has been attributed to the internalization and intracellular drug delivery capacity of the nanocapsules in association with a potential reversion of the multidrug resistance effect.

Importantly, the above indicated nanocapsules and those functionalized with a monoclonal antibody (anti TMEFF-2) have also been tested in a variety of animal models of cancer, such as: glyoma (Garcion et al., 2006), hepatocellular carcinoma (Lacoeuille et al., 2007), colon adenocarcinoma (Khalid et al., 2006), and lung cancer (Torrecilla et al., 2011). The results obtained so far have shown an improved or similar efficacy of the encapsulated drug as compared to that obtained for the free drug. These are promising preliminary data as the nanocapsules are expected to have a more acceptable toxicity profile (they avoid the use of toxic solubilizers) than the commercial drugs.

Stability studies of HA nanocapsules during storage

Stability is a critical issue in the development of a nanocarrier formulation. Variations on temperature are known to importantly compromise the stability of colloidal systems, and show evident importance during storage (Freitas and Müller, 1998). The size increase of the formulations could be attributed to the weakening/breaking of linkers between the molecules that forms the nanocarriers, and may alter their drug release and induce destabilization of the formulations. A decrease in size could also occur due to the detachment of components from the nanocarriers or to an increase on the interaction strengths between linkers, potentially affecting the desired efficacy of the nanocarrier. In the present study we evaluated the stability of the DCX-loaded nanocapsules prepared with the surfactant CTAB under storage at 4° and 37°C, for a period of 3 months. Figure 5 shows that nanocapsules were generally stable during storage

irrespective of the temperature conditions. The overall trend of prolonged stability is justified by the electrostatic repulsive effect due to the high zeta potential values of nanocapsules (around -40 mV). Similar results were obtained when the surfactant BKC was used for the elaboration of the nanocapsules (data not shown). This acceptable stability profile has been previously observed for other polymer nanocapsules (Prego et al., 2003; Lozano et al. 2011b); and attributed to the polymer corona surrounding the oily nanodroplets.

Figure 5: Stability study of DCX-loaded HA nanocapsules during 3 months of storage. Nanocapsules were prepared with CTAB and evaluated at 4°C (▲) and 37° C (●). (Mean ± S.D.; n=3).

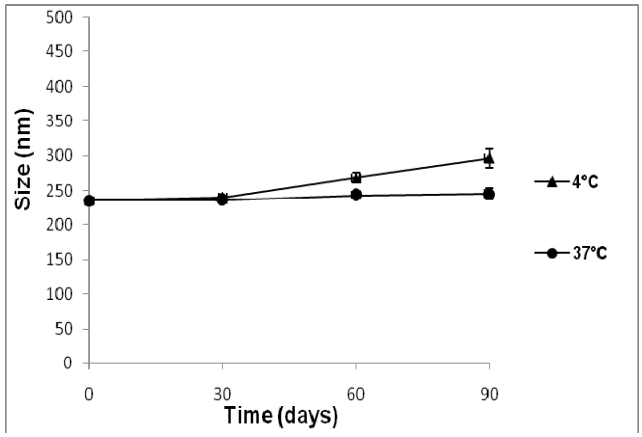

Formation of a lyophilized product of HA nanocapsules

Lyophilization is one of the most frequent and efficient methods for preserving the properties of nanoparticulate systems during storage. Nevertheless, this process becomes quite complex in the case of nanocapsules due to the fluidity of the polymer shell and also due to the presence of the oil core, which is susceptible of leakage (Choi et al., 2004). In order to facilitate the lyophilization of the nanocarriers and avoid their collapse, the use of cryoprotectant agents is necessary (Abdelwhaed et al.,

2006). The first evidence that polymeric nanocapsules were effectively protected, by isotonic concentrations of cryoprotectants derived from sugar, during a lyophilization process was carried out by Calvo et al. (1997). Subsequent works (Lozano et al 2011a, b) have indicated that trehalose is an adequate agent for preserving the stability of fluid nanosystems during lyophilization. The main arguments that support the use of this agent over others cryoprotectans is its less hygroscopicity together with its higher glass transition temperature.

Figure 6 shows the size of HA nanocapsules containing BKC upon reconstitution of the freeze-dried product. Overall the results indicate that at relatively high concentrations of nanocapsules (1% w/v) it is possible to achieve an adequate resuspension of the dried product without altering the size of the nanocapsules.

Figure 6: Particle size of the reconstituted freeze dried HA nanocapsules using BKC as surfactant. Different concentrations (w/v) of nanocapsules were lyophilized using trehalose at 10% (black bars) or 5% w/v (grey bars). (Mean ± S.D.; n=3).

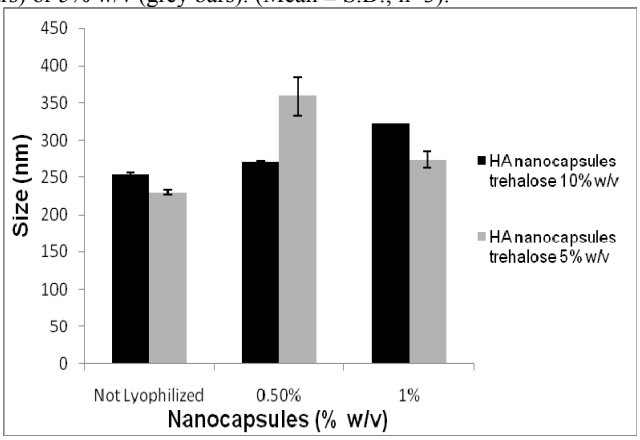

Conclusions

In this paper we report the formation and characterization of a new type of drug nanocarriers named as HA nanocapsules. Because of their hydrophobic core, these nanocarriers are able to successfully encapsulate the hydrophobic drug docetaxel. In addition, thanks to their HA hydrophilic coating, these nanocarriers have the capacity to interact with NCI-H460 cancer cells and improve the pharmacological effect of the model drug docetaxel. Finally, pharmaceutical parameters such as drug release, stability during storage and reconstitution of freeze-dried HA nanocapsules render these novel systems promising platforms for the intracellular delivery of anticancer drugs.

References

1. Akima K, Ito H, Iwata Y et al.: Evaluation of antitumor activities of hyaluronate binding antitumor drugs: synthesis, characterization and antitumor activity. J. Drug Target 4,1-8 (1996).
2. Abdelwhaed W, Degobert G, Fessi H.: Investigation of nanocapsules stabilization by amorphous excipients during freeze-drying and storage. Eur. J. Pharm. Biopharm. 63, 87-94 (2006).
3. Ahmed IS, Ayres JW: Comparison of in vitro and in vivo performance of a colonic delivery system. Int. J. Pharm. (2011), doi:10.1016/j.ijpharm.2011.02.061.
4. Auzenne E, Ghosh SC, Khodadadian M et al.:. Hyaluronic acid-paclitaxel: antitumor efficacy against CD44(+) human ovarian carcinoma xenografts. Neoplasia 9, 479–486 (2007).
5. Bae KH, Lee Y, Park TG. Oil-encapsulating PEO-PPO-PEO/PEG shell cross-linked nanocapsules for target-specific delivery of paclitaxel. Biomacromol. 8(2), 650-6 (2007).

6. Calvo P, Remuñan-López C, Vila-Jato JL, Alonso MJ: Development of positively charged colloidal drug carriers: Chitosan-coated polyester nanocapsules and submicron-emulsions. Colloid. Polym. Sci. 275, 46-53 (1997).
7. Choi M.J, Briancon S, Andrieu J, Min SG, Fessi H: Effect of freeze-drying process conditions on the stability of nanoparticles. Dry. Technol. 22, 335-346 (2004).
8. Choi KY, Min KH, Na JH et al.: Self-assembled hyaluronic acid nanoparticles as a potential drug carrier for cancer therapy: synthesis, characterization, and *in vivo* biodistribution J. Mater. Chem. 19, 4102-4107 (2009).
9. Crown J, O'Leary M: The taxanes: An update. Lancet 355(9210), 1176-8 (2000).
10. Cowman M, Matsuoka SH: Experimental approaches to hyaluronan structure. Carbohydr Res. 340(5):791-809 (2005).
11. Eliaz RE, Szoka FCJr: Liposome-encapsulated doxorubicin targeted to CD44: A strategy to kill CD44-overexpressing tumor cells. Cancer Res. 61(6), 2592-601 (2001).
12. Eliaz RE, Nir S, Marty C, Szoka FC Jr. Determination and modeling of kinetics of cancer cell killing by doxorubicin and doxorubicin encapsulated in targeted liposomes. Cancer Res. 64:711–718 (2004).
13. Freitas C, Müller RH: Effect of light and temperature on zeta potential and physical and physical stability in solid lipid nanoparticle (SLN^{TM}) dispersions. Int. J. Pharm. 168, 221-229 (1998).
14. Garcion E, Lamprecht A, Heurtault B et al.: A new generation of anticancer, drug-loaded, colloidal vectors reverses multidrug resistance in glioma and reduces tumor progression in rats. Mol. Cancer Ther. 5(7), 1710-22 (2006).

15. Heurtault B, Saulnier P, Pech B, Proust JE, Benoit JP: A novel phase inversion-based process for the preparation of lipid nanocarriers. Pharm. Res. 19(6), 875-80 (2002a).
16. Heurtault B, Saulnier P, Pech B, Proust JE, Benoit JP: Properties of polyethylene glycol 660 12-hydroxy stearate at a triglyceride/water interface. Int. J. Pharm. 242(1-2), 167-70 (2002b).
17. Principles of Colloidal and Surface Chemistry (third edition). Hiemenz PC, Rajagopalan R, (Editors). Dekker, New York, USA (1997).
18. Hyung W, Ko H, Park J et al.: Novel hyaluronic acid (HA) coated drug carriers (HCDCs) for human breast cancer treatment. Biotechnol Bioeng. 99(2), 442-54 (2008).
19. Khalid MN, Simard P, Hoarau D, Dragomir A, Leroux JC:. Long circulating poly(ethylene glycol)-decorated lipid nanocapsules deliver docetaxel to solid tumors. Pharm Res. 23(4), 752-8 (2006).
20. Lacoeuille F, Hindre F, Moal F et al.: In vivo evaluation of lipid nanocapsules as a promising colloidal carrier for paclitaxel. Int. J. Pharm. 344(1-2), 143-9 (2007).
21. Lee SH, Yoo SD, Lee KH: Rapid and sensitive determination of paclitaxel in mouse plasma by high-performance liquid chromatography. J. Chromatogr., B: Biomed. Sci. Appl., 724, 357-363 (1999).
22. Lozano MV, Torecilla D, Torres D, Vidal A, Dominguez F, Alonso MJ: Highly efficient system to deliver taxanes into tumor cells: docetaxel-loaded chitosan oligomer colloidal carriers. Biomacromol. 9, 2186-2193 (2008).
23. Lozano MV, Lollo G, Brea J, Torres D, Loza MI, Alonso MJ. Freeze-dried polysaccharide nanocapsules: efficient vehicles for the intracellular delivery of docetaxel. (submitted) (2011a).
24. Lozano MV, Lollo G, Brea J, Torres D, Loza MI, Alonso MJ. Polyarginine nanocapsules: a new platform for intracellular drug delivery. (submitted) (2011b).

25. Luo Y, Prestwich GD. Synthesis and selective cytotoxicity of a hyaluronic acid-antitumor bioconjugate. Bioconjug. Chem. 10, 755–763 (1999).
26. Mossman T: Rapid colorimetric assay for cellular growth and survival: application to proliferation and cytotoxicity assays. J. Immunol. Methods 65, 55-63 (1983).
27. Ossipov DA: Nanostructured hyaluronic acid-based materials for active delivery to cancer. Expert Opin. Drug Deliv. 7(6), 681-703 (2010).
28. Peer D, Margalit R: Tumor-targeted hyaluronan nanoliposomes increase the antitumor activity of liposomal Doxorubicin in syngeneic and human xenograft mouse tumor models. Neoplasia 6, 343-353 (2004a).
29. Peer D, Margalit R: Loading mitomycin C inside long circulating hyaluronan targeted nano-liposomes increases its antitumor activity in three mice tumor models. Int. J. Cancer 108, 780-789 (2004b).*
30. Peer D, Karp JM, Hong S, Farokhzad OC, Margalit R, Langer R: Nanocarriers as an emerging platform for cancer therapy. Nat. Nanotechnol. 2(12), 751-60 (2007).
31. Prego C, Fernandez-Megia E, Novoa-Carballal R, Quinoa E, Torres D, Alonso MJ. Chitosan and chitosan-PEG nanocapsules: new carriers for improving the oral absorption of calcitonin. Presented at: 30th Annual Meeting of the Controlled Release Society, Glasgow, UK, 19-23 July 2003.
32. Prego C, García M, Torres D, Alonso MJ: Transmucosal macromolecular drug delivery. J. Control Release 101(1-3), 151-62 (2005).
33. Prego C, Torres D, Alonso MJ: Chitosan nanocapsules: A new carrier for nasal peptide delivery. JDDST. 16, 331-337 (2006).
34. Rosato A, Banzato A, De Luca G et al.: HYTAD1-p20: a new paclitaxel-hyaluronic acid hydrosoluble bioconjugate for treatment of superficial bladder cancer. Urol. Oncol. 3, 207-15 (2006).

35. Handbook of pharmaceutical excipients (Sixth edition). Raymond C Rowe, Paul J Sheskey, Marian E Quinn (Editors). Pharmaceutical press, London-United Kingdom (2009).
36. Santander-Ortega MJ, Peula-García JM, Goycoolea FM, Ortega-Vinuesa JL: Chitosan nanocapsules: Effect of chitosan molecular weight and acetylation degree on electrokinetic behaviour and colloidal stability. Colloids Surf. B Biointerfaces. 82(2), 571-80 (2011).
37. Surace C, Arpicco S, Dufaÿ-Wojcicki A et al.: Lipoplexes targeting the CD44 hyaluronic acid receptor for efficient transfection of breast cancer cells. Mol Pharm. 6(4), 1062-73 (2009).
38. Ten Tije AJ, Verweij J, Loos WJ, Sparreboom A: Pharmacological effects of formulation vehicles : implications for cancer chemotherapy. Clin. Pharmacokinet. 42(7), 665-85 (2003).
39. Torrecilla D, Lozano MV, Lallana E: In Vivo Efficacy of Anti-TMEFF-2 Modified Chitosan-g-Poly(ethyleneglycol) Nanocapsules in Non-Small Cell Lung Tumors (submitted) (2011).

DISCUSIÓN

El ácido hialurónico (HA) es un polísacárido aniónico natural, no tóxico y biodegradable que se ha revelado como una propuesta muy interesante para el diseño de nanosistemas dirigidos específicamente al tratamiento de tumores sólidos[118;119;120;121]. Este polímero posee especificidad frente a los receptores CD-44 sobreexpresados en diferentes tipos de cáncer, entre otros los que cursan a nivel pulmonar como el cáncer de células no pequeñas, metaplasia escamosa y adenocarcinoma[122;123].

El HA posee además una demostrada capacidad mucoadhesiva [124;125] que lo posiciona como un material ideal para dotar a los nanosistemas de la mucoadhesión necesaria para favorecer el contacto con el epitelio pulmonar y potenciar la difusión de fármacos antitumorales hacia el entorno tumoral y su penetración intracelular.

Los nanosistemas que contienen un núcleo oleoso contituyen el vehículo ideal para fármacos antitumorales extremadamente hidrofóbicos, como son los taxanos[126;127;128;129]. Concretamente, el docetaxel ha sido incluído en el núcleo oleoso de sistemas nanométricos como

[118] **Surace C, Arpicco S, Dufaÿ-Wojcicki A, Marsaud V, Bouclier C, Clay D, Cattel L, Renoir JM, Fattal E.** (2009). Mol Pharm. 6(4):1062-73.
[119] **Taetz S, Bochot A, Surace C, Arpicco S, Renoir JM, Schaefer UF, Marsaud V, Kerdine-Roemer S, Lehr CM, Fattal E.** (2009). Oligonucleotides. 19(2):103-16.
[120] **Peer D, Margalit R.** (2004). Neoplasia. 6(4):343-53.
[121] **Eliaz RE, Nir S, Szoka FC Jr.** (2004) Methods Enzymol. 387:16-33.
[122] **Penno MB, August JT, Baylin SB, Mabry M, Linnoila RI, Lee VS, Croteau D, Yang XL, Rosada C.** (1994). Cancer Res. 54(5):1381-7.
[123] **Tran TA, Kallakury BV, Sheehan CE, Ross J.S.** (1997). Hum Pathol. 28(7):809-14.
[124] **Di Colo G**, **Zambito Y**, **Zaino C**, **Sansò M**. (2009). Drug Dev Ind Pharm. 35(8):941-9.
[125] **Saso L**, **Bonanni G**, **Grippa E**, **Gatto MT**, **Leone MG**, **Silvestrini B**. (1999). Res Commun Mol Pathol Pharmacol. 104(3):277-84.
[126] **Huynh N.T.; Passirani C, Saulnier P, Benoit J.P**. (2009). Int. J. Pharm. 379(2):201-9.
[127] **Bae K.H.; Lee Y.; Park T.G.** (2007). Biomacromolecules. 8: 650-656.
[128] **Khalid M.N.; Simard P.; Hoarau D.; Dragomir A.; Leroux J.C.** (2007). Pharm. Res. 23: 752-758.
[129] **Peltier S, Oger JM, Lagarce F, Couet W, Benoit J.P.** (2006). Pharm. Res. 23: 1243-1250.

nanocápsulas[126;128;130;131] y liposomas[132;133;134;135;136;137], lo que ha permitido con mayor o menor éxito potenciar su efecto antitumoral, evitando la utilización de los disolventes incluidos hasta ahora en la formulación comercial.

En nuestro grupo de investigación, la inclusión de docetaxel en nanocápsulas de quitosano[131] y poliarginina[138], ha confirmado la idoneidad de estos nanosistemas en cuanto a lograr una encapsulación adecuada del fármaco, y potenciar su vehiculización hacia el interior de las células tumorales.

El trabajo central de la segunda parte de esta tesis se ha dirigido a explorar un nuevo nanosistema, las nanocápsulas de HA, como vehículos del antitumoral docetaxel, con el fin último de lograr una aplicación localizada pulmonar.

Preparación y caracterización de las nanocápsulas de HA

Las nanocápsulas de HA se prepararon mediante la la técnica de desplazamiento de disolvente, adaptando un procedimiento desarrollado previamente en nuestro laboratorio para otros polímeros catiónicos, como el

[130] **Nassar T**, **Attili-Qadri S**, **Harush-Frenkel O**, **Farber S**, **Lecht S**, **Lazarovici P**, **Benita S**. (2011). Cancer Res. 71(8):3018-28.
[131] **Lozano MV, Torrecilla D, Torres D, Vidal A, Domínguez F, Alonso MJ.** (2008) Biomacromolecules. 9(8):2186-93.
[132] **Immordino ML**, **Brusa P**, **Arpicco S**, **Stella B**, **Dosio F**, **Cattel L**. (2003). J. Control Release. 91(3):417-29.
[133] **Qin Y**, **Song QG**, **Zhang ZR**, **Liu J**, **Fu Y**, **He Q**, **Liu J**. (2008) Arzneimittelforschung. 58(10):529-34.
[134] **Liang G**, **Jia-Bi Z**, **Fei X**, **Bin N**. (2007). J. Pharm. Pharmacol. 59(5):661-7.
[135] **Yuan Z, Chen D, Zhang S, Zheng Z.** (2010). Yakugaku Zasshi. 130(10):1353-9.
[136] **Yamamoto Y, Yoshida M, Sato M, Sato K, Kikuchi S, Sugishita H, Kuwabara J, Matsuno Y, Kojima Y, Morimoto M, Horiuchi A, Watanabe Y.** (2011). Int. J. Oncol. 38(1):33-9.
[137] **Zhai G, Wu J, Yu B, Guo C, Yang X, Lee R.J.** (2010). J. Nanosci. Nanotechnol. 10(8):5129-36.
[138] **Lozano MV, Lollo G, Brea J, Loza MI, Torres D, Alonso MJ.** (2011). Submitted.

quitosano[131;139] y la poliarginina[138]. En el caso de los polímeros catiónicos, la formación de nanocápsulas se producía gracias a la interacción de éstos con el tensoactivo aniónico, lecitina, incluido en el núcleo de una nanoemulsión. Para la formación de las nanocápsulas de HA, al tratarse de un polímero aniónico, fue necesario adaptar el método, mediante la incorporación de un tensoactivo catiónico. Básicamente, el proceso consistió en la adición, bajo agitación suave, de una fase orgánica etanol-acetona (conteniendo el aceite Mygliol 812®, lecitina y el tensoactivo catiónico) sobre una fase acuosa conteniendo poloxámero 188, tras lo cual se obtiene la nanoemulsión catiónica (Figura 1).

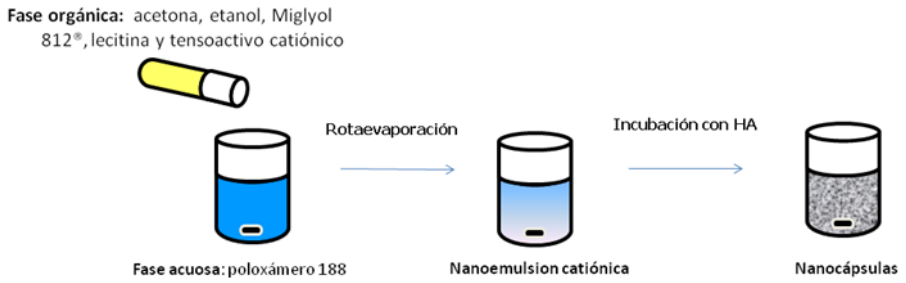

Figura 1. Esquema de preparación de las nanocápsulas de HA

Una vez eliminados los solventes en rotavapor, la nanoemulsión se incubó con una solución acuosa del HA en una relación de volúmenes 4:1.5. En estas condiciones, el HA se dispone, a través de interacciones electrostáticas, sobre la superficie de la nanoemulsión, originandose las nanocápsulas. Una estrategia similar, pero orientada a la formación de nanopartículas de poli-ε-caprolactona recubiertas con HA, ha sido previamente descrita por Barbault-Foucher y col[140].

Es importante señalar que las nanocápsulas se pueden formar igualmente en una sola etapa, es decir añadiendo directamente la fase

[139] **Prego C, García M, Torres D, Alonso MJ.** (2005). J Control Release. 101(1-3):151-62.
[140] **Barbault-Foucher S, Gref R, Russo P, Guechot J, Bochot A.** (2002). J. Control Release. 83(3):365-75.

orgánica sobre la fase acuosa conteniendo el polímero, dando lugar a resultados muy similares los discutidos en esta parte del trabajo (datos no mostrados).

Para la obtención de nanocáspulas estables, se ha evaluado el efecto de tres factores sobre el proceso de formación: tipo de tensoactivo catiónico, peso molecular y concentración de HA. Los tensoactivos catiónicos seleccionados para el estudio fueron el cloruro de benzalconio (BKC) y el bromuro de hexadeciltrimetilamonio (CTAB), los pesos moleculares de HA estudiados fueron bajo (29 KDa) y alto (160 KDa) peso molecular, y la concentración de polímero se evaluó a 8 y 9 niveles (Tablas 1 y 2).

Las cantidades de BKC y CTAB utilizadas en la preparación de las formulaciones fueron 4 y 1.8 mg, respectivamente. El criterio de selección de estas cantidades obedece a que fueron las mínimas necesarias para lograr nanoemulsiones catiónicas estables.

El efecto de la concentración de HA sobre el tamaño y carga superficial de las nanocápsulas formadas se muestra en las Tablas 1a y 1b, que corresponden a los tensoactivos BKC y CTAB, respectivamente. La incubación de las nanoemulsiones catiónicas con concentraciones adecuadas de HA permite la formación de poblaciones homogéneas de nanocápsulas con un tamaño medio aproximado de 250 nm. Este tamaño coincide con el presentado por nanocápsulas recubiertas con quitosano[131;139] y poliarginina[138], preparadas por un método similar. Mediante microscopía electrónica de transmisión (Figura 2) se confirmó la esfericidad de estas nanocápsulas, que muestran la estructura núcleo-cubierta similar a otros sistemas nanocapsulares de diferente cubierta[131;138].

En los valores de la carga superficial, se puede apreciar que, a medida que se aumenta la cantidad de HA, se presenta un enmascaramiento parcial o una completa inversión del potencial zeta de las nanoemulsiones

catiónicas originales, lo que sugiere que el polímero cargado negativamente se dispone en la superficie de los nanosistemas.

Tabla 1. Características físico-químicas de las nanocápsulas preparadas con distintas cantidades de HA (29 kDa), utilizando como tensoactivos (a) BKC o (b) CTAB (media ± d.e., n≥3).

(a)

HA (mg)	Tamaño (nm)	Índice de polidispersión	Potencial ζ (mV)
0	223 ± 10	0.1	27 ± 3
0.5	249 ± 10	0.2	9 ± 2
1.0	pp.	---	---
3.1	pp.	---	---
6.2	248 ± 10	0.2	-42 ± 2
12.5	235 ± 13	0.1	-45 ± 4
25.0	252 ± 19	0.1	-46 ± 2
50.0	pp.	---	---

(b)

HA (mg)	Tamaño (nm)	Índice de polidispersión	Potencial ζ (mV)
0	215 ± 7	0.1	35 ± 2
0.1	231 ± 8	0.1	18 ± 2
0.5	pp.	---	---
1.0	pp.	---	---
3.1	238 ± 2	0.1	-35 ± 2
6.2	238 ± 3	0.1	-37 ± 2
12.5	260 ± 20	0.2	-31 ± 3
25.0	pp.	---	---
50.0	pp.	---	---

pp.= precipitación

En las Tablas 1a y 1b se pueden apreciar 2 puntos críticos en los que ocurre la precipitación de los nanosistemas. Uno de ellos está bastante cercano a la zona en la que se produce la inversión de la carga superficial. En este caso, la precipitación ocurre, presumiblemente, debido a que la cantidad de HA no es suficiente para provocar la inversión del potencial zeta de los sistemas, favoreciendo únicamente la contraionización de la carga positiva de superficie. Esta contraionización provoca que el potencial zeta de las formulaciones se acerque a la neutralidad, impidiendo la repulsión eléctrica entre los nanosistemas, y ocasionando su precipitación.

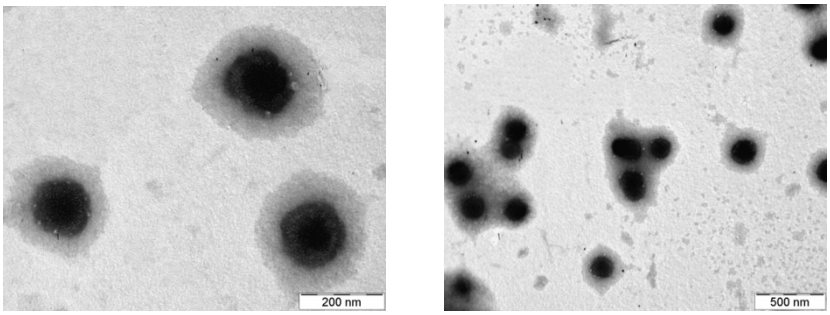

Figura 2. Imágenes de microscopía electrónica de transmisión de nanocápsulas obtenidas con 12.5 mg of HA (29 kDa).

El otro punto crítico en el que se observa precipitación se relaciona con el exceso de HA. Una combinación de factores como son la mayor fuerza iónica[141] (el HA está en forma de sal sódica) y la mayor viscosidad del medio, es lo que provocaría la precipitación de los nanosistemas[142].

Los valores correspondientes a tamaño, polidispersión y potencial zeta de las formulaciones preparadas con el HA de mayor peso molecular **(Capítulo 4, Tabla 3)** resultaron superiores a los obtenidos con el HA de bajo peso molecular Esta diferencia se atribuye a que la adsorción superficial del polímero de alto peso molecular produce un aumento en el grosor de la cubierta, lo que conlleva a un aumento en el tamaño de los nanosistemas. Este mayor grosor en la cubierta se asocia a un mayor número de grupos ionizables en superficie, lo que explicaría el aumento en el potencial zeta. Considerando esta información, se eligió el HA de peso molecular 29 KDa para continuar los experimentos de encapsulación del docetaxel y eficacia de los nanosistemas.

[141] **Hiemenz PC, Rajagopalan R.** (1997). Principles of Colloidal and Surface Chemistry. Dekker, New York.
[142] **Cowman M, Matsuoka SH.** (2005). Carbohydrates res. 340(5):791-809.

Encapsulación y liberación de docetaxel a partir de las nanocápsulas

Para llevar a cabo la encapsulación del antitumoral, hemos seleccionado las formulaciones elaboradas con 12.5 mg de HA. El docetaxel se encapsuló eficazmente (Tabla 2), sin que se produjesen modificaciones significativas en las características físico-químicas originales de las nanocápsulas. Estos datos coinciden con los mostrados en trabajos publicados previamente, y se atribuyen a la afinidad del fármaco por establecer interacciones hidrofóbicas con los componentes del núcleo de las nanocápsulas[128;131;138].

Tabla 2. Características físico-químicas y eficacia de encapsulación de las formulaciones de nanocápsulas de HA conteniendo docetaxel (DCX), elaboradas con los tensoactivos BKC y CTAB (media ± d.e., n≥3).

Formulación	Tamaño (nm)	Indice de polidispersión	Potencial ζ (mV)	Eficacia de encapsulación (%)
Nanocápsulas blancas de HA (BKC)	235 ± 13	0.1	-45 ± 4	-
Nanocápsulas de HA-DCX(BKC)	250 ± 20	0.1	-52 ± 11	65 ± 3
Nanocápsulas blancas de HA (CTAB)	267 ± 23	0.1	-31 ± 3	-
Nanocápsulas de HA-CX (CTAB)	276 ± 1	0.1	-36 ± 1	65 ± 3

La liberación de docetaxel a partir de las nanocápsulas muestra una evolución similar para ambos tensoactivos utilizados. El perfil es bifásico, caracterizado por una rápida liberación inicial seguida por una segunda etapa de estabilización. La etapa de liberación inicial, que es típica de este tipo de sistemas de naturaleza oleosa[128;131], se relaciona con la dilución de las nanocápsulas en el medio de incubación y el consiguiente reparto del fármaco entre el núcleo oleoso y el medio externo. La ausencia de liberación en la segunda etapa confirma la alta afinidad que posee el docetaxel para interaccionar con los componentes oleosos de los nanosistemas.

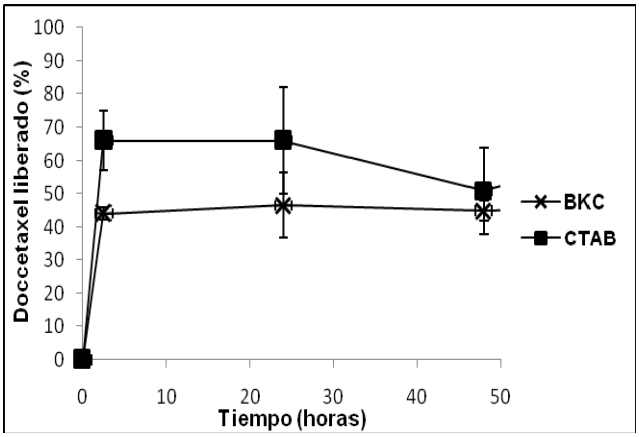

Figura 2: Perfiles de liberación *in vitro* de docetaxel a partir de las nanocápsulas de HA elaboradas con los tensoactivos BKC (X) o CTAB (■) (media± d.e., n=3).

En términos cuantitativos, la liberación del fármaco se muestra muy similar a la observada con nanocápsulas de quitosano[131] y poliarginina[138], lo que indica que la composición de la cubierta polimérica (HA, quitosano o poliarginina) no tiene una influencia significativa sobre la liberación del fármaco.

Eficacia antitumoral de las nanocápsulas de HA conteniendo docetaxel sobre la línea celular NCI-H460

Los estudios de viabilidad celular se realizaron en una línea de cáncer de pulmón que sobreexpresa el receptor CD-44 (NCI-H460). Este receptor se expresa de manera importante en tumores sólidos[143]; de tal manera que se utiliza como marcador celular para identificar el cáncer de células no pequeñas de pulmón, metaplasia escamosa y adenocarcinoma[89;90].

Los resultados de viabilidad celular, tras un contacto de 48 h con las nanocápsulas conteniendo docetaxel, o sus controles (Figuras 3a y 3b),

[143] **Naor D, Nedvetski S, Golan L, Melnik L, Faitelson Y.** (2002) CD44. Crit. Rev. Clin. Lab. Sci. 39(6):527-79.

indican una clara potenciación del efecto antitumoral del docetaxel, tras su inclusión en los nanosistemas. Este efecto resulta significativo para todas las concentraciones de fármaco ensayadas, en el caso de las nanocápsulas preparadas con el tensoactivo CTAB, mientras que con el BKC, lo es a partir de 12.5 nM de fármaco.

Los valores de la concentración de fármaco necesaria para producir el 50% de la muerte celular, IC_{50} (Tabla 4), confirman el incremento de la eficacia antitumoral logrado cuando el fármaco se incorpora a las nanocápsulas (3.4 y 2.4 veces más efectivas que el docetaxel en solución, para las elaboradas con CTAB y BCK, respectivamente).

En el caso de las nanocápsulas blancas elaboradas con BCK, se observa para las concentraciones más altas una cierta reducción de la viabilidad, atribuible al vehículo por si mismo. Este efecto se debe relacionar con la mayor toxicidad del BCK, en comparación con el CTAB[144], y con el hecho de que se necesita una mayor concentración del primero para conseguir formulaciones estables.

a

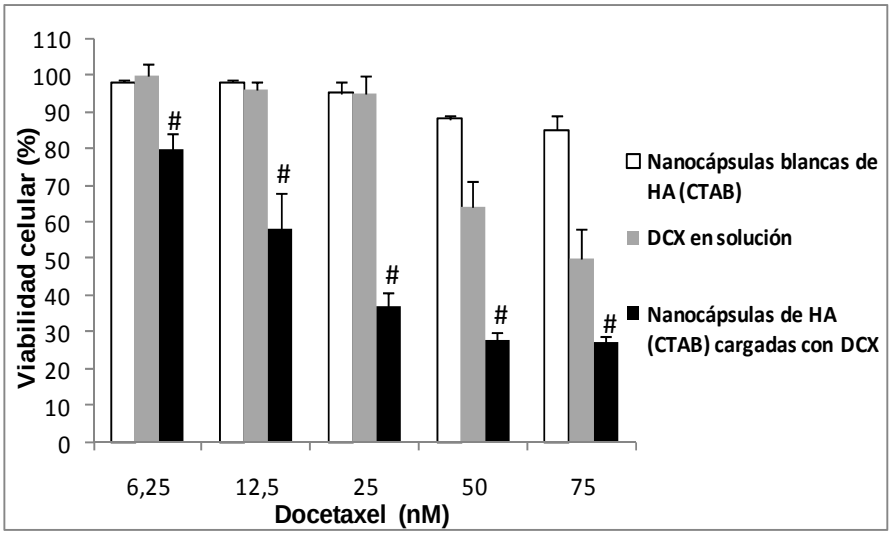

[144] **Rowe RC, Sheskey PJ, Quinn,** ed. Handbook of pharmaceutical excipients, 6th edn. United Kingdom: pharmaceutical press, 2009.

b

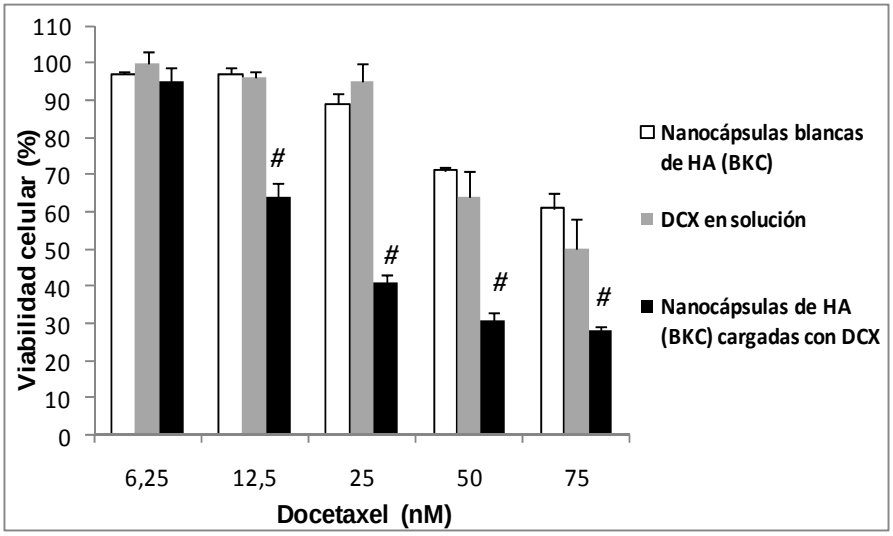

Figura 3: Efecto de las nanocápsulas de HA blancas (blanco), docetaxel (DCX) en solución (gris) y y nanocápsulas de HA conteniendo DCX (negro) sobre la viabilidad de células NCI-H460, tras 48 h de incubación, utilizando el tensoactivo CTAB (a) o BKC (b). #Diferencias significativas entre nanocápsulas conteniendo DCX vs. DCX en solución (p<0.005).

Tabla 4. Valores de IC_{50} (nM ;n=4), obtenidos tras el contacto de las formulaciones indicadas con células NCI-H460, durante un período de exposición de 48 h.

Formulación	IC_{50} (nM)
Nanocápsulas blancas de HA (CTAB)	n.d.
Nanocápsulas blancas de HA (BKC)	*
DCX en solución	36.4±4.0
Nanocápsulas de HA (CTAB) conteniendo DCX	$10.8\pm1.1^{\#}$
Nanocápsulas de HA (BKC) conteniendo DCX	$15.3\pm2.0^{\#}$

*: La máxima reducción en viabilidad celular fue de 39.0 ± 8.0%. $^{\#}$: P<0.01 con respecto a la IC_{50} de DCX (One-way ANOVA test, post-hoc Tukey test).

Los resultados de la viabilidad celular tras un contacto de 2 h con las formulaciones (Capítulo IV, Figuras 3a y 4a), indicaron cómo ya tras un período mínimo de contacto, el efecto del docetaxel encapsulado es marcadamente superior al del docetaxel en solución, lo que apunta a que las nanocápsulas favorecen la penetración intracelular del fármaco.

La significativa mejora de la eficacia antitumoral del docetaxel cuando se incorpora a las nanocápsulas de HA es concordante con lo observado en otros estudios en los que nanocápsulas cargadas con taxanos y recubiertas con PEG[145], quitosano[131] o poliarginina[138], se evaluaron en líneas celulares de glioma (9L y F98), carcinoma de mama (MCF-7) y cáncer de pulmón (A549 y NCI-H460), respectivamente. En el caso de las formulaciones recubiertas con PEG, la mejora se atribuyó a la capacidad de las nanoestructuras para contrarrestar el efecto de resistencia múltiple a fármacos. Para los nanosistemas de quitosano y poliarginina, el efecto se relacionó con la capacidad de los polímeros cargados positivamente para conseguir una mejor interacción/internalización de los nanosistemas. Estas formulaciones fueron también ensayadas *in vivo* en modelos animales a los que se implantaron subcutáneamente células de glioma[145], carcinoma hepatocelular[146], adenocarcinoma de colon[128] y cáncer de pulmón[147]. Los resultados de estos experimentos mostraron una eficacia similar o superior a la del fármaco sólo pero, a diferencia de lo que sucede con éste (formulación comercializada), los nanosistemas estudiados no necesitan ser administrados con solventes y tensoactivos que solubilizan el fármaco, a costa de producir importantes efectos de sensibilización y toxicidad.

Los resultados presentados son prometedores, y hacen esperar un mejor resultado tras la utilización de los nanosistemas de HA por vía inhalatoria, para el tratamiento localizado de cáncer de pulmón, ya que permitiría potenciar aun más la eficacia del antitumoral, disminuyendo la dosis utilizada por vía endovenosa[148].

---

[145] **Garcion E, Lamprecht A, Heurtault B, Paillard A, Aubert-Pouessel A, Denizot B, Menei P, Benoît JP**. (2006). Mol. Cancer Ther. 5(7):1710-22.
[146] **Lacoeuille F, Hindre F, Moal F, Roux J, Passirani C, Couturier O, Cales P, Le Jeune JJ, Lamprecht A, Benoit JP.** (2007). Int J Pharm. 344(1-2):143-9.
[147] **Torrecilla D, Lozano MV, Lallana E, Novoa-Carballal R, Vidal A, Torres D, Fernández-Megía E, Riguera E, Alonso MJ, Domínguez F.** (2011). Sometido.
[148] **Hureaux J, Lagarce F, Gagnadoux F, Vecellio L, Clavreul A, Roger E, Kempf M, Racineux JL, Diot P, Benoit JP, Urban T.** (2009). Eur J Pharm Biopharm. 73(2):239-46.

Estudios de estabilidad en almacenamiento de las nanocápsulas de HA conteniendo docetaxel

La inestabilidad es un problema crítico frecuente en el desarrollo de formulaciones de sistemas coloidales. En el presente estudio, se ha evaluado la estabilidad de las formulaciones de nanocápsulas de HA con docetaxel, en suspensión, almacenadas a 4 y 37° C, durante un periodo de 3 meses. En la Figura 5 se puede apreciar que todas las formulaciones se mantienen estables, en lo que se refiere al tamaño, durante el periodo de estudio. Esta prolongada estabilidad puede ser atribuida al potencial zeta altamente negativo que presentan los sistemas durante todo el experimento (~ -40 mV). Estos resultados concuerdan con los encontrados en otros sistemas nanocapsulares[149] en los que la estabilidad coloidal se ve favorecida por la presencia de la cubierta polimérica.

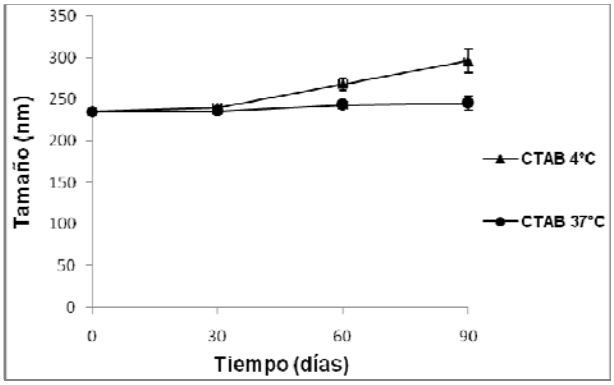

Figura 5: Evolución del tamaño de particula de las nanocápsulas de HA (tensoactivo CTAB) conteniendo docetaxel durante 3 meses de almacenamiento a 4 (▲) y 37° C (●). (Media ± d.e.; n=3).

[149] **Prego C, Torres D, Fernandez-Megia E, Novoa-Carballal R, Quiñoá E, Alonso MJ.** J Control Release. (2006). 111(3):299-308.

Obtención de un producto liofilizado de nanocápsulas de HA

Una de las limitaciones tecnológicas comunes a los nanosistemas es su deficiente estabilidad durante largos periodos de tiempo. La gelificación, cremación, fusión o agregación son los fenómenos más comunes de desestabilización que pueden sufrir estos sistemas durante su almacenamiento[150].

La liofilización es uno de los métodos más eficaces para preservar su estabilidad durante largos periodos de tiempo. Sin embargo, este proceso se puede tornar especialmente complejo en el caso de las nanocápsulas debido a la fluidez de la cubierta polimérica y a la presencia del núcleo oleoso que es susceptible de romperse[151].

El uso de agentes crioprotectores durante la liofilización de las nanoestructuras es fundamental pues facilita el proceso y previene el colapso de los nanosistemas[152]. La primera evidencia de que concentraciones isótónicas de criprotectores derivados de azúcares son capaces de proteger a las nanocápsulas durante su liofilización fue aportada por Calvo y col. (1997)[153]. Estudios posteriores llevados a cabo con diferentes estructuras como nanopartículas, liposomas y nanocápsulas han indicado que la trealosa es uno de los agentes más eficaces para asegurar un proceso de liofilización y reconstitución adecuada de los nanosistemas (su menor higroscopicidad y su mayor temperatura de transición vítrea son las características que la diferencian de otros azúcares).

---

[150] **Heurtault B, Saulnier P, Pech B, Proust JE, Benoit JP**. (2003). Biomaterials. 24:4283-4300.

[151] **Choi MJ, Briancon S, Andrieu J, Min SG, Fessi H.** (2004). Dry. Technol. 22:335-346.

[152] **Abdelwhaed W.; Degobert G.; Fessi H.** (2006). Eur. J. Pharm. Biopharm. 63:87-94.

[153] **Calvo P, Remuñan-López C, Vila-Jato JL, Alonso MJ.** (1997). Colloid. Polym. Sci. 275, 46-53.

Los resultados obtenidos con las nanocápsulas de HA (Figura 6) nos llevan a concluir que la trealosa es un agente que permite obtener un producto liofilizado adecuado, llegando a concentraciones del nanosistema del 1% p/v.

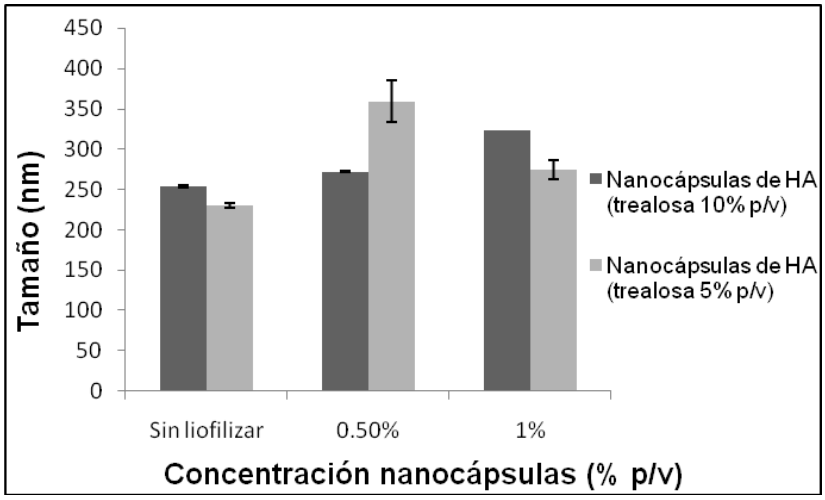

Figura 6: Tamaño de partícula de las nanocápsulas de HA conteniendo docetaxel (tensoactivo: BKC) tras el proceso de liofilización y reconstitución de la suspensión Las nanocápsulas se liofilizaron en presencia de trealosa al 5 y 10 % . (media ± d.e.; n=3).

CONCLUSIONES

CONCLUSIONES

El trabajo experimental expuesto pone de manifiesto el interés de las nanostructuras desarrolladas para cumplir el objetivo futuro de una administración pulmonar eficaz. Ello se ha podido constatar a través del estudio de la interacción de las nanoestructuras con las células diana (mastocitos y células de cáncer de pulmón) y de la cuantificación de la eficacia antiasmática y antitumoral de los fármacos asociados.

.

De todo ello, se han podido extraer las siguientes conclusiones:

PARTE I

1. Se han optimizado, utilizando el método de gelificación iónica, sistemas nanoparticulares constituídos por mezclas quitosano-ácido hialurónico y quitosano-carboximetil-β-ciclodextrina, con un elevado contenido en heparina.

2. El tamaño medio osciló en torno a 150-375 nm, dependiendo fundamentalmente del peso molecular de la heparina asociada, mostrando siempre una elevada carga superficial positiva. Los perfiles de estabilidad de los nanosistemas y de liberación de heparina de alto y bajo peso molecular, se mostraron muy dependientes de la composición de las formulaciones y medios utilizados.

3. Se evidenció, mediante microscopía confocal, que las nanopartículas, independientemente de su composición, fueron internalizadas por los mastocitos, demostrándose *ex vivo*, por primera vez para un sistema nanoparticular, y concretamente para las nanopartículas de quitosano-

ciclodextrina, la mejora del efecto antiasmático de la heparina, frente al de la molécula en solución.

PARTE II

1. Se ha diseñado, mediante la técnica de desplazamiento del disolvente, un nuevo sistema que denominamos "nanocápsulas de ácido hialurónico", constituído por un núcleo oleoso que contiene el principio activo y una cubierta de ácido hialurónico.

2. Los nanosistemas presentaron tamaño nanométrico (en torno a 250 nm) y carga superficial negativa (entre -30 y -50 mV), mostrando la capacidad de encapsular eficazmente el antitumoral hidrofóbico docetaxel y retenerlo en el núcleo oleoso tras su dilución en fluídos biológicos simulados

3. El docetaxel encapsulado incrementó significativamente su efecto citotóxico sobre células tumorales de cáncer de pulmón (NCI-H460), incremento que se atribuye a la internalización de las nanocápsulas y posterior liberación intracelular del docetaxel.

4. Las nanocápsulas almacenadas en forma de suspensión fueron estables durante al menos un período de 3 meses, independientemente de la temperatura de almacenamiento (4 ó 37° C).

5. Las nanocápsulas se pudieron liofilizar y reconstituir adecuadamente, tras la incorporación del crioprotector trealosa en concentraciones en torno al 5% p/v.

REFERENCIAS

REFERENCIAS

1. Abal M, Andreu JM, Barasoain I. Taxanes: microtubule and centrosome targets, and cell cycle dependent mechanisms of action. Curr Cancer Drug Targets. 3(3):193-203 (2003).
2. Abdelwahed W, Degobert G, Fessi H. Investigation of nanocapsules stabilization by amorphous excipients during freeze-drying and storage. Eur J Pharm Biopharm. 63(2):87-94 (2006).
3. Aboubakar M, Puisieux F, Couvreur P, Deyme M, Vauthier C. Study of the mechanism of insulin encapsulation in poly(isobutylcyanoacrylate) nanocapsules obtained by interfacial polymerization. J Biomed Mater Res. 47:568-576 (1999).
4. Ahmad Z, Sharma S, Khuller GK. Inhalable alginate nanoparticles as antitubercular drug carriers against experimental tuberculosis. Int. J. Antimicrob. Agents. 26(4):298-303 (2005).
5. Ahmed IS, Ayres JW: Comparison of in vitro and in vivo performance of a colonic delivery system. Int. J. Pharm. (2011), doi:10.1016/j.ijpharm.2011.02.061.
6. Ahmed T, Campo C, Abraham MK, Molinari JF, Abraham WM, Ashkin D, Syriste T, Andersson LO, Svahn CM. Inhibition of antigen-induced acute bronchoconstriction, airway hyperresponsiveness, and mast cell degranulation by a nonanticoagulant heparin: comparison with a low molecular weight heparin. Am J Respir Crit Care Med. 155(6):1848-55 (1997).
7. Ahmed T, Garrigo J, Danta I. Preventing bronchoconstriction in exercise-induced asthma with inhaled heparin. N Engl J Med. 329(2):90-5 (1993).

8. Ahmed T, Gonzalez BJ, Danta I. Prevention of exercise-induced bronchoconstriction by inhaled low-molecular-weight heparin. Am J Respir Crit Care Med. 160(2):576-81 (1999).
9. Ahmed T, Ungo J, Zhou M, Campo C. Inhibition of allergic late airway responses by inhaled heparin-derived oligosaccharides. J Appl Physiol. 88(5):1721-9 (2000).
10. Ahmed T, Syriste T, Mendelssohn R, Sorace D, Mansour E, Lansing M, Abraham WM, Robinson MJ. Heparin prevents antigen-induced airway hyperresponsiveness: interference with IP3-mediated mast cell degranulation? J Appl Physiol. 76(2):893-901 (1994).
11. Al Khouri Fallouh N, Roblot-Treupel L, Fessi H. Development of a new process for the manufacture of polyisobutylcyanoacrylate nanocapsules. Int J Pharm. 28:125-132 (1986).
12. Akima K, Ito H, Iwata Y, Matsuo K, Watari N, Yanagi M, Hagi H, Oshima K, Yagita A, Atomi Y, Tatekawa I. Evaluation of antitumor activities of hyaluronate binding antitumor drugs: synthesis, characterization and antitumor activity. J Drug Target. 4(1):1-8 (1996).
13. Alonso MJ. Nanomedicines for overcoming biological barriers. Biomed Pharmacother. 58:168-172 (2004).
14. Alonso MJ, Sanchez, A. The potential of chitosan in ocular drug delivery. J Pharm Pharmacol. 55:1451-1463 (2003).
15. Andrade F, Videira M, Ferreira D, Sarmento B. Nanocarriers for pulmonary administration of peptides and therapeutic proteins. Nanomedicine (Lond). 6(1):123-41 (2011).
16. Anton N, Gayet P, Benoit JP, Saulnier P. Nano-emulsions and nanocapsules by the PIT method: An investigation on the role of the temperature cycling on the emulsion phase inversion. Int J Pharm. 344:44-52 (2007).

17. Aspden TJ, Mason JD, Jones NS, Lowe J, Skaugrud O, Illum L. Chitosan as a nasal delivery system: the effect of chitosan solutions on in vitro and in vivo mucociliary transport rates in human turbinates and volunteers. J. Pharm Sci. 86(4):509-13 (1997).
18. Auzenne E, Ghosh SC, Khodadadian M, Rivera B, Farquhar D, Price RE, Ravoori M, Kundra V, Freedman RS, Klostergaard J. Hyaluronic acid-paclitaxel: antitumor efficacy against CD44(+) human ovarian carcinoma xenografts. Neoplasia. 9(6):479-86 (2007).
19. Bae KH, Lee Y, Park TG. Oil-encapsulating PEO-PPO-PEO/PEG shell cross-linked nanocapsules for target-specific delivery of paclitaxel. Biomacromolecules. 8(2):650-6 (2007).
20. Barar J, Javadzadeh AR, Omidi, Y. Ocular novel drug delivery: Impacts of membranes and barriers. Expert Opin Drug Deliv. 5:567-581 (2008).
21. Barbault-Foucher S, Gref R, Russo P, Guechot J, Bochot A. Design of poly-epsilon-caprolactone nanospheres coated with bioadhesive hyaluronic acid for ocular delivery. J Control Release. 83(3):365-75 (2002).
22. Barnes PJ. New therapies for asthma: is there any progress? Trends Pharmacol. Sci. 31(7):335-43 (2010).
23. Becquemin MH, Chaumuzeau JP. Inhaled insulin: a model for pulmonary systemic absorption? Rev. Mal. Respir. 27(8):e54-65 (2010).
24. Bivas-Benita M, Ottenhoff TH, Junginger HE, Borchard G. Pulmonary DNA vaccination: concepts, possibilities and perspectives. J Control Release. 107(1):1-29 (2005).
25. Bivas-Benita M, Romeijn S, Junginger HE, Borchard G. PLGA-PEI nanoparticles for gene delivery to pulmonary epithelium. Eur J Pharm Biopharm. 58(1):1-6 (2004).

26. Bivas-Benita M, van Meijgaarden KE, Franken KL, Junginger HE, Borchard G, Ottenhoff TH, Geluk A.Pulmonary delivery of chitosan-DNA nanoparticles enhances the immunogenicity of a DNA vaccine encoding HLA-A*0201-restricted T-cell epitopes of Mycobacterium tuberculosis. Vaccine. 22(13-14):1609-15 (2004).
27. Bivas-Benita M, Zwier R, Junginger HE, Borchard G. Non-invasive pulmonary aerosol delivery in mice by the endotracheal route. Eur J Pharm Biopharm. 61(3):214-8 (2005).
28. Bouclier Cl, Moine L, Hillaireau H, Marsaud VR, Connault E, Opolon P, Couvreur P, Fattal E, Renoir JM. Physicochemical Characteristics and Preliminary in Vivo Biological Evaluation of Nanocapsules Loaded with siRNA Targeting Estrogen Receptor Alpha. Biomacromolecules. 9:2881-2890 (2008).
29. Brigger I, Dubernet C, Couvreur P. Nanoparticles in cancer therapy and diagnosis. Adv Drug Deliv Rev. 54:631-651 (2002).
30. Brown SD, Nativo P, Smith JA, Stirling D, Edwards PR, Venugopal B, Flint DJ, Plumb JA, Graham D, Wheate NJ. Gold nanoparticles for the improved anticancer drug delivery of the active component of oxaliplatin. J Am Chem Soc. 132(13):4678-84 (2010).
31. Buceta M, Domínguez E, Castro M, Brea J, Alvarez D, Barcala J, Valdés L, Alvarez-Calderón P, Domínguez F, Vidal B, Díaz JL, Miralpeix M, Beleta J, Cadavid MI, Loza MI. A new chemical tool (C0036E08) supports the role of adenosine A(2B) receptors in mediating human mast cell activation. Biochem Pharmacol. 76(7):912-21 (2008).
32. Bur M, Henning A, Hein S, Schneider M, Lehr CM. Inhalative nanomedicine--opportunities and challenges. Inhal Toxicol. 1:137-43 (2009).

33. Calvo P, Alonso MJ, Vila-Jato JL, Robinson JR. Improved Ocular Bioavailability of Indomethacin by Novel Ocular Drug Carriers. J Pharm Pharmacol. 48:1147-1152 (1996).
34. Calvo P, Remuñan-López C, Vila-Jato JL, Alonso MJ: Development of positively charged colloidal drug carriers: Chitosan-coated polyester nanocapsules and submicron-emulsions. Colloid. Polym. Sci. 275, 46-53 (1997).
35. Calvo P, Remuñan-López C, Vila-Jato JL, Alonso MJ. Chitosan and chitosan/ethylene oxide-propylene oxide block copolymer nanoparticles as novel carriers for proteins and vaccines. Pharm Res. 14(10):1431-6 (1997).
36. Calvo P, Remuñan-Lopez C, Vila-Jato JL, Alonso M.J. Novel hydrophilic chitosan–polyethylene oxide nanoparticles as protein carriers. J. Appl. Polymer Sci. 63:125–132 (1997).
37. Calvo P, Sanchez A, Martinez J, Lopez MI, Calonge M, Pastor JC, Alonso MJ. Polyester nanocapsules as new topical ocular delivery systems for cyclosporin A. Pharm Res. 13: 311-315 (1996).
38. Calvo P, Thomas C, Alonso MJ, Vila-Jato JL, Robinson .R. Study of the mechanism of interaction of poly(E-caprolactone) nanocapsules with the cornea by confocal laser scanning microscopy. Int J Pharm. 103:283-291 (1994).
39. Calvo P, Vila-Jato JL, Alonso MJ. Comparative in vitro evaluation of several colloidal systems, nanoparticles, nanocapsules, and nanoemulsions, as ocular drug carriers. J Pharm Sci. 85:530-536 (1996).
40. Calvo P, Vila-Jato JL, Alonso MJ. Evaluation of cationic polymer-coated nanocapsules as ocular drug carriers. Int J Pharm. 153:41-50 (1997).

41. Cafaggi S, Russo E, Stefani R, Leardi R, Caviglioli G, Parodi B, Bignardi G, De Totero D, Aiello C, Viale M. Preparation and evaluation of nanoparticles made of chitosan or N-trimethyl chitosan and a cisplatin-alginate complex. J Control Release. 121(1-2):110-23 (2007).
42. Campo C, Molinari JF, Ungo J, Ahmed T. Molecular-weight-dependent effects of nonanticoagulant heparins on allergic airway responses. J Appl Physiol. 86(2):549-57 (1999).
43. Cauchetier E, Deniau M, Fessi H, Astier A, Paul M. Atovaquone-loaded nanocapsules: Influence of the nature of the polymer on their in vitro characteristics. Int J Pharm. 250: 273-281 (2003).
44. Chen Y, Siddalingappa B, Chan PH, Benson HA.Development of a chitosan-based nanoparticle formulation for delivery of a hydrophilic hexapeptide, dalargin. Biopolymers. 90(5):663-70 (2008).
45. Chen MC, Wong HS, Lin KJ, Chen HL, Wey SP, Sonaje K, Lin YH, Chu CY, Sung HW. The characteristics, biodistribution and bioavailability of a chitosan-based nanoparticulate system for the oral delivery of heparin.
46. Choi MJ, Briançon S, Andrieu J, Min SG, Fessi H. Effect of freeze-drying process conditions on the stability of nanoparticles. Dry. Technol. 22: 335-346 (2004).
47. Choi KY, Min KH, Na JH et al.: Self-assembled hyaluronic acid nanoparticles as a potential drug carrier for cancer therapy: synthesis, characterization, and in vivo biodistribution J. Mater. Chem. 19, 4102-4107 (2009).
48. Cournarie F, Auchere D, Chevenne D, Lacour B, Seiller M, Vauthier, C. Absorption and efficiency of insulin after oral administration of insulin-loaded nanocapsules in diabetic rats. Int J Pharm. 242:325-328 (2002).

49. Couvreur P, Barratt G, Fattal E, Legrand P, Vauthier C. Nanocapsule technology: A review. Crit Rev Ther Drug Carrier Syst. 19:99-134 (2002).
50. Couvreur P, Kante B, Roland, M. Polycyanoacrylate nanocapsules as potential lysosomotropic carriers: Preparation, morphological and sorptive properties. J Pharm Pharmacol. 31:331-332 (1979).
51. Couvreur P, Tulkens P, Roland, M. Nanocapsules: a new type of lysosomotropic carrier. FEBS Lett. 84: 323-326 (1977).
52. Cowman MK, Matsuoka S. Experimental approaches to hyaluronan structure. Carbohydr Res. 340(5):791-809 (2005).
53. Crown J, O'Leary M: The taxanes: An update. Lancet 355(9210), 1176-8 (2000).
54. Csaba N, Köping-Höggård M, Fernandez-Megia E, Novoa-Carballal R, Riguera R, Alonso MJ. Ionically crosslinked chitosan nanoparticles as gene delivery systems: effect of PEGylation degree on in vitro and in vivo gene transfer. J Biomed Nanotechnol. 5(2):162-71 (2009).
55. Csaba N, Garcia-Fuentes M, Alonso MJ. The performance of nanocarriers for transmucosal drug delivery. Expert Opin Drug Deliv. 3:463-478 (2006).
56. Csaba N, Garcia-Fuentes M, Alonso MJ. Nanoparticles for nasal vaccination. Adv Drug Deliv Rev. 61(2):140-57 (2009).
57. Csaba N, Köping-Höggård M, Alonso MJ. Ionically crosslinked chitosan/tripolyphosphate nanoparticles for oligonucleotide and plasmid DNA delivery. Int J Pharm. 382(1-2):205-14 (2009).
58. Damge C, Michel C, Aprahamian M, Couvreur P. New approach for oral administration of insulin with polyalkylcyanoacrylate nanocapsules as drug carrier. Diabetes. 37:246-251 (1988).

59. Damge C, Vranckx H, Balschmidt P, Couvreur P. Poly(alkyl cyanoacrylate) nanospheres for oral administration of insulin. J Pharm Sci. 86:1403-1409 (1997).
60. De Campos AM, Diebold Y, Carvalho EL, Sanchez A, Alonso MJ. Chitosan nanoparticles as newocular drug delivery systems: in vitro stability, in vivo fate, and cellular toxicity. Pharm. Res. 21:803–810 (2004).
61. De Campos AM, Sanchez A, Gref R, Calvo P, Alonso M.J. The effect of a PEG versus a chitosan coating on the interaction of drug colloidal carriers with the ocular mucosa. Eur J Pharm Sci. 20:73-81 (2003).
62. De la Fuente M, Csaba N, Garcia-Fuentes M, Alonso MJ. Nanoparticles as protein and gene carriers to mucosal surfaces. Nanomedicine (Lond). 3(6):845-57 (2008).
63. De la Fuente M, Seijo B, Alonso MJ. Novel hyaluronic acid-chitosan nanoparticles for ocular gene therapy. Invest Ophthalmol Vis Sci. 49(5):2016-24 (2008).
64. De la Fuente M, Seijo B, Alonso MJ. Bioadhesive hyaluronan–chitosan nanoparticles can transport genes across the ocular mucosa and transfect ocular tissue. Gene Ther. 15:668–676 (2008).
65. De la Fuente M, Seijo B, Alonso MJ. Novel hyaluronan-based nanocarriers for transmucosal delivery of macromolecules. Macromol. Biosci. 8:441–450 (2008).
66. Densmore CL, Kleinerman ES, Gautam A, Jia SF, Xu B, Worth LL, Waldrep JC, Fung YK, T'Ang A, Knight V.Growth suppression of established human osteosarcoma lung metastases in mice by aerosol gene therapy with PEI-p53 complexes. Cancer Gene Ther. 8(9):619-27 (2001).
67. Des Rieux A, Fievez V, Garinot M, Schneider YJ, Preat V. Nanoparticles as potential oral delivery systems of proteins and vaccines: A mechanistic approach. J Control Release. 116:1-27 (2006).

68. Desai MP, Labhasetwar V, Amidon GL, Levy RJ. Gastrointestinal Uptake of Biodegradable Microparticles: Effect of Particle Size. Pharm Res. 13:1838-1845 (1996).
69. Desai SD, Blanchard J. Pluronic® F127-based ocular delivery system containing biodegradable polyisobutylcyanoacrylate nanocapsules of pilocarpine. Drug Delivery: J Delivery and Targeting Therapeutic Agents. 7:201-207 (2000).
70. Dhanikula A, Khalid N, Lee SD, Yeung R, Risovic V, Wasan KM, Leroux JC. Long circulating lipid nanocapsules for drug detoxification. Biomaterials. 28:1248-1257 (2007).
71. Diamant Z, Page CP. Heparin and related molecules as a new treatment for asthma. Pulm Pharmacol Ther. 13(1):1-4 (2000).
72. Di Colo G, Zambito Y, Zaino C, Sansò M.Selected polysaccharides at comparison for their mucoadhesiveness and effect on precorneal residence of different drugs in the rabbit model. Drug Dev Ind Pharm. 35(8):941-9 (2009).
73. Edwards DA, Hanes J, Caponetti G, Hrkach J, Ben-Jebria A, Eskew ML, Mintzes J, Deaver D, Lotan N, Langer R. Large porous particles for pulmonary drug delivery. Science. 276(5320):1868-71 (1997).
74. Ehdaie B. Application of Nanotechnology in Cancer Research: Review of Progress in the National Cancer Institute's Alliance for nanotechnology (2008).
75. Eliaz RE, Nir S, Marty C, Szoka FC Jr. Determination and modeling of kinetics of cancer cell killing by doxorubicin and doxorubicin encapsulated in targeted liposomes. Cancer Res. 64:711–718 (2004).
76. Eliaz RE, Nir S, Szoka FC Jr.Interactions of hyaluronan-targeted liposomes with cultured cells: modeling of binding and endocytosis. Methods Enzymol. 387:16-33 (2004).

77. Eliaz RE, Szoka FC Jr. Liposome-encapsulated doxorubicin targeted to CD44: a strategy to kill CD44-overexpressing tumor cells. Cancer Res. 61(6):2592-601 (2001).
78. Engels FK, Mathot RA, Verweij J. Alternative drug formulations of docetaxel: a review. Anticancer Drugs. 18(2):95-103 (2007).
79. Fattal E. Bochot A. State of the art and perspectives for the delivery of antisense oligonucleotides and siRNA by polymeric nanocarriers. Int J Pharm. 364:237-248 (2008).
80. Fessi H, Puisieux F, Devissaguet JP, Ammoury N, Benita, S. Nanocapsule formation by interfacial polymer deposition following solvent deplacement. Int J Pharm. 55:25-28 (1989).
81. Freitas C, Müller RH: Effect of light and temperature on zeta potential and physical and physical stability in solid lipid nanoparticle (SLN^{TM}) dispersions. Int. J. Pharm. 168, 221-229 (1998).
82. Fresta M, Cavallaro G, Giammona G, Wehrli E, Puglisi G. Preparation and characterization of polyethyl-2-cyanoacrylate nanocapsules containing antiepileptic drugs. Biomaterials. 17:751-758 (1996).
83. Gallardo M, Couarraze G, Denizot B, Treupel L, Couvreur P, Puisieux F. Study of the mechanisms of formation of nanoparticles and nanocapsules of polyisobutyl-2-cyanoacrylate. Int J Pharm. 100:55-64 (1993).
84. Garcia-Contreras L, Fiegel J, Telko MJ, Elbert K, Hawi A, Thomas M, VerBerkmoes J, Germishuizen WA, Fourie PB, Hickey AJ, Edwards D. Inhaled large porous particles of capreomycin for treatment of tuberculosis in a guinea pig model. Antimicrob Agents Chemother. 51(8):2830-6 (2007).
85. Garcia-Fuentes M, Prego C, Torres D, Alonso MJ. A comparative study of the potential of solid triglyceride nanostructures coated with chitosan or poly(ethylene glycol) as carriers for oral calcitonin delivery. Eur. J. Pharm. Sci. 25:133–143 (2005).

86. Garcion E, Lamprecht A, Heurtault B, Paillard A, Aubert-Pouessel A, Denizot B, Menei P, Benoît JP.A new generation of anticancer, drug-loaded, colloidal vectors reverses multidrug resistance in glioma and reduces tumor progression in rats. Mol Cancer Ther. 5(7):1710-22 (2006).
87. Garrigo J, Danta I, Ahmed T. Time course of the protective effect of inhaled heparin on exercise-induced asthma. Am J Respir Crit Care Med. 153(5):1702-7 (1996).
88. Gelderblom H, Verweij J, Nooter K, Sparreboom A. Cremophor EL: the drawbacks and advantages of vehicle selection for drug formulation. Eur J Cancer. 37(13):1590-8 (2001).
89. Gottesman MM, Fojo T, Bates SE. Multidrug resistance in cancer: Role of ATP-dependent transporters. Nat Rev Cancer. 2:48-58 (2002).
90. Green WF, Konnaris K, Woolcock AJ. Effect of salbutamol, fenoterol, and sodium cromoglicate on the release of heparin fromsensitized human lung fragments challenged with Dermatophagoides pteronyssinus allergen. Am. J. Respir. Cell Mol. Biol. 8:518–521 (1993).
91. Greish K. Enhanced permeability and retention of macromolecular drugs in solid tumors: A royal gate for targeted anticancer nanomedicines. J Drug Target.15:457-464 (2007).
92. Guinebretiere S, Briançon S, Fessi H, Teodorescu VS, Blanchin MG. Nanocapsules of biodegradable polymers: Preparation and characterization by direct high resolution electron microscopy. Mater Sci Eng C. 21:137-142 (2002).
93. Guinebretiere S, Briancon S, Lieto J, Mayer C, Fessi H. Study of the emulsion-diffusion of solvent: Preparation and characterization of nanocapsules. Drug Dev Res. 57:18-33 (2002).
94. Halayko AJ, Rector E, Stephens NL. Characterization of molecular determinants of smooth muscle cell heterogeneity. Can J Physiol Pharmacol. 75(7):917-29 (1997).

95. Heinemann L. New ways of insulin delivery. Int J Clin Pract Suppl. 166:29-40 (2010).
96. Heurtault B, Saulnier P, Pech B, Benoit JP, Proust JE. Interfacial stability of lipid nanocapsules. Colloids Surf B Biointerfaces. 30:225-235 (2003).
97. Heurtault B, Saulnier P, Pech B, Proust JE, Benoit, JP. A novel phase inversion-based process for the preparation of lipid nanocarriers. Pharm Res. 19:875-880 (2002).
98. Heurtault B, Saulnier P, Pech B, Proust JE, Benoit JP: Properties of polyethylene glycol 660 12-hydroxy stearate at a triglyceride/water interface. Int. J. Pharm. 242(1-2), 167-70 (2002).
99. Heurtault B.; Saulnier P.; Pech B.; Proust J.E.; Benoit J.P. Physico-chemical stability of colloidal lipid particles. Biomaterials. 24:4283-4300 (2003).
100. Heurtault B, Saulnier P, Pech B, Venier-Julienne MC, Proust JE, Phan-Tan-Luu R, Benoit JP. The influence of lipid nanocapsule composition on their size distribution. Eur J Pharm Sci. 18:55-61 (2003).
101. Hiemenz PC, Rajagopalan R. Principles of Colloidal and Surface Chemistry, 3rd edition (1997). Dekker, New York, USA (Libro).
102. Hillaireau H, Le Doan T, Chacun H, Janin J, Couvreur P. Encapsulation of mono- and oligo-nucleotides into aqueous-core nanocapsules in presence of various water-soluble polymers. Int J Pharm. 331:148-152 (2007).
103. Hitzman CJ, Wattenberg LW, Wiedmann TS. Pharmacokinetics of 5-fluorouracil in the hamster following inhalation delivery of lipid-coated nanoparticles. J Pharm Sci. 95(6):1196-211 (2006).
104. Hohenegger M. Novel and current treatment concepts using pulmonary drug delivery. Curr Pharm Des. 16(22):2484-92 (2010).

105. Hong GY, Jeong YI, Lee SJ, Lee E, Oh JS, Lee HC. Combination of paclitaxel- and retinoic acid-incorporated nanoparticles for the treatment of CT-26 colon carcinoma. Arch Pharm Res. 34(3):407-17 (2011).

106. Hureaux J, Lagarce F, Gagnadoux F, Vecellio L, Clavreul A, Roger E, Kempf M, Racineux JL, Diot P, Benoit JP, Urban T. Lipid nanocapsules: ready-to-use nanovectors for the aerosol delivery of paclitaxel. Eur J Pharm Biopharm. 73(2):239-46 (2009).

107. Hureaux J, Lagarce F, Gagnadoux F, Rousselet MC, Moal V, Urban T, Benoit JP. Toxicological study and efficacy of blank and paclitaxel-loaded lipid nanocapsules after i.v. administration in mice. Pharm Res. 27(3):421-30 (2010).

108. Huynh NT, Passirani C, Saulnier P, Benoit JP. Lipid nanocapsules: a new platform for nanomedicine. Int J Pharm. 379(2):201-9 (2009).

109. Hyung W, Ko H, Park J, Lim E, Park SB, Park YJ, Yoon HG, Suh JS, Haam S, Huh YM. Novel hyaluronic acid (HA) coated drug carriers (HCDCs) for human breast cancer treatment. Biotechnol Bioeng. 99(2):442-54 (2008).

110. Immordino ML, Brusa P, Arpicco S, Stella B, Dosio F, Cattel L.Preparation, characterization, cytotoxicity and pharmacokinetics of liposomes containing docetaxel. J Control Release. 91(3):417-29 (2003).

111. Issa MM, Köping-Höggård M, Tømmeraas K, Vårum KM, Christensen BE, Strand SP, Artursson P. Targeted gene delivery with trisaccharide-substituted chitosan oligomers in vitro and after lung administration in vivo. J Control Release. 115(1):103-12 (2006).

112. Iyer AK, Khaled G, Fang J, Maeda H. Exploiting the enhanced permeability and retention effect for tumor targeting. Drug Discov Today. 11:812-818 (2006).

113. Jaques LB. Heparins--anionic polyelectrolyte drugs. Pharmacol Rev. 31(2):99-166 (1979).

114. Jin H, Kim TH, Hwang SK, Chang SH, Kim HW, Anderson HK, Lee HW, Lee KH, Colburn NH, Yang HS, Cho MH, Cho CS. Aerosol delivery of urocanic acid-modified chitosan/programmed cell death 4 complex regulated apoptosis, cell cycle, and angiogenesis in lungs of K-ras null mice. Mol Cancer Ther. 5(4):1041-9 (2006).
115. Johnson PR, Armour CL, Carey D, Black JL. Heparin and PGE2 inhibit DNA synthesis in human airway smooth muscle cells in culture. Am J Physiol. 269(4 Pt 1):L514-9 (1995).
116. Jones SE, Erban J, Overmoyer B, Budd GT, Hutchins L, Lower E, Laufman L, Sundaram S, Urba WJ, Pritchard KI, Mennel R, Richards D, Olsen S, Meyers ML, Ravdin PM. Randomized phase III study of docetaxel compared with paclitaxel in metastatic breast cancer. J Clin Oncol. 23(24):5542-51 (2005).
117. Kanabar V, Hirst SJ, O'Connor BJ, Page CP. Some structural determinants of the antiproliferative effect of heparin-like molecules on human airway smooth muscle. Br J Pharmacol. 146(3):370-7 (2005).
118. Khalid MN, Simard P, Hoarau D, Dragomir A, Leroux JC. Long circulating poly(ethylene glycol)-decorated lipid nanocapsules deliver docetaxel to solid tumors. Pharm Res. 23(4):752-8 (2006).
119. Kilfeather SA, Tagoe S, Perez AC, Okona-Mensa K, Matin R, Page CP. Inhibition of serum-induced proliferation of bovine tracheal smooth muscle cells in culture by heparin and related glycosaminoglycans. Br J Pharmacol. 114(7):1442-6 (1995).
120. Kimura S, Egashira K, Chen L, Nakano K, Iwata E, Miyagawa M, Tsujimoto H, Hara K, Morishita R, Sueishi K, Tominaga R, Sunagawa K. Nanoparticle-mediated delivery of nuclear factor kappaB decoy into lungs ameliorates monocrotaline-induced pulmonary arterial hypertension. Hypertension. 53(5):877-83 (2009).

121. Köping-Höggård M, Issa MM, Köhler T, Tronde A, Vårum KM, Artursson P. A miniaturized nebulization catheter for improved gene delivery to the mouse lung. J. Gene Med. 7(9):1215-22 (2005).
122. Köping-Höggård M, Sanchez A, Alonso MJ. Nanoparticles as carriers for nasal vaccine delivery. Exp. Rev. Vaccines 4:185–196 (2005).
123. Krauland AH, Alonso MJ. Chitosan/cyclodextrin nanoparticles as macromolecular drug delivery system. Int J Pharm. 340(1-2):134-42 (2007).
124. Kumar MN, Mohapatra SS, Kong X, Jena PK, Bakowsky U, Lehr CM. Cationic poly(lactide-co-glycolide) nanoparticles as efficient in vivo gene transfection agents. J Nanosci Nanotechnol. 4(8):990-4 (2004).
125. Kurmi BD, Kayat J, Gajbhiye V, Tekade RK, Jain NK. Micro- and nanocarrier-mediated lung targeting. Expert Opin Drug Deliv. 7(7):781-94 (2010).
126. Lacoeuille F, Hindre F, Moal F, Roux J, Passirani C, Couturier O, Cales P, Le Jeune JJ, Lamprecht A, Benoit JP. In vivo evaluation of lipid nanocapsules as a promising colloidal carrier for paclitaxel. Int J Pharm. 344(1-2):143-9 (2007).
128. Lago J, Alfonso A, Vieytes MR, Botana LM. Ouabain-induced enhancement of rat mast cells response. Modulation by protein phosphorylation and intracellular pH. Cell Signal. 13(7):515-24 (2001).
129. Lambert G, Bertrand JR, Fattal E, Subra F, Pinto-Alphandary H, Malvy C, Auclair C, Couvreur P. EWS Fli-1 antisense nanocapsules inhibits Ewing sarcoma-related tumor in mice. Biochem Biophys Res Commun.279:401-406 (2000).
130. Lambert G, Fattal E, Pinto-Alphandary H, Gulik A, Couvreur P. Polyisobutylcyanoacrylate nanocapsules containing an aqueous core as a novel colloidal carrier for the delivery of oligonucleotides. Pharm Res. 17:707-714 (2000).

131. Lambert G, Fattal E, Pinto-Alphandary H, Gulik A, Couvreur P. Polyisobutylcyanoacrylate nanocapsules containing an aqueous core for the delivery of oligonucleotides. Int J Pharm. 214:13-16 (2001).
132. Lang JC. Ocular drug delivery conventional ocular formulations. Adv Drug Deliv Rev. 16:39-43 (1995).
133. Le Bourlais CA, Chevanne F, Turlin B, Acar L, Zia H, Sado PA, Needham TE, Leverge R. Effect of cyclosporine A formulations on bovine corneal absorption: Ex-vivo study. J Microencapsulation. 14:457-467 (1997).
134. Lee DW, Yun KS, Ban HS, Choe W, Lee SK, Lee KY. Preparation and characterization of chitosan/polyguluronate nanoparticles for siRNA delivery. J Control Release. 139(2):146-52 (2009).
136. Lee SH, Yoo SD, Lee KH: Rapid and sensitive determination of paclitaxel in mouse plasma by high-performance liquid chromatography. J. Chromatogr., B: Biomed. Sci. Appl., 724, 357-363 (1999).
137. Legrand P, Barratt G, Mosqueira V, Fessi H, Devissaguet, JP. Polymeric nanocapsules as drug delivery systems: A review. STP Pharm. Sci. 9:411-418 (1999).
138. Lenaerts V, Labib A, Chouinard F, Rousseau J, Ali H, Van Lier J. Nanocapsules with a reduced liver uptake: Targeting of phthalocyanines to EMT-6 mouse mammary tumor in vivo. Eur J Pharm Biopharm. 41:38-43 (1995).
139. Li X. Chan WK. Transport, metabolism and elimination mechanisms of anti-HIV agents. Adv Drug Deliv Rev. 39:81-103 (1999).
140. Liang G, Jia-Bi Z, Fei X, Bin N. Preparation, characterization and pharmacokinetics of N-palmitoyl chitosan anchored docetaxel liposomes. J Pharm Pharmacol. 59(5):661-7 (2007).
141. Lim ST, Martin GP, Berry DJ, Brown MB. Preparation and evaluation of the in vitro drug release properties and mucoadhesion of novel

microspheres of hyaluronic acid and chitosan. J Control Release. 66(2-3):281-92 (2000).

142. Limayem Blouza I, Charcosset C, Sfar S, Fessi H. Preparation and characterization of spironolactone-loaded nanocapsules for paediatric use. Int J Pharm. 325:124-131 (2006).

143. Lindahl U, Bäckström G, Thunberg L. The antithrombin-binding sequence in heparin. Identification of an essential 6-O-sulfate group. J Biol Chem. 258(16):9826-30 (1983).

143. Liu D, Wang L, Liu Z, Zhang C, Zhang N. Preparation, characterization, and in vitro evaluation of docetaxel-loaded poly(lactic acid)-poly(ethylene glycol) nanoparticles for parenteral drug delivery. J Biomed Nanotechnol. 6(6):675-82 (2010).

144. Lopez-Leon T, Carvalho EL, Seijo B, Ortega-Vinuesa JL, Bastos-Gonzalez D. Physicochemical characterization of chitosan nanoparticles: electrokinetic and stability behavior. J. Colloid Interface Sci. 283:344–351 (2005).

144. Losa C, Marchal-Heussler L, Orallo F, Vila-Jato JL, Alonso MJ. Design of new formulations for topical ocular administration: Polymeric nanocapsules containing metipranolol. Pharm Res. 10:80-87 (1993).

145. Lowe PJ, Temple CS. Calcitonin and insulin in isobutylcyanoacrylate nanocapsules: Protection against proteases and effect on intestinal absorption in rats. J Pharm Pharmacol. 46:547-552 (1994).

146. Lozano MV, Torrecilla D, Lallana E, Vidal A, Fernández-Megía R, Riguera R, Dominguez F, Alonso M J and Torres D. Chitosan nanocapsules for active tumor targeting, 7th World Meeting on Pharmaceutics, Biopharmaceutics and Pharmaceutical Technology, Malta, 2010.

147. Lozano MV, Torrecilla D, Torres D, Vidal A, Domínguez F, Alonso MJ. Highly efficient system to deliver taxanes into tumor cells: docetaxel-loaded chitosan oligomer colloidal carriers. Biomacromolecules. 9(8):2186-93 (2008).

148. Lozano MV, Lollo G, Brea J, Torres D, Loza MI, Alonso MJ. Freeze-dried polysaccharide nanocapsules: efficient vehicles for the intracellular delivery of docetaxel. (submitted, 2011).

149. Lozano MV, Lollo G, Brea J, Torres D, Loza MI, Alonso MJ. Polyarginine nanocapsules: a new platform for intracellular drug delivery (submitted, 2011).

150. Lucio J, D'Brot J, Guo CB, Abraham WM, Lichtenstein LM, Kagey-Sobotka A, Ahmed T. Immunologic mast cell-mediated responses and histamine release are attenuated by heparin. J Appl Physiol. 73(3):1093-101 (1992).

151. Luo Y, Bernshaw NJ, Lu ZR, Kopecek J, Prestwich GD. Targeted delivery of doxorubicin by HPMA copolymer-hyaluronan bioconjugates. Pharm Res. 19(4):396-402 (2002).

152. Luo Y, Prestwich GD. Synthesis and selective cytotoxicity of a hyaluronic acid-antitumor bioconjugate. Bioconjug. Chem. 10, 755–763 (1999).

153. Ma Z, Lim LY. Uptake of chitosan and associated insulin in Caco-2 cell monolayers: a comparison between chitosan molecules and chitosan nanoparticles. Pharm Res. 20(11):1812-9 (2003).

154. Mansour HM, Rhee YS, Wu X. Nanomedicine in pulmonary delivery. Int J Nanomedicine. 4:299-319 (2009).

155. Marchal-Heussler L, Fessi H, Devissaguet JP, Hoffman M, Maincent P. Colloidal drug delivery systems for the eye. A comparison of the efficacy of three different polymers: Polyisobutylcyanoacrylate,

polylactic-co-glycolic acid, poly-epsilon-caprolactone. STP Pharma Sciences. 2:98-104 (1992).

156. Marchal-Heussler L, Sirbat D, Hoffman M, Maincent P. Poly(ε-caprolactone) nanocapsules in carteolol ophthalmic delivery. Pharm Res. 10:386-390 (1993).
157. Martinez-Salas J, Mendelssohn R, Abraham WM, Hsiao B, Ahmed T. Inhibition of allergic airway responses by inhaled low-molecular-weight heparins: molecular-weight dependence. J Appl Physiol. 84(1):222-8 (1998).
158. McNeil SE. Nanotechnology for the biologist. J Leukoc Biol. 78:585-594 (2005).
159. Misra A, Hickey AJ, Rossi C, Borchard G, Terada H, Makino K, Fourie PB, Colombo P. Inhaled drug therapy for treatment of tuberculosis. Tuberculosis (Edinb). 91(1):71-81 (2011).
160. Mitchison DA, Fourie PB. The near future: improving the activity of rifamycins and pyrazinamide. Tuberculosis (Edinb). 90(3):177-81 (2010).
161. Moinard-Checot D, Chevalier Y, Briancon S, Beney L, Fessi H. Mechanism of nanocapsules formation by the emulsion-diffusion process. J Colloid Interface Sci. 317:458-468 (2008).
162. Molinari JF, Campo C, Shakir S, Ahmed T. Inhibition of antigen-induced airway hyperresponsiveness by ultralow molecular-weight heparin. Am J Respir Crit Care Med. 157(3 Pt 1):887-93 (1998).
163. Mora-Huertas CE, Fessi H, Elaissari A. Polymer-based nanocapsules for drug delivery. Int J Pharm. 385(1-2):113-42 (2010).
164. Mosqueira VCF, Legrand P, Gulik A, Bourdon O, Gref R, Labarre D, Barratt G. Relationship between complement activation, cellular uptake and surface physicochemical aspects of novel PEG-modified nanocapsules. Biomaterials. 22:2967-2979 (2001).

165. Mosqueira VCF, Legrand P, Morgat JL, Vert M, Mysiakine E, Gref R, Devissaguet JP, Barratt G. Biodistribution of long-circulating PEG-grafted nanocapsules in mice: Effects of PEG chain length and density. Pharm Res. 18:1411-1419 (2001).

166. Mossman T: Rapid colorimetric assay for cellular growth and survival: application to proliferation and cytotoxicity assays. J. Immunol. Methods 65, 55-63 (1983).

167. Motlekar NA, Youan BB. The quest for non-invasive delivery of bioactive macromolecules: a focus on heparins. J Control Release. 113(2):91-101 (2006).

168. Nafee N, Taetz S, Schneider M, Schaefer UF, Lehr CM. Chitosan-coated PLGA nanoparticles for DNA/RNA delivery: effect of the formulation parameters on complexation and transfection of antisense oligonucleotides. Nanomedicine. 3(3):173-83 (2007).

169. Nakada Y, Fattal E, Foulquier M, Couvreur P. Pharmacokinetics and biodistribution of oligonucleotide adsorbed onto poly(isobutylcyanoacrylate) nanoparticles after intravenous administration in mice. Pharm Res. 13:38-43 (1996).

170. Naor D, Nedvetzki S, Golan I, Melnik L, Faitelson Y. CD44 in cancer. Crit Rev Clin Lab Sci. 39(6):527-79 (2002).

171. Nassar T, Attili-Qadri S, Harush-Frenkel O, Farber S, Lecht S, Lazarovici P, Benita S. High plasma levels and effective lymphatic uptake of docetaxel in an orally available nanotransporter formulation. Cancer Res. 71(8):3018-28 (2011).

172. Nassar T, Rom A, Nyska A, Benita S. A novel nanocapsule delivery system to overcome intestinal degradation and drug transport limited absorption of P-glycoprotein substrate drugs. Pharm Res. 25:2019-2029 (2008).

173. Nassar T, Rom A, Nyska A, Benita S. Novel double coated nanocapsules for intestinal delivery and enhanced oral bioavailability of tacrolimus, a P-gp substrate drug. J Control Release. 133:77-84 (2009).
174. Neumiller JJ, Campbell RK.Technosphere insulin: an inhaled prandial insulin product. BioDrugs. 2010 Jun;24(3):165-72. doi: 10.2165/11536700-000000000-00000.
175. Niven AS, Argyros G. Alternate treatments in asthma. Chest. 123(4):1254-65 (2003).
176. Ohashi K, Kabasawa T, Ozeki T, Okada H. One-step preparation of rifampicin/poly(lactic-co-glycolic acid) nanoparticle-containing mannitol microspheres using a four-fluid nozzle spray drier for inhalation therapy of tuberculosis. J Control Release. 135(1):19-24. (2009).
177. Ortner MJ, Chignell CF. The effect of concentration on the binding of compound 48/80 to rat mast cells: a fluorescence microscopy study. Immunopharmacology. 3(3):187-91 (1981).
178. Ossipov DA: Nanostructured hyaluronic acid-based materials for active delivery to cancer. Expert Opin. Drug Deliv. 7(6), 681-703 (2010).
179. Oyarzun-Ampuero FA, Brea J, Loza MI, Torres D, Alonso MJ. Chitosan-hyaluronic acid nanoparticles loaded with heparin for the treatment of asthma. Int J Pharm. 381(2):122-9 (2009).
180. Page CP. One explanation of the asthma paradox: inhibition of natural anti-inflammatory mechanism by beta 2-agonist. Lancet. 337:717–720 (1991).
181. Page S, Ammit AJ, Black JL, Armour CL. Human mast cell and airway smooth muscle cell interactions: implications for asthma. Am. J. Physiol. Lung Cell. Mol. Physiol. 281: L1313–L1323 (2001).
182. Pandey R, Sharma A, Zahoor A, Sharma S, Khuller GK, Prasad B. Poly (DL-lactide-co-glycolide) nanoparticle-based inhalable sustained drug

delivery system for experimental tuberculosis. J Antimicrob Chemother. 52(6):981-6 (2003).

183. Pandita D, Ahuja A, Lather V, Dutta T, Velpandian T, Khar RK. Development, characterization and in vitro assessement of stearylamine-based lipid nanoparticles of paclitaxel. Pharmazie. 66(3):171-7 (2011).
184. Paraskar AS, Soni S, Chin KT, Chaudhuri P, Muto KW, Berkowitz J, Handlogten MW, Alves NJ, Bilgicer B, Dinulescu DM, Mashelkar RA, Sengupta S. Harnessing structure-activity relationship to engineer a cisplatin nanoparticle for enhanced antitumor efficacy. Proc Natl Acad Sci U S A. 107(28):12435-40 (2010).
185. Peer D, Margalit R.Tumor-targeted hyaluronan nanoliposomes increase the antitumor activity of liposomal Doxorubicin in syngeneic and human xenograft mouse tumor models. Neoplasia. 6(4):343-53 (2004).
186. Peer D, Margalit R: Loading mitomycin C inside long circulating hyaluronan targeted nano-liposomes increases its antitumor activity in three mice tumor models. Int. J. Cancer 108:780-789 (2004).
187. Peer D, Karp JM, Hong S, Farokhzad OC, Margalit R, Langer R: Nanocarriers as an emerging platform for cancer therapy. Nat. Nanotechnol. 2(12), 751-60 (2007).
188. Peltier S, Oger JM, Lagarce F, Couet W, Benoît JP.Enhanced oral paclitaxel bioavailability after administration of paclitaxel-loaded lipid nanocapsules. Pharm Res. 23(6):1243-50 (2006).
189. Penno MB, August JT, Baylin SB, Mabry M, Linnoila RI, Lee VS, Croteau D, Yang XL, Rosada C. Expression of CD44 in human lung tumors. Cancer Res. 54(5):1381-7 (1994).
190. Pinto-Alphandary H, Aboubakar M, Jaillard D, Couvreur P, Vauthier C. Visualization of insulin-loaded nanocapsules: In vitro and in vivo studies after oral administration to rats. Pharm Res. 20:1071-1084 (2003).

191. Pinto Reis C, Neufeld RJ, Ribeiro AJ, Veiga F. Nanoencapsulation II. Biomedical applications and current status of peptide and protein nanoparticulate delivery systems. Nanomedicine. 2:53-65 (2006).

192. Prego C, Fabre M, Torres D, Alonso M.J. Efficacy and mechanism of action of chitosan nanocapsules for oral peptide delivery. Pharm Res .23:549-556 (2006).

193. Prego C, Fernandez-Megia E, Novoa-Carballal R, Quinoa E, Torres D, Alonso MJ. Chitosan and chitosan-PEG nanocapsules: new carriers for improving the oral absorption of calcitonin. Presented at: 30th Annual Meeting of the Controlled Release Society, Glasgow, UK, 19-23 July 2003.

194. Prego C, García M, Torres D, Alonso MJ. Transmucosal macromolecular drug delivery. J Control Release. 101(1-3):151-62 (2005).

195. Prego C, Torres D, Alonso M.J. Chitosan nanocapsules: A new carrier for nasal peptide delivery. JDDST. 16:331-337 (2006).

196. Prego C, Torres D, Alonso MJ. Chitosan nanocapsules as carriers for oral peptide delivery: Effect of chitosan molecular weight and type of salt on the in vitro behaviour and in vivo effectiveness. J Nanosci Nanotechnol. 6:2921-2928 (2006).

197. Prego C, Torres D, Fernandez-Megia E, Novoa-Carballal R, Quiñoá E, Alonso MJ. Chitosan-PEG nanocapsules as new carriers for oral peptide delivery. Effect of chitosan pegylation degree. J Control Release. 111(3):299-308 (2006).

198. Preetz C, Rube A, Reiche I, Hause G, Mader K. Preparation and characterization of biocompatible oil-loaded polyelectrolyte nanocapsules. Nanomedicine. 4:106-114 (2008).

199. Pritchard, K., Lansley, A.B., Martin, G.P., Helliwell, M., Marriott, C., Benedetti, L.M. Evaluation of the bioadhesive properties of hyaluronan

derivatives:detachment weight and mucociliary transport rate studies. Int. J. Pharm. 129,137–145 (1996).

200. Puglisi G, Fresta HTM, Giammona G, Ventura CA. Influence of the preparation conditions on poly(ethylcyanoacrylate) nanocapsule formation. Int J Pharm. 125:283-287 (1995).
201. Qin Y, Song QG, Zhang ZR, Liu J, Fu Y, He Q, Liu J. Ovarian tumor targeting of docetaxel-loaded liposomes mediated by luteinizing hormone-releasing hormone analogues. In vive distribution in nude mice. Arzneimittelforschung. 58(10):529-34 (2008).
202. Quintanar-Guerrero D, Allemann E, Doelker E, Fessi, H. Preparation and characterization of nanocapsnles from preformed polymers by a new process based on emulsification-diffusion technique. Pharm Res. 15:1056-1062 (1998).
203. Raviña M, Cubillo E, Olmeda D, Novoa-Carballal R, Fernandez-Megia E, Riguera R, Sánchez A, Cano A, Alonso MJ. Hyaluronic acid/chitosan-g-poly(ethylene glycol) nanoparticles for gene therapy: an application for pDNA and siRNA delivery. Pharm Res. 27(12):2544-55 (2010).
204. Robinson DS. The role of the mast cell in asthma: induction of airway hyperresponsiveness by interaction with smooth muscle? J. Allergy Clin. Immunol. 114:58–65 (2004).
205. Rosato A, Banzato A, De Luca G, Renier D, Bettella F, Pagano C, Esposito G, Zanovello P, Bassi P. HYTAD1-p20: a new paclitaxel-hyaluronic acid hydrosoluble bioconjugate for treatment of superficial bladder cancer. 65 Urol Oncol. 24(3):207-15 (2006).
206. Rowe RC, Sheskey PJ, Quinn. Handbook of pharmaceutical excipients, 6th edition (2009). pharmaceutical press, United Kingdom (libro).
207. Rowinsky EK, Donehower RC. Paclitaxel (taxol). N Engl J Med. 332(15):1004-14 (1995).

207. Rube A, Hause G, Mader K, Kohlbrecher J. Core-shell structure of Miglyol/poly(D,L-lactide)/Poloxamer nanocapsules studied by small-angle neutron scattering. J Control Release. 107:244-252 (2005).

209. Rusch V, Klimstra D, Venkatraman E, Pisters PW, Langenfeld J, Dmitrovsky E. Overexpression of the epidermal growth factor receptor and its ligand transforming growth factor alpha is frequent in resectable non-small cell lung cancer but does not predict tumor progression. Clin Cancer Res. 3(4):515-22 (1997).

210. Santander-Ortega MJ, Peula-García JM, Goycoolea FM, Ortega-Vinuesa JL: Chitosan nanocapsules: Effect of chitosan molecular weight and acetylation degree on electrokinetic behaviour and colloidal stability. Colloids Surf. B Biointerfaces. 82(2), 571-80 (2011).

211. Saso L, Bonanni G, Grippa E, Gatto MT, Leone MG, Silvestrini B.Interaction of hyaluronic acid with mucin, evaluated by gel permeation chromatography. Res Commun Mol Pathol Pharmacol. 104(3):277-84 (1999).

212. Schwab G, Chavany C, Duroux I, Goubin G, Lebeau J, Helene C, Saison-Behmoaras T. Antisense oligonucleotides adsorbed to polyalkylcyanoacrylate nanoparticles specifically inhibit mutated Ha-ras-mediated cell proliferation and tumorigenicity in nude mice. Proc Natl Acad Sci U S A. 91:10460-10464 (1994).

213. Sharma A, Sharma S, Khuller GK. Lectin-functionalized poly (lactide-co-glycolide) nanoparticles as oral/aerosolized antitubercular drug carriers for treatment of tuberculosis. J Antimicrob Chemother. 54(4):761-6 (2004).

214. Sparreboom A, Scripture CD, Trieu V, Williams PJ, De T, Yang A, Beals B, Figg WD, Hawkins M, Desai N. Comparative preclinical and clinical pharmacokinetics of a cremophor-free, nanoparticle albumin-bound paclitaxel (ABI-007) and paclitaxel formulated in Cremophor (Taxol). Clin Cancer Res. 11(11):4136-43 (2005).

215. Staniscuaski Guterres S, Fessi H, Barratt G, Puisieux F, Devissaguet JP. Poly(D,L-Lactide) nanocapsules containing non-steroidal anti-inflammatory drugs: Gastrointestinal tolerance following intravenous and oral administration. Pharm Res. 12:1545-1547 (1995).

216. Surace C, Arpicco S, Dufaÿ-Wojcicki A, Marsaud V, Bouclier C, Clay D, Cattel L, Renoir JM, Fattal E. Lipoplexes targeting the CD44 hyaluronic acid receptor for efficient transfection of breast cancer cells. Mol Pharm. 6(4):1062-73 (2009).

217. Taetz S, Bochot A, Surace C, Arpicco S, Renoir JM, Schaefer UF, Marsaud V, Kerdine-Roemer S, Lehr CM, Fattal E. Hyaluronic acid-modified DOTAP/DOPE liposomes for the targeted delivery of anti-telomerase siRNA to CD44-expressing lung cancer cells. Oligonucleotides. 19(2):103-16 (2009).

218. Taetz S, Nafee N, Beisner J, Piotrowska K, Baldes C, MürdterTE, Huwer H, Schneider M, Schaefer UF, Klotz U, Lehr CM.The influence of chitosan content in cationic chitosan/PLGA nanoparticles on the delivery efficiency of antisense 2'-O-methyl-RNA directed against telomerase in lung cancer cells. Eur J Pharm Biopharm. 72(2):358-69 (2009).

219. Teijeiro-Osorio D, Remuñán-López C, Alonso MJ. Chitosan/cyclodextrin nanoparticles can efficiently transfect the airway epithelium in vitro. Eur J Pharm Biopharm. 71(2):257-63 (2009).

220. Teijeiro-Osorio D, Remuñán-López C, Alonso MJ.New generation of hybrid poly/oligosaccharide nanoparticles as carriers for the nasal delivery of macromolecules. Biomacromolecules. 10(2):243-9 (2009).

221. Ten Tije AJ, Verweij J, Loos WJ, Sparreboom A: Pharmacological effects of formulation vehicles : implications for cancer chemotherapy. Clin. Pharmacokinet. 42(7), 665-85 (2003).

222. Tomoda K, Ohkoshi T, Hirota K, Sonavane GS, Nakajima T, Terada H, Komuro M, Kitazato K, Makino K.Preparation and properties of inhalable nanocomposite particles for treatment of lung cancer. Colloids Surf B Biointerfaces. 71(2):177-82 (2009).

223. Torrecilla D, Lozano MV, Lallana E, Novoa-Carballal R, Vidal A, Torres D, Fernández-Megía E, Riguera E, Alonso MJ, Domínguez F (Sometido, 2011).

224. Toub N, Bertrand JR, Malvy C, Fattal E, Couvreur P. Antisense oligonucleotide nanocapsules efficiently inhibit EWS-Fli1 expression in a Ewing's sarcoma model. Oligonucleotides. 16:158-168 (2006).

225. Toub N, Bertrand JR, Tamaddon A, Elhamess H, Hillaireau H, Maksimenko A, Maccario J, Malvy C, Fattal E, Couvreur P. Efficacy of siRNA nanocapsules targeted against the EWS-Fli1 oncogene in Ewing sarcoma. Pharm Res. 23:892-900 (2006).

226. Tran TA, Kallakury BV, Sheehan CE, Ross JS. Expression of CD44 standard form and variant isoforms in non-small cell lung carcinomas. Hum Pathol. 28(7):809-14 (1997).

227. Trudeau ME, Eisenhauer EA, Higgins BP, Letendre F, Lofters WS, Norris BD, Vandenberg TA, Delorme F, Muldal AM. Docetaxel in patients with metastatic breast cancer: a phase II study of the National Cancer Institute of Canada-Clinical Trials Group. J Clin Oncol. 14(2):422-8 (1996).

228. Tseng CL, Su WY, Yen KC, Yang KC, Lin FH. The use of biotinylated-EGF-modified gelatin nanoparticle carrier to enhance cisplatin accumulation in cancerous lungs via inhalation. Biomaterials. 30(20):3476-85 (2009).

229. Tyrell DJ, Kilfeather S, Page CP. Therapeutic uses of heparin beyond its traditional role as an anticoagulant. Trends Pharmacol Sci. 16(6):198-204 (1995).

230. Ubrich N, Schmidt C, Bodmeier R, Hoffman M, Maincent P. Oral evaluation in rabbits of cyclosporin-loaded Eudragit RS or RL nanoparticles. Int J Pharm. 288:169-175 (2005).
231. van Zuylen L, Verweij J, Sparreboom A. Role of formulation vehicles in taxane pharmacology. Invest New Drugs. 19(2):125-41 (2001).
232. Vauthier C, Bouchemal K. Methods for the preparation and manufacture of polymeric nanoparticles. Pharm Res. 26(5):1025-58 (2009).
233. Vauthier C, Labarre D, Ponchel G. Design aspects of poly(alkylcyanoacrylate) nanoparticles for drug delivery. J Drug Target. 15:641-663 (2007).
234. Vila A, Gill H, McCallion O, Alonso MJ. Transport of PLA-PEG particles across the nasal mucosa: effect of particle size and PEG coating density. J Control Release. 98:231-244 (2004).
235. Vila A, Sánchez A, Janes K, Behrens I, Kissel T, Vila Jato JL, Alonso MJ. Low molecular weight chitosan nanoparticles as new carriers for nasal vaccine delivery in mice. Eur J Pharm Biopharm. 57(1):123-31 (2004).
236. Vranckx H, Demoustier M, Deleers M. A new nanocapsule formulation with hydrophilic core: Application to the oral administration of salmon calcitonin in rats. Eur J Pharm Biopharm. 42:345-347 (1996).
237. Watnasirichaikul S, Davies NM, Rades T, Tucker IG. Preparation of biodegradable insulin nanocapsules from biocompatible microemulsions. Pharm Res. 17:684-689 (2000).
238. Wohlgemuth M, Mayer C. Pulsed field gradient NMR on polybutylcyanoacrylate nanocapsules. J Colloid Interface Sci. 260:324-331 (2003).
239. Wong WS, Koh DS. Advances in immunopharmacology of asthma. Biochem Pharmacol. 59(11):1323-35 (2000).
240. Xin D, Wang Y, Xiang J. The use of amino acid linkers in the conjugation of paclitaxel with hyaluronic acid as drug delivery system:

synthesis, self-assembled property, drug release, and in vitro efficiency. Pharm Res. 27(2):380-9 (2010).

241. Xu CX, Jere D, Jin H, Chang SH, Chung YS, Shin JY, Kim JE, Park SJ, Lee YH, Chae CH, Lee KH, Beck GR Jr, Cho CS, Cho MH. Poly(ester amine)-mediated, aerosol-delivered Akt1 small interfering RNA suppresses lung tumorigenesis. Am J Respir Crit Care Med. 178(1):60-73 (2008).
242. Yamamoto H, Kuno Y, Sugimoto S, Takeuchi H, Kawashima Y. Surface-modified PLGA nanosphere with chitosan improved pulmonary delivery of calcitonin by mucoadhesion and opening of the intercellular tight junctions. J Control Release. 102(2):373-81 (2005).
243. Yamamoto Y, Yoshida M, Sato M, Sato K, Kikuchi S, Sugishita H, Kuwabara J, Matsuno Y, Kojima Y, Morimoto M, Horiuchi A, Watanabe Y. Feasibility of tailored, selective and effective anticancer chemotherapy by direct injection of docetaxel-loaded immunoliposomes into Her2/neu positive gastric tumor xenografts. Int J Oncol. 38(1):33-9 (2011).
244. Yi D, Wiedmann TS. Inhalation adjuvant therapy for lung cancer. J Aerosol Med Pulm Drug Deliv. 23(4):181-7 (2010).
245. Yin Win K, Feng S. Effects of particle size and surface coating on cellular uptake of polymeric nanoparticles for oral delivery of anticancer drugs. Biomaterials. 26:2713-2722 (2005).
246. Yuan Z, Chen D, Zhang S, Zheng Z. Preparation, characterization and evaluation of docetaxel-loaded, folate-conjugated PEG-liposomes. Yakugaku Zasshi. 130(10):1353-9 (2010).
247. Zhai G, Wu J, Yu B, Guo C, Yang X, Lee RJ. A transferrin receptor-targeted liposomal formulation for docetaxel. J Nanosci Nanotechnol. 10(8):5129-36 (2010).

ANEXOS

Anexo 1: Artículo relacionado

Chitosan-coated lipid nanocarriers for therapeutic applications

F.A. Oyarzun-Ampuero, M. Garcia-Fuentes, D. Torres, M.J. Alonso

Departamento de Farmacia y Tecnología Farmacéutica, Facultad de Farmacia, Universidad de Santiago de Compostela, 15782-Santiago de Compostela, Spain

Adapted from: Journal of drug delivery science and technology. (2010). 20 (4): 259-265.

Abstract

This article reports the efforts made over the last two decades by our group regarding the design of chitosan-coated lipid nanostructures as well as their potential for two different applications: i) as transmucosal delivery vehicles for complex macromolecules and ii) as carriers for anticancer drug delivery. The nanostructures described here share a core coating structure, in which the core consists of a liquid (Miglyol 812) or a solid (tripalmitin) lipid surrounded by a chitosan coating. Both polymer-coated nanostructures have displayed outstanding properties in relation to the favored transport of large complex molecules (e.g. peptides and vaccines) across the nasal and intestinal barriers, as well as to facilitate
the intracellular delivery of anticancer drugs into tumor cells.

Keywords: Chitosan; Nanocapsules; Lipid nanoparticles; Transmucosal peptide delivery; Cancer therapy.

Chitosan-coated lipid nanostructures, rationale and historical perspective

For better comprehension of our contribution to the development of chitosan-coated lipid nanocarriers, the reader should refer to the past, more precisely, to the context of the mid 90s. At that time, lipid nanocarriers such as submicron nanoemulsions, nanocapsules and solid lipid nanoparticles, were revealed as interesting systems for the administration of hydrophobic drugs by different routes [1-3]. Most of these colloidal drug carriers were characterized by a negative surface charge, which was mainly attributed to the presence of natural lipidic compounds [3, 4] or to polyester polymers [1, 5]. The presence of this negative surface charge helped prevent the destabilization of the carriers; however, it also had certain negative consequences. On the one hand, it promoted the adsorption of cationic proteins and sodium and calcium ions present in biological fluids, thereby leading to the neutralization of the surface charge, breakdown of the system and leakage of the entrapped agents [6]. On the other, these negatively charged colloidal systems can suffer an electrostatic repulsion with biological membranes, since they are also negatively charged [6]. In the light of the above, it was reasonable to believe that positively charged drug carriers would be favorable in terms of facilitating interactions with the epithelia and improving the capacity for drug transport [7, 8]. In fact, several authors proposed the use of positive phospholipid derivates and other cationic surfactants in the preparation and stabilization of liposomes and submicron emulsions [9-11]. As an alternative, we proposed a new approach based on the incorporation of the cationic polysaccharide chitosan (CS) on the surface of the nanocarrriers simply through ionic interactions between the negatively charged nanocarrier surface and the polymer [6]. The polysaccharide CS was chosen to coat these colloidal systems due to its cationic character and because it showed critical features for drug delivery, including

mucoadhesivity and biocompatibility. Indeed, several authors had reported low or absent signs of toxicity upon CS administration by different routes [12-13]. Our first attempts conducted with the newly developed CS-coated lipid nanocarriers focused on the ocular route, in which several problems such as removal mechanisms, rapid nasolachrymal drainage and non-productive drug absorption into the systemic circulation constrains the effects of conventional formulations. With the benefits obtained with these CS-coated lipid nanocarriers, we can achieve a higher drug concentration in ocular tissues and improve most pharmacokinetic parameters when compared to other cationic- coated carriers or to commercial formulations [14]. This information together with the low ocular toxicity of the nanosystems [14], inspired us to extend applications of these novel formulations to other administration routes.

This work aims to review and to summarize our group's contribution in aspects concerning the design and *in vivo* fate of the developed CS-coated lipid nanocarriers.

Design and characterization of CS-coated lipid nanocarriers

CS nanocapsules

The initially designed CS-coated nanosystems were formed by promoting the ionic interaction of CS onto the surface of the negatively charged poly-ε-caprolactone (PεCL) nanocapsules or onto the negatively charged submicron nanoemulsion [6]. In the first case, CScoated PεCL nanocapsules were obtained by modifying the method of interfacial deposition of polyester polymers, proposed by Al Khouri *et al.* [15]. PεCL nanocapsules were formed by means of the spontaneous emulsification of a lipid core (Mygliol and lecithin) in water due to the diffusion of the organic solvent, in which the polymer and lipids were dissolved [15, 16]. To obtain CS-coated polyester nanocapsules, the polysaccharide CS was incorporated

in the aqueous phase during the manufacturing process, thus allowing the adsorption of CS onto the negatively charged surface of the systems [6].

In the second case, CS nanocapsules were prepared using a similar procedure to the one described above, the only difference being that the PεCL was eliminated from the formulation. Thus, the method of preparation was not a polymeric interfacial deposition, but rather a direct electrostatic interaction between CS and lecithin located in the inner core of the systems [6]. We also described the possibility of incubating the polysaccharide CS with the preformed lecithin-containing nanoemulsions for obtaining these nanocapsules [17].

Characterization by photon correlation spectroscopy of CS-coated polyester and CS nanocapsules indicated that nanocarriers between 150-300 nm were obtained, showing a monomodal dispersity. Laser doppler anemometry showed that all systems without CS displayed negative zeta potential values, while the addition of CS to the aqueous phase resulted in highly positive values, supporting the successful formation of a CS layer surrounding the lipid cores. Micrographs obtained by transmission electron microscopy (TEM), showed spherical structures in all cases (*Figure 1*).

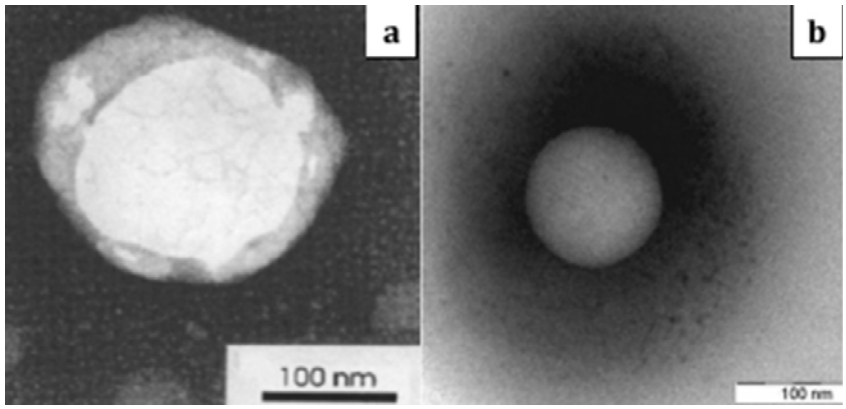

Figure 1 - Transmission electron micrographs of (a) CS-coated polyester nanocapsules and (b) CS nanocapsules (reproduced with permission from Springer and Editions de Santé, respectively).

Considering the hydrophobic nature of the inner components in CS-coated nanosystems, it was reasonable to postulate that a variety of molecules with low water solubility could be efficiently encapsulated. The drugs that we effectively encapsulated in the CS-coated nanosystems included: diazepam [6], triclosan [18] and docetaxel [19]. Additionally, the cationic CS coating allowed the adsorption of negatively charged hydrophilic macromolecules such as the recombinant hepatitis B surface antigen [20].

The presence of the negatively charged lecithin in the oily core of the nanocapsules further allowed the incorporation of positively charged hydrophilic molecules such as salmon calcitonin [21]. The peptide was encapsulated into CS nanocapsules with an efficiency of 44 %, which was significantly lower than that shown by the uncoated nanoemulsion (> 90 %). This effect was attributed to a competition between the peptide and the CS, both positively charged, in their association with the surface of the nanoemulsion. The encapsulation efficiency was also dependent on the CS molecular weight. In fact, CS oligomer (~10 kDa) nanocapsules showed higher encapsulation efficiency (60 %) than medium molecular weight (~100 kDa) CS nanocapsules. This indicates that the CS oligomer coating was not able to displace salmon calcitonin to the same extent as medium molecular weight CS.

CS-coated lipid nanoparticles

Solid triglycerides are interesting biomaterials for the production of nanocarriers due to: i) their excellent biocompatibility [22]; ii) their capacity to form highly hydrophobic matrices capable of restricting the penetration of peptidases and other degradative enzymes present in biological fluids or in the intestinal epithelia, thus protecting the loaded cargo; iii) their capacity to enhance intestinal drug transport, which has been observed even in the case

of peptidic drugs [23]. Taking these reasons into account, we decided to prepare CS-coated solid triglyceride nanoparticles as alternative formulations to CS nanocapsules. More concretely, our aim was to compare the suitability of the different core structures, based on liquid or solid lipids, for protecting and promoting the intestinal absorption of peptide drugs. Solid triglyceride nanoparticles are typically prepared by high-pressure homogenization of molten lipid mixtures, by formation of microemulsions above the melting temperature of the triglycerides or by solventemulsification techniques [24]. These preparation techniques allow simple microencapsulation of hydrophobic molecules such as doxorubicin, paclitaxel, prednisolone or progesterone, among others [25]. On the other hand, solid triglyceride matrices present low affinity for hydrophilic macromolecules. Indeed, early attempts to include proteins and peptides into nanomatrices of solid lipids were undertaken by solubilizing these molecules in molten lipid mixtures that were subsequently dispersed as nanometric matrices [26, 27]. These methods frequently resulted in low protein loadings and potential peptide denaturation processes arising from contact with the molten lipids [24]. To avoid the use of high temperatures, we decided to adapt a solvent casting method and more specifically, a w/o/w doubleemulsion solvent-evaporation technique [28]. The double-emulsion solvent-evaporation method has been applied to the encapsulation of insulin and salmon calcitonin, leading to moderate/high encapsulation efficiencies and drug loadings close to 1 % (w/w) [28, 29]. Such encapsulation values represented a significant improvement over previous attempts based on peptide solubilization in the triglyceride mixture [27]. Notably, double-emulsion solvent-evaporation techniques have found application in the encapsulation of other biopharmaceutics such as antigenic proteins [30]. CS-coated lipid nanoparticles can be prepared by the deposition of CS on the nanoparticle surface, a process that is triggered by electrostatic forces. Presence of CS in the external phase of the solvent emulsification method used for lipid nanoparticle preparation destabilizes the

colloidal system. For that reason, our method of CS-coated lipid nanoparticles preparation comprises first the preparation of the lipid nanoparticle cores and secondly, the formation of the CS coating by electrostatic interactions between the anionic cores and polycationic CS [29]. Typical CS-coated nanoparticles prepared by this method present a particle size between 400 and 600 nm and a positive zeta potential, as confirmed by photon correlation spectroscopy and laser doppler anemometry. Lipid nanoparticle composition and nanostructure can be further characterized by liquid-state NMR techniques, taking advantage of the different relaxation constants of the triglyceride core and polymeric shell and of the possibility of performing the analysis over the lipid mixture melting temperature [31, 32].

CS-coated nanostructures for the transmucosal delivery of macromolecules

The beginning of this decade witnessed large research efforts dedicated to finding the "holy grail" of transmucosal delivery, a carrier capable of promoting the oral absorption of protein and DNA-based medicines [33]. The expectation of realizing such groundbreaking technology was fuelled by major advances from the late 80s and 90s, that demonstrated the capacity of nanometric matter to interact with the intestinal epithelium, ultimately leading to the first proofs-of-principle of their capacity to enhance the bioavailability of macromolecules delivered by transmucosal routes. Some of these first key contributions came from the Florence group, which in a systematic work demonstrated the capacity of submicrometric matter to be taken up by the intestinal epithelium and to a lesser extent, to be internalized [34-36]. Simultaneously, the Couvreur group presented the first evidence of efficient peptide delivery by the oral route using polycyanoacrylate nanocapsules [37]. This concept of oral delivery of therapeutic

macromolecules was further explored by the Mathiowitz group, this time using biodegradable, solid-core nanoparticles [38].

During the 90s, our group also studied the capacity of polymeric nanocarriers to interact with several epithelial barriers. Our results indicated the capacity of nanocarriers to tightly interact with the corneal, nasal and intestinal epithelia and even more importantly, that this interaction can lead to significant improvements in the transmucosal absorption of drugs [39-41].

All of this collected evidence pointed us to a potential opportunity to apply specifically optimized nanostructures for the transmucosal delivery of macromolecules. The blueprint of an ideal transmucosal nanocarrier would be a system capable of protecting the macromolecule of interest from enzymatic degradation in the administration route [42], but also capable of enhancing macromolecule transport through biological barriers.

CS is a biocompatible polymer with mucoadhesive and penetration-enhancing properties, which makes it a promising candidate for nanocarrier surface modification [43]. Additionally, studies performed by our group have confirmed that CS-coated nanostructures present improved stability in biological fluids compared to lipid nanocores [29]. The modification of nanocarriers with CS applied as a mucoadhesive polymer coating for transmucosal delivery was reported simultaneously by the Kawashima group and our own. These works comprised CScoating strategies implemented into PεCL nanocapsules, poly(lactic-co-glycolic acid) nanoparticles and liposomes as transmucosal peptide carriers [6, 44-46]. In the next part of the review, we will summarize our main findings in the field of transmucosal delivery using the proposed CS-coated lipid nanocarriers. The interaction of the nanocarriers with mucosal surfaces and the administration of peptidic drugs by oral and nasal routes will be reviewed. As an alternative application, the utilization of CS nanocapsules in cancer therapy will be presented.

Interaction of CS-coated nanostructures with mucosal surfaces

We had previously reported a study showing the preferential internalization of CS nanoparticles compared with poly(ethylene glycol) (PEG)-coated nanoparticles in the Caco-2 cell model [47]. These results were even more remarkable when the formulations were assayed in the mucus-secreting cells MTX-E12, suggesting that mucoadhesivity of CS nanoparticles is an important factor for interacting with mucosal surfaces. The above findings contrast with those obtained with CS-coated lipid nanostructures in Caco-2 cells. Here, the amount of associated CS-coated lipid nanoparticles or CS nanocapsules was similar to those obtained with PEG-coated nanoparticles or with a nanoemulsion, respectively [17, 48]. A further goal was to elucidate the possible internalization together with the intracellular localization of CS-coated lipid nanostructures. For this, CS nanocapsules were visualized after their incubation with Caco-2 cells and with a coculture of enterocytes and mucus-secreting cells using confocal laser scanning microscopy [21]. The results indicated that i) while in Caco-2 cells nanosystems interacted with a random distribution, in the coculture they interacted highly and preferentially with the mucus secreting cells; ii) the systems were not capable of crossing the monolayer and were preferentially located in the apical region of the cells (*Figure 2*). The higher interaction with mucus secreting cells of CS-coated nanosystems was attributed to the strong mucoadhesive character of the polymer which is related to the formation of hydrogen and ionic bonds between the positively charged amino groups of CS and the negatively charged sialic acid residues of mucin glycoproteins [49]. Consequently, we can infer from this study that the mucoadhesive character of CS nanocapsules is a determinant factor of their ability to interact with the intestinal mucosa. Theoretically, this mechanistic behavior would also be applicable to other CS-coated nanostructures such as lipid nanoparticles [29]. We have also checked the capacity of our polymer-coated lipid nanostructures to modify the permeability of the cell monolayers.

In this case, it is known that CS has a capacity to cause a dose-dependent decrease in transepithelial electric resistance (TEER) [50] while PEG is assumed to be inert in terms of cellular interaction. In agreement with this, we observed that PEG-coated lipid cores did not cause a reduction in the TEER of Caco-2 monolayers in the range of concentrations investigated (220-330 μg/cm2). In contrast, CS-coated lipid nanostructures induced a dose-dependent drop in the TEER of Caco-2 monolayers, reaching significant reductions for the concentration range of 83-330 μg/cm2 [17, 48] (*Figure 3*). The values of the TEER reduction were additionally supported by the observation of enhanced paracellular transport of the macromolecular marker dextran-Texas Red (Mw = 3000 Da) [48].

However, it should be added that these values were, in the case of nanocapsules, close to those that comprised cell viability (220 μg/cm2) [17]. Therefore, it could be expected that this change in epithelium permeability could only be seen when an important amount of the nanocarriers accumulate in the epithelium. Interestingly, we observed that the normal TEER values slowly recuperated after the exposure of CS-coated nanostructures.

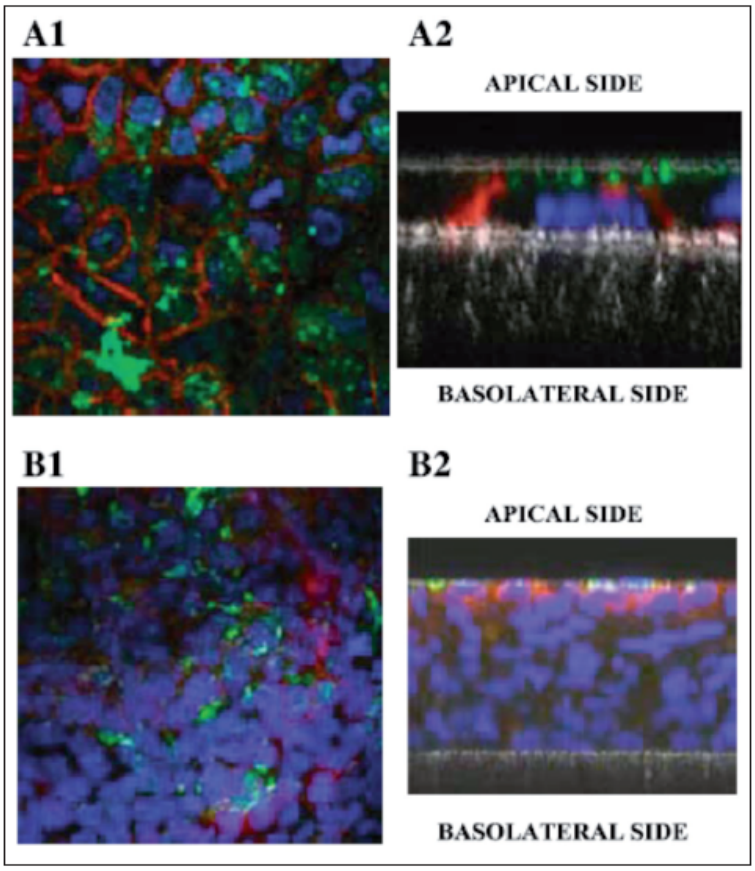

Figure 2 - Confocal scanning microscopy images showing the association of fluorescent nanocapsules (green) with Caco-2 cells and coculture Caco-2/HT29-M6 (E-cadherin in red and nucleus in blue). Caco-2: (A1) Montage of 24 horizontal cross sections illustrating the interaction of fluorescent CS nanocapsules to the cells (step size in z axis of 0.5 2 m.); (A2) confocal xz section showing the accumulation of fluorescent CS nanocapsules in the apical side of the monolayer. Caco-2/HT29-M6 coculture: (B1) Montage of microscopy images showing the association of fluorescent CS nanocapsules with the coculture Caco-2:HT29-M6. (B2) Confocal scanning microscopy xz section showing the accumulation of fluorescent CS nanocapsules (green) in the apical side of the HT29-M6 cells (reprinted with permission from Springer).

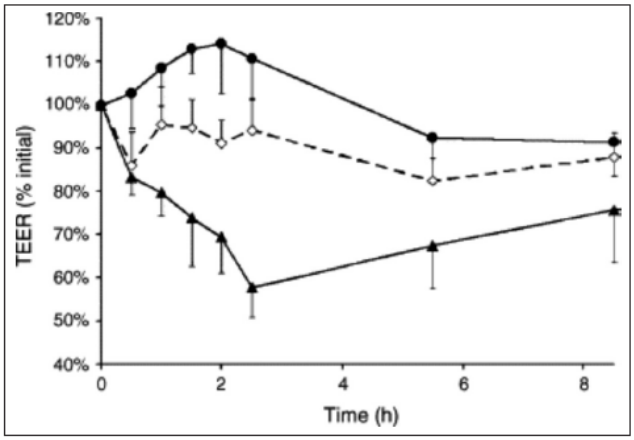

Figure 3 - Transepithelial electric resistance (TEER) of Caco-2 monolayers exposed to PEG-coated nanoparticles (1 mg/mL) (◊), CS-coated nanoparticles (1 mg/mL) (s) or their respective controls (HBSS (Hanks' balanced salt solution) (p); HBSS pH 6.5 (l)) (mean ± SD, n = 3-6) (reprinted with permission from Elsevier).

Application of CS-coated nanocarriers for oral peptide delivery – case of study: salmon calcitonin

The efficacy of CS nanocapsules and CS-coated lipid nanoparticles as oral carriers for peptide delivery was investigated using salmon calcitonin (sCT) as a model [17, 48]. The reduction of the serum calcium levels after oral administration of peptide-loaded CS nanocapsules was monitored in rats, using an aqueous solution and a nanoemulsion containing sCT as controls. Importantly, as shown in *Figure 4*, a marked hypocalcemic response was noted when the peptide was associated with the nanocapsules. The importance of the CS coating was evident because sCT was ineffective when administered in the uncoated nanoemulsion. Moreover, this reduction in the serum calcium levels was maintained for more than 24 h following administration of the CS-coated nanocapsules. This pronounced and longlasting hypocalcemic effect led us to speculate that the mucoadhesive properties of CS might be determinant in facilitating the intestinal absorption of sCT and in assuring the sustained release of the peptide from the absorptive epithelium towards the bloodstream. In the same way, sCT-loaded

CS-coated lipid nanoparticles administered orally to rats have shown a very marked and prolonged pharmacological effect, which contrasted with the lack of response observed for the controls of sCT solution and PEG-coated lipid nanoparticles [48].

Application of CS-coated nanocarriers for nasal peptide delivery-case of study: salmon calcitonin

Our research group was the first to explore the potential of CS nanocapsules to increase the nasal absorption of peptide drugs. Several strategies had been proposed to enhance the bioavailability of peptides by the nasal route, with the use of penetration enhancers being a frequent option. Importantly, a major limitation of the majority of enhancers is related to their ability for inducing morphological changes on the nasal mucosa and/or inhibition of the ciliary movement [51, 52]. Among the penetration enhancers, CS is a special case because, in addition to being a mucoadhesive material, the penetration enhancing effect of this polymer is reversible; therefore, it does not compromise the integrity and functionality of the epithelia [53, 54]. The efficacy of this material in terms of increasing the nasal absorption of peptides has already been illustrated for insulin, leuprolide, parathyroid hormone and sCT [54-56]. In our study, the model peptide sCT was incorporated in the nasally administered formulations and the serum calcium levels obtained with the CS nanocapsules were compared with those obtained with the uncoated nanoemulsion and with an aqueous solution containing or not containing the CS [57]. The results shown in *Figure 5* indicate that the hypocalcemic effect observed after administration of the colloidal systems (uncoated nanoemulsion and CS nanocapsules) was significantly greater than that obtained with the other formulations, with results being clearly better for the CS nanocapsules. Interestingly, the slight but significant decrease in calcium levels observed for the uncoated

nanoemulsion might be related to the lipids' absorptionenhancing effect [23, 58] and/or to their drug-protecting properties [59, 60]. The results obtained with CS nanocapsules compared to the other formulations, highlight the critical role of CS in enhancing the transport of the associated drug and consequently underline the potential of this polymer for nasal peptide delivery. We have also prepared and tested CS nanocapsules for nasal vaccination. In that case, the recombinant hepatitis B surface antigen was adsorbed ionically onto the surface of the nanocapsules. These systems were capable of inducing an effective protective response against the disease [20, 61]. This subject will be extensively reviewed in the article "From single-dose vaccine delivery systems to nanovaccines" published in this same issue.

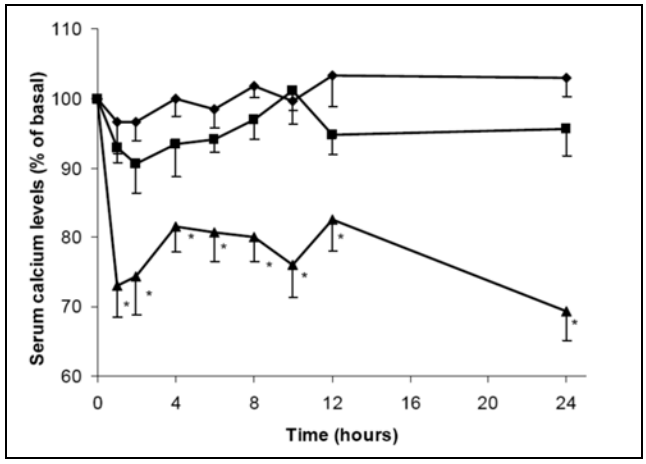

Figure 4 - Serum calcium levels after oral administration in rats of CS nanocapsules as well as the control nanoemulsion and an aqueous solution of sCT (mean ± SE; n = 6). ◆ sCT solution; ■ nanoemulsion; ▲ CS nanocapsules. *Statistically significant differences from sCT solution ($p < 0.05$) (reprinted with permission from Elsevier).

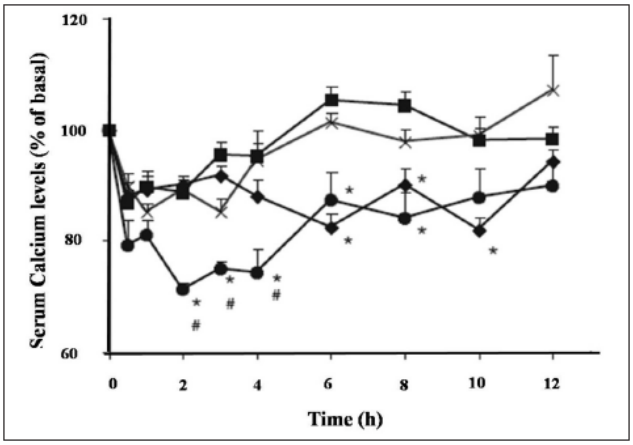

Figure 5 - Serum calcium levels after nasal administration in rats of salmon calcitonin (sCT, dose: 15 IU/kg) in aqueous solution (with or without CS) or encapsulated in the control nanoemulsion or in CS nanocapsules; (mean ± SE; n = 6). ■ sCT solution; X sCT solution + CS; ◆ nanoemulsion; ● CS nanocapsules. *Significantly different from salmon sCT solution ($p < 0.05$). #Significantly different from nanoemulsion ($p < 0.05$) (reproduced with permission from Editions de Santé).

CS nanocapsules for anticancer drug delivery

The advances in nanomedicine are especially well perceived in cancer therapy, mainly because the efficacy of current treatments is still very limited [62]. The main problems related to conventional cancer therapies include: unspecific biodistribution, suboptimal cell internalization and the toxicity of standard excipients required for drug solubilization. In this context, nanocapsule technology emerges as apromising approach for the formulation of anticancer drugs, offering the possibility of facilitating the accumulation of the drug in the tumor tissue by the well-known enhanced permeability and retention effect (EPR) [63]. Nanocapsules may also improve the cellular internalization of the drug because of its ability to inhibit the multi-drug resistance barrier expressed in many kinds of cancers [64] and allowing the incorporation of hydrophobic drugs directly into the formulation, thus limiting the toxicity of excipients while protecting the drug from biological fluids [65].

Taxanes (paclitaxel, docetaxel) have established themselves as an important class of currently available antitumor drugs. They have greatly contributed to the improvement in cancer patient survival and have proven clinical efficacy against a wide range of solid tumors, such as advanced breast, ovarian or non-small cell lung cancer [66-68]. Despite their positive therapeutic features, taxanes suffer from such drawbacks as aqueous insolutibilty and dose-limiting toxicities at the clinically administered doses, especially related to the solubilizing solvents and surfactants included in their marketed formulations. Importantly, the potential of nanoformulated taxanes to solve this inherent toxicity was reinforced by the Food and Drug Administration's approval of Abraxane, consisting of nanoparticles containing albumin-bound paclitaxel [69].

CS nanocapsules developed by our research group were proposed as carriers for the taxane drug docetaxel with the aim of reducing the side effects of the free drug and improving docetaxel's efficacy by tumor targeting [19]. In this study oligomers of CS were chosen because a low molecular weight of the polymer was considered safer to be administered by intravenous route.

Docetaxel-loaded CS nanocapsules were incubated with MCF7 (breast tumor cell line) and A549 (lung tumor cell line) cells for 24 and 48 h, showing an effect on cell proliferation at 24 h that was significantly greater than that of free docetaxel in both cell lines. This information was corroborated by the lower growth inhibition 50 % (GI50) values obtained for the loaded nanocapsules compared to the free drug in both cell cultures (*Table I*). Importantly, in *Table I* is also possible to appreciate that blank CS nanocapsules had no significant effects in the cell growth.

Interestingly, after 48 h of incubation, the effects on cell proliferation observed for docetaxel-loaded nanocapsules and free docetaxel were similar, which suggests that the differential effect found at 24 h was due to an accelerated uptake of the docetaxel-loaded nanocarriers. In order to provide evidence of the uptake intensity of the CS nanocapsules, a fluorescent dye was encapsulated and its interaction was evaluated at 2 h by flow cytometry in MCF-7 and A549 cell lines. *Figure 6* shows that the encapsulated fluorescent dye interacted with almost every cell, while the non encapsulated dye remained mainly excluded from this interaction. This improved uptake could be related to a favorable interaction of the CS coating with the cancer cells, as it was also found with CS nanocapsules in different cell types such as those of corneal epithelium [70].

More recently, a comparative efficacy study with docetaxel-loaded CS-nanocapsules and a control docetaxel formulation (Taxotere) was performed in a A549 tumor xenograf model in mice, by administering an intratumoral dose of 9 mg/kg, each four days, for a complete dose of 27 mg/kg. In this work, we have shown that the efficacy of docetaxel-loaded CS-nanocapsules was comparable to that of the classical docetaxel formulation [71]. Moreover, by analyzing the effect of each single injection of both docetaxel formulations in the tumor size, it was found that free docetaxel has a faster effect but docetaxel-loaded CS nanocapsules can continue their antiproliferative effect for longer periods of time. Besides this hypothetical advantage which needs to be corroborated, CS oligomer nanocapsules exhibit the great advantage to avoid the use of Tween 80 for the solubilization and formulation of docetaxel, this vehicle being responsible for severe side effects. Therefore, CS oligomer nanocapsules can be proposed as a new drug delivery system for docetaxel, although toxicological and biodistribution studies need to be undertaken to support the potential of this formulation.

Table I - GI50 (growth inhibitory 50, drug concentration resulting in a 50 % reduction in absorbance in control cells) in MCF7 and A549 cells for blank CS nanocapsules, free docetaxel, and docetaxel-loaded CS nanocapsules (mean ± SD; n = 4) (Reproduced with permission from ACS publications).

	MCF7		A549	
	24 h	48 h	24 h	48 h
Blank CS nanocapsules	n.d.	n.d.	n.d.	n.d.
Docetaxel	62.5	5.6	36.5	12.8
Docetaxel-loaded CS nanocapsules	4.7	2.7	5.3	4.5

nd: non determined; none of the concentrations tested resulted in a 50 % reduction of the absorbance.

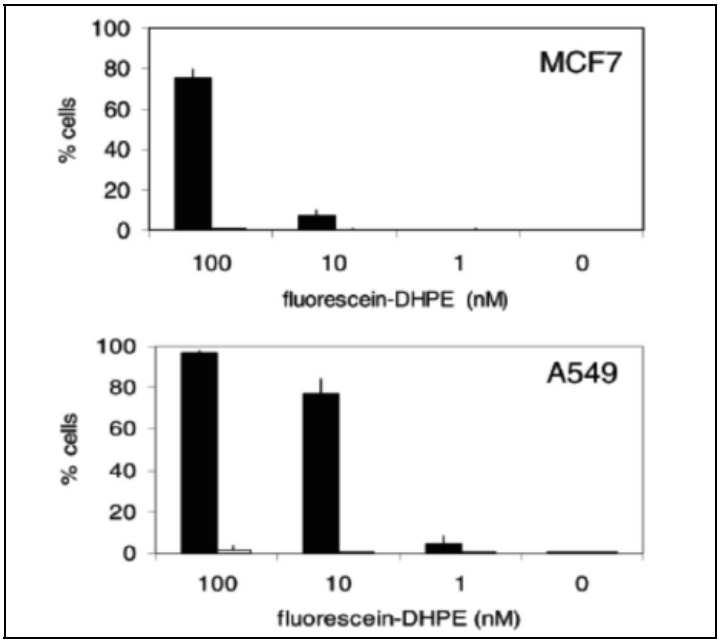

Figure 6 - Uptake studies of fluorescent CS nanocapsules assessed by flow cytometry in MCF7 and A549 cells. Percentage of stained cells after a 2 h incubation with fluorescein-DHPE CS nanocapsules (black bars) or free fluorescein-DHPE (white bars). Mean values of three independent experiments. (Reproduced with permission from ACS publications).

5. Main remarks

CS-coated lipid nanostructures are a versatile tool suitable for encapsulating lipophilic or hydrophilic drugs with a considerable efficiency and capable of exhibiting sustained-release functions at the site of delivery or action. These CS lipid nanocarriers have shownpotential as transmucosal carriers for the delivery of large complex molecules and also as intracellular drug delivery vehicles. Besides the capacity of these nanocarriers to protect sensitive molecules in their lipid core, the presence of the CS coating has been identified as a critical parameter for their efficacy. This coating is responsible for the interaction of the nanostructures with the epithelial and cellular barriers. More specifically, these interactions are known to favor the residence of the nanostructures in the intestinal epithelium and facilitate the rapid uptake into the cancer cell lines. A proof-of-principle has been described for drugs such as salmon calcitonin and docetaxel. Current experiments are aimed at evidencing the clinical relevance of these findings and identifying potential drug/vaccine candidates which could greatly benefit from these findings.

References

1. Calvo P., Vila-Jato J.L., Alonso M.J. - Comparative *in vitro* evaluation of several coloidal systems, nanoparticles, nanocapsules, and nanoemulsions, as ocular drug carriers. - J. Pharm. Sci., **85**, 530-536, 1996.
2. Losa C., Marchal-Heussler L ., Orallo F., Vila-Jato J.L. Alonso M.J. - Desing of new formulations for topical ocular administration: polymeric nanocapsules containing metipranolol. - Pharm. Res., **10**, 80-87, 1993.
3. Müller R.H., Maassen S., Weyhers H., Mehner T. – Phagocityc uptake and cytotoxicity of solid lipid nanoparticles (SLN) sterically stabilized

with poloxamine 908 and poloxamer 407. - J. Drug. Target., **4** (3), 161-170, 1996.

4. Benita S., Levy M.Y. - Submicron emulsions as colloidal drug carriers for intravenous administration: comprehensive physicochemical characterization. - J. Pharm. Sci., **82** (11), 1069-1079, 1993.
5. Guterres S.S., Fessi H., Barratt G., Puisieux F., Devissaguet J.P. - Poly(D,L-lactide) nanocapsules containing non-steroidal anti-inflammatory drugs: gastrointestinal tolerance following intravenous and oral administration. - Pharm Res., **12** (10), 1545-1547, 1995.
6. Calvo P., Vila-Jato J.L., Alonso M.J. - Development of positively charged coloidal drug carriers: chitosan-coated polyester nanocapsules and submicron-emulsions. - Colloid. Polym. Sci., **275**, 46-53, 1997.
7. Meisner D., Pringle J., Mezei M. - Liposomal ophthalmic drug delivery. III. Pharmacodynamic and biodisposition studies of atropine. - Int. J. Pharm., **55**, 105-113, 1989.
8. Robinson J.R. - Ocular drug delivery. Mechanism(s) of corneal drug transport and mucoadhesive delivery systems. – STP Pharma, **5**, 839-846, 1989.
9. Guo L.S.S., Radhakrishnan R., Redemann C.T. - Adhesion of positivively charged liposomes to mucosal tissues. - J. Liposomal Res., **1**, 319-337, 1989.
10. Lee H.V.L., Carson L.W. - Ocular disposition of inulin from single & multiple doses of positively charged multilamellar liposomes: evidence for alterations in tear dynamics and ocular surface characteristics. - J. Ocular Pharmacol., **2**, 353-364, 1986.
11. Elbaz E., Zeevi A., Klang S., Benita S. - Positively charged submicron emulsions- a new type of colloidal drug carrier. - Int. J. Pharm., **96**, R1-R6, 1993.

12. Weiner M.L. - In: Advances in Chitin and Chitosan, C.J. Brine., P.A. Sandford., J.P. Zikakis Eds., Elsevier Science Publishers Ltd., London, 1993, pp. 663-672.
13. Hirano S., Seino H., Akiyama Y., Nonaka I. - In: Progress in Biomedical Polymers, C.G. Gebelein., R.L. Dunn Eds., Plenum Press, New York, 1990, pp. 283-289.
14. Calvo P., Vila-Jato J.L., Alonso M.J. - Evaluation of cationic polymer-coated nanocapsules as ocular drug carriers. - Int. J. Pharm., **153**, 41-50, 1997.
15. Al-Khouri F.N., Roblot-Treupel L., Fessi H. - Development of a new process for the manufacture of polyisobutylcyanoacrylate nanocapsules. - Int. J. Pharm., **28**, 125-132, 1986.
16. Fessi H., Puisieux F., Devissaguet J.P., Ammoury N., Benita S. - Nanocapsule formation by interfacial polymer deposition following solvent deplacement. - Int. J. Pharm., **55**, 25-28, 1989.
17. Prego C., Garcia M., Torres D., Alonso M.J. – Transmucosal macromolecular drug delivery. - J. Control Release., **101**, 151-162, 2005.
18. Maestrelli F., Mura P., Alonso M.J. - Formulation and characterization of triclosan sub-micron emulsions and nanocapsules. - J. Microencapsul., **21** (8), 857-64, 2004.
19. Lozano M.V., Torecilla D., Torres D., Vidal A., Dominguez F., Alonso M.J. - Highly efficient system to deliver taxanes into tumor cells: docetaxel-loaded chitosan oligomer colloidal carriers. - Biomacromol., **9**, 2186-2193, 2008.
20. Vicente S., Sanchez A., Diaz B., Gonzalez A., Alonso M.J. - Polysaccharide based nanocarriers for intranasal vaccination: application to rHBs antigen. - EUFEPS Workshop: Opportunities and Challenges in Vaccine Delivery, Geneva, 15-17 September 2008, EUFEPS, p. 35.

21. Prego C., Fabre M., Torres D., Alonso M.J. - Efficacy and mechanism of action of chitosan nanocapsules for oral peptide delivery. - Pharm Res., **23**, 549-56, 2006.
22. Schöler N., Hahn H., Muller R.H., Liesenfeld O. - Effect of lipid matrix and size of solid lipid nanoparticles (SLN) on the viability and cytokine production of macrophages. - Int. J. Pharm., **231**, 167-176, 2002.
23. Muranishi S. - Absorption enhancers. - Crit. Rev. Therap. Drug Carrier Systems, **7**, 1-33, 1990.
24. Almeida A.J., Souto E. - Solid lipid nanoparticles as a drug delivery system for peptides and proteins. - Adv. Drug Deliv. Rev., **59**, 478-490, 2007.
25. Wissing S.A., Kayser O., Müller R. - Solid lipid nanoparticles for parenteral drug delivery. - Adv. Drug Deliv. Rev., **56**, 1257-1272, 2004.
26. Morel S., Ugazio E., Cavalli R., Gasco M.R. - Thymopentin in solid lipid nanoparticles. - Int. J. Pharm., **132**, 259-261, 1996.
27. Almeida A.J., Runge S., Muller R.H. - Peptide-loaded solid lipid nanoparticles (SLN): Influence of production parameters. - Int. J. Pharm., **149**, 255-265, 1997.
28. Garcia-Fuentes M., Torres D., Alonso M.J. - Design of lipid nanoparticles or the oral delivery of hydrophilic macromolecules. - Colloid Surf. B-Biointerfaces, **27**, 159-168, 2003.
29. Garcia-Fuentes M., Alonso M.J., Torres D. - New surface-modified lipid nanoparticles as delivery vehicles for salmon calcitonin. - Int. J. Pharm., **296**, 122-132, 2005.
30. Saraf S., Mishra D., Asthana A., Jain R., Singh S., Jain N.K. - Lipid microparticles for mucosal immunization against hepatitis B. - Vaccine, **24**, 45-56, 2006.
31. Garcia-Fuentes M., Torres D., Martin-Pastor M., Alonso M.J. - Application of NMR spectroscopy to the characterization of PEG-stabilized lipid nanoparticles. - Langmuir, **20**, 8839-8845, 2004.

32. Garcia-Fuentes M., Alonso M.J., Torres D. - Design and characterization of a new drug nanocarrier made from solid-liquid lipid mixtures. - J. Colloid. Interf. Sci., **285**, 590-598, 2005.
33. Csaba N., Garcia-Fuentes M., Alonso M.J. - The performance of nanocarriers for transmucosal drug delivery. - Expert. Opin. Drug Deliv., **3**, 463-478, 2006.
34. Jani P., Halbert G.W., Langridge J., Florence A.T. - The uptake and translocation of latex nanospheres and microspheres after oral administration to rats. - J. Pharm. Pharmacol., **41**, 809-812, 1989.
35. Florence A.T. - The oral absorption of micro- and nanoparticulates: neither exceptional nor unusual. - Pharm. Res., **14**, 259-266, 1997.
36. Florence A.T., Hussain N. - Transcytosis of nanoparticle and dendrimer delivery systems: evolving vistas. - Adv. Drug Deliv. Rev., **50**, S69-89, 2001.
37. Damgé C., Michel C., Aprahamian M., Couvreur P. - New approach for oral adiminstration of insulin with polyalkylcyanoacrylate nanocapsules as drug carrier. - Diabetes, **37**, 246-251, 1988.
38. Mathiowitz E., Jacob J.S., Jong Y.S., Carino G.P. – Biologically erodable microsphere as potential oral drug delivery system. - Nature, **386**, 410-414, 1997.
39. Calvo P., Alonso, M.J., Vila-Jato J.L., Robinson J.R. – Improved ocular bioavailability of indomethacin by novel ocular drugs carriers. - J. Pharm. Pharmacol., **48** (11), 1147-52, 1996.
40. Tobio M., Gref R., Sanchez A., Langer R., Alonso M.J. – Stealth PLA-PEG nanoparticles as protein carriers for nasal administration. - Pharm. Res., **15**, 270-275, 1998.
41. Tobio M., Sanchez A., Vila A., Soriano I., Évora C., Vila-Jato J.L., Alonso M.J. - The role of PEG on the stability in digestive fluids and *in vivo* fate of PEG-PLA nanoparticles following oral administration. - Colloid. Surf. B-Biointerfaces, **18**, 315-323, 2000.

42. Lee Y.H., Sinko P.J. - Oral delivery of salmon calcitonin. - Adv. Drug Deliv. Rev., **42**, 225-238, 2000.
43. Janes K.A., Calvo P., Alonso M.J. - Polysaccharide colloidal particles as delivery systems for macromolecules. - Adv. Drug Deliv. Rev., **47**, 83-97, 2001.
44. Kawashima Y., Yamamoto H., Takeuchi H., Kuno Y. – Mucoadhesive DL-lactide/glycolide copolymer nanospheres coated with chitosan to improve oral delivery of elcatonin. - Pharm. Dev. Technol., **5**, 77-85, 2000.
45. Takeuchi H., Yamamoto H., Niwa T., Hino T., Kawashima Y. - Enteral absorption of insulin in rats from mucoadhesive chitosan-coated liposomes. - Pharm. Res., **13**, 896-901, 1996.
46. Takeuchi H., Matsui Y., Yamamoto H., Kawashima Y. – Mucoadhesive properties of carbopol or chitosan-coated liposomes and their effectiveness in the oral administration of calcitonin to rats. - J. Control. Release, **86**, 235-242, 2003.
47. Behrens I., Pena A.I., Alonso M.J., Kissel T. - Comparative up-take studies of bioadhesive and non-bioadhesive nanoparticles in human intestinal cell lines and rats: the effect of mucus on particle adsorption and transport. - Pharm. Res., **19**, 1185-93, 2002.
48. Garcia-Fuentes M., Prego C., Torres D., Alonso M.J. - A comparative study of the potential of solid triglyceride nanostructures coated with chitosan or poly(ethylene glycol) as carriers for oral calcitonin delivery. - Eur. J. Pharm. Sci., **25**, 133-43, 2005.
49. Rossi S., Ferrari F., Bonferoni M.C., Caramella C. – Characterization of chitosan hydrochloride-mucin interaction by means of viscosimetric and turbidimetric measurements. - Eur. J. Pharm. Sci., **10**, 251-257, 2000.
50. Borchard G., Lueben H, De Boer A.G., Verhoef J.C., Lehr C.M., Junginger H.E. - The potential of mucoadhesive polymers in enhancing intestinal peptide drug absorption. III. Effects of chitosan-glutamate and

carbomer on epithelial tight junctions *in vitro*. - J. Control Rel., **39**, 131-138, 1996.

51. Merkus F.W.H.M., Schipper N.G.M., Hermens W.A.J.J., Romeijn S.G., Verhoef J.C. - Absorption enhancers in nasal drug delivery: efficacy and safety. - J. Control. Release, **24**, 201- 208, 1993.
52. Marttin E., Verhoef J.C., Romeijn S.G., Merkus F.W.H.M. – Effects of absorption enhancers on rat nasal epithelium *in vivo*: release of marker compounds in the nasal cavity. - Pharm. Res., **12**, 1151-1157, 1995.
53. Tengamnuay P., Sahamethapat A., Sailasuta A., Mitra A.K. - Chitosan as nasal absorption enhancers of peptides: comparison between free amine chitosans and soluble salts. - Int. J. Pharm., **197**, 53-67, 2000.
54. Illum L., Farraj N.F., Davis S.S. - Chitosan as a novel nasal delivery system for peptide drugs. - Pharm. Res., **11**, 1186-1189, 1994.
55. Illum L. - Nasal drug delivery-possibilities, problems and solutions. - J. Control. Release, **87**, 187-198, 2003.
56. Sinswat P., Tengamnuay P. - Enhancing effect of chitosan on nasal absorption of salmon calcitonin in rats: comparison with hydroxypropyl- and dimethyl-ß-ciclodextrins. - Int. J. Pharm., **257**, 15-22, 2003.
57. Prego C., Torres D., Alonso M.J. - Chitosan nanocapsules: A new carrier for nasal peptide delivery. - J. Drug Del. Sci. Tech., **16**, 331-337, 2006.
58. Mitra R., Pezron I., Chuw A., Mitra A.K. - Lipid emulsions as vehicles for enhanced nasal delivery of insulin. - Int. J. Pharm., **205**, 127-134, 2000.
59. Lowe P.J., Temple C.S. - Calcitonin and insulin in isobutylcyanoacrylate nanocapsules: Protection against proteases and effect on intestinal absorption. - J. Pharm. Pharmacol., **46**, 547-552, 1994.

60. Yoo H.S., Park T.G. - Biodegradable nanoparticles containing protein-fatty acid complexes for oral delivery of salmon calcitonin. - J. Pharm. Sci., **93**, 488-495 2004.
61. Csaba N., Garcia-Fuentes M., Alonso MJ. - Nanoparticles for nasal vaccination. - Adv. Drug. Deliv. Rev., **61**, 140-57, 2009.
62. Tanaka T., Decuzzi P., Cristofanilli, Sakamoto J.H., Tasciotti E., Robertson F.M., Ferrari M. - Nanotechnology for breast cancer therapy. - Biomed. Microdevices, **11**, 49-63, 2009.
63. Iyer A.K., Khaled G., Fang J., Maeda H. - Exploiting the enhanced permeability and retention effect for tumor targeting. – Drug Discov. Today, **11**, 812-818, 2006.
64. Garcion E., Lamprecht A., Heurtault B., Paillard A., Aubert- Pouessel A., Denizot B., Menei P., Benoit J.P. - A new generation of anticancer, drug-loaded, colloidal vectors reverses multidrug resistance in glioma and reduces tumor progression in rats. - Mol. Cancer Ther., **5**, 1710-1722, 2006.
65. Couvreur P., Barratt G., Fattal E., Legrand P., Vauthier C. – Nanocapsule technology: A review. - Crit. Rev. Ther. Drug Carrier Syst., **19**, 99-134, 2002.
66. Twelves C. - Docetaxel weekly with metastatic breast cancer. - Onkologie, **30**, 407-408, 2007.
67. Ferrandina G., Ludovisi M., De Vincenzo R., Salutari V., Lorusso D., Colangelo M., Prantera T., Valerio M.R., Scambia G. - Docetaxel and oxaliplatin in the second-line treatment of platinum-sensitive recurrent ovarian cancer: a phase II study. - Ann. Oncol., **18**, 1348-1353, 2007.
68. Jiang Z., Yan W., Ming J., Yu Y. - Docetaxel weekly regimen in conjunction with RF hyperthermia for pretreated locally advanced non-small cell lung cancer: a preliminary study. - BMC Cancer, **7**, 189-193, 2007.

69. Green M. R., Manikhas G. M., Orlov S., Afanasyev B., Makhson A. M., Bhar P., Hawkins M. J. - Abraxane, a novel Cremophorfree, albumin-bound particle form of paclitaxel for the treatment of advanced non-small-cell lung cancer. - Ann. Oncol., **17**, 1263-1268, 2006.
70. De Campos A.M., Sanchez A., Gref R., Calvo P., Alonso M.J. - The effect of a PEG versus a chitosan coating on the interaction of drug coloidal carriers with the ocular mucosa. - Eur. J. Pharm. Sci., **20**, 73-81, 2003.
71. Lozano M.V., Torecilla D., Lallana E., Vidal A., Fernandez-Megía E., Riguera R., Dominguez F., Alonso M.J., Torres D. – Chitosan Nanocapsules for active tumor targeting. - Proceedings of the 7th World Meeting on Pharmaceutics, Biopharmaceutics and Pharmaceutical Technology, Malta, 8-11 March 2010.

Acknowledgements

The studies reported in this review were performed in our laboratory and have been supported by grants from the Ministry of Science and Technology (Consolider Nanobiomed, CSD 2006-00012) and the Xunta de Galicia (PGIDIT 08CSA045209PR), Spain. Felipe Oyarzun-Ampuero was granted a CONICYT scholarship.

Manuscript

Received 7 April 2010, accepted for publication 28 May 2010.

Anexo 2: Artículo relacionado

A new drug nanocarrier consisting of polyarginine and hyaluronic acid

F. A. Oyarzun-Ampuero[a], F.M. Goycoolea[a], D. Torres[a], M.J. Alonso[a]

Department of Pharmacy and Pharmaceutical Technology, Faculty of Pharmacy 15782, University of Santiago de Compostela, Spain.

Adapted from: European Journal of Pharmaceutics and Biopharmaceutics. (2011). 79(1): 54-57.

Abstract

The purpose of this study was to produce and characterize a variety of nanostructures comprised of the polyaminoacid polyarginine (PArg) and the polysaccharide hyaluronic acid (HA) as a preliminary stage before evaluating their potential application in drug delivery. PArg was combined with high- or low-molecular-weight HA (HMWHA or LMWHA, respectively) to form nanoparticles by simply mixing polymeric aqueous solutions at room temperature. The average size of the resulting nanocarriers was between 116 and 155 nm, and their zeta potential value ranged from +31.3 to -35.9 mV, indicating that the surface composition of the particle could be conveniently modified according to the mass ratio of the polymers. Importantly, the systems prepared with HMWHA remained stable after isolation by centrifugation and in conditions that mimic the physiological medium, whereas particles that incorporated LMWHA were unstable. Transmission electron microscopy showed that the nanostructures made with HMWHA were spherical. Finally, the systems were stable for at least three months at storage conditions (4°C).

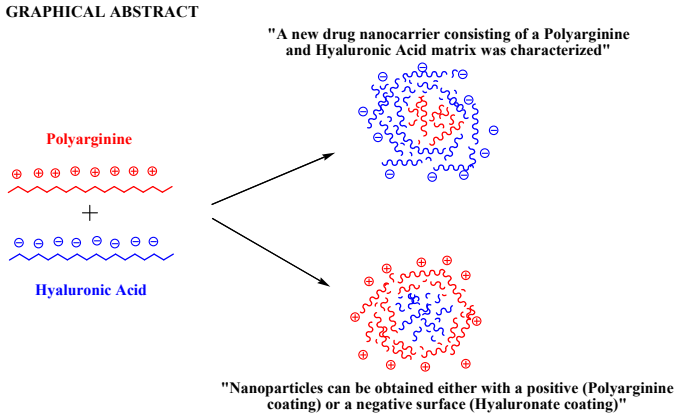

Keywords: Nanoparticles; hyaluronic acid; polyarginine; drug delivery; complexes.

Introduction

Because of their unique size and surface characteristics, nanostructures have emerged as a platform for the delivery of macromolecules and low-molecular-weight drugs for the treatment of a variety of diseases. In nanomedicine, there is a need for suitable biomaterials for optimization of the interaction/transport of drug carriers to target tissues. Concerning their characteristics, glycosaminoglycan hyaluronic acid (HA) and polyaminoacid polyarginine (PArg) are molecules used for the transport and biorecognition of nanomedicines.

HA is a natural non-toxic mucoadhesive polysaccharide that is negatively charged and biodegradable. It is widely distributed throughout the human body but primarily resides in connective tissue, eyes, intestine, and lungs. Importantly, the overexpression in a variety of tissues of the CD-44 receptor, the endogenous ligand for HA, makes this biopolymer a viable candidate for specific targeting. Several studies have tested the efficacy of nanosystems based on HA using various applications, namely gene delivery [1], cancer [2], and asthma [3] among others.

In turn, polyaminoacids are promising tools for the development of drug delivery systems, mainly due to their safety profile. These molecules are structurally similar to polypeptides and are thus degraded by human enzymes; their accumulation within the organism is minimal. Interestingly, the cationic PArg is able to translocate through cell membranes and facilitate the uptake of molecules associated with polyaminoacid [4]. This interesting feature of PArg has been exploited to harness drug delivery systems used for gene therapy [5], protein/vaccine delivery [6], and cancer [7]. Furthermore, PArg enhances the absorption of hydrophilic compounds across the nasal epithelium [8], a property that may be utilized for mucosal drug delivery.

The nanoparticles preparation method can affect its pharmacological and functional properties. Some procedures include the use of organic

solvents or covalent cross-linkers that can compromise the safety of the formulation. Other preparation protocols use stringent processes, such as high temperature or sonication, which may destroy or alter drug bioactivity. In addition, nanoparticle stability in conditions that mimic biological medium or during long-term storage is a key factor that may determine the success of the formulation.

The aim of the present work was to develop and characterize a variety of PArg-containing nanostructures that were formed by the combination of the polyaminoacid with HA, wich have also addressed the possible influence of the molecular weight of HA on the physicochemical and stability characteristics of the systems by using a high and a low-molecular-weight hyaluronic acid (HMWHA or LMWHA, respectively). These particles were formed using an extremely mild and simple procedure that involves mixing two aqueous phases at room temperature. The prepared nanostructures could be applied in different fields considering the established properties such as mucoadhesivity and cell- penetrating capacity of the constituent polymers. Of note, a recent study by Kim et al. reported the formation of a nanosystem composed of HA (19 kDa), PArg (15-70 kDa), and small interference RNA (siRNA) [9]. Such study focused on the biological behavior of siRNA-loaded nanosystems and not on the physicochemical and technological parameters of the unloaded nanoparticles.

Materials and methods

Chemicals

HMWHA (Mw ~165 kDa) was a gift from Bioiberica (Barcelona, Spain). LMWHA (Mw ~29 kDa) was purchased from Inquiaroma (Barcelona, Spain), and polyarginine (PArg, Mw ~5-15 kDa) was purchased from Sigma Aldrich (Madrid, Spain). All other reagents were of the highest analytical grade. MilliQ water was used for experimentation.

Preparation of nanoparticles

Nanoparticles were prepared by mixing HA and PArg aqueous solutions. Briefly, 4.5 mL of an aqueous solution containing HA (0.44-2.67 mg/mL) was added to 4.5 mL of a solution containing PArg (0.53 mg/mL) by stirring at room temperature. For isolation, 1 mL of the nanoparticles was transferred to Eppendorf tubes and centrifuged (16000×*g*, 30 min, 25 º C) in 20 μL of a glycerol bed. Supernatants were discarded, and the nanoparticles were resuspended in water by vigorous shaking. It is thought that the nanosystems were formed by electrostatic interactions between the positively charged amino group of the guanidine moiety on the PArg and the negatively charged carboxylate groups with the HA.

Physicochemical characterization of nanoparticles

The size and zeta potential of the colloidal systems were determined by photon correlation spectroscopy and laser Doppler anemometry using a Zetasizer Nano-ZS (Malvern Instruments, Worcestershire, United Kingdom), MilliQ water was used as solvent. Each batch was analyzed in triplicate. Morphological examination of the nanoparticles was carried out by transmission electron microscopy (TEM) (CM12 Phillips, Eindhoven,

Netherlands). The samples were stained with 1% (w/v) phosphotungstic acid for 10 s, immobilized on copper grids with Formvar® and dried overnight before TEM analysis.

Stability of nanoparticles

Nanoparticle formulations were prepared and centrifuged in the presence of glycerol. The stability of the nanoparticles was evaluated according to size and precipitation in phosphate-buffered saline (PBS, pH 7.4) at 37 °C and in MilliQ water at 4 °C.

The composition of PBS was as follows: 137 mM NaCl, 2.7 mM KCl, 1.4 mM NaH_2PO_4 and 1.3 mM Na_2HPO_4.

Results and discussion

Table 1a and b show the mass ratio, charge [HA]/[PArg] ratio, size, polydispersity index and zeta potential of the tested formulations prepared with either HMWHA or LMWHA, respectively. Our data show that when the [HA]/[PArg] charge ratio was lower than 0.975, nanostructures with a positive zeta potential were obtained, indicating that the surface of these systems is mainly composed of positively charged PArg. This feature is attributed to excess of PArg (relative to that of HA) in the formulation. Consequently, when the [HA]/[PArg] charge ratio increased to 0.975 and higher, inversion of the zeta potential values was observed, indicating that the nanocarrier surface was now shielded by excess of HA, which bears a negative charge. It can be appreciated that the zeta potential values (and average size) are not further modified beyond this ratio. This indicates that HA is incorporated into the nanoparticles up to saturation limit while surplus HA remains unassociated in solution and is in agreement with yield studies (data not shown).

Table 1: Physicochemical properties of the nanocarriers prepared with different ratios of HMWHA-PArg (a) or LMWHA-PArg (b) and evaluated in MilliQ water. (mean ± S.D., n=3).

a)

Mass ratio HMWHA-PArg	Charge ratio [HA]/[PArg]	Size (nm)	Polydispersity index	Zeta potential (mV)
2-2.4	0.325	128 ± 8	0.2-0.3	+31.3 ± 1
4-2.4	0.65	136 ± 16	0.1-0.2	+25.3 ± 4
6-2.4	0.975	154 ± 7	0.1-0.2	-32.5 ± 5
8-2.4	1.3	150 ± 7	0.1-0.2	-33.4 ± 4
10-2.4	1.625	147 ± 7	0.1-0.2	-35.9 ± 5
12-2.4	1.95	155 ± 7	0.1-0.2	-33.8 ± 4

b)

Mass ratio LMWHA-PArg	Charge ratio [HA]/[PArg]	Size (nm)	Polydispersity index	Zeta potential (mV)
2-2.4	0.325	Not formed	Not formed	Not formed
4-2.4	0.65	131 ± 26	0.1-0.2	+25 ± 1
6-2.4	0.975	172 ± 18	0.1-0.2	-19 ± 1
8-2.4	1.3	139 ± 9	0.1-0.2	-27 ± 3
10-2.4	1.625	137 ± 13	0.1-0.2	-31 ± 3
12-2.4	1.95	146 ± 13	0.1-0.2	-33 ± 3

Alteration of the surface charge of the nanocarriers as a function of the polymer ratio allows optimization of the surface composition (and, presumably, the biological behavior) to interact with targets that have affinity for PArg or HA. Additionally, knowledge of the relative contribution of each charged species to the nanosystems may allow nanoparticle customization for the incorporation of positively or negatively charged drug molecules.

The transmission electron micrographs indicated that each formulation was reasonable spherical, which is in agreement with previous works describing a spherical shape of nanoparticles made with either natural or synthetic polymers [3]. Figure 1 shows a micrograph of a formulation with a [HMWHA]/[PArg] charge ratio of 1.3.

Figure 1: Transmission electron micrograph of HMWHA-PArg nanocarriers; HA-PArg charge ratio= 1.3.

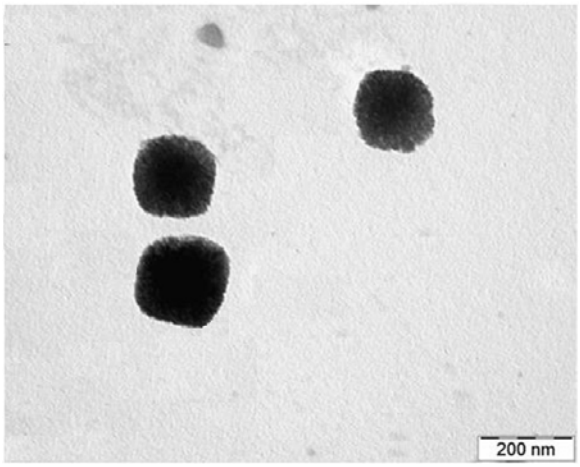

Importantly, characterization of HMWHA-containing systems was conducted after isolation of the nanocarriers by centrifugation, whereas characterization of LMWHA-containing systems was performed without isolation. The reason for that was because the latter nanoparticles were unstable during the centrifugation process (the lower tested conditions of centrifugation were 500*g* during 30 min) as evidenced by the disappearance of the turbidity of the system and by photon correlation spectroscopy (PCS) size measurements. The systems containing HMWHA were effectively isolated at 16000*g* during 30 min, maintaining the same characteristics that the non-isolated formulations had. As shown in Table 1a and b, at a charge ratio of 0.325, nanosystems were obtained that incorporated HMWHA, whereas those containing LMWHA were not formed. In addition, the ς values

of the LMWHA-containing systems were generally lower than those containing HMWHA systems. Thus, fewer charged species were located on the surface of the low-molecular-weight polymer surface. Greater charge compensation for systems that have low-molecular-weight species may also account for the lower ς values.

Hence, we postulate that the observed differences among nanostructures comprising HMWHA or LMWHA are probably due to the preferential organization of the polymers, particularly at the nanoparticle surface. Variance in particle assembly may also account for the instability of LMWHA nanosystems during centrifugation. The formation of local regions with a large number of consecutive associated residues (i.e., greater cooperativity) of both polyelectrolytes in the HMWHA-containing systems may explain its superior stability during centrifugation in comparison with LMWHA-containing systems, which presumably have lower cooperativity. These regions, in which charges are compensated, become more hydrophobic due to their neutral character and, hence, they are expected to lie within the inner core of the nanostructure. This distribution would provide the systems with more stability. A similar interpretation was offered in a previous work studying the behavior of hybrid nanoparticles of chitosan and alginate (of various molecular weight) cross-linked with tripolyphosphate [10]. It is important to point out that the ability to isolate formulations by simple centrifugation avoids tedious time-consuming procedures, such as those performed by Kim et al. [9], whose developed nanosystems were isolated by dialysis over 2 days.

Colloidal stability under physiological conditions is a crucial characteristic for successful biomedical application of the nanosystems. Therefore, we investigated the stability of the systems composed of HMWHA and LMWHA in PBS at pH 7.4 and 37 °C. Figure 2 shows the stability profiles of the HMWHA-containing systems. The majority of the formulations were stable for at least 2 h, indicating that the stability of the

nanosystems was maintained independent of their surface composition (PArg or HMWHA). The stability profiles of each LMWHA-containing formulation and those of 0.65 charge-ratio containing HMWHA are not shown in the plot because they either immediately aggregated after addition to the medium or were larger than ~1000 nm. Differences in the stability of HMWHA- and LMWHA-containing nanostructures may also be related to the specific organization of HA and PArg on the nanoparticle surface. This would affect the colloidal stability conferred by charge repulsion and steric hindrance. In the case of the formulation of charge ratio 0.65 with HMWHA, its instability could be attributed that this formulation shows the lowest magnitude in zeta potential before the point of charge inversion, thus effectively perturbing the stability of the systems mediated by charge repulsion. Importantly, in Figure 2 it is possible to appreciate that, from the beginning of the experiment (0 h), all the formulations showed an increased size compared with the original one evaluated in MilliQ water (Table 1). Considering that PBS presents a significant quantity of salt, this can weaken and dissociate the anionic interactions between the oppositely charged polymers leading to swelling of the systems. Additionally, the salt ions could diffuse inside the nanosystems and attracting, by osmotic forces, water inside the nanosystems also exerting a possible swelling of the formulations.

Figure 2: Stability profiles of HMWHA-PArg nanocarriers in phosphate-buffered saline pH 7.4 at 37°C; HA-PArg charge ratios: 0.325 (x), 0.975 (+), 1.3 (▲), 1.625 (○) and 1.95 (□) (mean ± S.D., n=3).

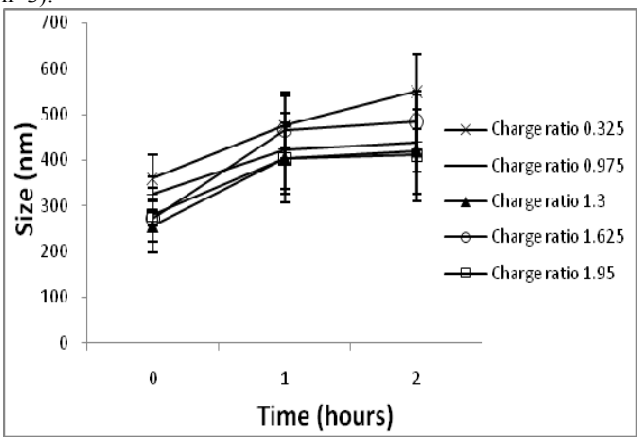

Finally, the stability of nanocarriers during long-term storage is an important step for the adequate handling of the formulations. Figure 3 shows the stability profiles of each formulation composed of HMWHA at 4 °C for 3 months. Every formulation was stable and showed no significant change in particle size. Each system composed of LMWHA was also stable during storage (data not shown).

Figure 3: Stability profiles of HMWHA-PArg nanocarriers in water during storage at 4°C; HA-PArg charge ratios: 0.325 (x), 0.65 (■), 0.975 (+), 1.3 (▲), 1.625 (○) and 1.95 (□) (mean ± S.D., n=3).

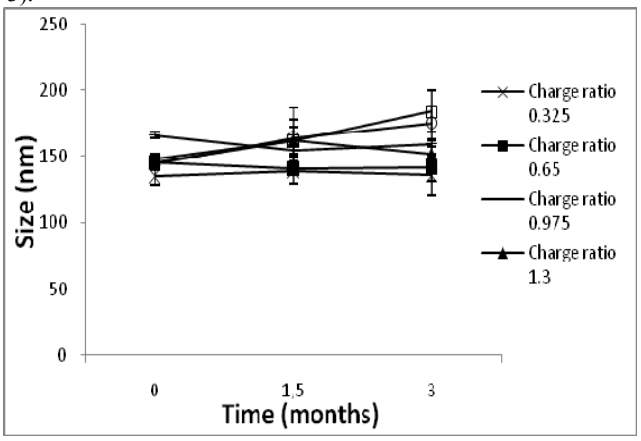

As future work, we are planning to introduce macromolecular hydrophilic drugs into the nanocarriers whose final targets could be solid tumor cells (where CD-44 receptors are overexpressed), or mucosal surfaces (that can avidly interact with both hyaluronic acid and polyarginine). More concretely, oral peptide delivery, in which polyarginine has demonstrated to be very promising, will be explored.

Conclusions

In conclusion, a nanoparticulate system composed of PArg and HA was successfully prepared using an extremely mild process. Negatively and positively charged nanoparticle formulations with surfaces composed preferentially of HA or PArg, were obtained. Importantly, we demonstrated that the molecular weight of HA is a crucial determinant of formulation stability during mechanical isolation and in physiological conditions. This knowledge is useful not only for systems comprising polyarginine and hyaluronic acid but also for systems composed by other polymers. Further studies testing the potential of these systems as mucoadhesive nanocarriers for targeted drug delivery will be carried out, and the in vitro-in vivo behavior of these systems will be also evaluated.

Acknowledgements

The authors acknowledge the Spanish Government for financial support (Consolider-Ingenio CSD 2006-00012 and Xunta de Galicia PGIDIT 08CSA045209PR) and CONICYT for a scholarship to F.A. Oyarzun-Ampuero.

References

1. M. de la Fuente, N. Csaba, M. Garcia-Fuentes, M.J. Alonso, Nanoparticles as protein and gene carriers to mucosal surfaces, Nanomed. 3 (2008) 845-57.
2. V.M. Platt, F.C.Jr. Szoka, Anticancer therapeutics: targeting macromolecules and nanocarriers to hyaluronan or CD44, a hyaluronan receptor, Mol. Pharm. 5 (2008) 474-86.
3. F.A. Oyarzun-Ampuero, J. Brea, M.I. Loza, D. Torres, M.J. Alonso, Chitosan-hyaluronic acid nanoparticles loaded with heparin for the treatment of asthma, Int. J. Pharm. 381 (2009) 122-129.
4. Lundberg M.; Wikström S.; Johansson M. (2003). Cell Surface Adherence and Endocytosis of Protein Transduction Domains. Mol. Ther. 8 (2003) 143-150.
5. V.P. Torchilin, TAT peptide-mediated intracelular delivery of pharmaceutical nanocarriers, Adv. Drug Deliv. Rev. 60 (2008) 548-58.
6. K. Lingnau, K. Riedl, A. von Gabain, IC31® and IC30, novel types of vaccine adjuvant based on peptide delivery systems, Expert Rev. Vaccines. 6 (2007) 741-746.
7. Z. Miklán, E. Orbán, G. Csík, G. Schlosser, A. Magyar, F. Hudecz, New daunomycin-oligoarginine conjugates: synthesis, characterization, and effect on human leukemia and human hepatoma cells, Biopolymers. 92 (2009) 489-501.
8. M. Miyamoto, H. Natsume, S. Iwata, K. Ohtake, M. Yamaguchi, D. Kobayashi, K. Sugibayashi, M. Yamashina, Y. Morimoto, Improved nasal absorption of drugs using poly-L-arginine: effects of concentration and molecular weight of poly-L-arginine on the nasal absorption of fluorescein isothiocyanate-dextran in rats, Eur. J. Pharm. Biopharm. 52 (2001) 21-30.

9. E.J. Kim, G. Shim, K. Kim, I.C. Kwon, Y.K. Oh, C.K. Shim, Hyaluronic acid complexed to biodegradable poly-L-arginine for targeted delivery of siRNA, J. Gene Med. 11 (2009) 791-803.
10. F.M. Goycoolea, G. Lollo, C. Remuñán-López, F. Quaglia, M.J. Alonso, Chitosan-alginate blended nanoparticles as carriers for the transmucosal delivery of macromolecules. Biomacromolecules. 10 (2009) 1736-1743.

Anexo 3

Patentes Solicitadas:

M.J. Alonso, D. Torres, G. Rivera-Rodríguez, F. Oyarzún-Ampuero, G. Lollo, T. Gonzalo-Lázaro, M. García-Fuentes. Nanocápsulas con cubierta polimérica. Número de solicitud P201130015 (Oficina Española de Patentes y Marcas), fecha de recepción 10-01-2011.